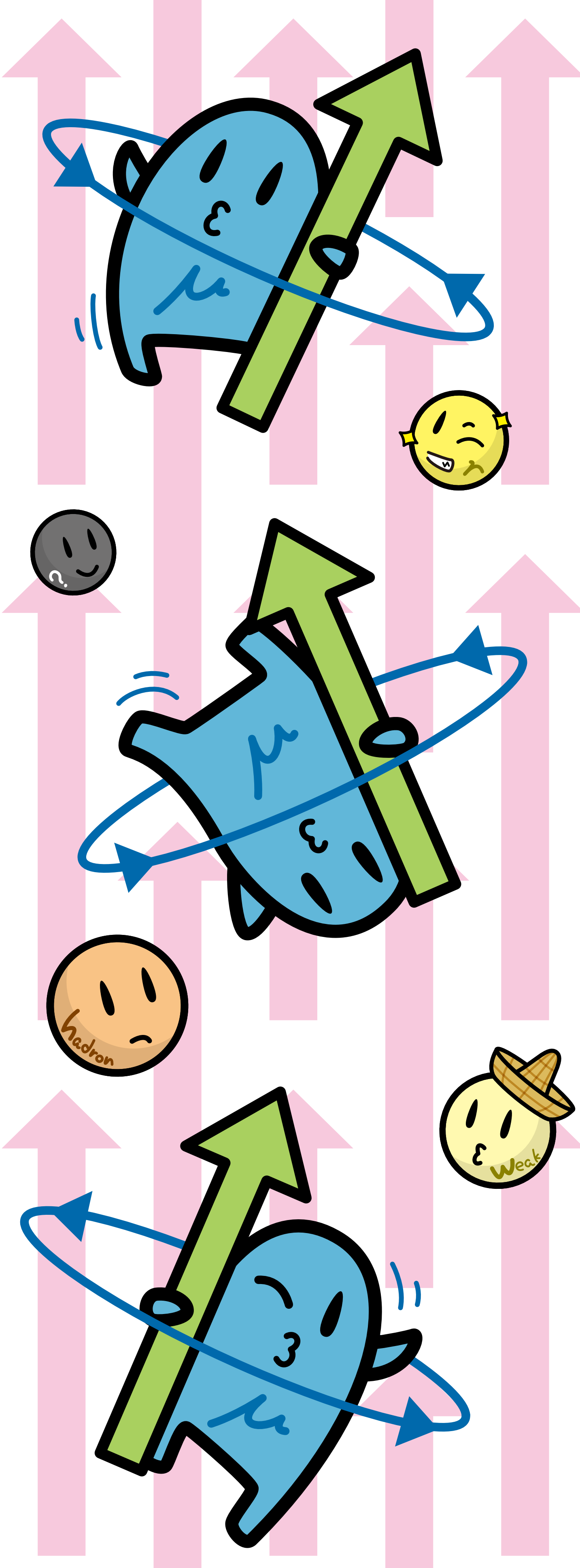

HADRONIC LIGHT-BY-LIGHT SCATTERING CONTRIBUTION

— PHENOMENOLOGY —

Franziska Hagelstein

(JGU Mainz & PSI Villigen)

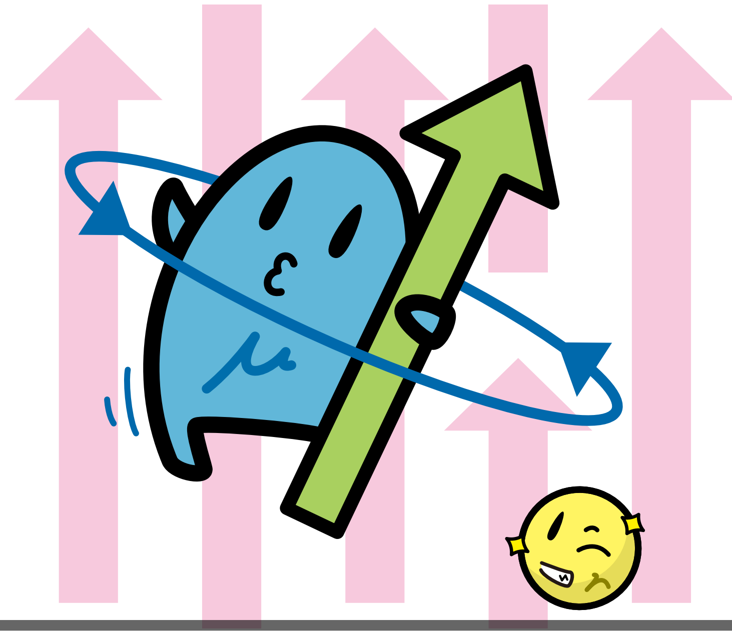

— Short Recap —

$(g-2)_\mu$ Uncertainty Budget & Hadronic Contributions

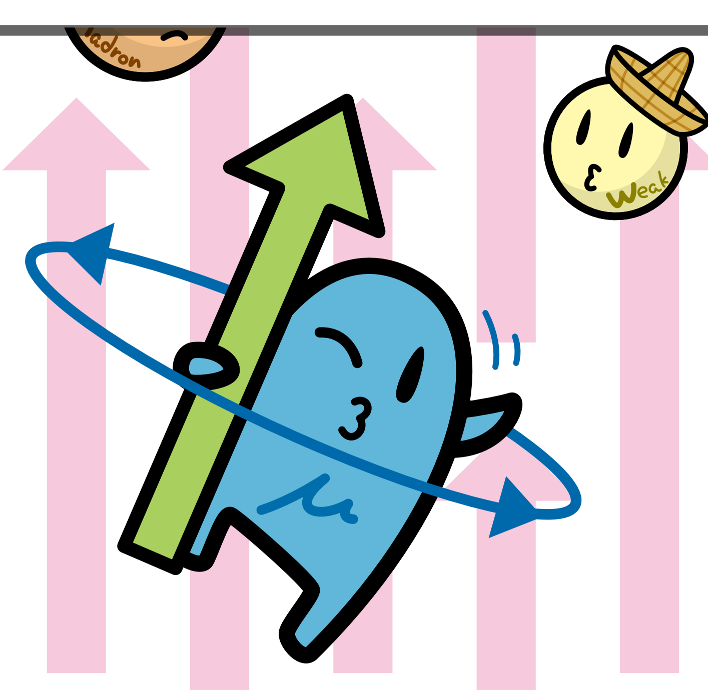

HISTORY

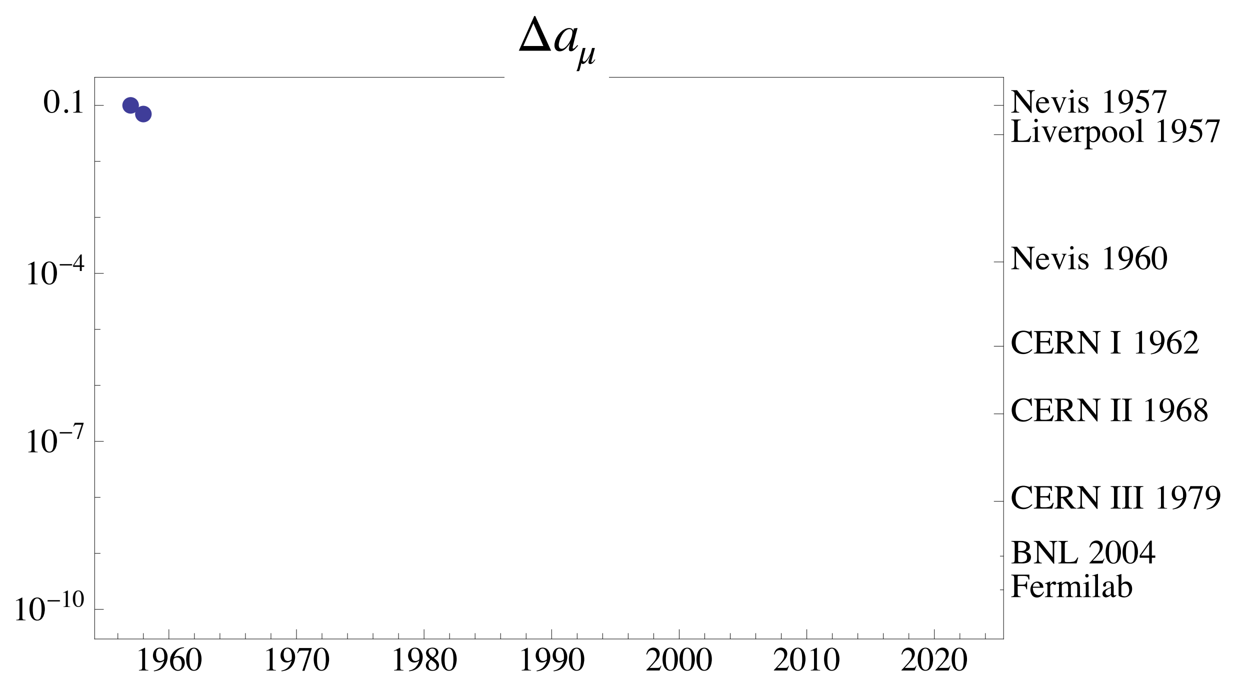
Δa_μ
0.1
10^{-4}
10^{-7}
10^{-10}
1960
1970
1980
1990
2000
2010
2020
Nevis 1957
Liverpool 1957
Nevis 1960
CERN I 1962
CERN II 1968
CERN III 1979
BNL 2004
Fermilab

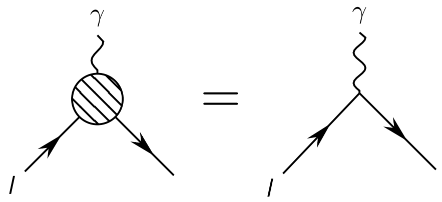
γ
γ
=

HISTORY

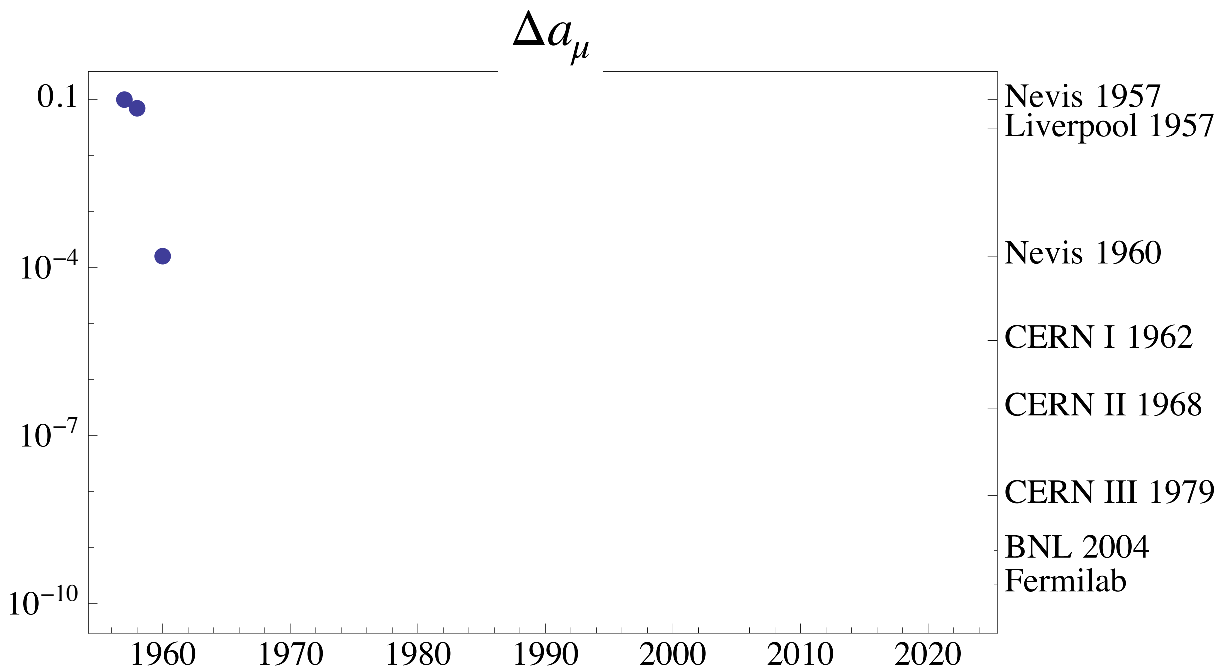

Schwinger term
$a_\mu = \alpha/2\pi$

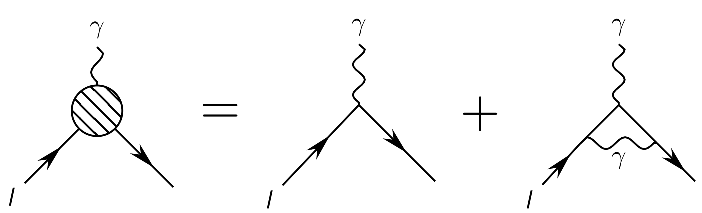

1-loop QED [1 diagram]

HISTORY

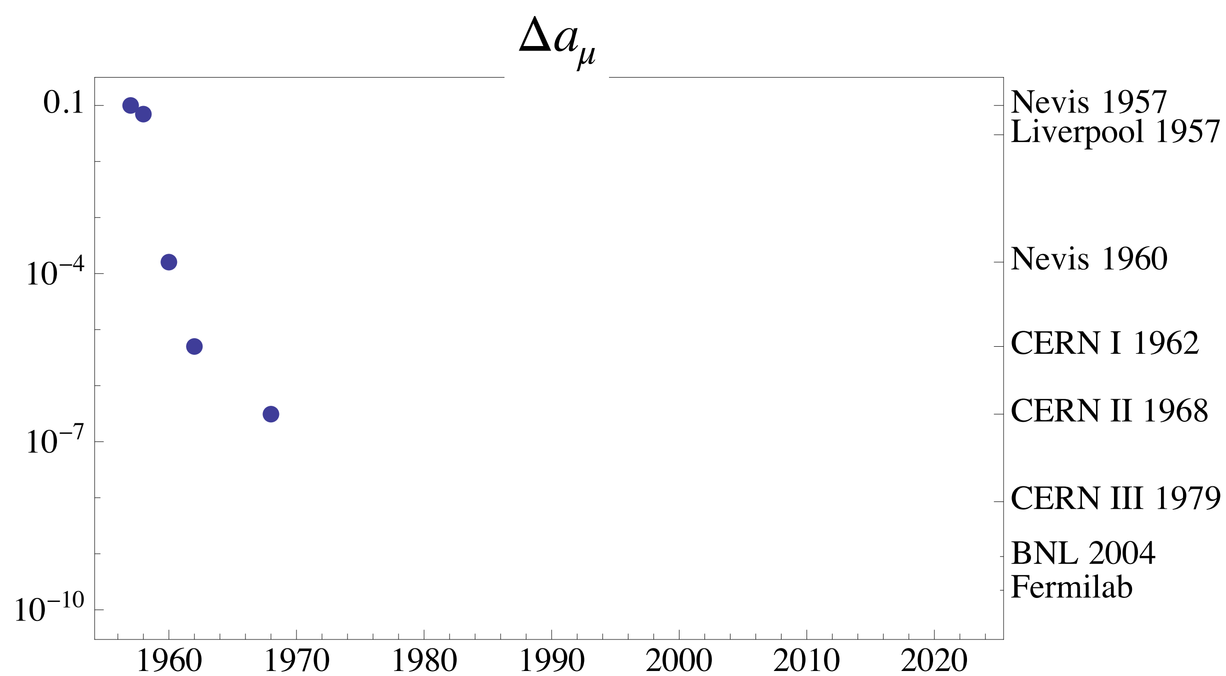

Schwinger term
$a_\mu = \alpha/2\pi$

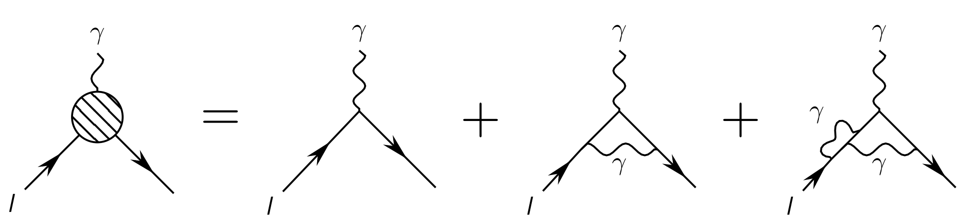

1-loop QED [1 diagram]
2-loop QED [7 diagrams]
3-loop QED [72 diagrams]

HISTORY

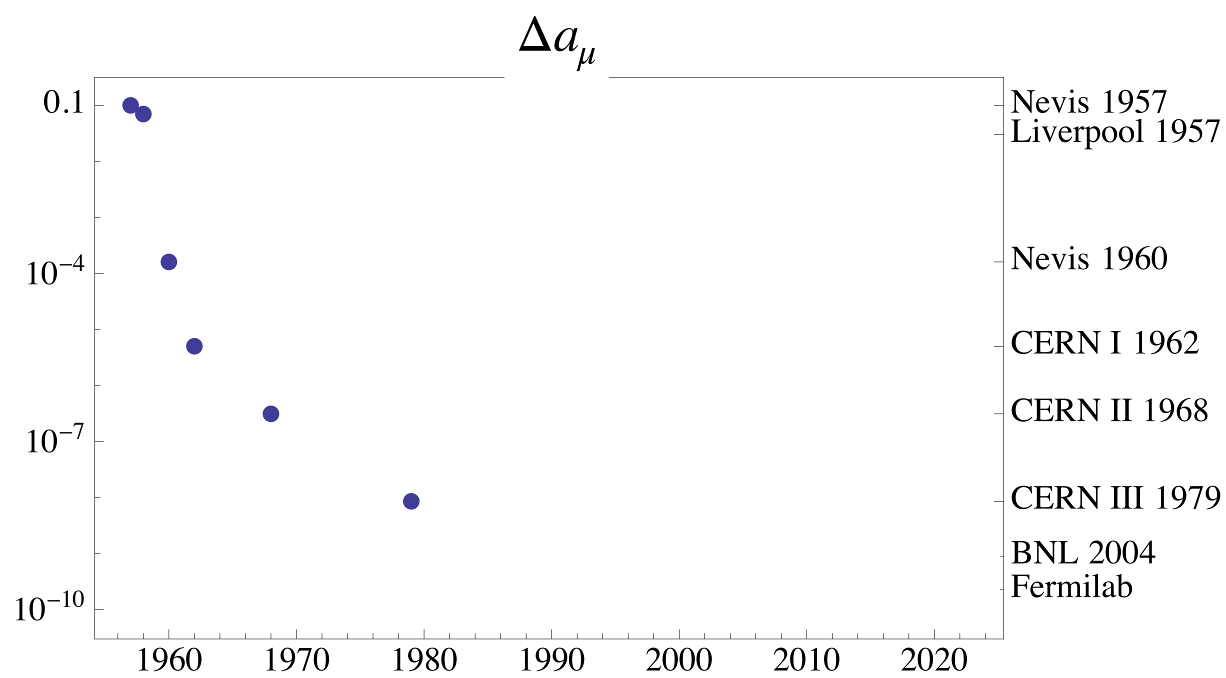

Schwinger term
$a_\mu = \alpha/2\pi$

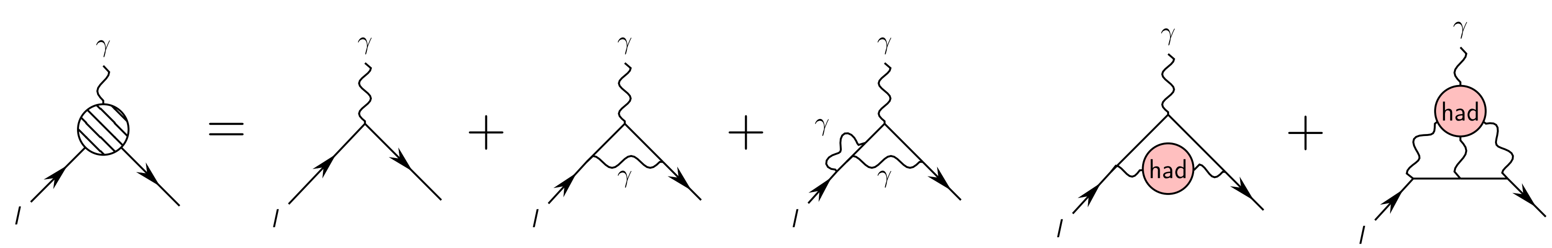

1-loop QED [1 diagram]
2-loop QED [7 diagrams]
3-loop QED [72 diagrams]

HISTORY

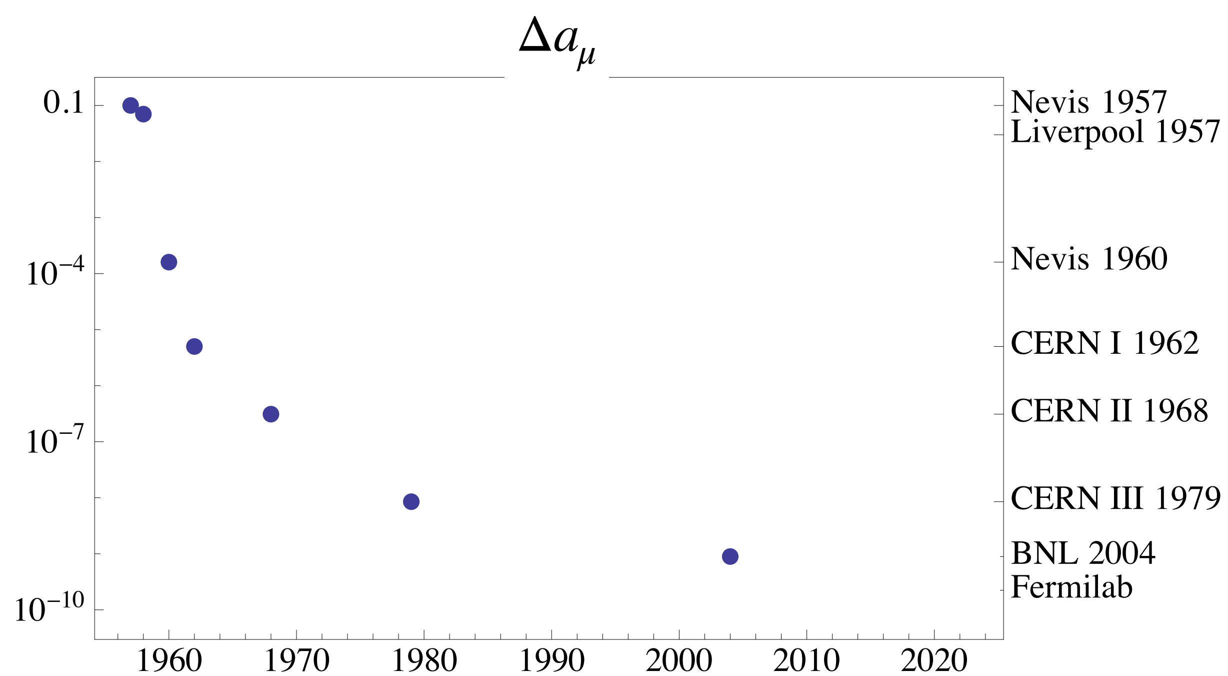

Schwinger term
$a_\mu = \alpha/2\pi$

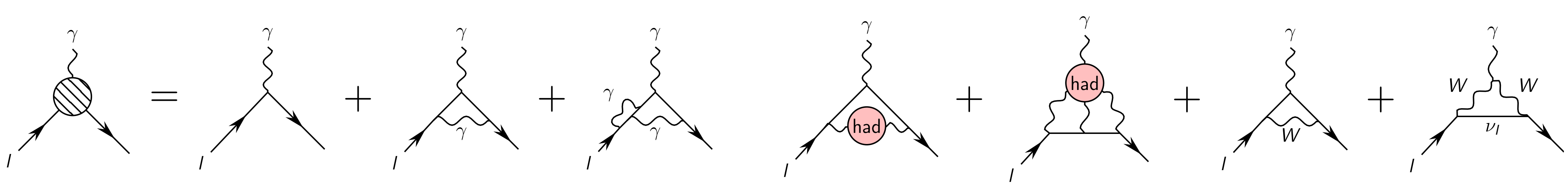

1-loop QED [1 diagram]
2-loop QED [7 diagrams]
3-loop QED [72 diagrams]
4-loop QED [891 diagrams]
5-loop QED [12 672 diagrams]

HISTORY

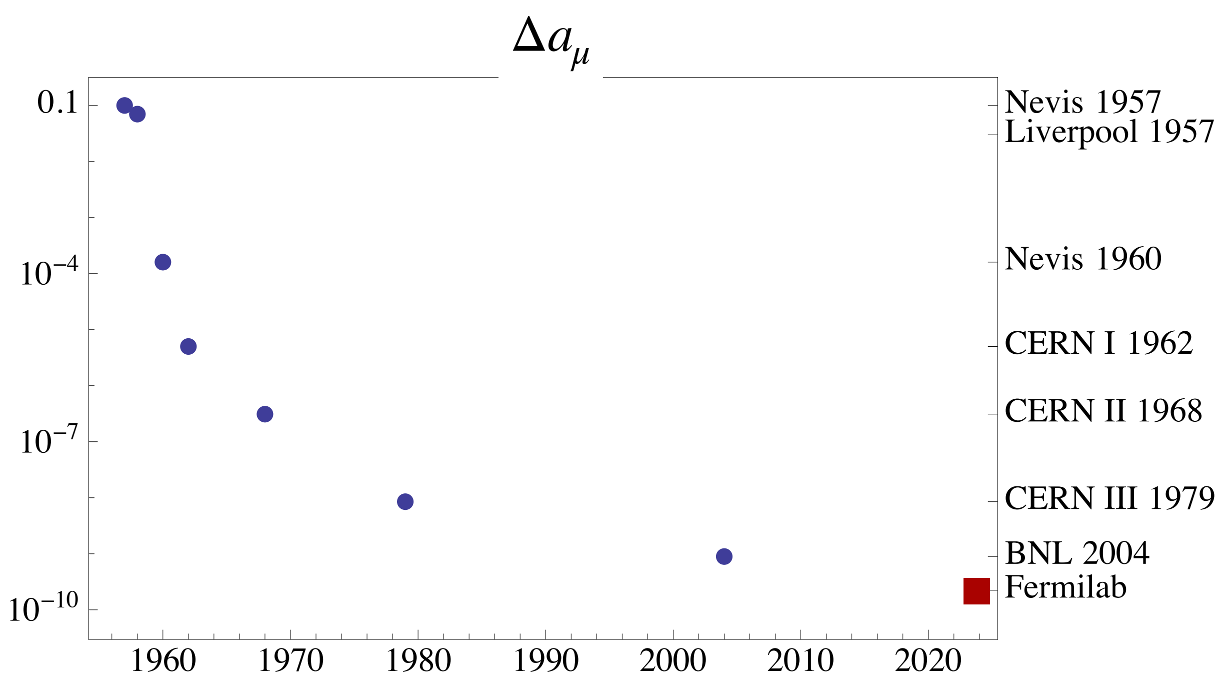

- Fermilab Run 1-3 & BNL: 0.19 ppm uncertainty

Schwinger term
$a_\mu = \alpha/2\pi$

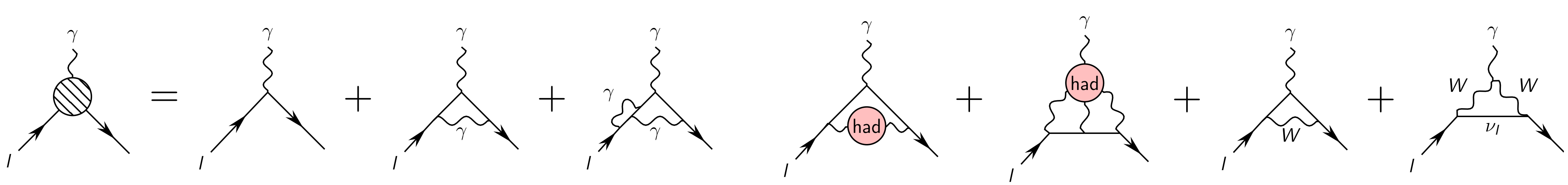

1-loop QED [1 diagram]
2-loop QED [7 diagrams]
3-loop QED [72 diagrams]
4-loop QED [891 diagrams]
5-loop QED [12 672 diagrams]

HISTORY

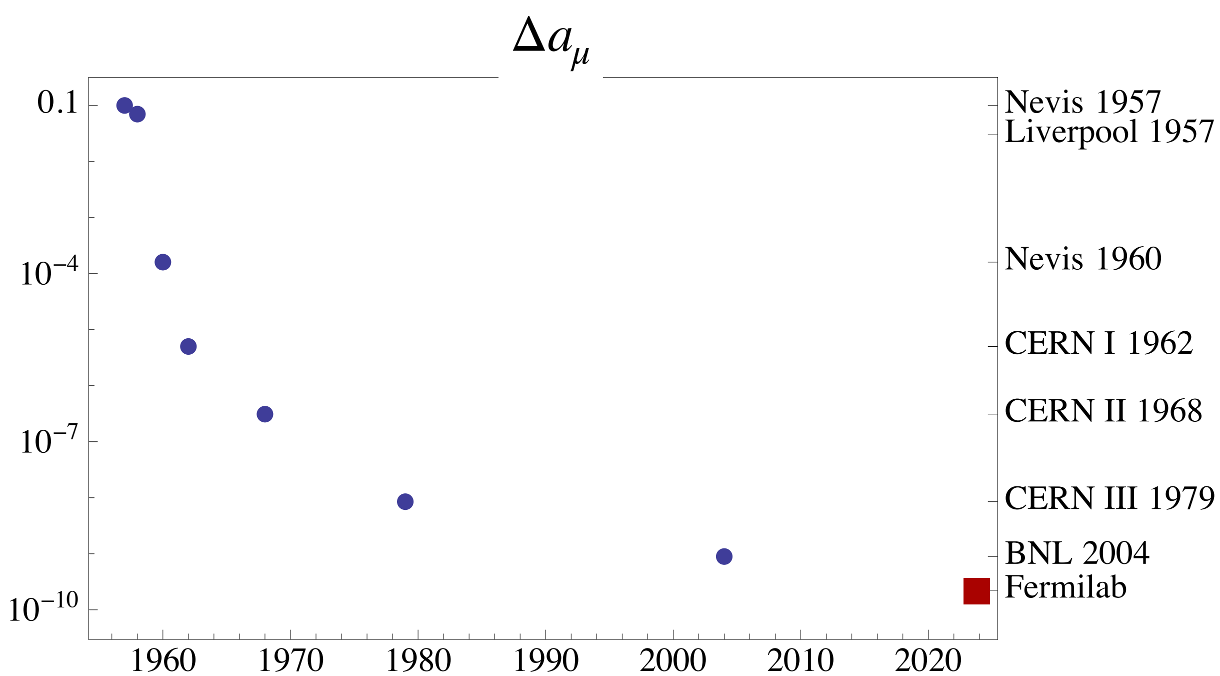

- Fermilab Run 1-3 & BNL: 0.19 ppm uncertainty
- Fermilab Run 4 & 5 will reduce statistical uncertainty by another factor of 2

Schwinger term
$a_\mu = \alpha/2\pi$

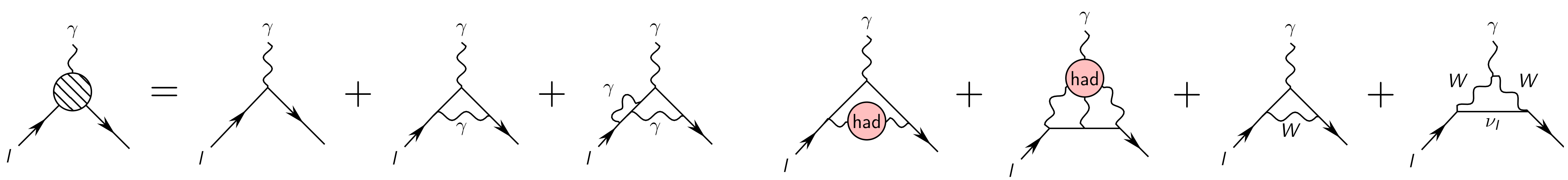

1-loop QED [1 diagram]
2-loop QED [7 diagrams]
3-loop QED [72 diagrams]
4-loop QED [891 diagrams]
5-loop QED [12 672 diagrams]

HISTORY

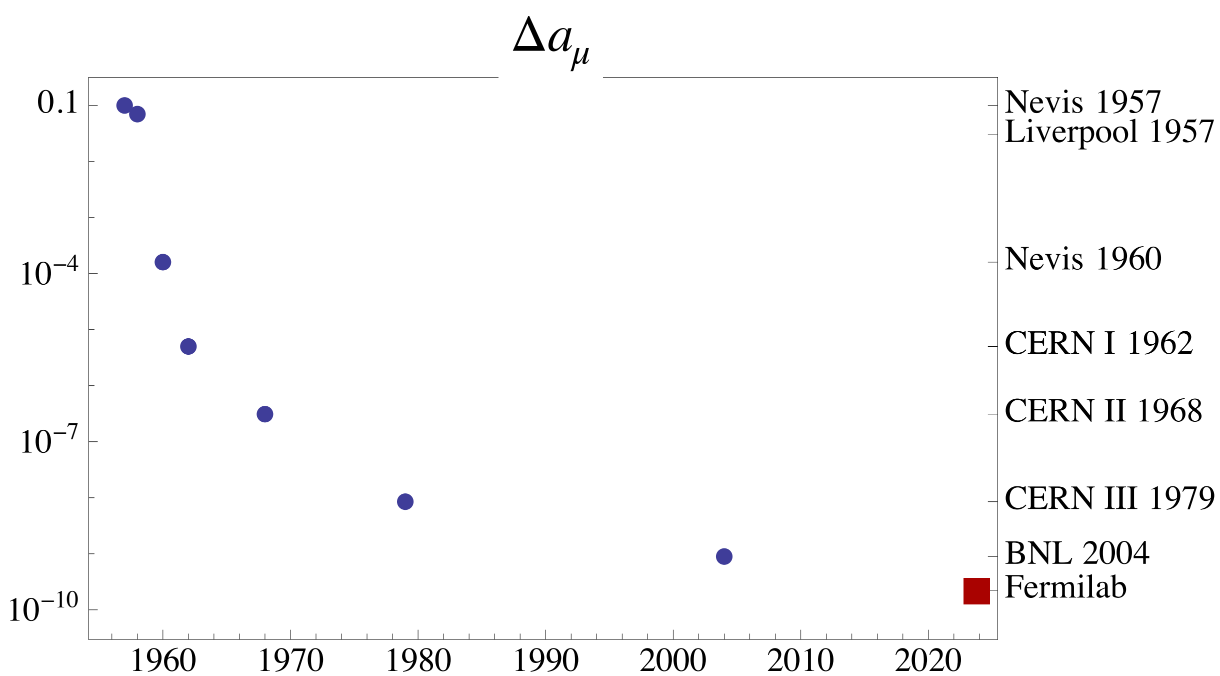

- Fermilab Run 1-3 & BNL: 0.19 ppm uncertainty
- Fermilab Run 4 & 5 will reduce statistical uncertainty by another factor of 2
- J-PARC experiment will provide independent cross check

Schwinger term
$a_\mu = \alpha/2\pi$

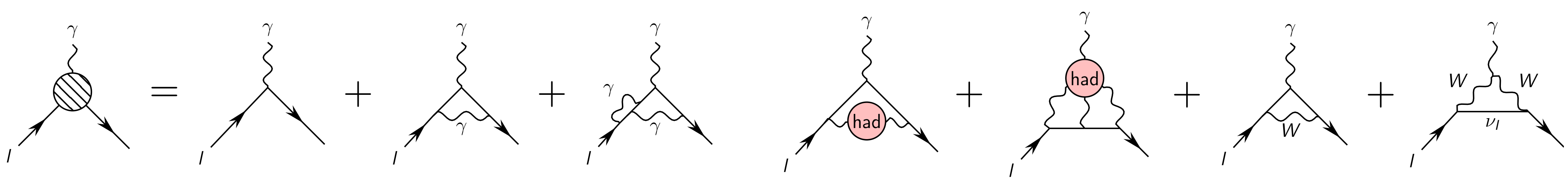

1-loop QED [1 diagram]
2-loop QED [7 diagrams]
3-loop QED [72 diagrams]
4-loop QED [891 diagrams]
5-loop QED [12 672 diagrams]

HISTORY

Anna Driutti / Elia Bottalico & Masato Kimura (KEK, Monday)

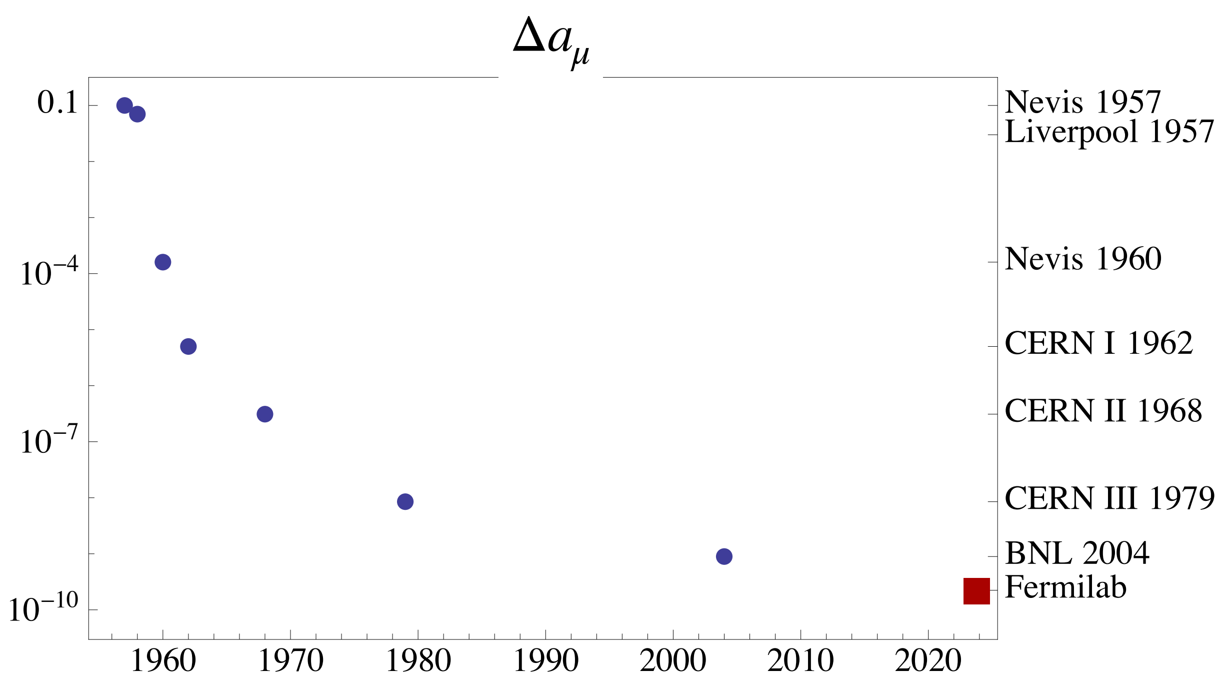

- Fermilab Run 1-3 & BNL: 0.19 ppm uncertainty
- Fermilab Run 4 & 5 will reduce statistical uncertainty by another factor of 2
- J-PARC experiment will provide independent cross check

Schwinger term
$a_\mu = \alpha/2\pi$

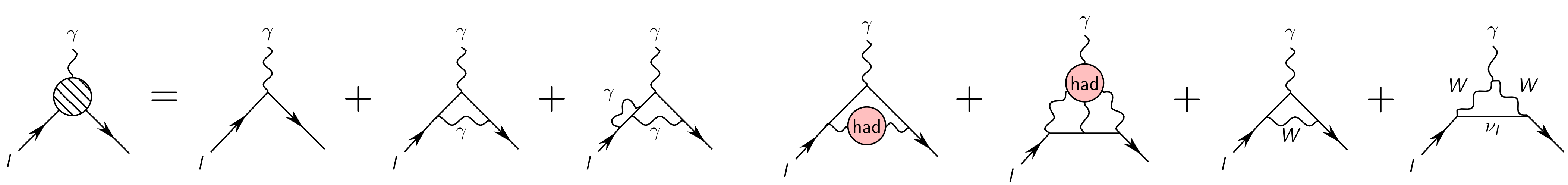

1-loop QED [1 diagram]
2-loop QED [7 diagrams]
3-loop QED [72 diagrams]
4-loop QED [891 diagrams]
5-loop QED [12 672 diagrams]

PRESENT STATUS

Aguillard, et al., Phys. Rev. Lett. 131 (2023) 16, 161802

Aoyama, et al., Phys. Rept. 887 (2020) 1-166

	$a_\mu \times 10^{14}$	$\Delta a_\mu \times 10^{14}$	$\Delta a_\mu / a_\mu$
Experiment	116 592 059 000	22 000	2×10^{-7}
SM	116 591 810 000	43 000	4×10^{-7}

PRESENT STATUS

Aguillard, et al., Phys. Rev. Lett. 131 (2023) 16, 161802

Aoyama, et al., Phys. Rept. 887 (2020) 1-166

	$a_\mu \times 10^{14}$	$\Delta a_\mu \times 10^{14}$	$\Delta a_\mu / a_\mu$
Experiment	116 592 059 000	22 000	2×10^{-7}
SM	116 591 810 000	43 000	4×10^{-7}
QED	116 584 718 931	104	9×10^{-10}

PRESENT STATUS

Aguillard, et al., Phys. Rev. Lett. 131 (2023) 16, 161802

Aoyama, et al., Phys. Rept. 887 (2020) 1-166

	$a_\mu \times 10^{14}$	$\Delta a_\mu \times 10^{14}$	$\Delta a_\mu / a_\mu$
Experiment	116 592 059 000	22 000	2×10^{-7}
SM	116 591 810 000	43 000	4×10^{-7}
QED	116 584 718 931	104	9×10^{-10}
HVP	6 845 000	40 000	6×10^{-3}

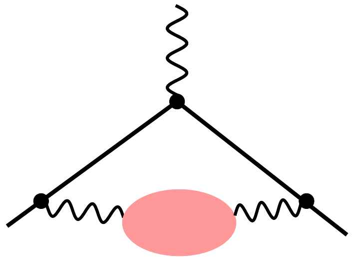

Hadronic vacuum polarization (HVP)

PRESENT STATUS

Aguillard, et al., Phys. Rev. Lett. 131 (2023) 16, 161802

Aoyama, et al., Phys. Rept. 887 (2020) 1-166

	$a_\mu \times 10^{14}$	$\Delta a_\mu \times 10^{14}$	$\Delta a_\mu / a_\mu$
Experiment	116 592 059 000	22 000	2×10^{-7}
SM	116 591 810 000	43 000	4×10^{-7}
QED	116 584 718 931	104	9×10^{-10}
HVP	6 845 000	40 000	6×10^{-3}
Electroweak	153 600	1 000	7×10^{-3}

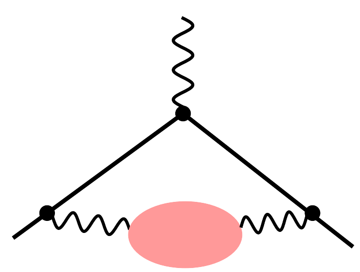

Hadronic vacuum polarization (HVP)

PRESENT STATUS

Aguillard, et al., Phys. Rev. Lett. 131 (2023) 16, 161802

Aoyama, et al., Phys. Rept. 887 (2020) 1-166

	$a_\mu \times 10^{14}$	$\Delta a_\mu \times 10^{14}$	$\Delta a_\mu / a_\mu$
Experiment	116 592 059 000	22 000	2×10^{-7}
SM	116 591 810 000	43 000	4×10^{-7}
QED	116 584 718 931	104	9×10^{-10}
HVP	6 845 000	40 000	6×10^{-3}
Electroweak	153 600	1 000	7×10^{-3}
HLbL	92 000	18 000	2×10^{-1}

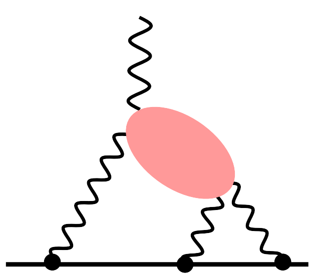

Hadronic light-by-light scattering (HLbL)

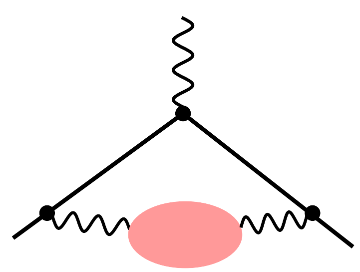

Hadronic vacuum polarization (HVP)

PRESENT STATUS

Aguillard, et al., Phys. Rev. Lett. 131 (2023) 16, 161802

Aoyama, et al., Phys. Rept. 887 (2020) 1-166

	$a_\mu \times 10^{14}$	$\Delta a_\mu \times 10^{14}$	$\Delta a_\mu / a_\mu$
Experiment	116 592 059 000	22 000	2×10^{-7}
SM	116 591 810 000	43 000	4×10^{-7}
QED	116 584 718 931	104	9×10^{-10}
HVP	6 845 000	40 000	6×10^{-3}
Electroweak	153 600	1 000	7×10^{-3}
HLbL	92 000	18 000	2×10^{-1}

Mismatch implies "New Physics" or insufficient understanding of the SM!

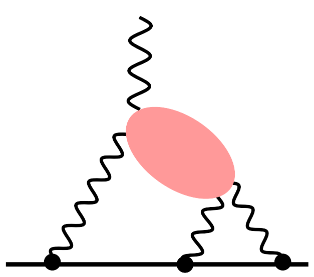

Hadronic light-by-light scattering (HLbL)

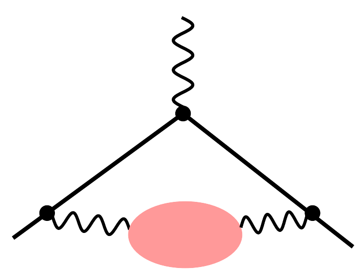

Hadronic vacuum polarization (HVP)

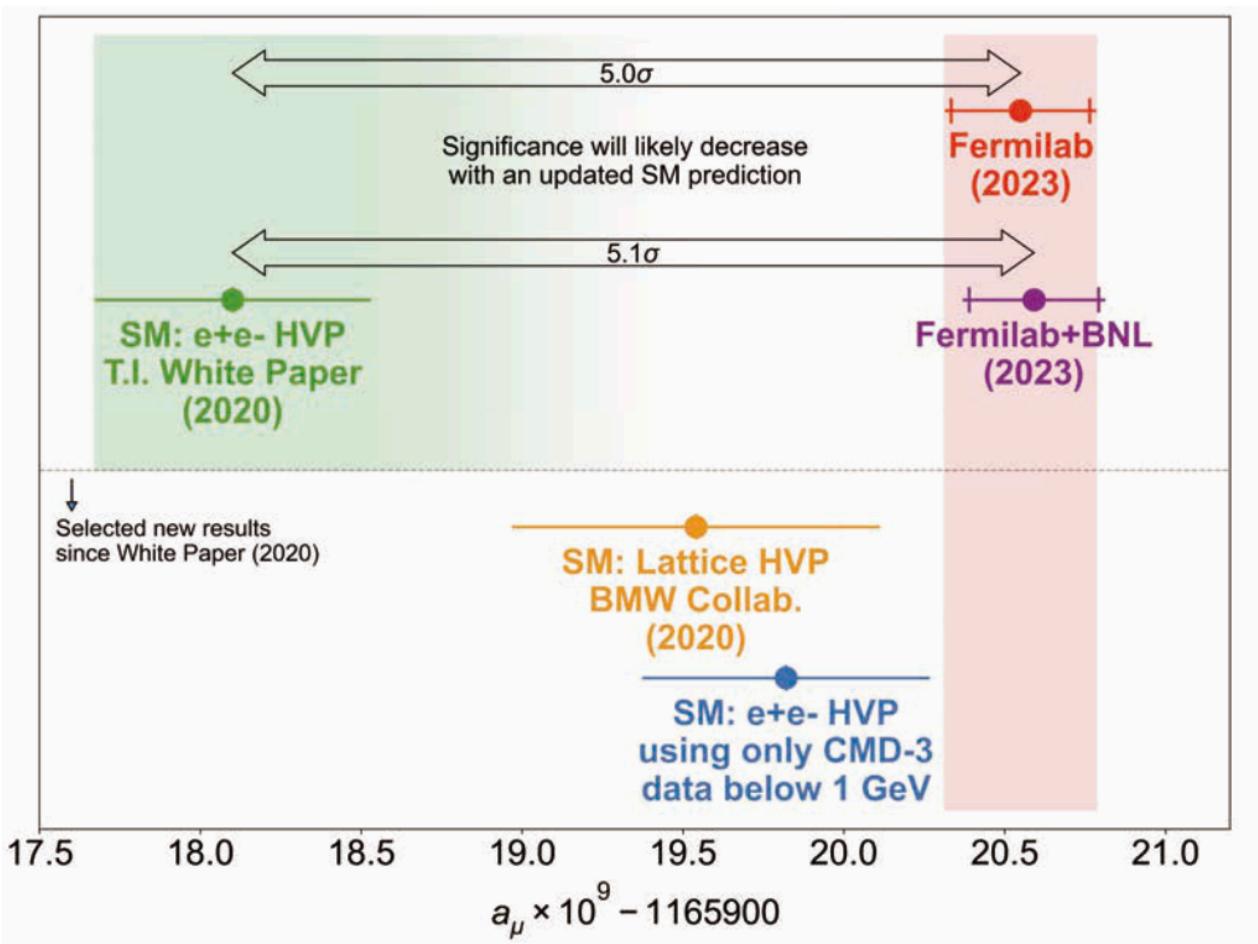

THEORY SUMMARY

Physics Reports 887 (2020) 1–166

Contents lists available at ScienceDirect

Physics Reports

journal homepage: www.elsevier.com/locate/physrep

ELSEVIER

The anomalous magnetic moment of the muon in the Standard Model

Contribution	Section	Equation	Value $\times 10^{11}$	References
Experiment (E821)		Eq. (8.13)	116 592 089(63)	Ref. [1]
HVP LO (e^+e^-)	Section 2.3.7	Eq. (2.33)	6931(40)	Refs. [2–7]
HVP NLO (e^+e^-)	Section 2.3.8	Eq. (2.34)	−98.3(7)	Ref. [7]
HVP NNLO (e^+e^-)	Section 2.3.8	Eq. (2.35)	12.4(1)	Ref. [8]
HVP LO (lattice, *udsc*)	Section 3.5.1	Eq. (3.49)	7116(184)	Refs. [9–17]
HLbL (phenomenology)	Section 4.9.4	Eq. (4.92)	92(19)	Refs. [18–30]
HLbL NLO (phenomenology)	Section 4.8	Eq. (4.91)	2(1)	Ref. [31]
HLbL (lattice, *uds*)	Section 5.7	Eq. (5.49)	79(35)	Ref. [32]
HLbL (phenomenology + lattice)	Section 8	Eq. (8.10)	90(17)	Refs. [18–30,32]
QED	Section 6.5	Eq. (6.30)	116 584 718.931(104)	Refs. [33,34]
Electroweak	Section 7.4	Eq. (7.16)	153.6(1.0)	Refs. [35,36]
HVP (e^+e^-, LO + NLO + NNLO)	Section 8	Eq. (8.5)	6845(40)	Refs. [2–8]
HLbL (phenomenology + lattice + NLO)	Section 8	Eq. (8.11)	92(18)	Refs. [18–32]
Total SM Value	Section 8	Eq. (8.12)	116 591 810(43)	Refs. [2–8,18–24,31–36]
Difference: $\Delta a_\mu := a_\mu^{\text{exp}} - a_\mu^{\text{SM}}$	Section 8	Eq. (8.14)	279(76)	

https://muon-gm2-theory.illinois.edu

THEORY SUMMARY

Submitted to the Proceedings of the US Community Study
on the Future of Particle Physics (Snowmass 2021)

FERMILAB-CONF-22-236-T LTH 1303 MITP-22-030

Prospects for precise predictions of a_μ in the Standard Model

hep-ph/2203.15810

Contribution	Value $\times 10^{11}$	References
Experiment (E821 + E989)	$116\,592\,061(41)$	Refs. [1, 5]
HVP LO (e^+e^-)	$6931(40)$	Refs. [17–22]
HVP NLO (e^+e^-)	$-98.3(7)$	Ref. [22]
HVP NNLO (e^+e^-)	$12.4(1)$	Ref. [23]
HVP LO (lattice, $udsc$)	$7116(184)$	Refs. [24–32]
HLbL (phenomenology)	$92(19)$	Refs. [33–45]
HLbL NLO (phenomenology)	$2(1)$	Ref. [46]
HLbL (lattice, uds)	$79(35)$	Ref. [47]
HLbL (phenomenology + lattice)	$90(17)$	Refs. [33–45, 47]
QED	$116\,584\,718.931(104)$	Refs. [48, 49]
Electroweak	$153.6(1.0)$	Refs. [50, 51]
HVP (e^+e^-, LO + NLO + NNLO)	$6845(40)$	Refs. [17–23]
HLbL (phenomenology + lattice + NLO)	$92(18)$	Refs. [33–47]
Total SM Value	$116\,591\,810(43)$	Refs. [17–23, 33–39, 46–51]
Difference: $\Delta a_\mu := a_\mu^{\text{exp}} - a_\mu^{\text{SM}}$	$251(59)$	

THEORY SUMMARY

Submitted to the Proceedings of the US Community Study
on the Future of Particle Physics (Snowmass 2021)

FERMILAB-CONF-22-236-T LTH 1303 MITP-22-030

Prospects for precise predictions of a_μ in the Standard Model

hep-ph/2203.15810

Contribution	Value $\times 10^{11}$	References
Experiment (E821 + E989)	$116\,592\,061(41)$	Refs. [1, 5]
HVP LO (e^+e^-)	$6931(40)$	Refs. [17–22]
HVP NLO (e^+e^-)	$-98.3(7)$	Ref. [22]
HVP NNLO (e^+e^-)	$12.4(1)$	Ref. [23]
HVP LO (lattice, $udsc$)	$7116(184)$	Refs. [24–32]
HLbL (phenomenology)	$92(19)$	Refs. [33–45]
HLbL NLO (phenomenology)	$2(1)$	Ref. [46]
HLbL (lattice, uds)	$79(35)$	Ref. [47]
HLbL (phenomenology + lattice)	$90(17)$	Refs. [33–45, 47]
QED	$116\,584\,718.931(104)$	Refs. [48, 49]
Electroweak	$153.6(1.0)$	Refs. [50, 51]
HVP (e^+e^-, LO + NLO + NNLO)	$6845(40)$	Refs. [17–23]
HLbL (phenomenology + lattice + NLO)	$92(18)$	Refs. [33–47]
Total SM Value	$116\,591\,810(43)$	Refs. [17–23, 33–39, 46–51]
Difference: $\Delta a_\mu := a_\mu^{\text{exp}} - a_\mu^{\text{SM}}$	$251(59)$	

THEORY SUMMARY

Submitted to the Proceedings of the US Community Study
on the Future of Particle Physics (Snowmass 2021)

FERMILAB-CONF-22-236-T LTH 1303 MITP-22-030

Prospects for precise predictions of a_μ in the Standard Model

hep-ph/2203.15810

Contribution	Value $\times 10^{11}$	References
Experiment (E821 + E989)	$116\,592\,061(41)$	Refs. [1, 5]
HVP LO (e^+e^-)	$6931(40)$	Refs. [17–22]
HVP NLO (e^+e^-)	$-98.3(7)$	Ref. [22]
HVP NNLO (e^+e^-)	$12.4(1)$	Ref. [23]
HVP LO (lattice, $udsc$)	$7116(184)$	Refs. [24–32]
HLbL (phenomenology)	$92(19)$	Refs. [33–45]
HLbL NLO (phenomenology)	$2(1)$	Ref. [46]
HLbL (lattice, uds)	$79(35)$	Ref. [47]
HLbL (phenomenology + lattice)	$90(17)$	Refs. [33–45, 47]
QED	$116\,584\,718.931(104)$	Refs. [48, 49]
Electroweak	$153.6(1.0)$	Refs. [50, 51]
HVP (e^+e^-, LO + NLO + NNLO)	$6845(40)$	Refs. [17–23]
HLbL (phenomenology + lattice + NLO)	$92(18)$	Refs. [33–47]
Total SM Value	$116\,591\,810(43)$	Refs. [17–23, 33–39, 46–51]
Difference: $\Delta a_\mu := a_\mu^{\text{exp}} - a_\mu^{\text{SM}}$	$251(59)$	

Harvey Meyer

THEORY SUMMARY

Submitted to the Proceedings of the US Community Study
on the Future of Particle Physics (Snowmass 2021)

FERMILAB-CONF-22-236-T LTH 1303 MITP-22-030

Prospects for precise predictions of a_μ in the Standard Model

hep-ph/2203.15810

Contribution	Value $\times 10^{11}$	References
Experiment (E821 + E989)	$116\,592\,061(41)$	Refs. [1, 5]
HVP LO (e^+e^-)	$6931(40)$	Refs. [17–22]
HVP NLO (e^+e^-)	$-98.3(7)$	Ref. [22]
HVP NNLO (e^+e^-)	$12.4(1)$	Ref. [23]
HVP LO (lattice, $udsc$)	$7116(184)$	Refs. [24–32]
HLbL (phenomenology)	$92(19)$	Refs. [33–45]
HLbL NLO (phenomenology)	$2(1)$	Ref. [46]
HLbL (lattice, uds)	$79(35)$	Ref. [47]
HLbL (phenomenology + lattice)	$90(17)$	Refs. [33–45, 47]
QED	$116\,584\,718.931(104)$	Refs. [48, 49]
Electroweak	$153.6(1.0)$	Refs. [50, 51]
HVP (e^+e^-, LO + NLO + NNLO)	$6845(40)$	Refs. [17–23]
HLbL (phenomenology + lattice + NLO)	$92(18)$	Refs. [33–47]
Total SM Value	$116\,591\,810(43)$	Refs. [17–23, 33–39, 46–51]
Difference: $\Delta a_\mu := a_\mu^{\text{exp}} - a_\mu^{\text{SM}}$	$251(59)$	

Harvey Meyer

HLBL SUMMARY

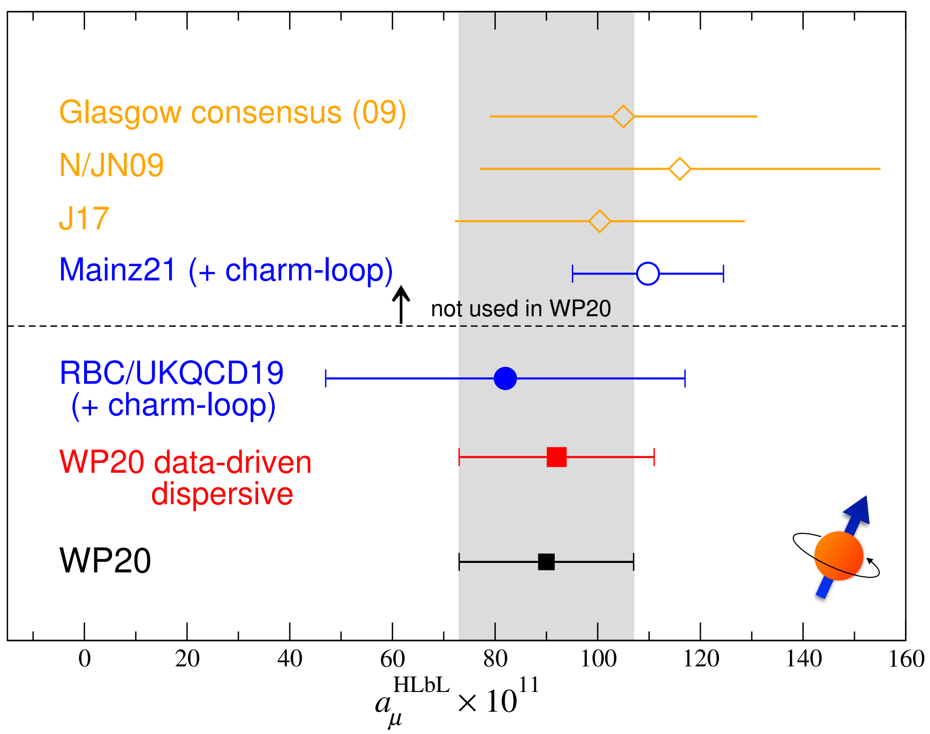

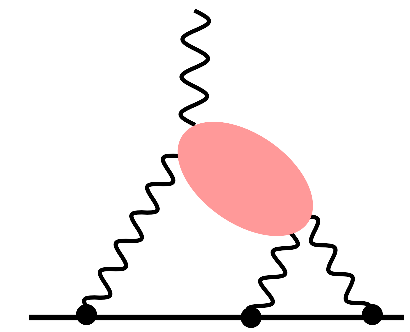

$$a_\mu^{\mathrm{HLbL}}(\text{phenomenology + lattice QCD}) + a_\mu^{\mathrm{HLbL,\,NLO}} = 92(18) \times 10^{-11}$$

- Data-driven and lattice QCD predictions are consistent

$\Longrightarrow$ 10% uncertainty feasible (by 2025) [Snowmass '21]

Contribution	PdRV(09) [471]	N/JN(09) [472, 573]	J(17) [27]	Our estimate
π^0, η, η'-poles	114(13)	99(16)	95.45(12.40)	93.8(4.0)
π, K-loops/boxes	−19(19)	−19(13)	−20(5)	−16.4(2)
S-wave $\pi\pi$ rescattering	−7(7)	−7(2)	−5.98(1.20)	−8(1)
subtotal	88(24)	73(21)	69.5(13.4)	69.4(4.1)
scalars	–	–	–	} − 1(3)
tensors	–	–	1.1(1)	}
axial vectors	15(10)	22(5)	7.55(2.71)	6(6)
u, d, s-loops / short-distance	–	21(3)	20(4)	15(10)
c-loop	2.3	–	2.3(2)	3(1)
total	105(26)	116(39)	100.4(28.2)	92(19)

Table 15: Comparison of two frequently used compilations for HLbL in units of 10^{-11} from 2009 and a recent update with our estimate. PdRV = Prades, de Rafael, Vainshtein ("Glasgow consensus"); N/JN = Nyffeler / Jegerlehner, Nyffeler; J = Jegerlehner.

HLBL SUMMARY

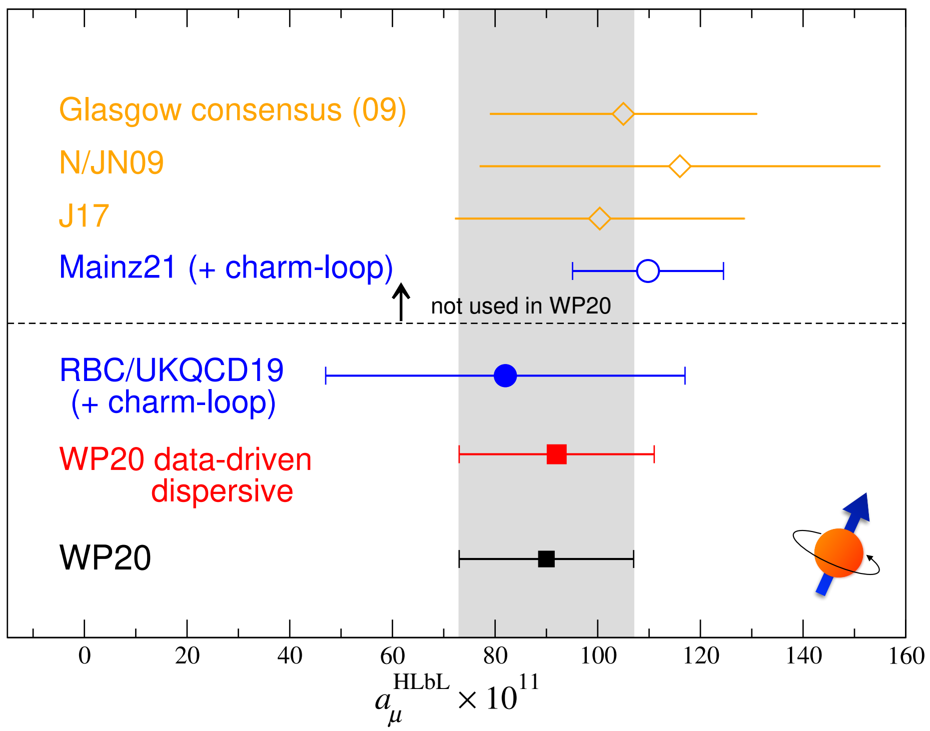

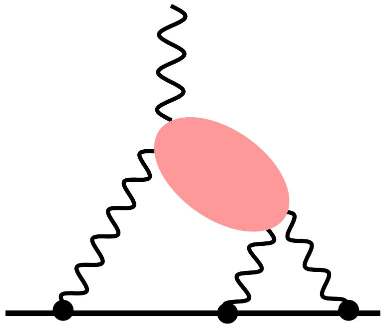

$$a_\mu^{\mathrm{HLbL}}(\text{phenomenology + lattice QCD}) + a_\mu^{\mathrm{HLbL,\,NLO}} = 92(18) \times 10^{-11}$$

- Data-driven and lattice QCD predictions are consistent

$\Longrightarrow$ 10% uncertainty feasible (by 2025) [Snowmass '21]

Contribution	PdRV(09) [471]	N/JN(09) [472, 573]	J(17) [27]	Our estimate
π^0, η, η'-poles	114(13)	99(16)	95.45(12.40)	93.8(4.0)
π, K-loops/boxes	−19(19)	−19(13)	−20(5)	−16.4(2)
S-wave $\pi\pi$ rescattering	−7(7)	−7(2)	−5.98(1.20)	−8(1)
subtotal	88(24)	73(21)	69.5(13.4)	69.4(4.1)
scalars	–	–	–	} − 1(3)
tensors	–	–	1.1(1)	
axial vectors	15(10)	22(5)	7.55(2.71)	6(6)
u, d, s-loops / short-distance	–	21(3)	20(4)	15(10)
c-loop	2.3	–	2.3(2)	3(1)
total	105(26)	116(39)	100.4(28.2)	92(19)

Bastian Kubis
(g-2 school 2021)

Table 15: Comparison of two frequently used compilations for HLbL in units of 10^{-11} from 2009 and a recent update with our estimate. PdRV = Prades, de Rafael, Vainshtein ("Glasgow consensus"); N/JN = Nyffeler / Jegerlehner, Nyffeler; J = Jegerlehner.

HLBL SUMMARY

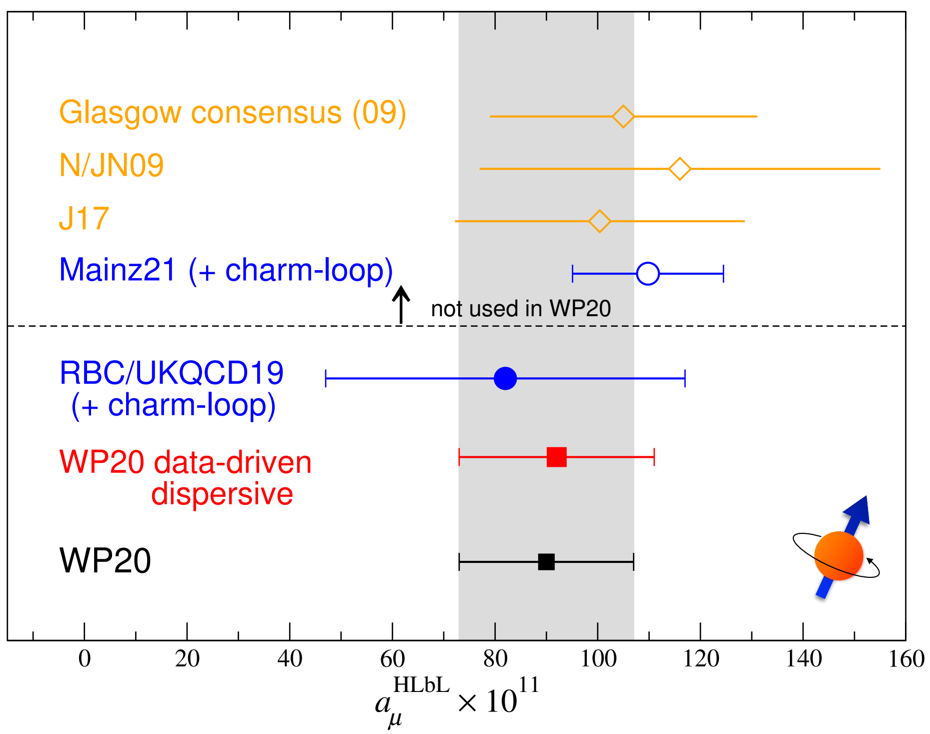

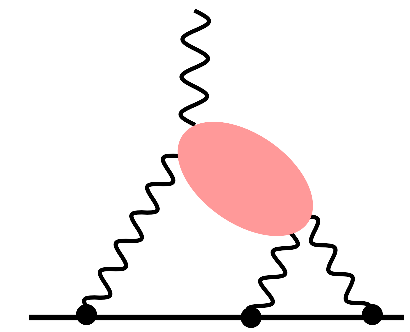

$$a_\mu^{\text{HLbL}}(\text{phenomenology + lattice QCD}) + a_\mu^{\text{HLbL, NLO}} = 92(18) \times 10^{-11}$$

- Data-driven and lattice QCD predictions are consistent

$\Longrightarrow$ 10% uncertainty feasible (by 2025) [Snowmass '21]

Contribution	PdRV(09) [471]	N/JN(09) [472, 573]	J(17) [27]	Our estimate
π^0, η, η'-poles	114(13)	99(16)	95.45(12.40)	93.8(4.0)
π, K-loops/boxes	−19(19)	−19(13)	−20(5)	−16.4(2)
S-wave $\pi\pi$ rescattering	−7(7)	−7(2)	−5.98(1.20)	−8(1)
subtotal	88(24)	73(21)	69.5(13.4)	69.4(4.1)
scalars	–	–	–	− 1(3)
tensors	–	–	1.1(1)	
axial vectors	15(10)	22(5)	7.55(2.71)	6(6)
u, d, s-loops / short-distance	–	21(3)	20(4)	15(10)
c-loop	2.3	–	2.3(2)	3(1)
total	105(26)	116(39)	100.4(28.2)	92(19)

Table 15: Comparison of two frequently used compilations for HLbL in units of 10^{-11} from 2009 and a recent update with our estimate. PdRV = Prades, de Rafael, Vainshtein ("Glasgow consensus"); N/JN = Nyffeler / Jegerlehner, Nyffeler; J = Jegerlehner.

Bastian Kubis
(g-2 school 2021)

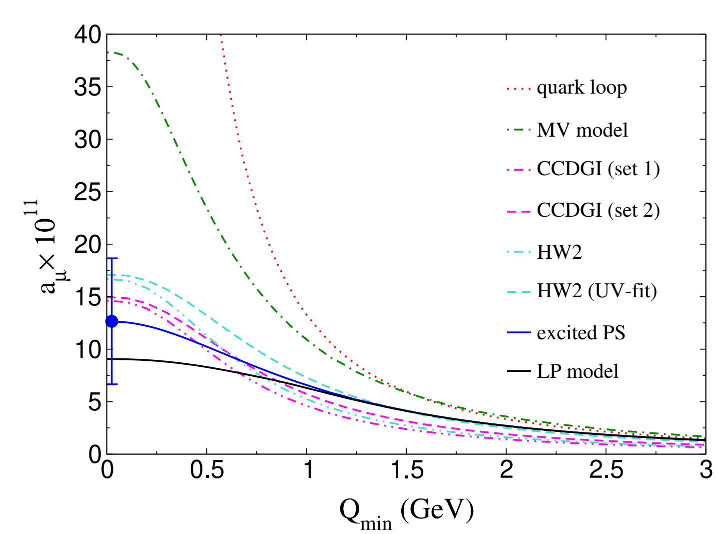

HADRONIC CORRECTIONS

- Low-energy observables measured to high precision provide stringent tests of the Standard Model (SM) of particle physics

HADRONIC CORRECTIONS

- Low-energy observables measured to high precision provide stringent tests of the Standard Model (SM) of particle physics
- Uncertainty of the SM prediction is dominated by hadronic corrections
- QCD is non-perturbative at low energies, therefore we use dispersion relations, lattice QCD and effective field theories

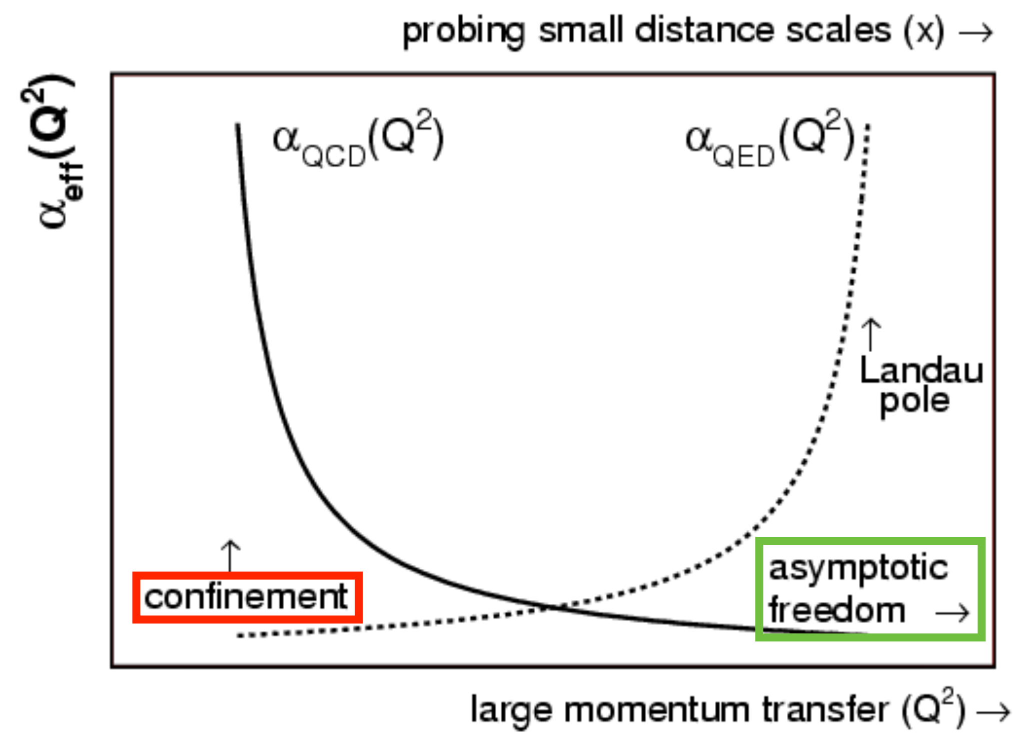

HADRONIC CORRECTIONS

- Low-energy observables measured to high precision provide stringent tests of the Standard Model (SM) of particle physics
- Uncertainty of the SM prediction is dominated by hadronic corrections
- QCD is non-perturbative at low energies, therefore we use dispersion relations, lattice QCD and effective field theories

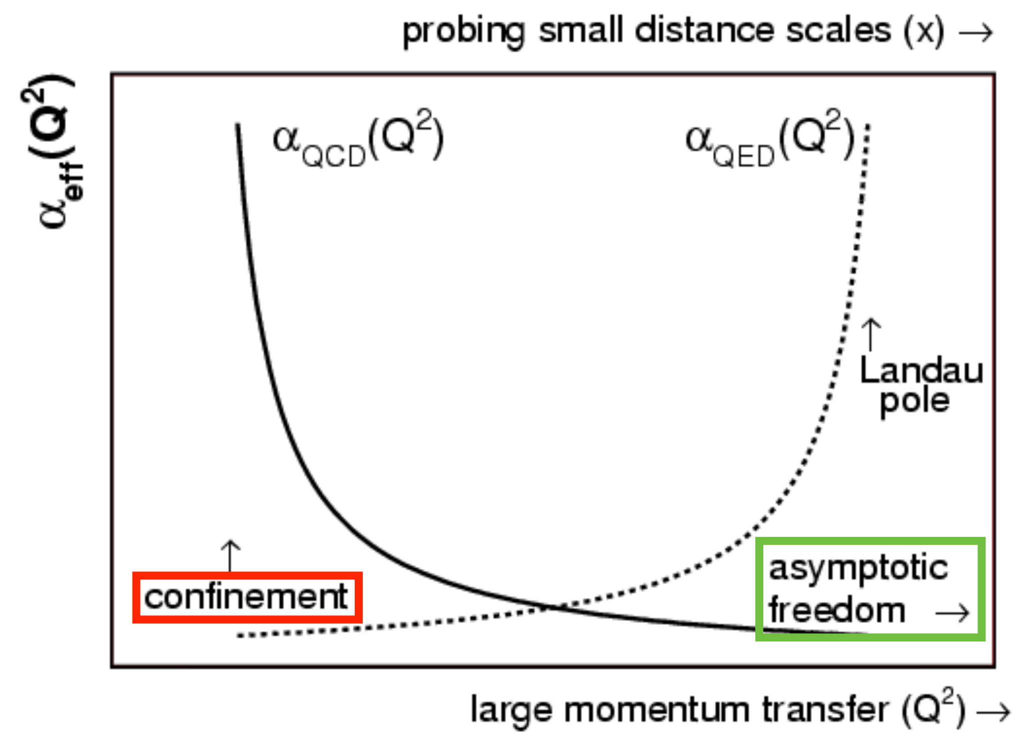

- Leading uncertainty presently comes from hadronic vacuum polarization
- Soon hadronic light-by-light scattering will be leading uncertainty

HADRONIC CORRECTIONS

- Low-energy observables measured to high precision provide stringent tests of the Standard Model (SM) of particle physics
- Uncertainty of the SM prediction is dominated by hadronic corrections
- QCD is non-perturbative at low energies, therefore we use dispersion relations, lattice QCD and effective field theories

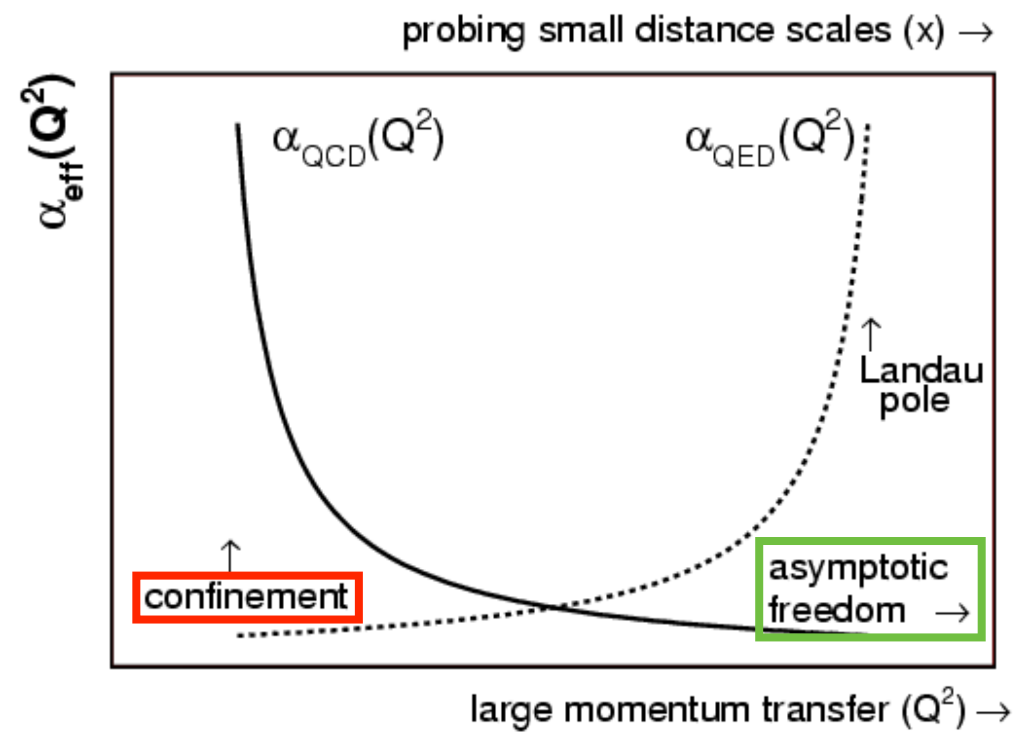

- Leading uncertainty presently comes from hadronic vacuum polarization
- Soon hadronic light-by-light scattering will be leading uncertainty
- Pseudoscalar-pole contributions are the leading HLbL contributions:
  $a_\mu^{\rm PS} = 93.8(4.0) \times 10^{-11}$

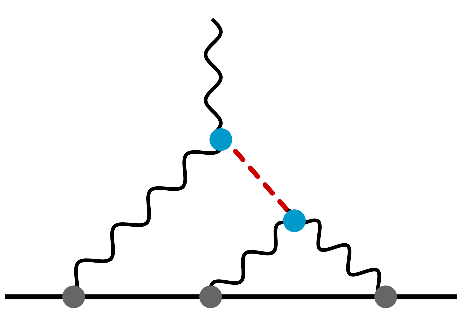

HADRONIC CORRECTIONS

- Low-energy observables measured to high precision provide stringent tests of the Standard Model (SM) of particle physics

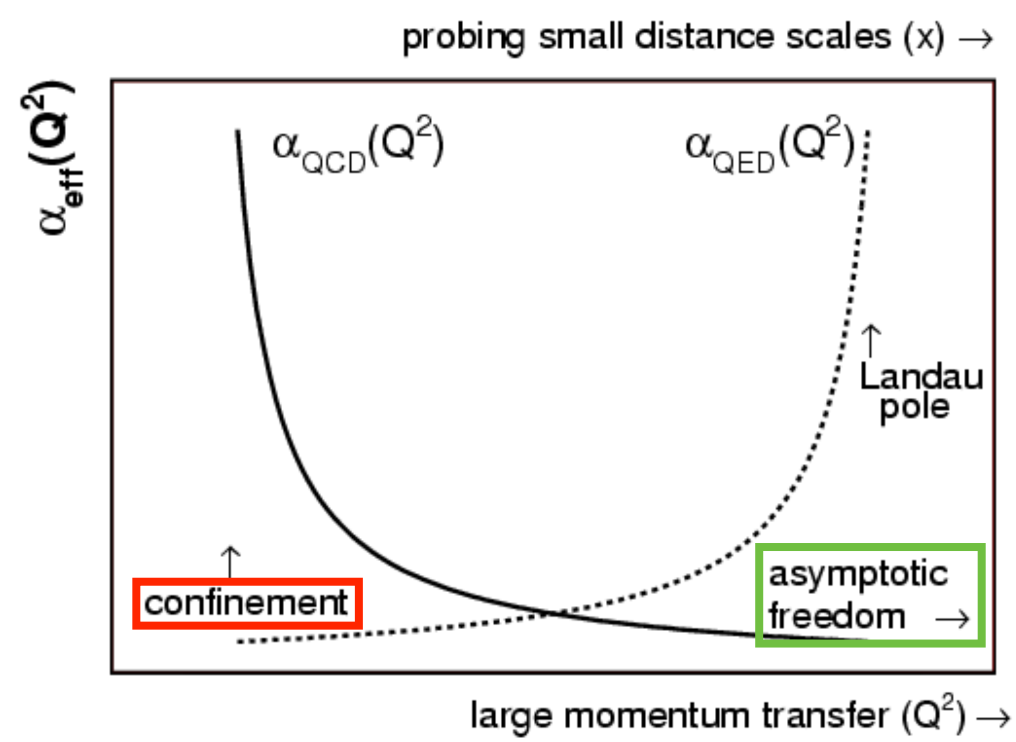

- Uncertainty of the SM prediction is dominated by hadronic corrections
- QCD is non-perturbative at low energies, therefore we use dispersion relations, lattice QCD and effective field theories
- Leading uncertainty presently comes from hadronic vacuum polarization
- Soon hadronic light-by-light scattering will be leading uncertainty
- Pseudoscalar-pole contributions are the leading HLbL contributions: $a_\mu^{\mathrm{PS}} = 93.8(4.0) \times 10^{-11}$

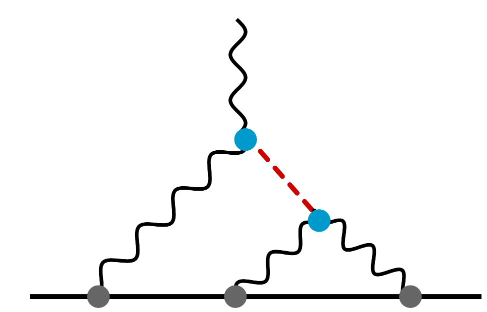

- Short-distance constraints are important for a model-independent evaluation, because mixed- and high-energy regions cannot be constrained from data

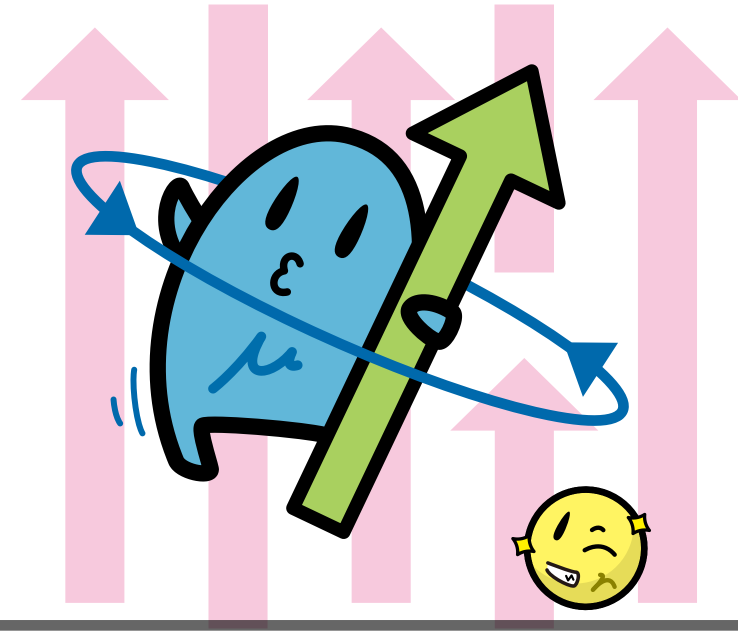

— Short Recap —

Hadronic Vacuum Polarization Phenomenology

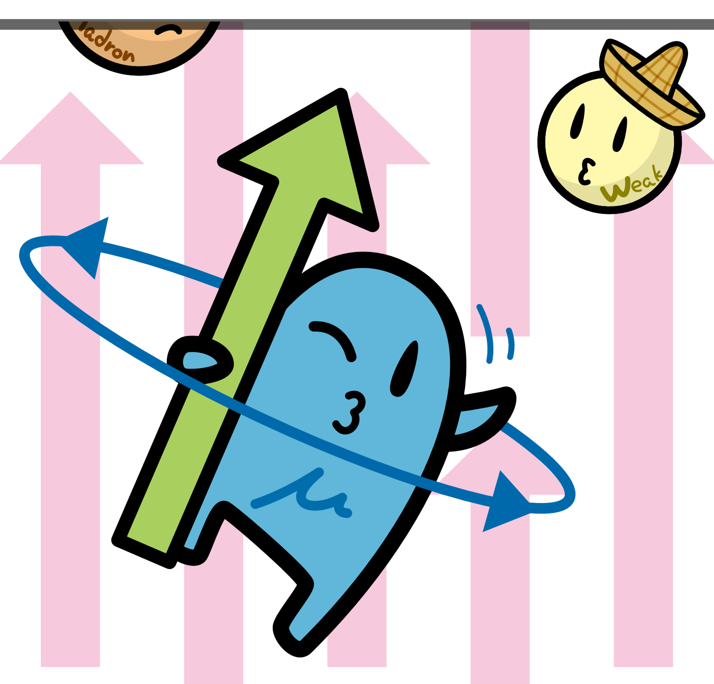

VACUUM POLARIZATION

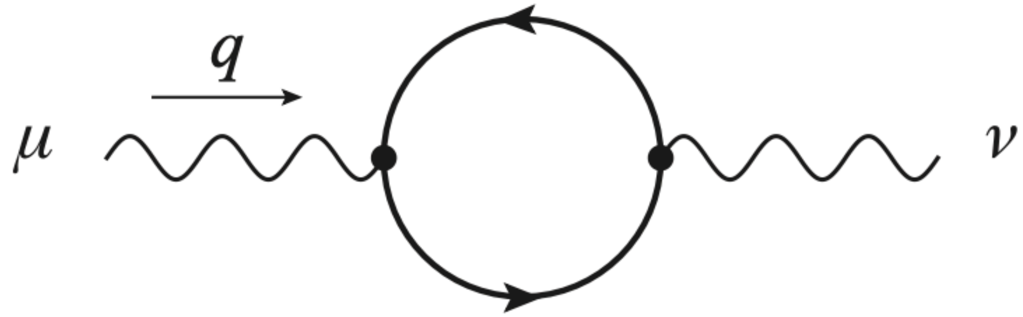

- E.m. gauge invariance $q_\mu \Pi^{\mu\nu} = 0,\ q_\nu \Pi^{\mu\nu} = 0$
  → only one scalar amplitude $\Pi^{\mu\nu}(q) = \left[q^2 g^{\mu\nu} - q^\mu q^\nu\right] \Pi(q^2)$

VACUUM POLARIZATION

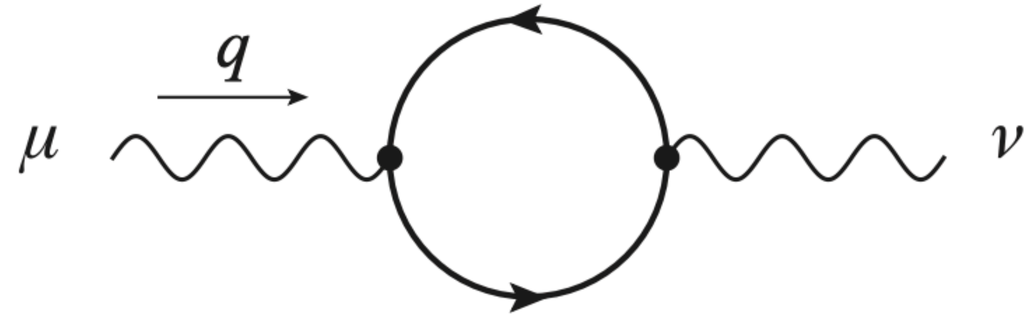

- E.m. gauge invariance $q_\mu \Pi^{\mu\nu} = 0,\ q_\nu \Pi^{\mu\nu} = 0$
  → only one scalar amplitude $\Pi^{\mu\nu}(q) = \left[q^2 g^{\mu\nu} - q^\mu q^\nu\right] \Pi(q^2)$

- Dressed photon propagator as Dyson series of self–energy insertions:

$$\tilde{\Delta}_{\mu\nu}(q) = \Delta_{\mu\nu}(q) + \Delta_{\mu\rho}(q) i \Pi^{\rho\sigma} \Delta_{\sigma\nu}(q) + \ldots = \frac{\Delta_{\mu\nu}(q)}{1 - \Pi(q^2)} \overset{q^2 \to 0}{=} \Delta_{\mu\nu}(q)$$

- Analyticity in the $s = q^2$ plane allows to write a once-subtracted dispersion relation (Cauchy's theorem):

$$\Pi(s) - \Pi(0) = \frac{s}{\pi} \int_{s_0}^{\infty} ds' \frac{\mathrm{Im}\, \Pi(s')}{s'(s' - s)}$$

DISPERSION RELATION

- Cauchy integral formula $f(z) = \frac{1}{2\pi i} \oint_{\mathscr{C}} \mathrm{d}\zeta \frac{f(\zeta)}{\zeta - z} = I_R(z) + I_+(z) + I_-(z) + I_r(z)$

  with closed contour $\mathscr{C}$ inside analyticity domain avoiding branch cut on real axis:

  - $I_R(z) = \frac{1}{2\pi} \int_a^{2\pi - a} \mathrm{d}\phi \, e^{i\phi} \frac{f(Re^{i\phi})}{e^{i\phi} - z/R} \overset{R\to\infty}{=} 0$
  - $I_r(z) = -\frac{r}{2\pi} \int_{\pi/2}^{3\pi/2} \mathrm{d}\phi \, e^{i\phi} \frac{f(\omega_0 + re^{i\phi})}{\omega_0 + re^{i\phi} - z} \overset{r\to 0}{=} 0$
  - $I_\pm(z) = \pm \frac{1}{2\pi i} \int_{\omega_0}^{R} \mathrm{d}\zeta \frac{f(\zeta \pm ir)}{\zeta \pm ir - z}$

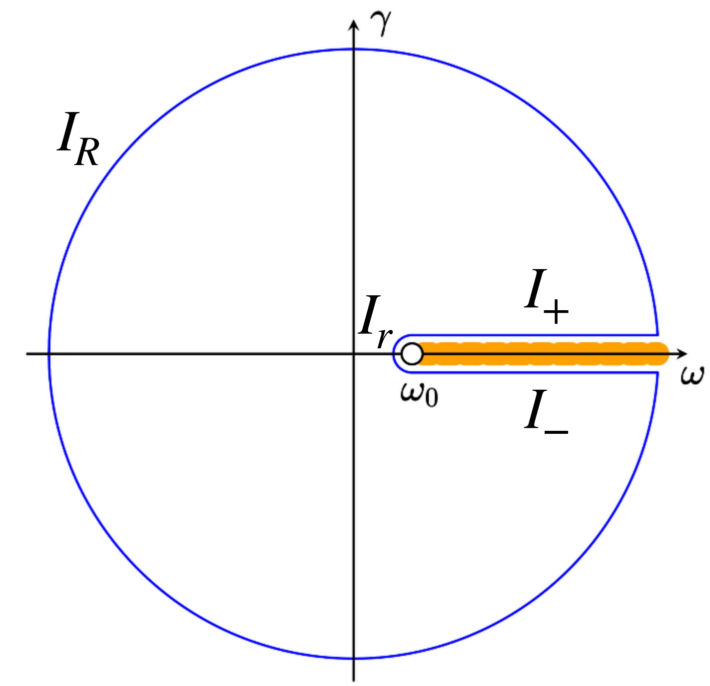

Figure 2.1. Analytic structure of a typical amplitude $f(z)$, with $z = \omega + i\gamma$, exhibiting a branch cut starting at ω_0. Enclosed in the contour is the domain of analyticity.

DISPERSION RELATION

- Cauchy integral formula $f(z) = \dfrac{1}{2\pi i} \oint_{\mathscr{C}} \mathrm{d}\zeta \, \dfrac{f(\zeta)}{\zeta - z} = I_R(z) + I_+(z) + I_-(z) + I_r(z)$

  with closed contour $\mathscr{C}$ inside analyticity domain avoiding branch cut on real axis:

  - $$I_R(z) = \frac{1}{2\pi} \int_a^{2\pi - a} \mathrm{d}\phi \, e^{i\phi} \frac{f(Re^{i\phi})}{e^{i\phi} - z/R} \overset{R\to\infty}{=} 0$$
  - $$I_r(z) = -\frac{r}{2\pi} \int_{\pi/2}^{3\pi/2} \mathrm{d}\phi \, e^{i\phi} \frac{f(\omega_0 + re^{i\phi})}{\omega_0 + re^{i\phi} - z} \overset{r\to 0}{=} 0$$
  - $$I_\pm(z) = \pm \frac{1}{2\pi i} \int_{\omega_0}^{R} \mathrm{d}\zeta \, \frac{f(\zeta \pm ir)}{\zeta \pm ir - z}$$

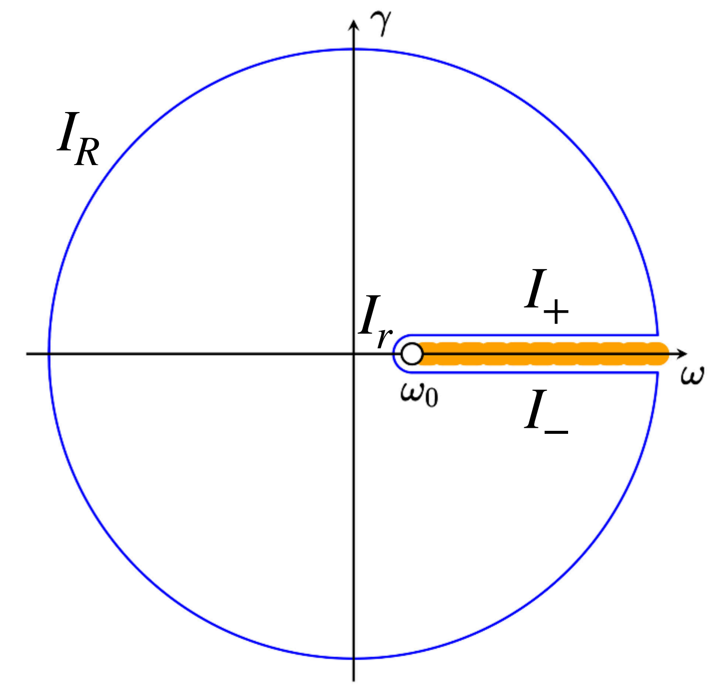

Figure 2.1. Analytic structure of a typical amplitude $f(z)$, with $z = \omega + i\gamma$, exhibiting a branch cut starting at ω_0. Enclosed in the contour is the domain of analyticity.

- Applying Schwarz reflection principle: $f^*(z) = f(z^*)$

$$f(z) = \lim_{r\to 0} \frac{1}{2\pi i} \int_{\omega_0}^{\infty} \mathrm{d}\zeta \left[\frac{f(\zeta + ir)}{\zeta + ir - z} - \frac{f^+(\zeta + ir)}{\zeta - ir - z} \right] = \frac{1}{\pi} \int_{\omega_0}^{\infty} \mathrm{d}\zeta \, \frac{\mathrm{Im}\, f(\zeta)}{\zeta - z}$$

DISPERSION RELATION

- We can reconstruct the function in the entire complex plane from an integral of its imaginary part associated with the branch cut(s):

$$\mathrm{Re}\,f(\omega) = \lim_{\gamma\to 0}\frac{1}{\pi}\int_{\omega_0}^{\infty}\mathrm{d}\zeta\,\frac{(\zeta-\omega)f(\zeta)}{(\zeta-\omega)^2+\gamma^2} = \frac{1}{\pi}\mathscr{P}\int_{\omega_0}^{\infty}\mathrm{d}\zeta\,\frac{\mathrm{Im}\,f(\zeta)}{\zeta-\omega}$$

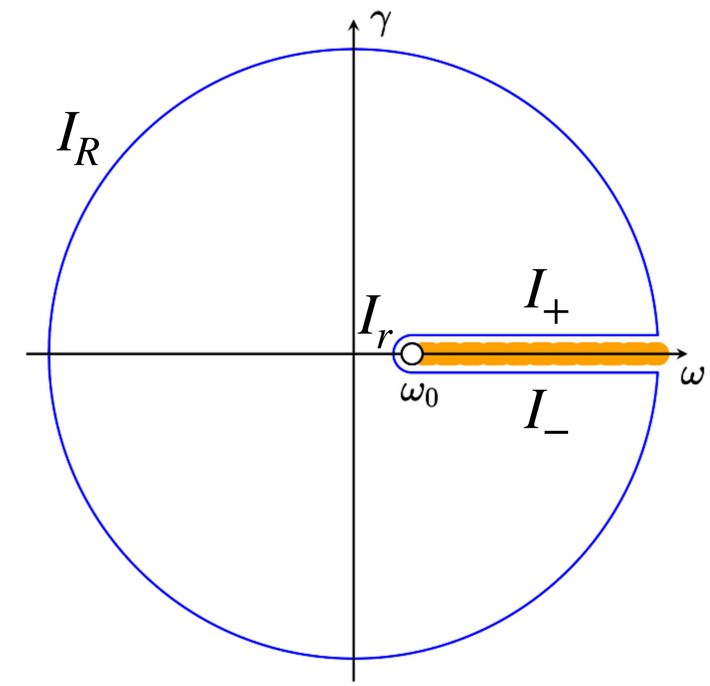

Figure 2.1. Analytic structure of a typical amplitude $f(z)$, with $z = \omega + i\gamma$, exhibiting a branch cut starting at ω_0. Enclosed in the contour is the domain of analyticity.

DISPERSION RELATION

- We can reconstruct the function in the entire complex plane from an integral of its imaginary part associated with the branch cut(s):

$$\mathrm{Re}\, f(\omega) = \lim_{\gamma\to 0} \frac{1}{\pi} \int_{\omega_0}^{\infty} \mathrm{d}\zeta \, \frac{(\zeta-\omega) f(\zeta)}{(\zeta-\omega)^2+\gamma^2} = \frac{1}{\pi} \mathscr{P} \int_{\omega_0}^{\infty} \mathrm{d}\zeta \, \frac{\mathrm{Im}\, f(\zeta)}{\zeta-\omega}$$

$$\mathrm{Im}\, f(\omega+i\gamma) = \frac{1}{\pi} \int_{\omega_0}^{\infty} \mathrm{d}\zeta \, \frac{\gamma\, \mathrm{Im} f(\zeta)}{(\zeta-\omega)^2+\gamma^2}$$

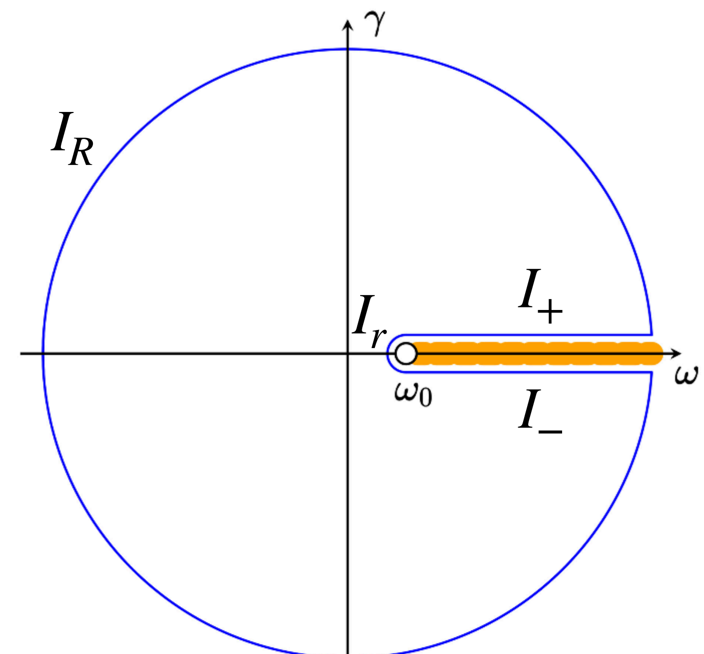

Figure 2.1. Analytic structure of a typical amplitude $f(z)$, with $z = \omega + i\gamma$, exhibiting a branch cut starting at ω_0. Enclosed in the contour is the domain of analyticity.

HADRONIC INTERMEDIATE STATES

- Unitarity (optical theorem) relates discontinuity across the branch cut to experimental observable:

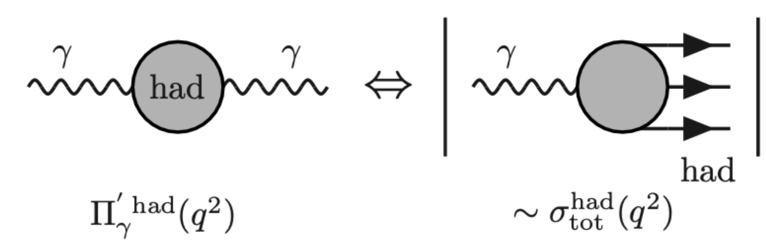

$$\mathrm{Im}\,\Pi_{\mathrm{had}}(s) = -\frac{\alpha}{3s}\sigma_{\mathrm{e^+e^-\to had}}(s) = \mathrm{Im}\,\Pi_{\mu^+\mu^-}(s)\,R_\gamma^{\mathrm{had}}(s)$$

with $R_\gamma^{\mathrm{had}}(s) = \dfrac{\sigma_{e^+e^-\to\gamma^*\to\mathrm{had}}}{\sigma_{e^+e^-\to\gamma^*\to\mu^+\mu^-}}$ where the QED part can be calculated exactly

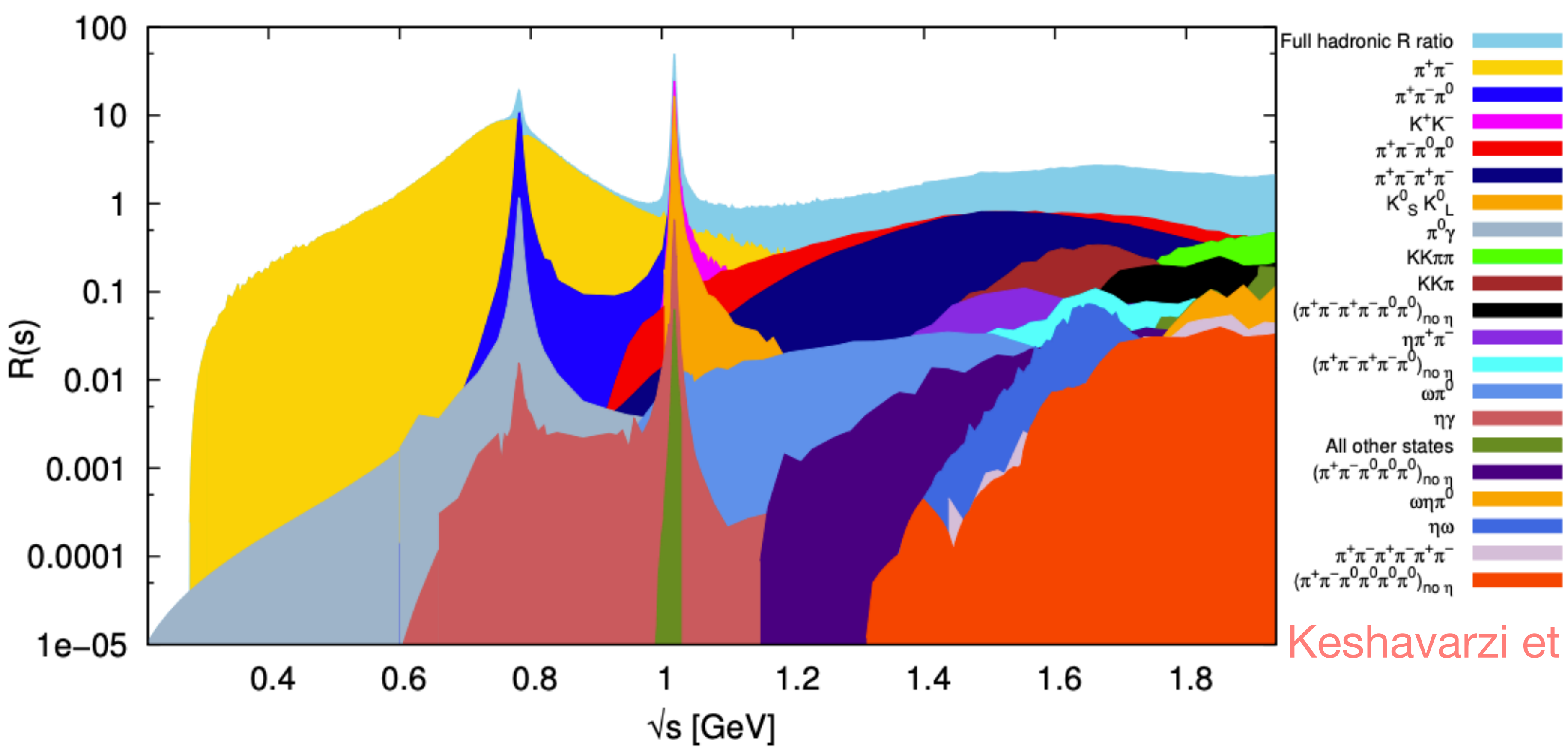

Keshavarzi et al. (2018)

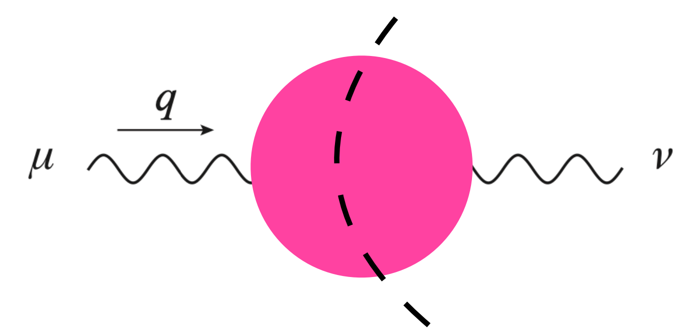

DATA-DRIVEN DISPERSIVE APPROACH TO HVP

$$\boxed{a^{\mathrm{HVP}} = \frac{\alpha^2}{3\pi^2}\int_{m_\pi^2}^{\infty} \mathrm{d}s\, \frac{R_\gamma^{\mathrm{had}}(s)\, K(s/m^2)}{s}}$$

$$K(s/m^2) = \int_0^1 \mathrm{d}x\, \frac{x^2(1-x)}{x^2 + (1-x)\, s/m^2}$$

$$R_\gamma^{\mathrm{had}}(s) = \frac{\sigma(e^+e^- \to \gamma^* \to \text{hadrons})}{\sigma(e^+e^- \to \gamma^* \to \mu^+\mu^-)}$$

HVP

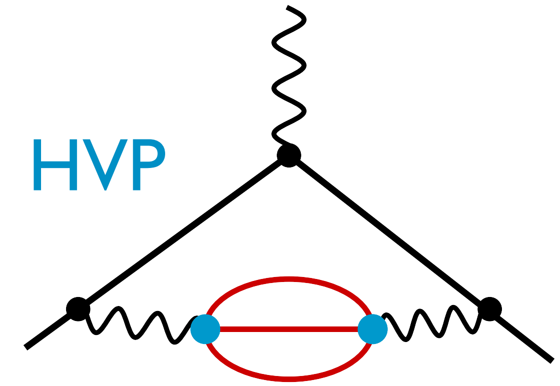

- HVP is calculated with a simple data-driven dispersive approach:
  - No conceptual problems
  - Systematic improvements possible
  - Tensions in data-base, in particular, $\pi^+\pi^-$channel (cf. CMD-3, KLOE vs. BaBar)

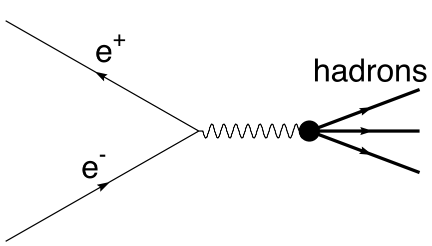

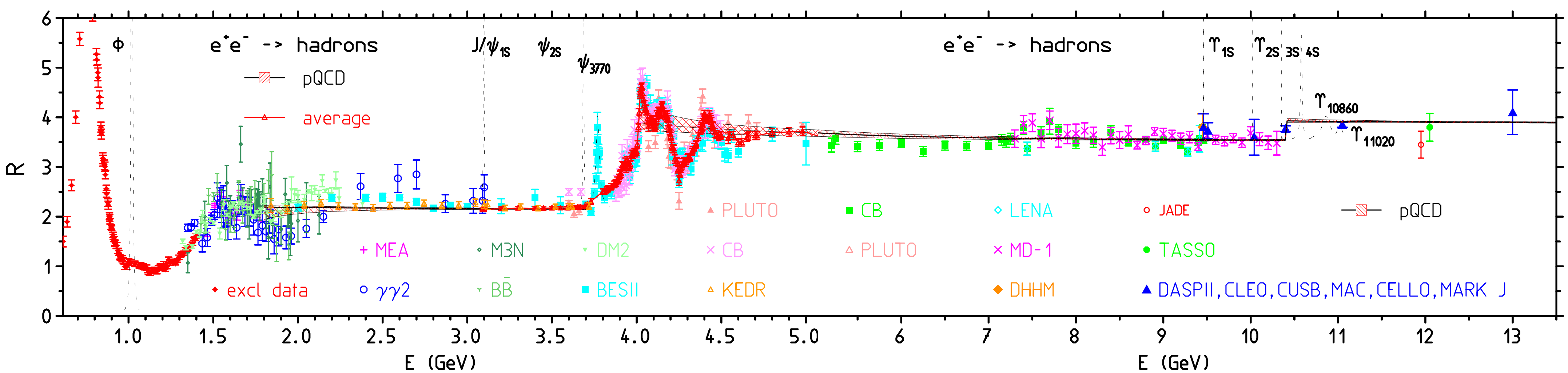

F. Jegerlehner, Springer Tracts Mod. Phys. 274 (2017)

M. Davier, Nucl. Part. Phys. Proc. 287-288, 70 (2017)

DATA-DRIVEN DISPERSIVE APPROACH TO HVP

	Ref. [21]	Ref. [22]	Difference
$\pi^+\pi^-$	507.85(0.83)(3.23)(0.55)	504.23(1.90)	3.62
$\pi^+\pi^-\pi^0$	46.21(0.40)(1.10)(0.86)	46.63(94)	−0.42
$\pi^+\pi^-\pi^+\pi^-$	13.68(0.03)(0.27)(0.14)	13.99(19)	−0.31
$\pi^+\pi^-\pi^0\pi^0$	18.03(0.06)(0.48)(0.26)	18.15(74)	−0.12
K^+K^-	23.08(0.20)(0.33)(0.21)	23.00(22)	0.08
K_SK_L	12.82(0.06)(0.18)(0.15)	13.04(19)	−0.22
$\pi^0\gamma$	4.41(0.06)(0.04)(0.07)	4.58(10)	−0.17
Sum of the above	626.08(0.95)(3.48)(1.47)	623.62(2.27)	2.46
$[1.8, 3.7]$ GeV (without $c\bar{c}$)	33.45(71)	34.45(56)	−1.00
J/ψ, $\psi(2S)$	7.76(12)	7.84(19)	−0.08
$[3.7, \infty)$ GeV	17.15(31)	16.95(19)	0.20
Total $a_\mu^{\text{HVP, LO}}$	$694.0(1.0)(3.5)(1.6)(0.1)_\psi(0.7)_{\text{DV+QCD}}$	692.8(2.4)	1.2

Table 2: Comparison of selected exclusive-mode contributions to $a_\mu^{\text{HVP, LO}}$ from Refs. [21, 22], for the energy range ≤ 1.8 GeV, in units of 10^{-10}, see Ref. [6] for details.

Strong weight at the low-energy part:
>70% from $\pi^+\pi^-[\rho(770)]$ channel

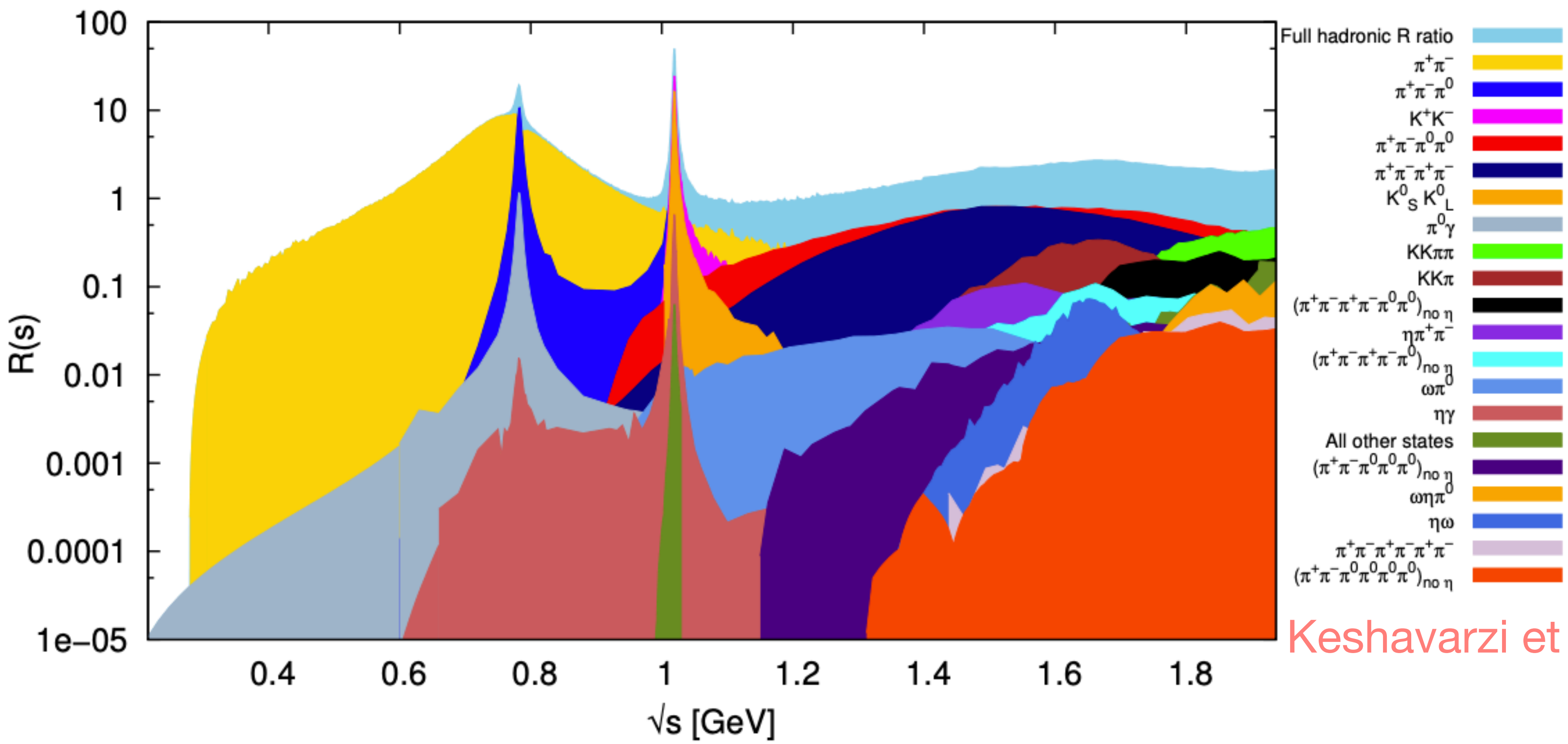

Keshavarzi et al. (2018)

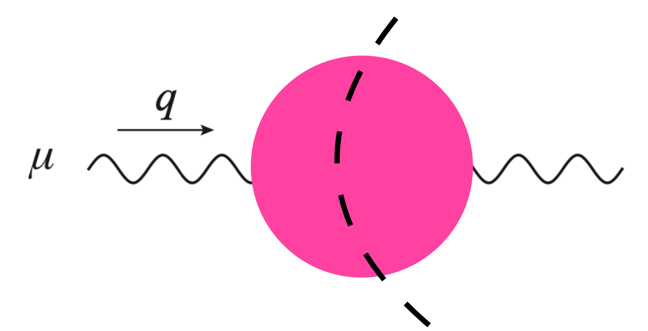

DISPERSIVE APPROACH TO HLBL

dispersive formula for the e.m. vertex function:

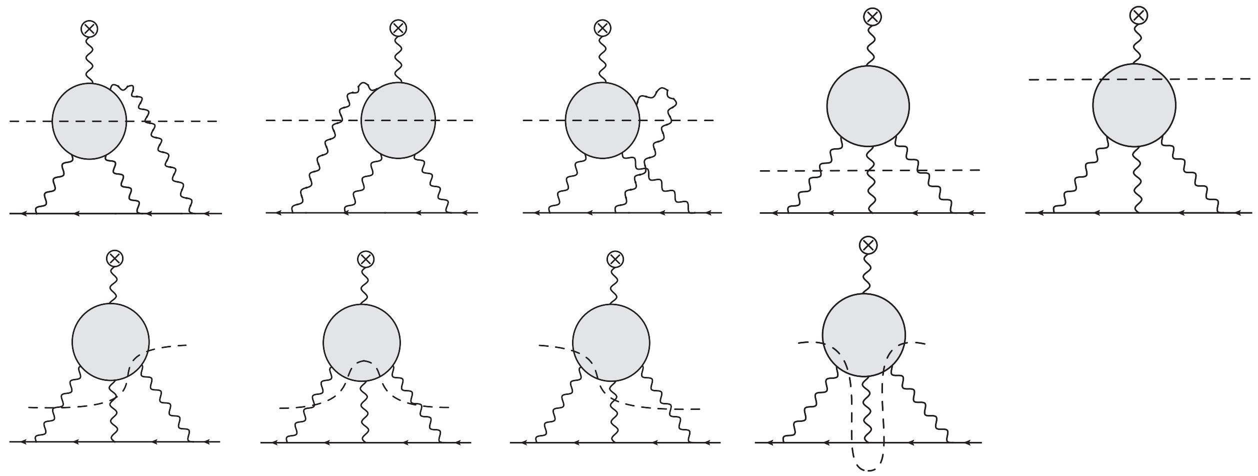

V. Pauk and M. Vanderhaeghen, Phys. Rev. D 90, 113012 (2014)

HLBL is more complicated than HVP!

DISPERSIVE APPROACH TO HLBL

dispersive formula for the e.m. vertex function:

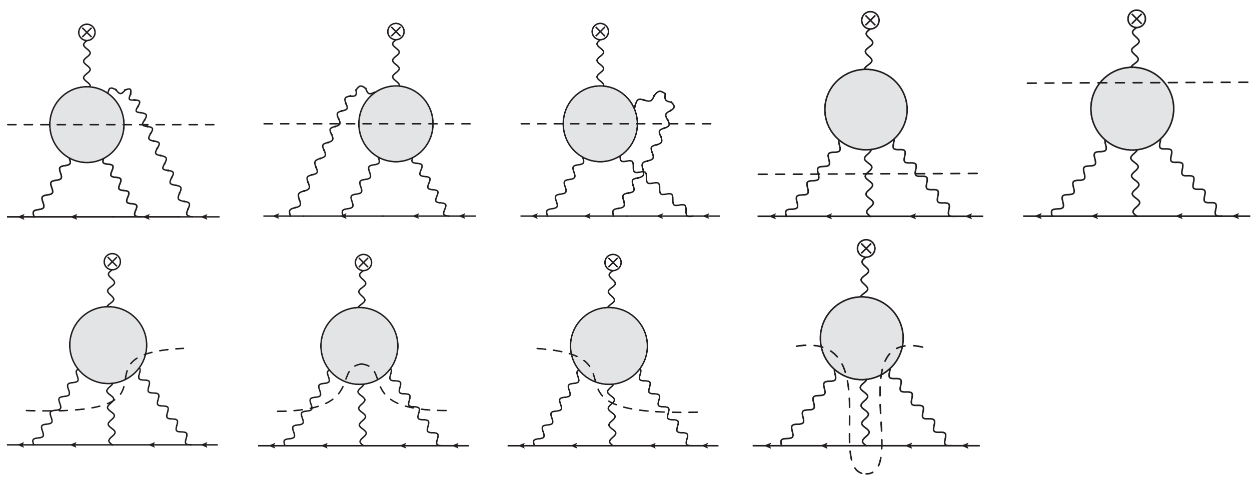

V. Pauk and M. Vanderhaeghen, Phys. Rev. D 90, 113012 (2014)

HLBL is more complicated than HVP!

dispersive formula for the
light-by-light scattering amplitude:

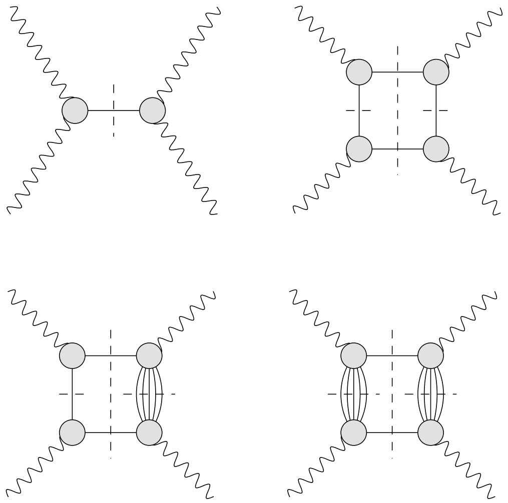

G. Colangelo, et al., JHEP 1509 (2015) 074

DISPERSIVE APPROACH TO HLBL

dispersive formula for the e.m. vertex function:

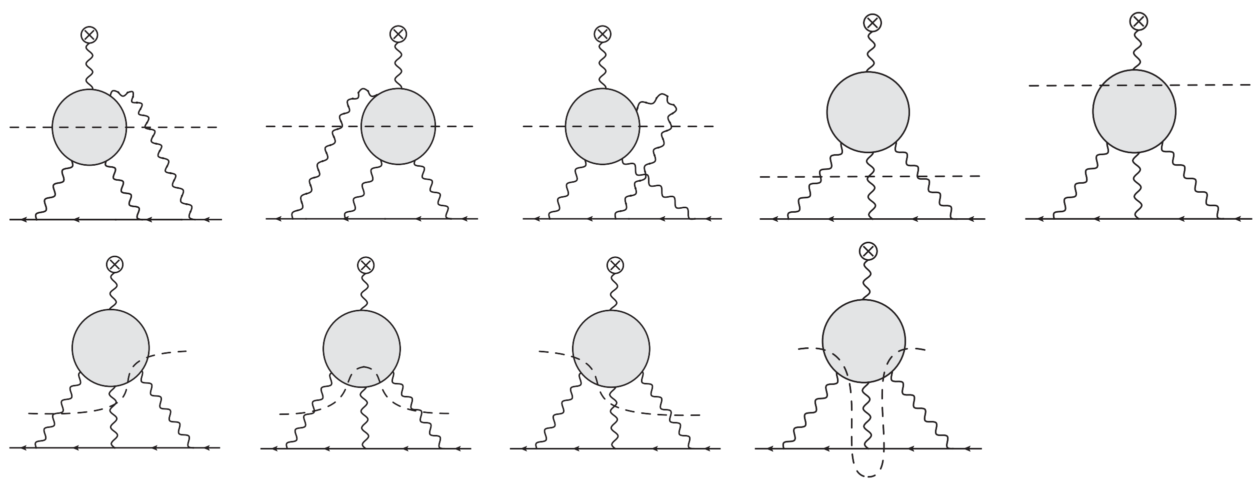

V. Pauk and M. Vanderhaeghen, Phys. Rev. D 90, 113012 (2014)

HLBL is more complicated than HVP!

dispersive formula for the
light-by-light scattering amplitude:

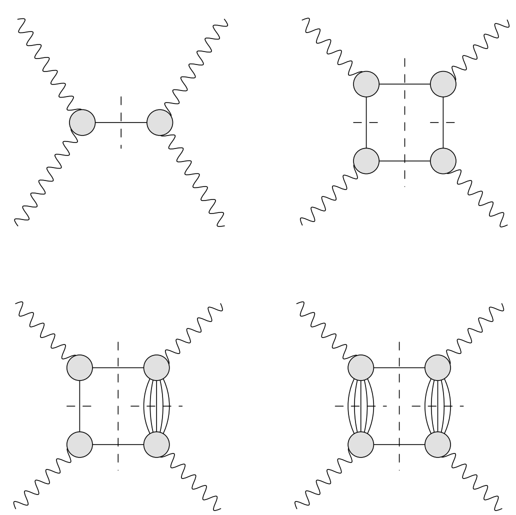

G. Colangelo, et al., JHEP 1509 (2015) 074

Is there an exact dispersive formula which needs simple experimental input and treats HLbL (and everything else) in the same way as HVP?

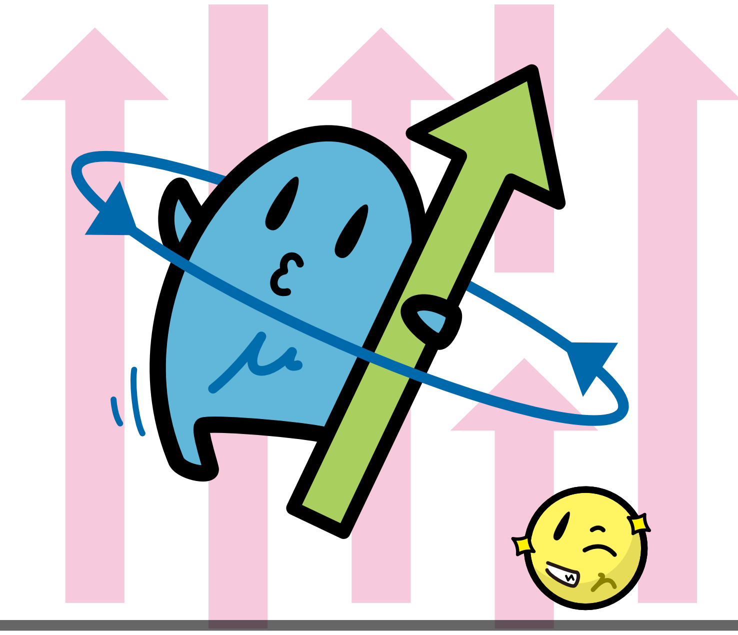

Schwinger Sum Rule

— One Rule To Rule Them All —

QED & QCD

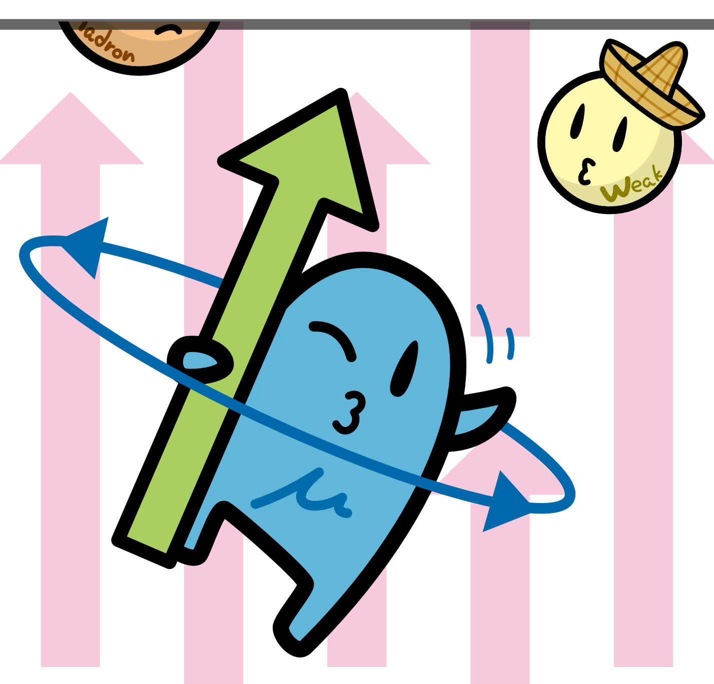

SUM RULES

- Forward Compton scattering sum rules:

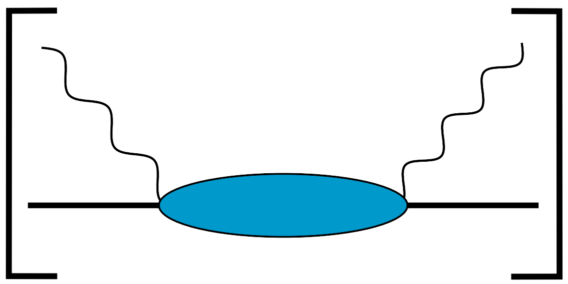

$$(\nu, Q^2) = \frac{2}{\pi}\int_{\nu_0}^{\infty} \mathrm{d}\nu' \frac{\nu'}{\nu'^2 - \nu^2}$$

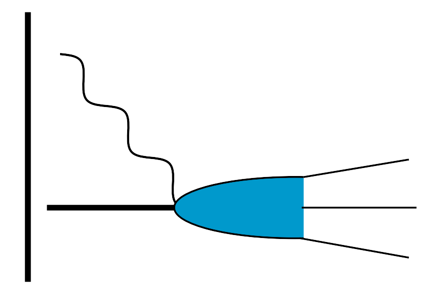

$^2 (\nu', Q^2)$

CS amplitudes

photoabsorption cross section

- Sum rules are model-independent relations based on very general principles:
  - Dispersion relation (analyticity/causality): $f(z) = \frac{1}{\pi}\int_{\omega_0}^{\infty} \mathrm{d}\zeta \frac{\mathrm{Im} f(\zeta)}{\zeta - z}$
  - Optical theorem (unitarity): Im 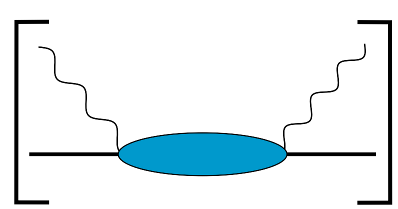 $\propto$ 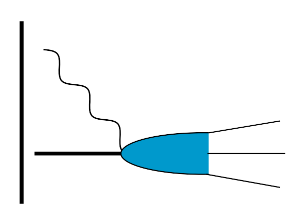 ^{2}
  - Crossing symmetry
  - Low-energy expansion: charge, anomalous magnetic moment, polarizabilities, …

OPTICAL THEOREM

- Scattering matrix $\mathscr{S} = 1 + i\mathscr{T}$ transforms asymptotic initial into final states (well-separated, non-interacting, free particles):

$$_{out}\langle \boldsymbol{p}_1'\boldsymbol{p}_2'\cdots | \boldsymbol{p}_1\boldsymbol{p}_2\rangle_{in} = \langle \boldsymbol{p}_1'\boldsymbol{p}_2'\cdots | \mathscr{S} | \boldsymbol{p}_1\boldsymbol{p}_2\rangle$$

- Scattering amplitude:

$$\langle \boldsymbol{p}_1'\boldsymbol{p}_2'\cdots | \mathscr{T} | \boldsymbol{p}_1\boldsymbol{p}_2\rangle = (2\pi)^4\,\delta^{(4)}\left(p_1 + p_2 - p_1' - p_2' - \cdots\right)\mathscr{A}\left(p_1, p_2 \to p_1', p_2', \cdots\right)$$

- Unitarity relation: $\mathscr{S}\mathscr{S}^\dagger = 1 \quad \longrightarrow \quad i\left(\mathscr{T} - \mathscr{T}^\dagger\right) = -\,\mathscr{T}^\dagger\mathscr{T}$

- It follows: $i\left\langle \boldsymbol{p}_1'\boldsymbol{p}_2' \left| \mathscr{T} - \mathscr{T}^\dagger \right| \boldsymbol{p}_1\boldsymbol{p}_2\right\rangle = -\left\langle \boldsymbol{p}_1'\boldsymbol{p}_2' \left| \mathscr{T}^\dagger\mathscr{T} \right| \boldsymbol{p}_1\boldsymbol{p}_2\right\rangle$

- Forward limit: $\mathrm{Im}\mathscr{A}\left(p_1, p_2 \to p_1, p_2\right) \propto \sigma\left(p_1, p_2 \to \text{anything}\right)$

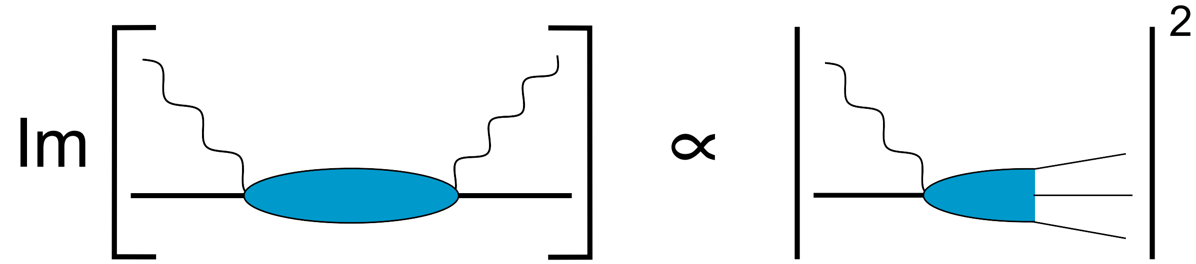

CROSSING SYMMETRY

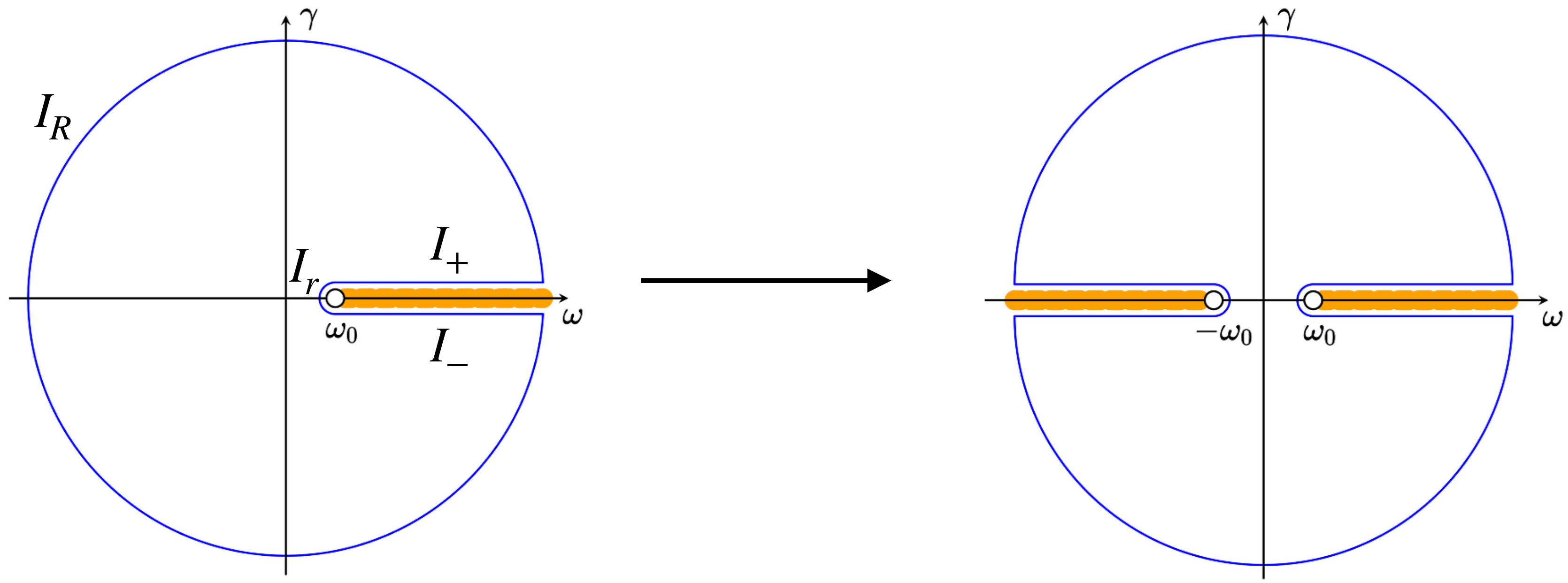

- Forward scattering, e.g. forward Compton or light-by-light scattering, should be invariant under the interchange of incident and outgoing particles
  - Crossing symmetry $f(-\omega) = \pm f(\omega)$
- Analytic structure is mirrored with respect to imaginary axis:

$$\mathrm{Re}\, f_{\mathrm{even}}(z) = \frac{2}{\pi} \int_{\omega_0}^{\infty} \mathrm{d}\zeta \, \frac{\zeta \, \mathrm{Im}\, f(\zeta)}{\zeta^2 - z^2}$$

$$\mathrm{Re}\, f_{\mathrm{odd}}(z) = \frac{2\omega}{\pi} \int_{\omega_0}^{\infty} \mathrm{d}\zeta \, \frac{\mathrm{Im}\, f(\zeta)}{\zeta^2 - z^2}$$

GERASIMOV DRELL HEARN SUM RULE

Gerasimov—Drell—Hearn sum rule

$$\boxed{I_{\mathrm{GDH}} = \frac{2\pi^2\alpha}{m^2}a^2 = -\,2\int_{\nu_0}^{\infty}\mathrm{d}\nu\,\frac{\sigma_{TT}(\nu)}{\nu}}$$

$a_p \approx 1.7929$ and
I_{GDH}= 204.784481 μb [CODATA]

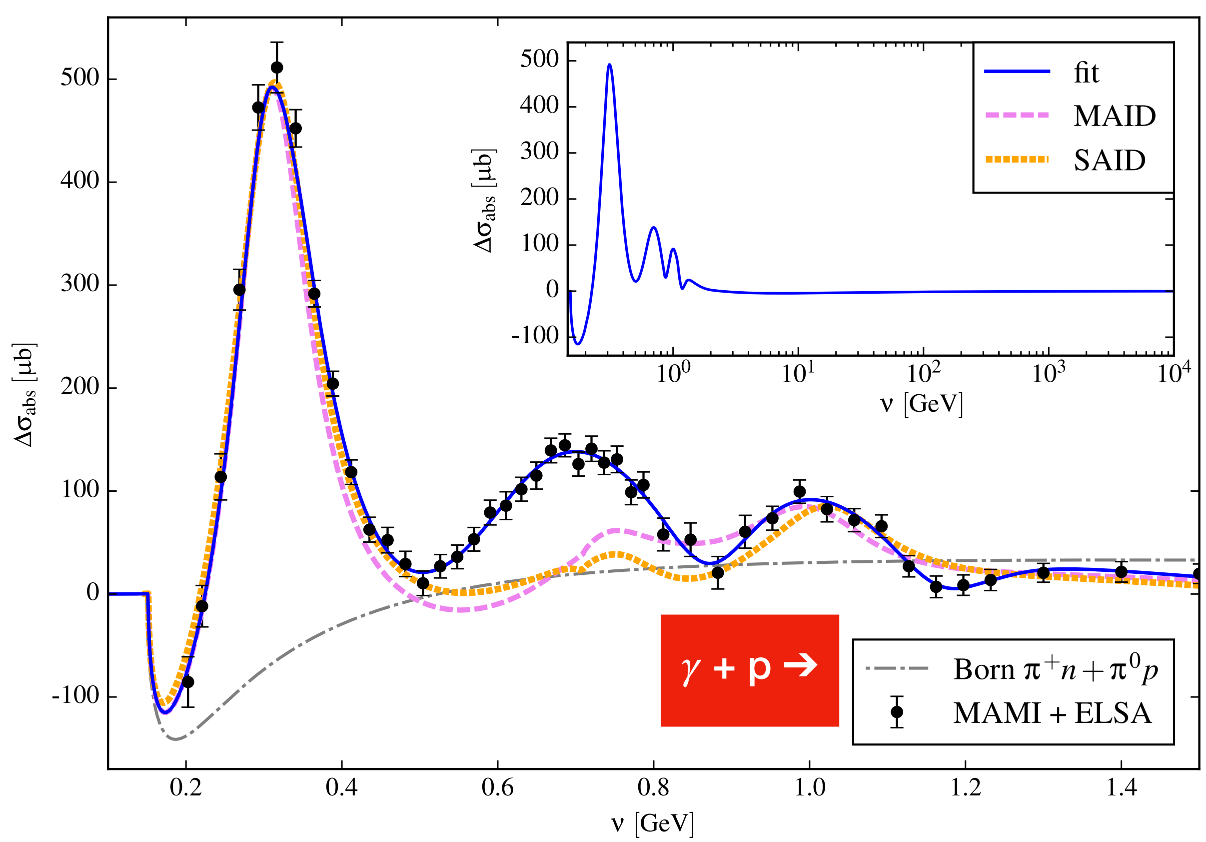

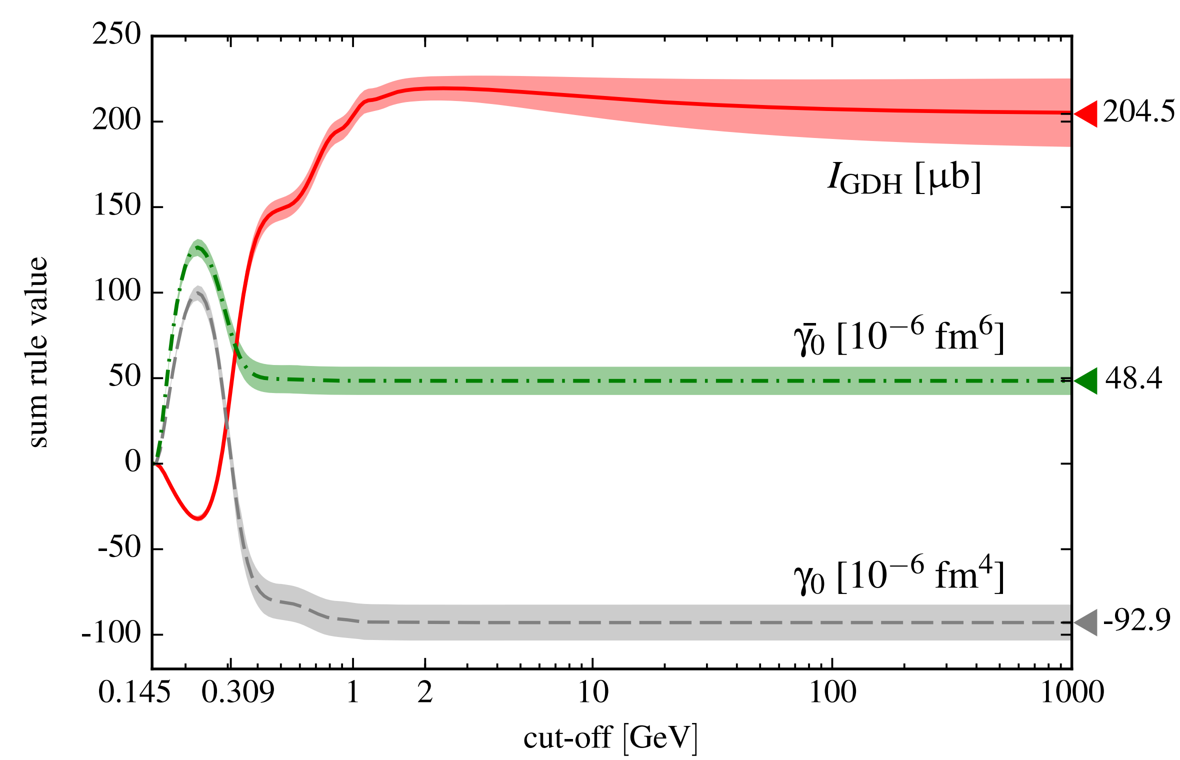

GERASIMOV DRELL HEARN SUM RULE

Gerasimov—Drell—Hearn sum rule

$$\boxed{I_{\text{GDH}} = \frac{2\pi^2\alpha}{m^2}a^2 = -2\int_{\nu_0}^{\infty} d\nu \frac{\sigma_{TT}(\nu)}{\nu}}$$

$a_\mu \approx 0.0011659209(6)$ [BNL]

$a_p \approx 1.7929$ and
$I_{\text{GDH}} = 204.784481\ \mu$b [CODATA]

- GDH sum rule for the muon:
  - Huge cancelation requires measurements with incredible accuracy
    - l.h.s.: HVP starts at $\mathcal{O}(\alpha^2)$, I_{GDH} starts at $\mathcal{O}(\alpha^5)$
    - r.h.s.: hadronic photo-production cross section starts at $\mathcal{O}(\alpha^3)$

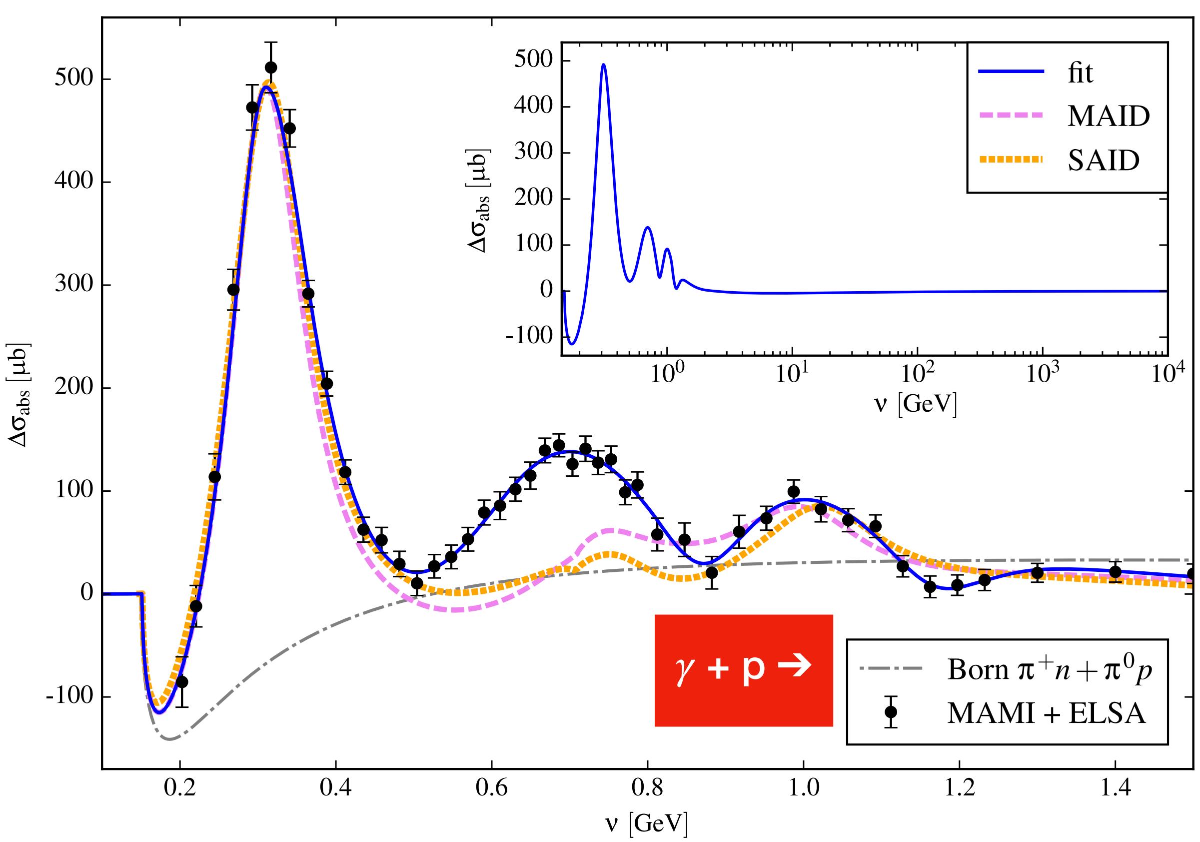

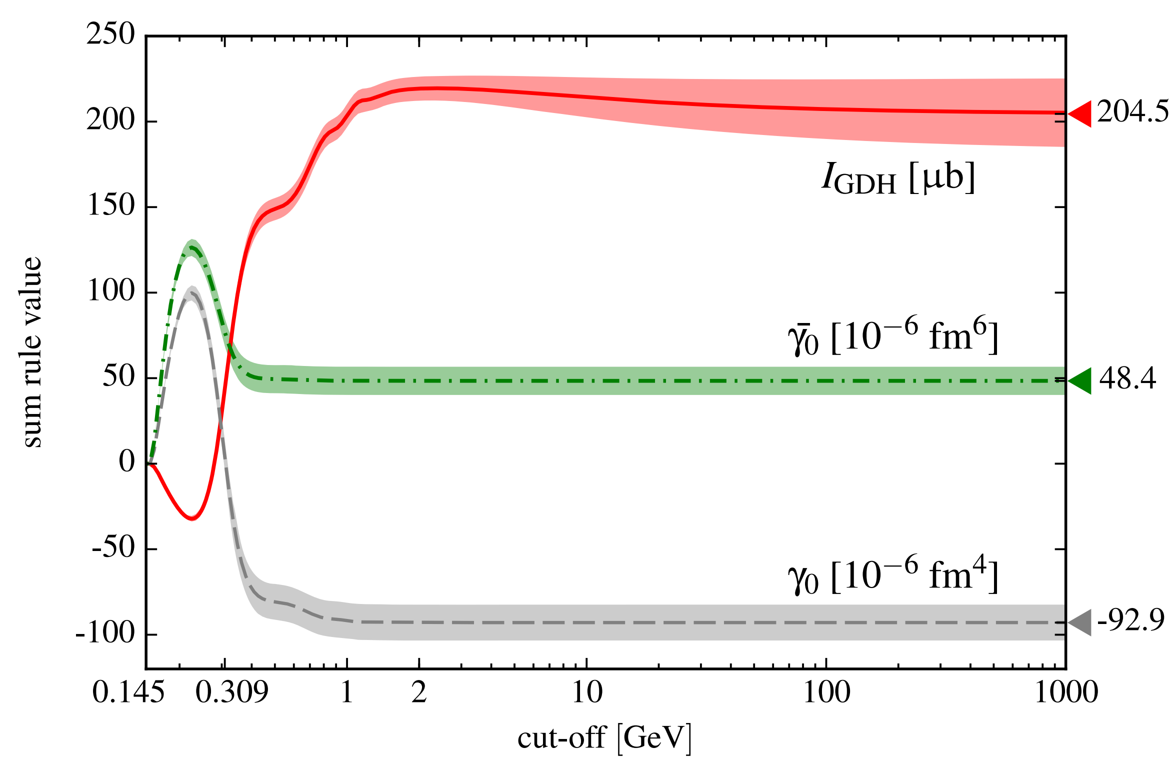

SCHWINGER, GDH AND BC SUM RULES

- Some sum rules for Compton scattering (CS) off a spin-1/2 particle:

Burkhardt—Cottingham sum rule (1970)

$$(1+a)a = \frac{m^2}{\pi^2\alpha}\int_{\nu_0}^{\infty} \mathrm{d}\nu \left[\frac{\sigma_{LT}}{Q} - \frac{\sigma_{TT}}{\nu}\right]_{Q^2=0}$$

Gerasimov—Drell—Hearn sum rule (1966)

$$a^2 = -\frac{m^2}{\pi^2\alpha}\int_{\nu_0}^{\infty} \mathrm{d}\nu\, \frac{\sigma_{TT}(\nu)}{\nu}$$

SCHWINGER, GDH AND BC SUM RULES

- Some sum rules for Compton scattering (CS) off a spin-1/2 particle:

Burkhardt—Cottingham sum rule (1970)

$$(1+a)a = \frac{m^2}{\pi^2\alpha}\int_{\nu_0}^{\infty} \mathrm{d}\nu \left[\frac{\sigma_{LT}}{Q} - \frac{\sigma_{TT}}{\nu}\right]_{Q^2=0}$$

Gerasimov—Drell—Hearn sum rule (1966)

$$\ominus \quad a^2 = -\frac{m^2}{\pi^2\alpha}\int_{\nu_0}^{\infty} \mathrm{d}\nu \, \frac{\sigma_{TT}(\nu)}{\nu}$$

Schwinger sum rule (1975)

$$a = \frac{m^2}{\pi^2\alpha}\int_{\nu_0}^{\infty} \mathrm{d}\nu \left[\frac{\sigma_{LT}(\nu, Q^2)}{Q}\right]_{Q^2=0}$$

linear dependence

THE SCHWINGER SUM RULE (1975)

J. S. Schwinger, Proc. Nat. Acad. Sci. 72, 1 (1975); ibid. 72, 1559 (1975) [Acta Phys. Austriaca Suppl. 14, 471 (1975)].
A. M. Harun ar-Rashid, Nuovo Cim. A 33, 447 (1976).
FH and V. Pascalutsa, PRL 120 (2018) 072002 and PoS CD2018 (2019) 066.

anomalous magnetic moment (a.m.m.) $a = ½(g-2)_\mu$

muon mass m

photon lab-frame energy ν and virtuality $Q^2 = -q^2$

$$a = \frac{m^2}{\pi^2 \alpha} \int_{\nu_0}^{\infty} \mathrm{d}\nu \left[\frac{\sigma_{LT}(\nu, Q^2)}{Q} \right]_{Q^2=0}$$

fine-structure constant $\alpha \approx 1/137$

photo-absorption threshold ν_0

longitudinal-transverse photo-absorption cross section σ_{LT}

THE SCHWINGER SUM RULE (1975)

J. S. Schwinger, Proc. Nat. Acad. Sci. 72, 1 (1975); ibid. 72, 1559 (1975) [Acta Phys. Austriaca Suppl. 14, 471 (1975)].
A. M. Harun ar-Rashid, Nuovo Cim. A 33, 447 (1976).
FH and V. Pascalutsa, PRL 120 (2018) 072002 and PoS CD2018 (2019) 066.

anomalous magnetic moment (a.m.m.) $a = ½(g-2)_\mu$

muon mass m

photon lab-frame energy ν and virtuality $Q^2 = -q^2$

$$a = \frac{m^2}{\pi^2 \alpha} \int_{\nu_0}^{\infty} \mathrm{d}\nu \left[\frac{\sigma_{LT}(\nu, Q^2)}{Q} \right]_{Q^2=0}$$

fine-structure constant $\alpha \approx 1/137$

photo-absorption threshold ν_0

longitudinal-transverse photo-absorption cross section σ_{LT}

- Linear relation between g-2 and a single experimental observable — the photo-absorption cross section

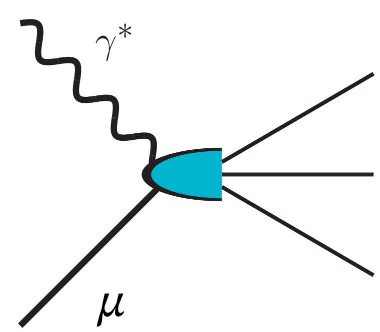

$\rightarrow \mu\gamma, \mu\gamma\gamma, \mu\pi^0, \mu\gamma\pi^0, \ldots$

inelastic cross section

THE SCHWINGER SUM RULE (1975)

J. S. Schwinger, Proc. Nat. Acad. Sci. 72, 1 (1975); ibid. 72, 1559 (1975) [Acta Phys. Austriaca Suppl. 14, 471 (1975)].
A. M. Harun ar-Rashid, Nuovo Cim. A 33, 447 (1976).
FH and V. Pascalutsa, PRL 120 (2018) 072002 and PoS CD2018 (2019) 066.

anomalous magnetic moment (a.m.m.) $a = \frac{1}{2}(g-2)_\mu$

muon mass m

photon lab-frame energy ν and virtuality $Q^2 = -q^2$

$$a = \frac{m^2}{\pi^2 \alpha} \int_{\nu_0}^{\infty} \mathrm{d}\nu \left[\frac{\sigma_{LT}(\nu, Q^2)}{Q} \right]_{Q^2=0}$$

fine-structure constant $\alpha \approx 1/137$

photo-absorption threshold ν_0

longitudinal-transverse photo-absorption cross section σ_{LT}

- Linear relation between g-2 and a single experimental observable — the photo-absorption cross section
- Puts all contributions to a_μ on the same footing: HVP, HLbL, …, QED

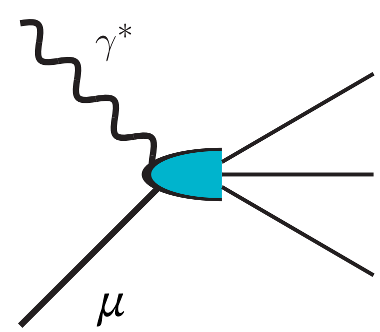

$\rightarrow \mu\gamma, \mu\gamma\gamma, \mu\pi^0, \mu\gamma\pi^0, \ldots$

inelastic cross section

LONGITUDINAL-TRANSVERSE CROSS SECTION

- Example: tree-level QED Compton scattering cross section

$$\mathrm{d}\sigma_{\lambda'_\gamma \lambda'_\mu \lambda_\gamma \lambda_\mu} = (2\pi)^4 \delta^{(4)}(p_f - p_i) \sum_{\lambda''_\gamma, \lambda''_\mu} \frac{\mathcal{M}^\dagger_{\lambda'_\gamma \lambda'_\mu \lambda''_\gamma \lambda''_\mu} \mathcal{M}_{\lambda''_\gamma \lambda''_\mu \lambda_\gamma \lambda_\mu}}{4I} \prod_a \frac{\mathrm{d}^3 p'_a}{(2\pi)^3 2E'_a},$$

with conserved helicity: $H=\lambda'_\gamma-\lambda'_\mu=\lambda_\gamma-\lambda_\mu$

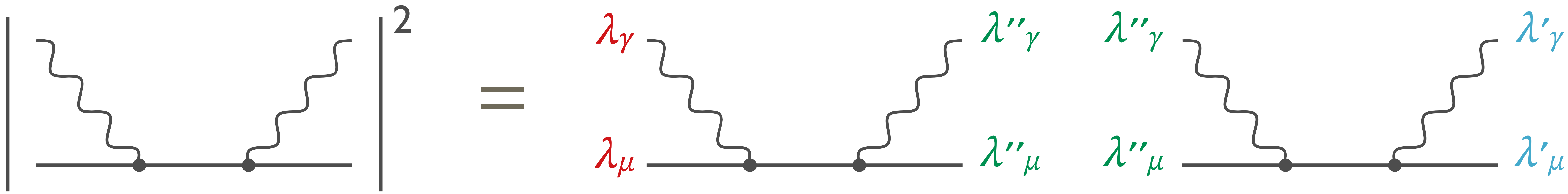

LONGITUDINAL-TRANSVERSE CROSS SECTION

- Example: tree-level QED Compton scattering cross section

$$\mathrm{d}\sigma_{\lambda'_\gamma\lambda'_\mu\lambda_\gamma\lambda_\mu} = (2\pi)^4\delta^{(4)}(p_f - p_i)\sum_{\lambda''_\gamma,\lambda''_\mu}\frac{\mathcal{M}^\dagger_{\lambda'_\gamma\lambda'_\mu\lambda''_\gamma\lambda''_\mu}\mathcal{M}_{\lambda''_\gamma\lambda''_\mu\lambda_\gamma\lambda_\mu}}{4I}\prod_a\frac{\mathrm{d}^3p'_a}{(2\pi)^3 2E'_a},$$

with conserved helicity: $H=\lambda'_\gamma-\lambda'_\mu=\lambda_\gamma-\lambda_\mu$

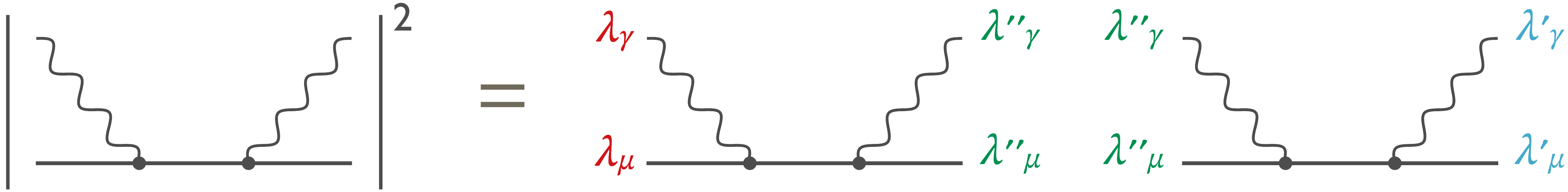

- helicity difference photo-absorption cross section: $\boxed{\sigma_{TT} = {}^1\!/_2\,(\sigma_{1/2} - \sigma_{3/2})}$

LONGITUDINAL-TRANSVERSE CROSS SECTION

- Example: tree-level QED Compton scattering cross section

$$\mathrm{d}\sigma_{\lambda'_\gamma \lambda'_\mu \lambda_\gamma \lambda_\mu} = (2\pi)^4 \delta^{(4)}(p_f - p_i) \sum_{\lambda''_\gamma, \lambda''_\mu} \frac{\mathcal{M}^\dagger_{\lambda'_\gamma \lambda'_\mu \lambda''_\gamma \lambda''_\mu} \mathcal{M}_{\lambda''_\gamma \lambda''_\mu \lambda_\gamma \lambda_\mu}}{4I} \prod_a \frac{\mathrm{d}^3 p'_a}{(2\pi)^3 2E'_a},$$

with conserved helicity: $H=\lambda'_\gamma-\lambda'_\mu=\lambda_\gamma-\lambda_\mu$

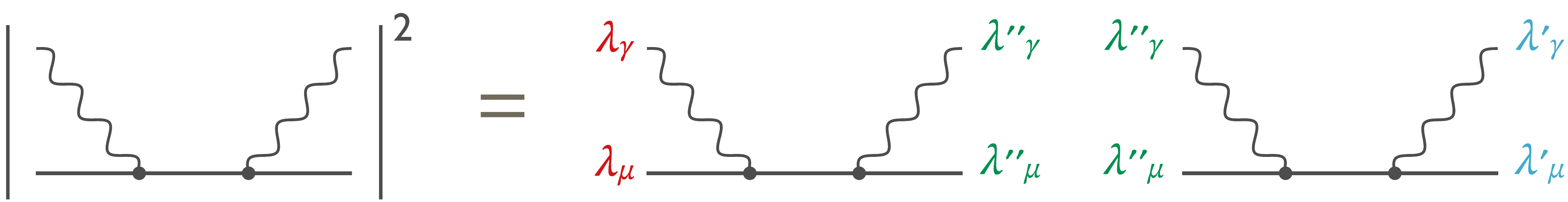

- helicity difference photo-absorption cross section: $\boxed{\sigma_{TT} = {}^1\!/_2\,(\sigma_{1/2} - \sigma_{3/2})}$
- longitudinal-transverse photo-absorption cross section:

$\gamma^*(\lambda_\gamma=0) + \mu(\lambda_\mu=-1/2) \to \gamma(\lambda'_\gamma=1) + \mu(\lambda'_\mu=1/2)$

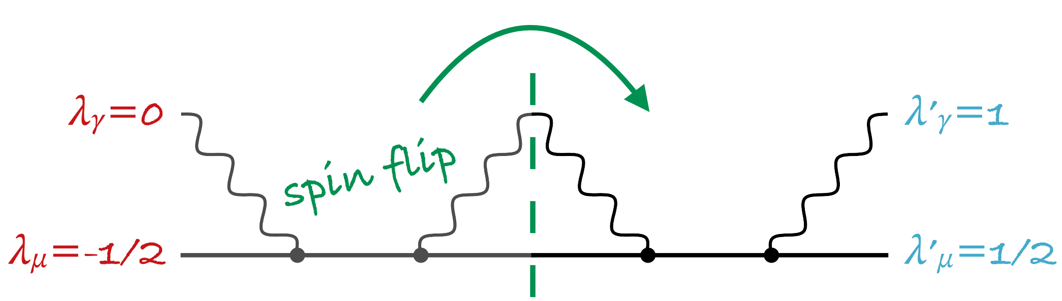

THE SCHWINGER TERM

- Schwinger sum rule: $a = \frac{m^2}{\pi^2 \alpha} \int_{\nu_0}^{\infty} \mathrm{d}\nu \left[\frac{\sigma_{LT}(\nu, Q^2)}{Q} \right]_{Q^2=0}$
- Input: longitudinal-transverse photo-absorption cross section

tree-level QED
Compton scattering

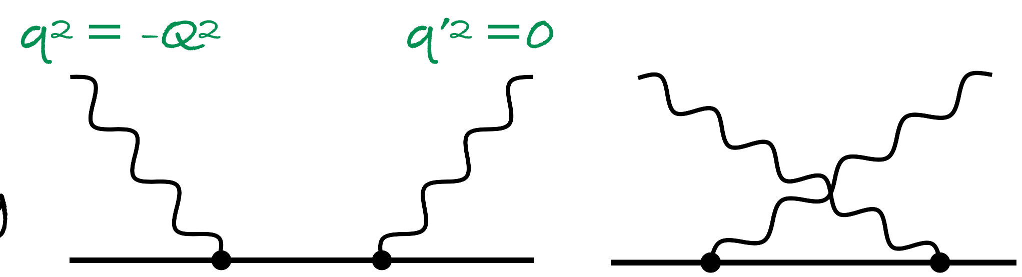

$$\sigma_{LT}^{\gamma^* \mu \to \gamma \mu}(\nu, Q^2) = \frac{\pi \alpha^2 Q \, (s - m^2)^2}{4 m^3 \nu^2 \, (\nu^2 + Q^2)} \left(-2 - \frac{m(m+\nu)}{s} + \frac{3m + 2\nu}{\sqrt{\nu^2 + Q^2}} \operatorname{arccoth} \frac{m + \nu}{\sqrt{\nu^2 + Q^2}} \right)$$

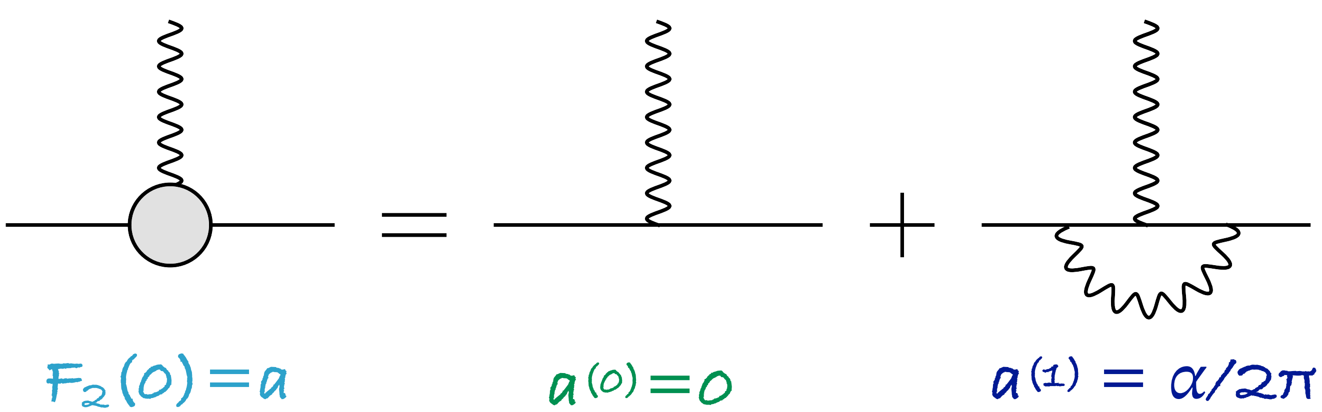

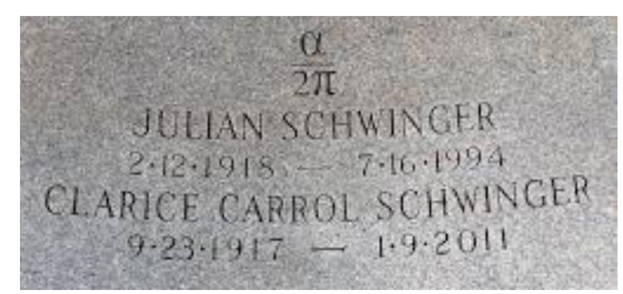

$\boxed{\text{Schwinger term — the leading QED result}}$

HVP — STANDARD FORMULA

- Hadronic vacuum polarization: 2 Data-driven approaches based on dispersion theory
  - A) Standard Formula
  - B) Schwinger Sum Rule

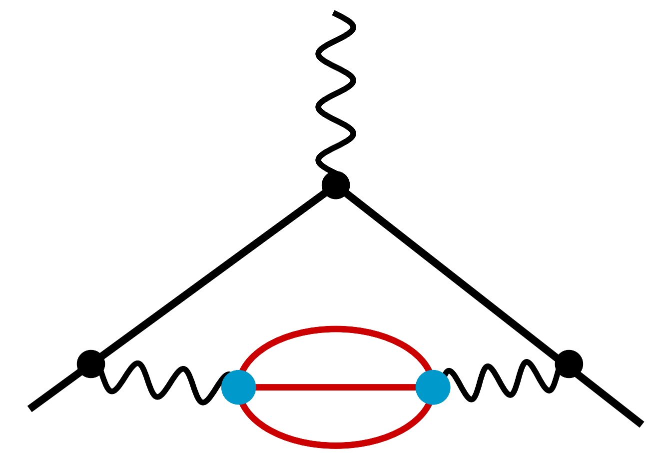

$$\boxed{a^{\mathrm{HVP}} = \frac{\alpha}{\pi^2} \int_{4m_\pi^2}^{\infty} \frac{\mathrm{d}s}{s} \, \mathrm{Im}\, \Pi^{\mathrm{had}}(s) \int_0^1 \mathrm{d}x \, \frac{x^2(1-x)}{x^2 + (1-x)(s/m^2)}}$$

$$\mathrm{Im}\, \Pi^{\mathrm{had}}(s) = \frac{s}{4\pi\alpha} \, \sigma(\gamma^* \to \text{anything}) = \frac{\alpha}{3} R_\gamma^{\mathrm{had}}(s)$$

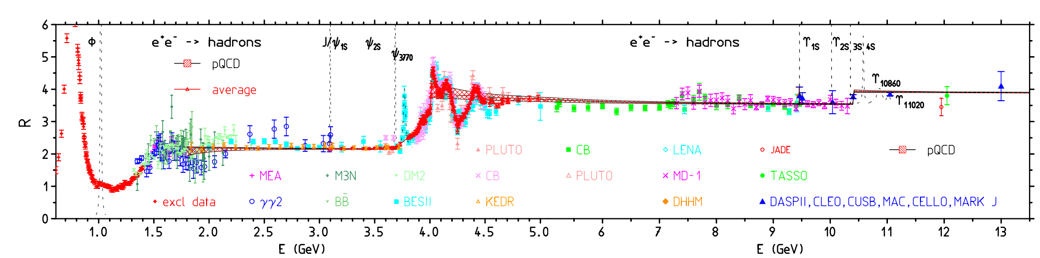

photon selfenergy

decay rate of a virtual timelike photon into hadrons

HVP — SCHWINGER SUM RULE

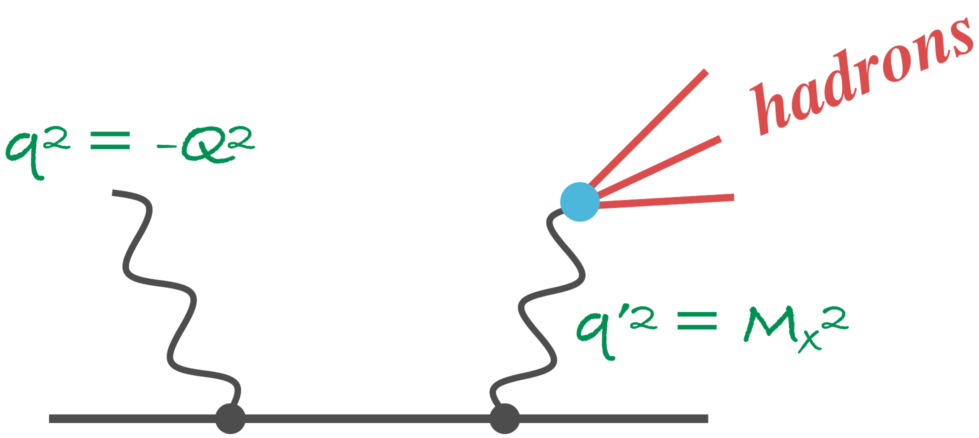

+ crossed diagram

- Cross section of hadron production through timelike Compton scattering:

factories into: $\sigma(\gamma\mu \to \mu X) = \frac{1}{\pi}\int_{4m_\pi^2}^{\infty} \frac{\mathrm{d}M_X^2}{M_X^2}\, \sigma(\gamma\mu \to \gamma^*\mu)\, \mathrm{Im}\,\Pi_X(M_X^2)$

HVP — SCHWINGER SUM RULE

+ crossed diagram

- Cross section of hadron production through timelike Compton scattering:

factories into: $$\sigma(\gamma\mu \to \mu X) = \frac{1}{\pi}\int_{4m_\pi^2}^{\infty} \frac{\mathrm{d}M_X^2}{M_X^2}\, \sigma(\gamma\mu \to \gamma^*\mu)\, \mathrm{Im}\,\Pi_X(M_X^2)$$

timelike

Compton scattering

- Timelike Compton scattering cross section:

$$\boxed{\left[\frac{\sigma_{LT}^{\gamma\mu\to\gamma^*\mu}(\nu,Q^2)}{Q}\right]_{Q^2=0} = \frac{\pi\alpha^2}{2m^2\nu^3}\left[-(5s+m^2+M_X^2)\lambda + (s+2m^2-2M_X^2)\log\frac{\beta+\lambda}{\beta-\lambda}\right]}$$

$$\beta = (s+m^2-M_X^2)/2s, \quad s = m^2+2m\nu$$
$$\lambda = (1/2s)\sqrt{[s-(m+M_X)^2]\,[s-(m-M_X)^2]}$$

HVP — SCHWINGER SUM RULE

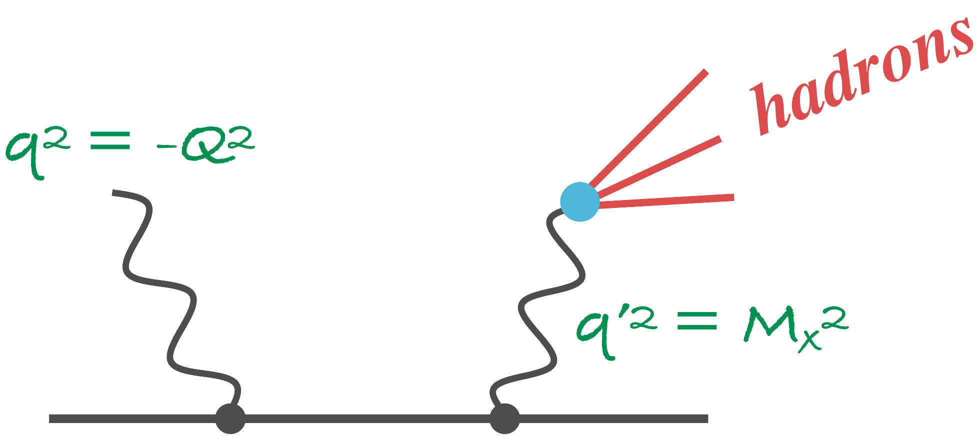

+ crossed diagram

- Cross section of hadron production through timelike Compton scattering:

factories into: $$\sigma(\gamma\mu \to \mu X) = \frac{1}{\pi}\int_{4m_\pi^2}^{\infty} \frac{\mathrm{d}M_X^2}{M_X^2}\, \underbrace{\sigma(\gamma\mu \to \gamma^*\mu)}_{\text{timelike Compton scattering}}\, \underbrace{\mathrm{Im}\,\Pi_X(M_X^2)}_{\text{virtual-photon decay into hadrons}}$$

- Timelike Compton scattering cross section:

$$\boxed{\left[\frac{\sigma_{LT}^{\gamma\mu\to\gamma^*\mu}(\nu,Q^2)}{Q}\right]_{Q^2=0} = \frac{\pi\alpha^2}{2m^2\nu^3}\left[-(5s+m^2+M_X^2)\lambda + (s+2m^2-2M_X^2)\log\frac{\beta+\lambda}{\beta-\lambda}\right]}$$

$$\beta = (s+m^2-M_X^2)/2s, \quad s = m^2+2m\nu$$
$$\lambda = (1/2s)\sqrt{[s-(m+M_X)^2]\,[s-(m-M_X)^2]}$$

HVP — SCHWINGER SUM RULE

- HVP from the Schwinger sum rule with the cross section of hadron production through timelike Compton scattering:

$$\boxed{a = \frac{m^2}{\pi^2\alpha}\int\limits_{4m_\pi^2}^{\infty} \mathrm{d}M_X^2 \int\limits_{\nu_0}^{\infty}\mathrm{d}\nu \left[\frac{1}{Q}\frac{\mathrm{d}\sigma_{LT}^{\gamma\mu\to\mu X}(\nu,Q^2)}{\mathrm{d}M_X^2}\right]_{Q^2=0}}$$

$$= \frac{1}{\pi}\int\limits_{4m_\pi^2}^{\infty} \mathrm{d}M_X^2\, \frac{\mathrm{Im}\,\Pi^{\mathrm{had}}(M_X^2)}{M_X^2}\,\frac{m^2}{\pi^2\alpha}\int\limits_{\nu_0}^{\infty}\mathrm{d}\nu \left[\frac{\sigma_{LT}^{\gamma\mu\to\gamma^*\mu}(\nu,Q^2)}{Q}\right]_{Q^2=0}$$

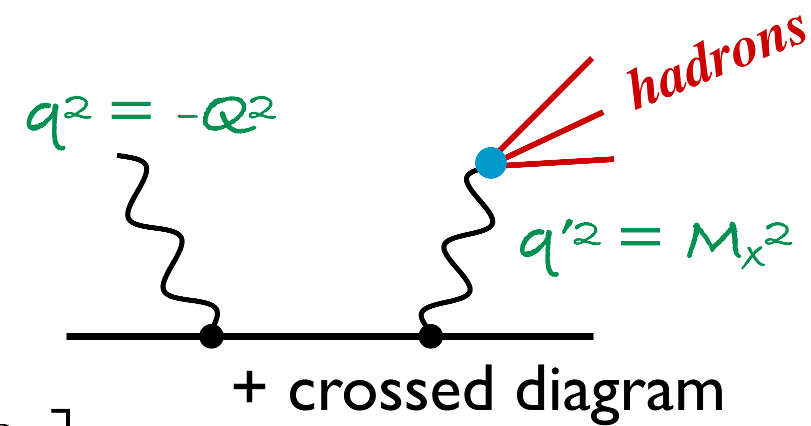

HVP — SCHWINGER SUM RULE

- HVP from the Schwinger sum rule with the cross section of hadron production through timelike Compton scattering:

$$\boxed{a = \frac{m^2}{\pi^2\alpha}\int\limits_{4m_\pi^2}^{\infty} \mathrm{d}M_X^2 \int\limits_{\nu_0}^{\infty}\mathrm{d}\nu \left[\frac{1}{Q}\frac{\mathrm{d}\sigma_{LT}^{\gamma\mu\to\mu X}(\nu,Q^2)}{\mathrm{d}M_X^2}\right]_{Q^2=0}}$$

$$= \frac{1}{\pi}\int\limits_{4m_\pi^2}^{\infty} \mathrm{d}M_X^2 \, \frac{\mathrm{Im}\,\Pi^{\mathrm{had}}(M_X^2)}{M_X^2} \underbrace{\frac{m^2}{\pi^2\alpha}\int\limits_{\nu_0}^{\infty}\mathrm{d}\nu \left[\frac{\sigma_{LT}^{\gamma\mu\to\gamma^*\mu}(\nu,Q^2)}{Q}\right]_{Q^2=0}}$$

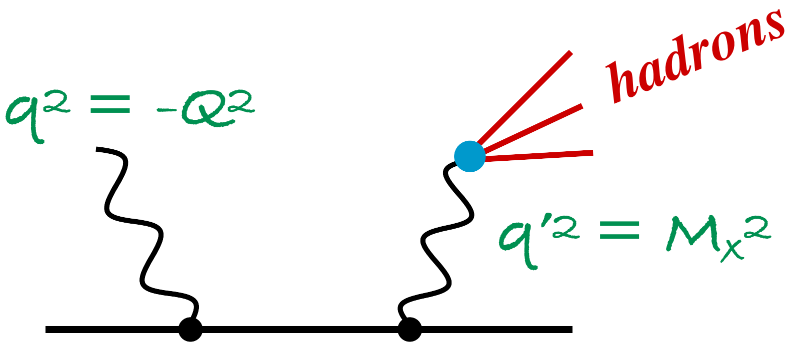

+ crossed diagram

kernel function: $\frac{\alpha}{\pi}K(M_X^2/m^2) \equiv \frac{\alpha}{\pi}\int_0^1 \mathrm{d}x \frac{x^2(1-x)}{x^2+(1-x)(M_X^2/m^2)}$

HVP — SCHWINGER SUM RULE

- HVP from the Schwinger sum rule with the cross section of hadron production through timelike Compton scattering:

$$\boxed{a = \frac{m^2}{\pi^2\alpha}\int_{4m_\pi^2}^{\infty} \mathrm{d}M_X^2 \int_{\nu_0}^{\infty} \mathrm{d}\nu \left[\frac{1}{Q}\frac{\mathrm{d}\sigma_{LT}^{\gamma\mu\to\mu X}(\nu,Q^2)}{\mathrm{d}M_X^2}\right]_{Q^2=0}}$$

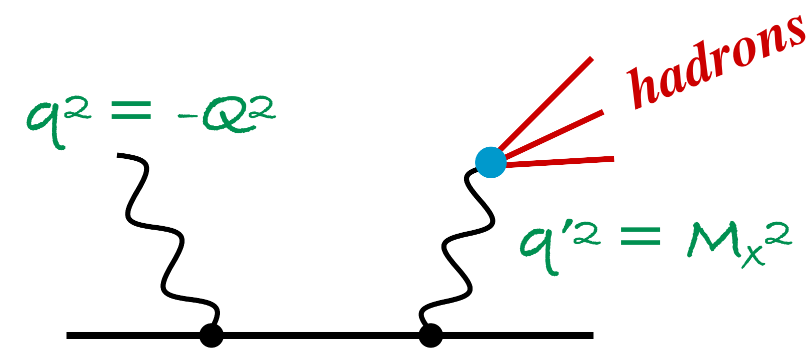

+ crossed diagram

$$= \frac{1}{\pi}\int_{4m_\pi^2}^{\infty} \mathrm{d}M_X^2 \,\frac{\mathrm{Im}\,\Pi^{\mathrm{had}}(M_X^2)}{M_X^2}\, \frac{m^2}{\pi^2\alpha}\int_{\nu_0}^{\infty} \mathrm{d}\nu \left[\frac{\sigma_{LT}^{\gamma\mu\to\gamma^*\mu}(\nu,Q^2)}{Q}\right]_{Q^2=0}$$

kernel function: $\frac{\alpha}{\pi}K(M_X^2/m^2) \equiv \frac{\alpha}{\pi}\int_0^1 \mathrm{d}x \frac{x^2(1-x)}{x^2+(1-x)(M_X^2/m^2)}$

- Schwinger sum rule can reproduce the HVP standard formula

$$\boxed{a^{\mathrm{HVP}} = \frac{\alpha}{\pi^2}\int_{4m_\pi^2}^{\infty}\frac{\mathrm{d}s}{s}\,\mathrm{Im}\,\Pi^{\mathrm{had}}(s)\int_0^1 \mathrm{d}x\,\frac{x^2(1-x)}{x^2+(1-x)(s/m^2)}}$$

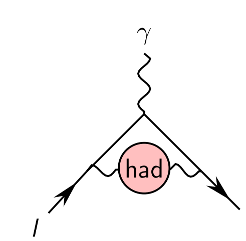

HVP — SCHWINGER SUM RULE

- HVP from the Schwinger sum rule with the cross section of hadron production through timelike Compton scattering:

$$\boxed{a=\frac{m^2}{\pi^2\alpha}\int\limits_{4m_\pi^2}^{\infty}\mathrm{d}M_X^2\int\limits_{\nu_0}^{\infty}\mathrm{d}\nu\left[\frac{1}{Q}\frac{\mathrm{d}\sigma_{LT}^{\gamma\mu\to\mu X}(\nu,Q^2)}{\mathrm{d}M_X^2}\right]_{Q^2=0}}$$

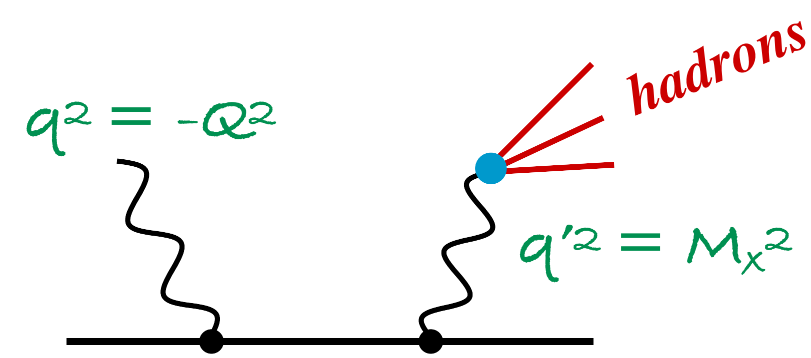

+ crossed diagram

$$=\frac{1}{\pi}\int\limits_{4m_\pi^2}^{\infty}\mathrm{d}M_X^2\,\frac{\mathrm{Im}\,\Pi^{\mathrm{had}}(M_X^2)}{M_X^2}\,\frac{m^2}{\pi^2\alpha}\int\limits_{\nu_0}^{\infty}\mathrm{d}\nu\left[\frac{\sigma_{LT}^{\gamma\mu\to\gamma^*\mu}(\nu,Q^2)}{Q}\right]_{Q^2=0}$$

kernel function: $\frac{\alpha}{\pi}K(M_X^2/m^2)\equiv\frac{\alpha}{\pi}\int_0^1\mathrm{d}x\,\frac{x^2(1-x)}{x^2+(1-x)(M_X^2/m^2)}$

for $M_x=0$, we find $K(0)=1/2$, and therefore the Schwinger term: $\varkappa^{(1)}=\alpha/2\pi$

- Schwinger sum rule can reproduce the HVP standard formula

$$\boxed{a^{\mathrm{HVP}}=\frac{\alpha}{\pi^2}\int_{4m_\pi^2}^{\infty}\frac{\mathrm{d}s}{s}\,\mathrm{Im}\,\Pi^{\mathrm{had}}(s)\int_0^1\mathrm{d}x\,\frac{x^2(1-x)}{x^2+(1-x)(s/m^2)}}$$

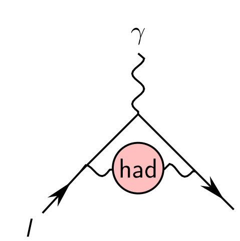

SUGAWARA-KANAZAWA THEOREM

- Sugawara-Kanazawa (SK) theorem:

$$\lim_{\nu\to\infty} S_{LT}(\nu \pm i\epsilon) = S_{LT}(\infty \pm i\epsilon) < \infty \quad \Longrightarrow \quad \lim_{|z|\to\infty} S_{LT}(z) = S_{LT}(\infty + \mathrm{sgn}(\mathrm{Im}\, z)\, i\epsilon)$$

the contribution of the integral of the amplitude over the big (semi)circle in the complex plane is given by the asymptotic value of the amplitude

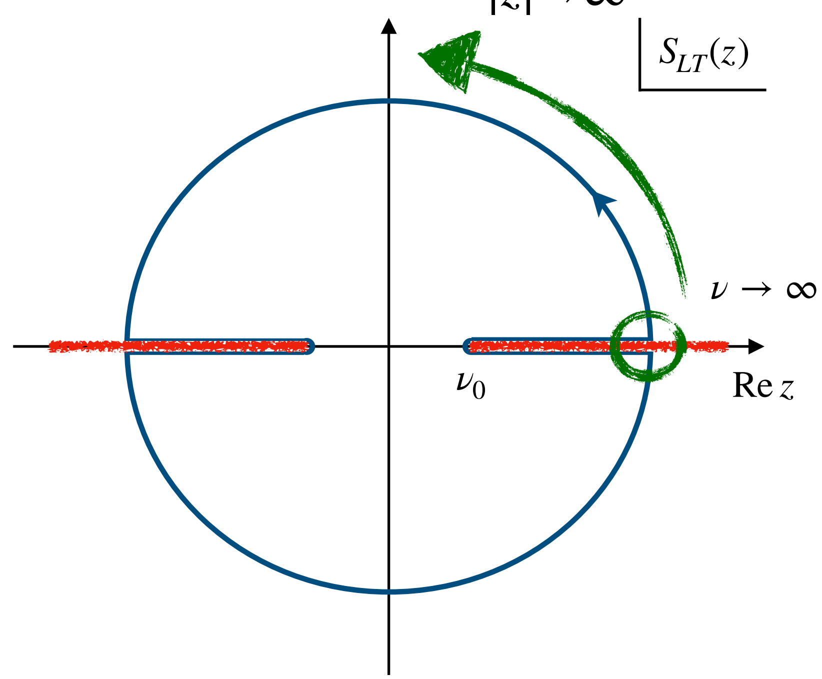

- Schwinger sum rule including asymptotic value of the amplitude:

$$a_\mu = \lim_{\nu\to\infty} S_{LT}(\nu) + \frac{m_\mu^2}{\pi^2\alpha}\int_{\nu_0}^{\infty} \mathrm{d}\nu \left[\frac{\sigma_{LT}(\nu, Q^2)}{Q}\right]_{Q^2\to 0}$$

S-K THEOREM — TOY MODEL EXAMPLE

- Consider the one-loop contributions of neutral scalar (S), pseudoscalar (P), vector (V) and axial-vector (A) massive particles to a_μ:

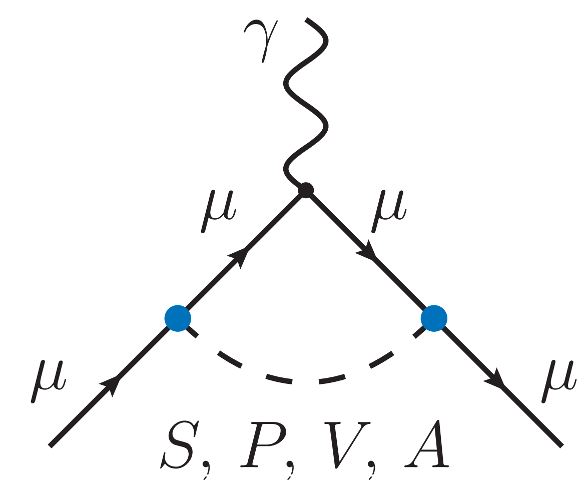

$$a_\mu^i = \Delta^i + \frac{m_\mu^2}{\pi^2\alpha}\int_{\nu_0}^{\infty} \mathrm{d}\nu \left[\frac{\sigma_{LT}^i(\nu,Q^2)}{Q}\right]_{Q^2\to 0}$$

$$\Delta^{\mathrm{S}}(\nu) = \frac{C_S^2}{8\pi^2}, \quad \Delta^{\mathrm{P}}(\nu) = -\frac{C_P^2}{8\pi^2}, \quad \Delta^{\mathrm{V}}(\nu) = 0, \quad \Delta^{\mathrm{A}}(\nu) = -\frac{C_A^2}{8\pi^2}\left(\frac{2m_\mu}{M_A}\right)^2$$

- Δ^i are associated with the asymptotic values of the Compton amplitude at infinite energy: $\Delta^i \equiv \lim_{\nu\to\infty} S_{LT}^i(\nu)$
- Perturbative checks indicate the absence of any sum-rule-violating asymptotic constants in a full ultraviolet-complete theory

S-K THEOREM — HIGGS & Z BOSON

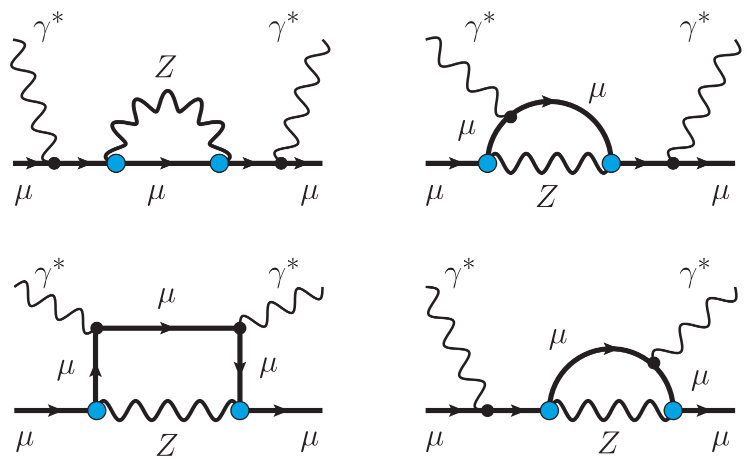

cs amplitudes

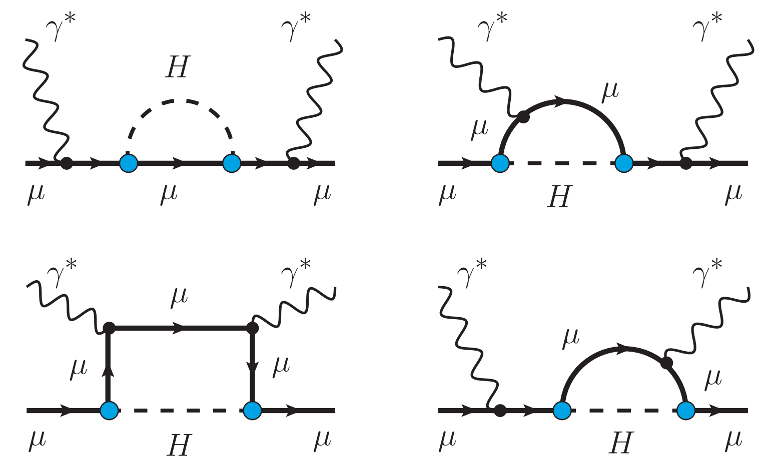

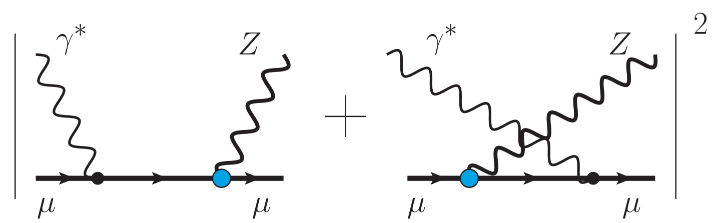

photoabsorption cross sections

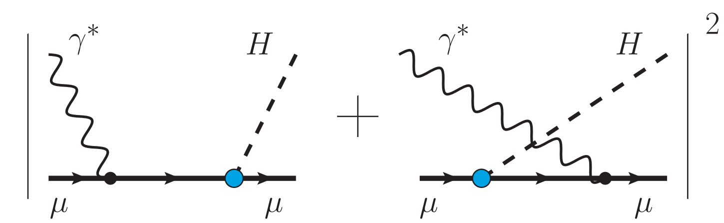

$$\lim_{\nu\to\infty} S_{\mathrm{LT}}^{Z^0}(\nu, Q=0) = \frac{[g/4\cos\Theta_W]^2}{8\pi^2}\left(\frac{2m_\mu}{M_Z}\right)^2$$

asymptotic value

$$\lim_{\nu\to\infty} S_{\mathrm{LT}}^{H}(\nu, Q=0) = \frac{1}{8\pi^2}\left(\frac{g m_\mu}{2M_Z\cos\Theta_W}\right)^2$$

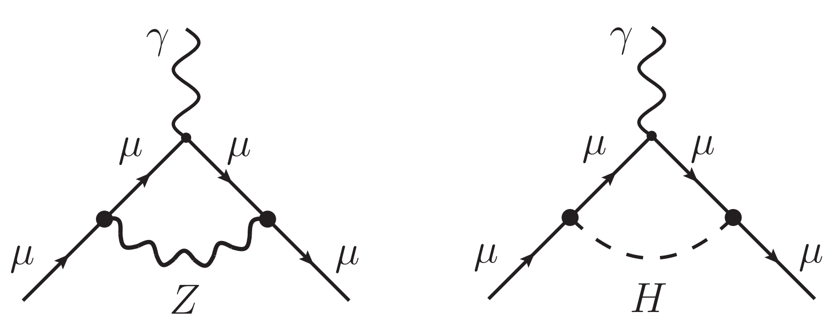

$$\lim_{\nu\to\infty} \left(S_{\mathrm{LT}}^{Z^0} + S_{\mathrm{LT}}^{H}\right)\Big|_{Q\to 0} = 0$$

Schwinger sum rule holds for Z+H!

PHOTOABSORPTION CROSS SECTIONS

- Hadron photo-production off the muon

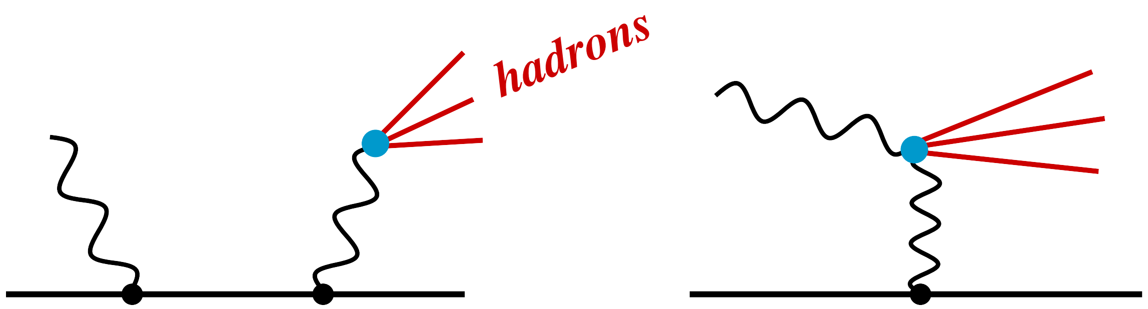

(a) (b)

(a) Timelike Compton scattering

(b) Primakoff effect

$\mu\gamma \to \mu + \text{hadrons}$

$\mu\gamma \to \mu\gamma + \text{hadrons}$

- Electromagnetic channels — HLbL contribution to Compton scattering

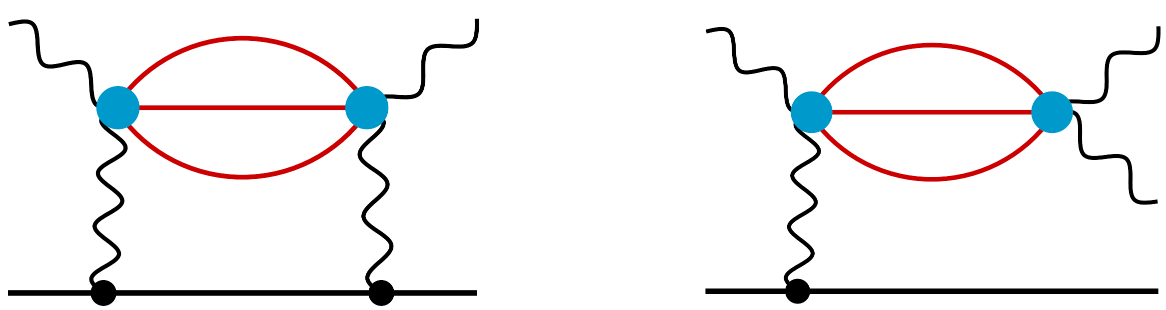

$\mu\gamma \to \mu\gamma$

$\mu\gamma \to \mu\gamma\gamma$

PROOF OF VANISHING PRIMAKOFF CONTR.

- Contribution of the Primakoff cross section is vanishing by itself [would be of order $\mathcal{O}(\alpha^2)$]
- Calculate the real part of the Compton scattering box diagram:

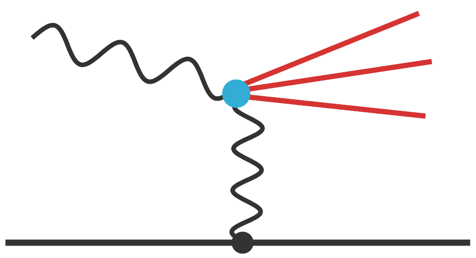

$$\boxed{\varkappa = -\frac{m^2}{2\pi\alpha}\lim_{Q^2\to 0}\lim_{\nu\to 0}\frac{T_{TL}(\nu,Q^2)}{Q}}$$

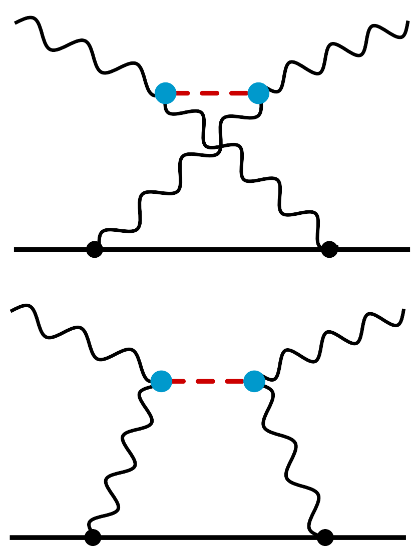

$$\begin{aligned}
&\lim_{Q^2\to 0}\frac{T_{LT}^{\mathrm{Box}}}{Q}\\
&=\lim_{Q^2\to 0}\frac{2}{3\pi^4}\int_0^\infty \mathrm{d}K\int_0^\pi \mathrm{d}\chi\,\sin^2\chi\int_{\nu_0}^\infty \mathrm{d}\tilde{\nu}'\\
&\times\left\{S_1(iK\cos\chi,K^2)\left[\frac{\tau_{TL}^a}{Q}+\frac{K\cos^2\chi}{2}\,\frac{\tau_{TT}^a}{\tilde{\nu}'}\right]-\frac{iK\cos\chi}{m}S_2(iK\cos\chi,K^2)\left[\frac{\tau_{TL}^a}{Q}+\frac{K}{2}\,\frac{\tau_{TT}^a}{\tilde{\nu}'}\right]\right\}\\
&=0
\end{aligned}$$

- LbL sum rules:

$$\lim_{Q^2\to 0}\int_{\nu_0}^\infty \mathrm{d}\tilde{\nu}'\,\frac{1}{\tilde{\nu}'}\,\tau_{TT}^a(\tilde{\nu}',K^2,Q^2)=0$$

$$\lim_{Q^2\to 0}\int_{\nu_0}^\infty \mathrm{d}\tilde{\nu}'\,\frac{1}{Q}\,\tau_{TL}^a(\tilde{\nu}',K^2,Q^2)=0$$

Pascalutsa et al.,
Phys. Rev. D 85 (2012) 116001.

PION-EXCHANGE CONTRIBUTION

WP-2020: $a_\mu^{\pi^0\text{-pole}}(\text{disp.}) = 63.0^{+2.7}_{-2.1} \times 10^{-11}$

$\boxed{\text{Schwinger sum rule: } a_\mu^{\pi^0} = 68(6) \times 10^{-11}}$

- Main contribution from π^0-photoproduction channel: $a_\mu^{\mu\pi^0-\text{channel}} = 63(5) \times 10^{-11}$

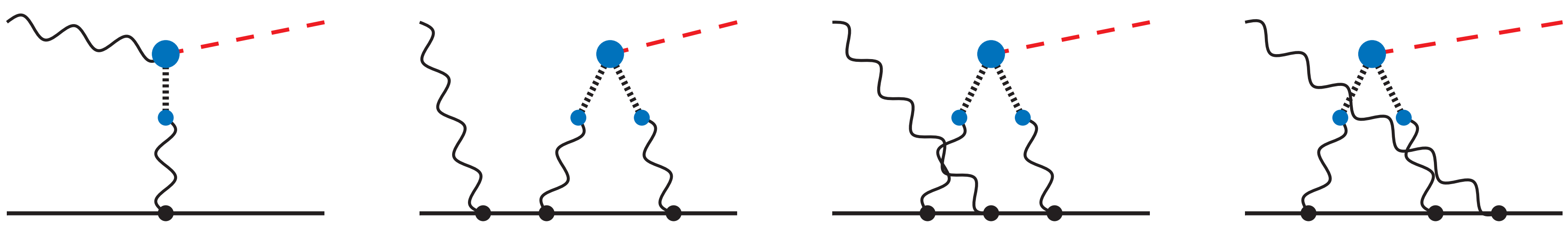

  - Including off-shell effects, $\pi^0\gamma\gamma$ vertex (Knecht & Nyffeler VMD model)

- Small corrections from electromagnetic channels, e.g.: $a_\mu^{\mu\gamma-\text{channel}\,(\pi^0)} \approx 5(3) \times 10^{-11}$
  - Highly model-dependent calculation

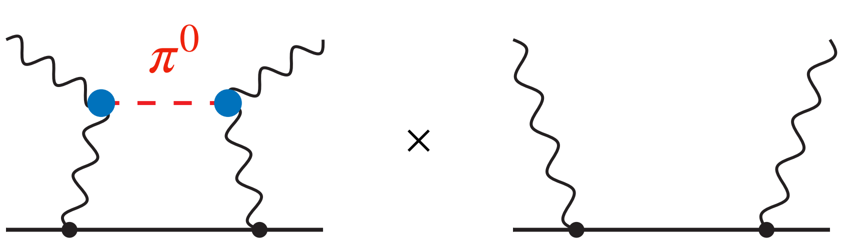

Feasibility of measurement at COMPASS as part of MUonE ?

cf. The Workshop on
Evaluation of the Leading Hadronic Contribution
to the Muon Anomalous Magnetic Moment
Mainz (Germany), 2 - 5 April 2017

$\mu e \to \mu e \pi^0$

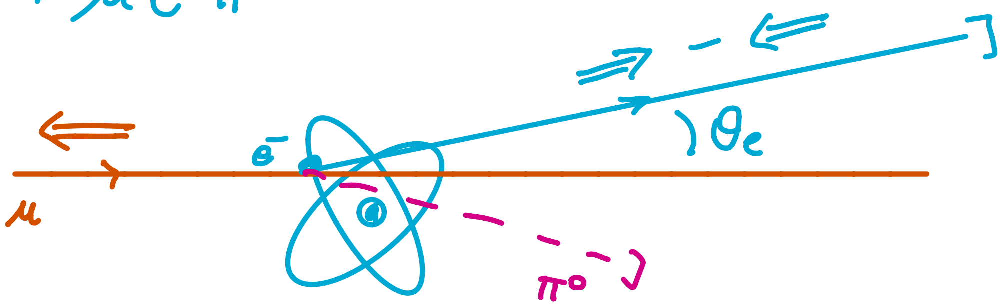

$E_\mu = 150,\ 200$ GeV

$E_e' \simeq 1$ GeV

$\theta_e \simeq 10$ mrad

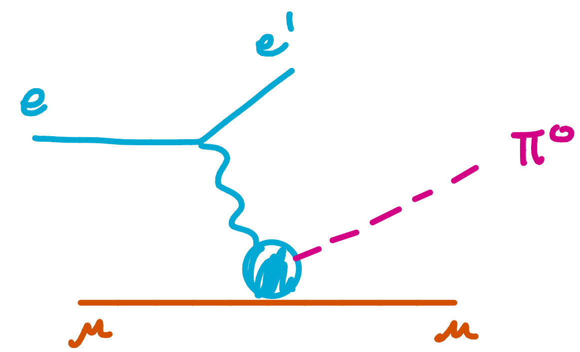

$$Q^2 \simeq 2 m_e E_e' \simeq 10^{-3}\,\mathrm{GeV}^2$$

$$\nu \simeq \frac{m_e E_\mu}{m_\mu}\left(1 - 2\frac{E_e'}{m_e}\sin^2\frac{\theta}{2}\right) = (\nu_{\pi^0},\ 1\,\mathrm{GeV})$$

$$\nu_{\pi^0} = \frac{m_{\pi^0}}{m_\mu}\left(\frac{1}{2}m_{\pi^0} + m_\mu\right) \simeq 230\,\mathrm{MeV}$$

slide: V. Pascalutsa @CIPANP'18

MUON STRUCTURE FUNCTIONS

- Muon spin structure functions could be measured in inelastic electron-muon scattering
  - Polarized electron-muon collisions?
  - Fixed-target μ-on-e scattering?
- Double-polarized spin asymmetries:

$$\frac{\mathrm{d}^2\sigma}{\mathrm{d}E'\mathrm{d}\Omega}(\downarrow\Uparrow - \uparrow\Uparrow) = \frac{4\alpha^2}{mQ^2}\frac{E'}{\nu E}\left[(E+E'\cos\theta)\,g_1(x,Q^2) - \frac{Q^2}{\nu}\,g_2(x,Q^2)\right]$$

$$\frac{\mathrm{d}^2\sigma}{\mathrm{d}E'\mathrm{d}\Omega}(\downarrow\Rightarrow - \uparrow\Rightarrow) = \frac{4\alpha^2\sin\theta}{mQ^2}\frac{E'^{\,2}}{\nu^2 E}\left[\nu\,g_1(x,Q^2) - 2E\,g_2(x,Q^2)\right]$$

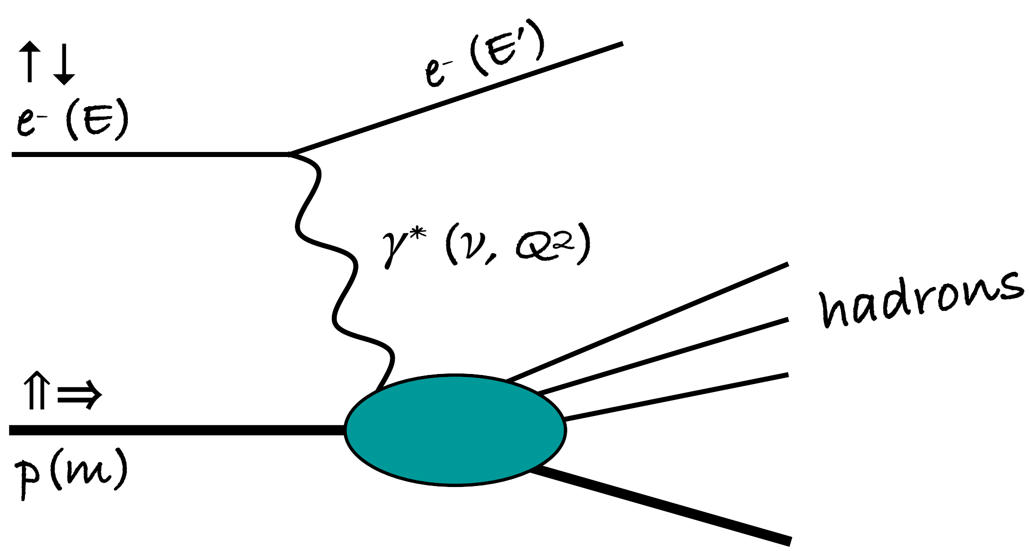

DISPERSIVE APPROACH TO HLBL

- HLBL more complicated than HVP $\Longrightarrow$ no analogue of the simple HVP formula

dispersive formula for the e.m. vertex function:

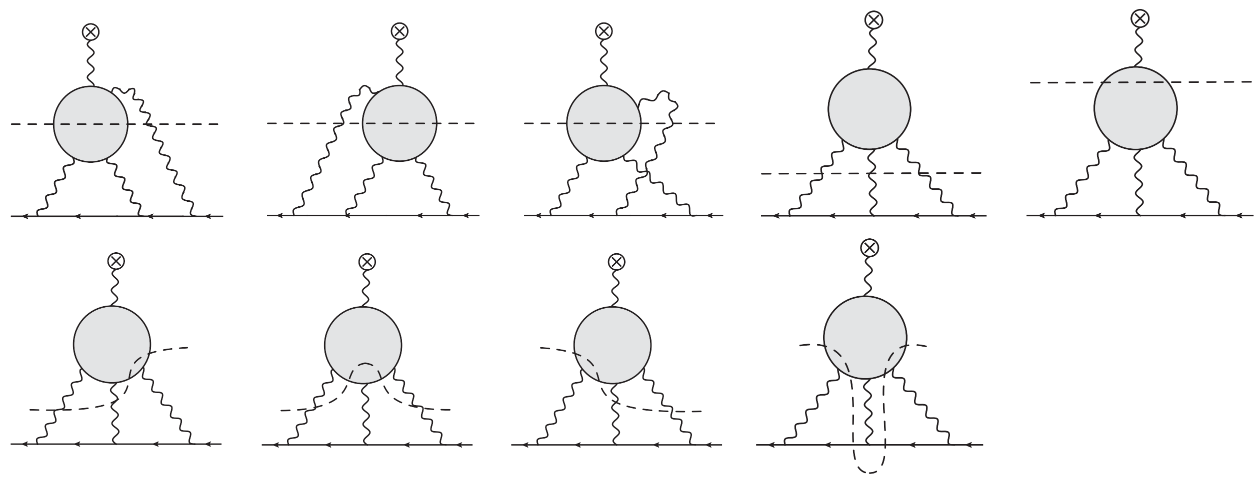

V. Pauk and M. Vanderhaeghen, Phys. Rev. D 90, 113012 (2014)

dispersive formula for the light-by-light scattering amplitude:

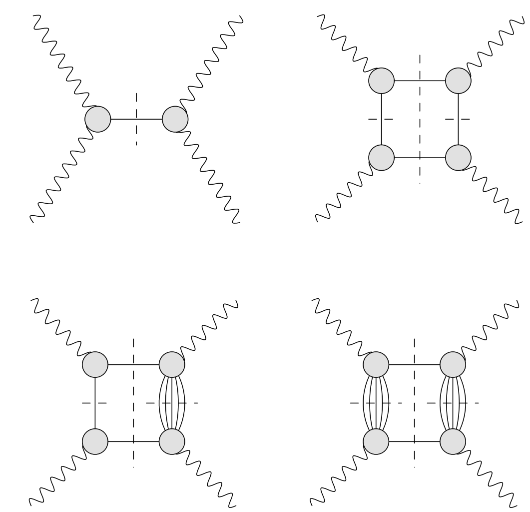

G. Colangelo, et al., JHEP 1509 (2015) 074

Schwinger sum rule (a dispersive formula for Compton scattering):

$$a_\mu = \frac{m^2}{\pi^2 \alpha} \int_{\nu_0}^{\infty} \mathrm{d}\nu \left[\frac{\sigma_{LT}(\nu, Q^2)}{Q} \right]_{Q^2=0}$$

CS amplitude, a_μ

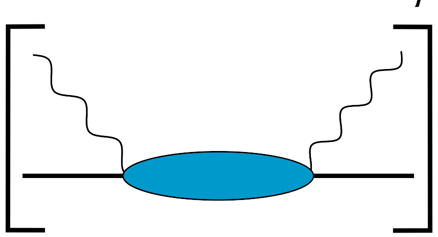

$$(\nu, Q^2) = \frac{2}{\pi} \int_{\nu_0}^{\infty} \mathrm{d}\nu' \frac{\nu'}{\nu'^2 - \nu^2}$$

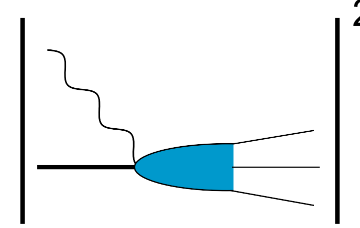

$$(\nu', Q^2)$$

Cross sections, structure functions

FH and V. Pascalutsa, PRL 120 (2018) 072002 and 1907.06927 (2019)

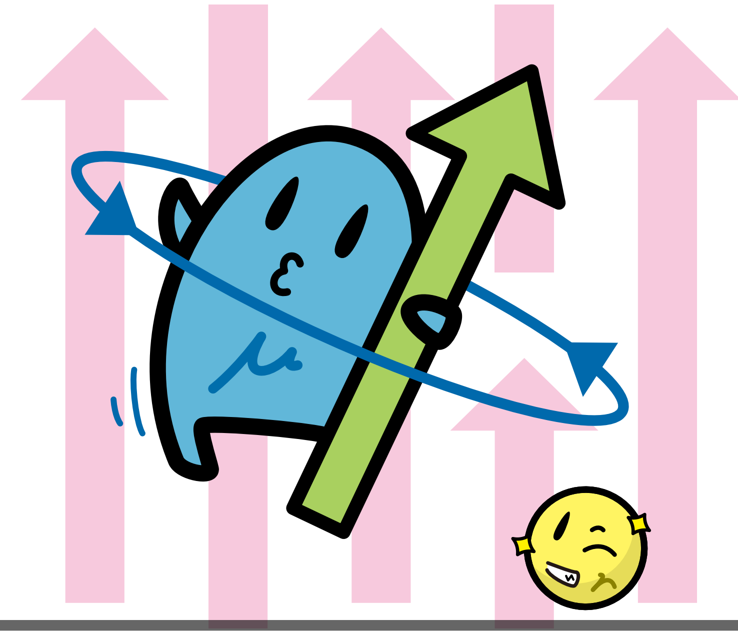

Light-by-Light Scattering

— General Concept and Formalism —

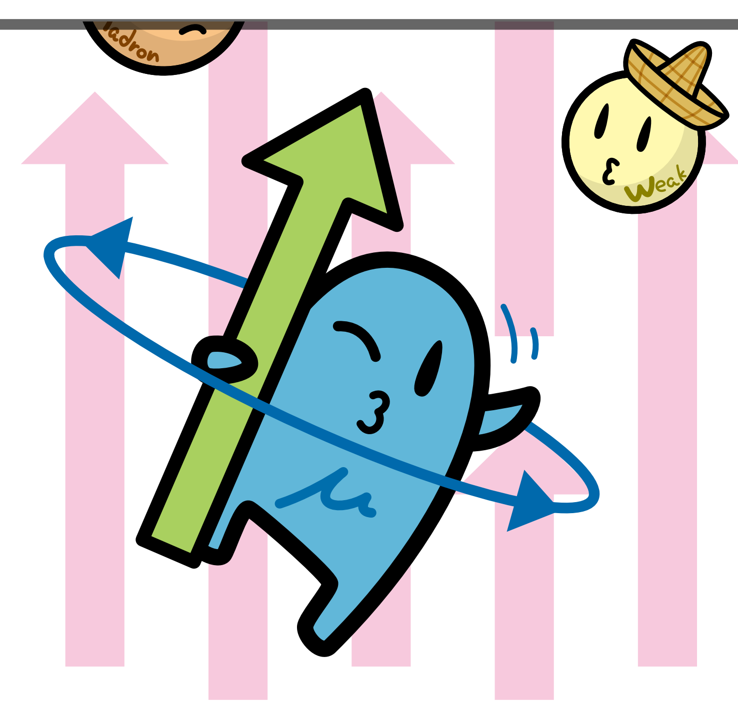

HVP VS HLBL

- HLbL is suppressed by a factor of α compared to HVP
- HLbL contribution to g-2 has larger relative uncertainty than HVP contribution
  - presently ~20%, needs to be <10% to meet the FNAL goal

HVP VS HLBL

- HLbL is suppressed by a factor of α compared to HVP
- HLbL contribution to g-2 has larger relative uncertainty than HVP contribution
  - presently ~20%, needs to be <10% to meet the FNAL goal

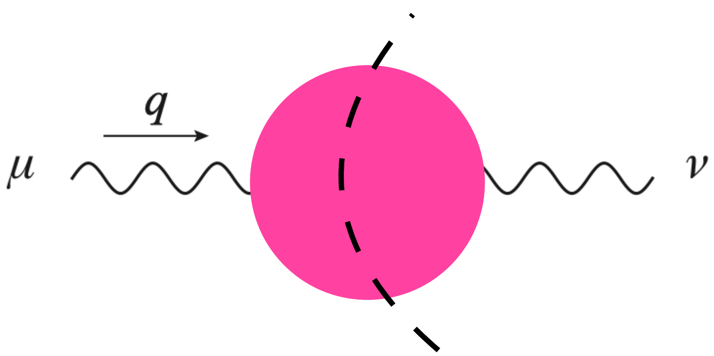

Data-driven HLbL evaluation is more complicated

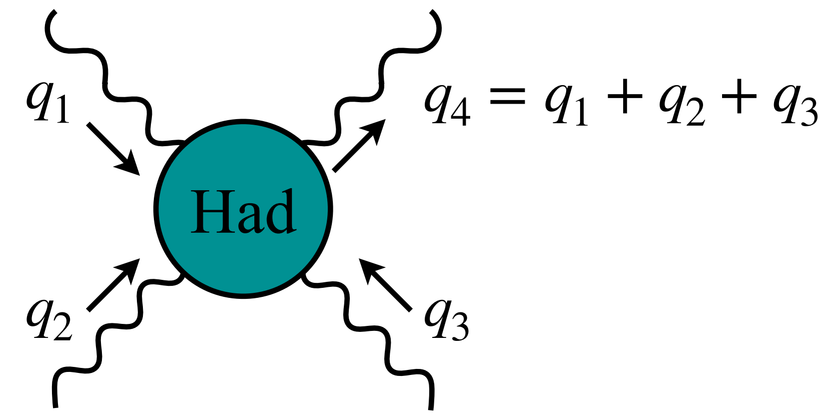

HVP VS HLBL

- HLbL is suppressed by a factor of α compared to HVP
- HLbL contribution to g-2 has larger relative uncertainty than HVP contribution
  - presently ~20%, needs to be <10% to meet the FNAL goal

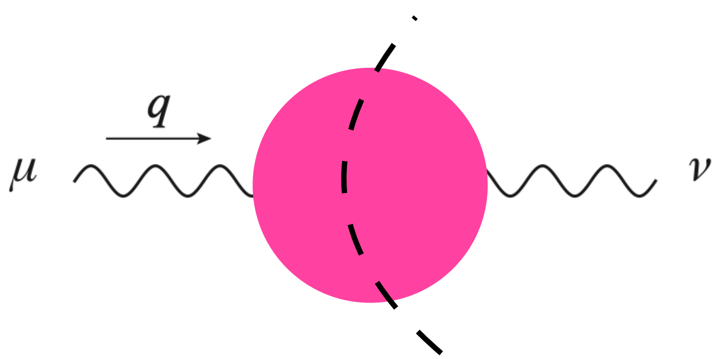

Data-driven HLbL evaluation is more complicated

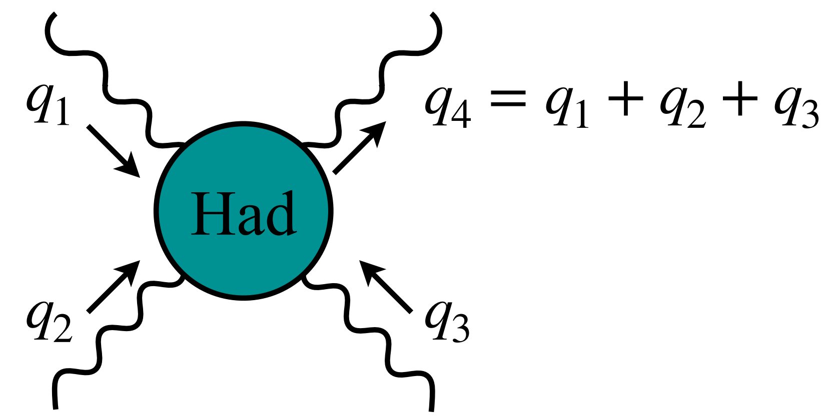

- HVP is described by a single function $\Pi(q^2)$ of a single variable

HVP VS HLBL

- HLbL is suppressed by a factor of α compared to HVP
- HLbL contribution to g-2 has larger relative uncertainty than HVP contribution
  - presently ~20%, needs to be <10% to meet the FNAL goal

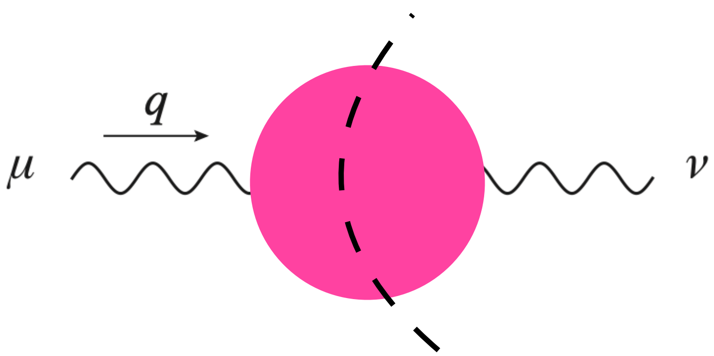

Data-driven HLbL evaluation is more complicated

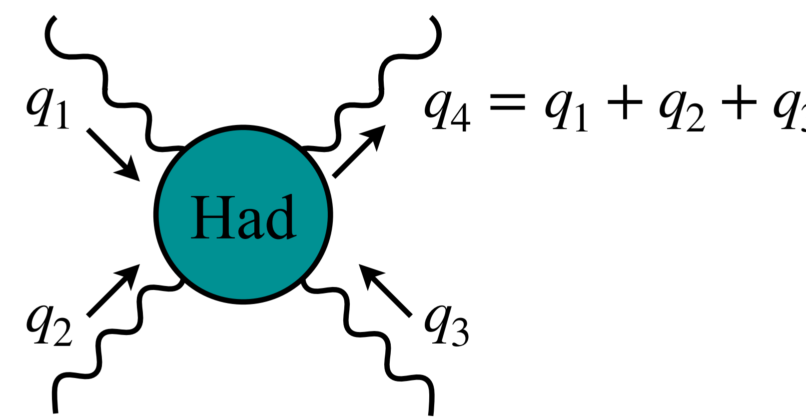

- HVP is described by a single function $\Pi(q^2)$ of a single variable
- Light-by-light 4-point function
  - Finding suitable “basis" / tensor structures is much more complicated
  - Dependence on two Mandelstam variables requires double-spectral representations

HLBL TENSOR

- **HLbL tensor:**

$$\Pi^{\mu\nu\lambda\sigma}(q_1, q_2, q_3) = -i \int d^4x\, d^4y\, d^4z\, e^{-i(q_1\cdot x + q_2\cdot y + q_3\cdot z)} \langle 0 \,|\, T\{j^\mu(x) j^\nu(y) j^\lambda(z) j^\sigma(0)\} \,|\, 0\rangle$$

with $q_1 + q_2 + q_3 = q_4$ and $q_4^2 = 0$

- General Lorentz invariant decomposition consists of 138 scalar functions
- Constraints due to gauge invariance?
  - **Bardeen-Tung-Tarrach (BTT) decomposition:** 54 tensor structures Π_i with scalar functions free of kinematic singularities / amenable to a dispersive treatment
  - 43 basis tensors (41 helicity amplitudes in $d = 4$) $\Rightarrow$ form of singularities follows from projection of the BTT decomposition
  - Crossing symmetry $\Rightarrow$ only 7 distinct structures

see Colangelo, Hoferichter, Procura, Stoffer 2014, 2015, 2017 for details

HLBL CONTRIBUTION TO $(g-2)_\mu$

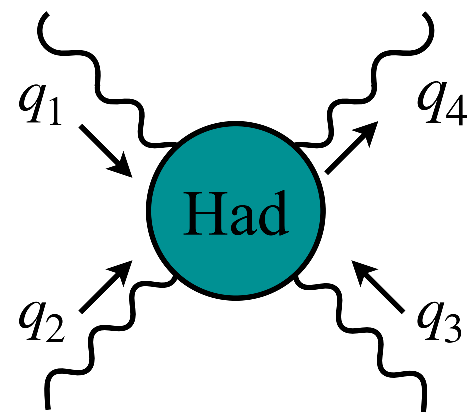

$q_4 = q_1 + q_2 + q_3$ and $q_4^2 = 0$

- Master formula:

$$a_\mu^{\text{HLbL}} = \frac{2\alpha^3}{3\pi^2} \int_0^\infty dQ_1 \int_0^\infty dQ_2 \int_{-1}^{1} d\tau \sqrt{1-\tau^2} Q_1^3 Q_2^3 \sum_{i=1}^{12} T_i(Q_1, Q_2, \tau)\, \bar{\Pi}_i(Q_1, Q_2, \tau)$$

  - $s = q_3^2 = -Q_3^2 = -Q_1^2 - 2Q_1Q_2\tau - Q_2^2, \quad t = q_2^2 = -Q_2^2, \quad u = q_1^2 = -Q_1^2$
  - τ is the four-dimensional angle between Euclidean momenta
  - T_i are known kernel functions
  - $\bar{\Pi}_i$ are scalar amplitudes suitable for dispersive treatment $\Rightarrow$ imaginary parts related to measurable sub-processes

see Colangelo, Hoferichter, Procura, Stoffer 2014, 2015, 2017 for details

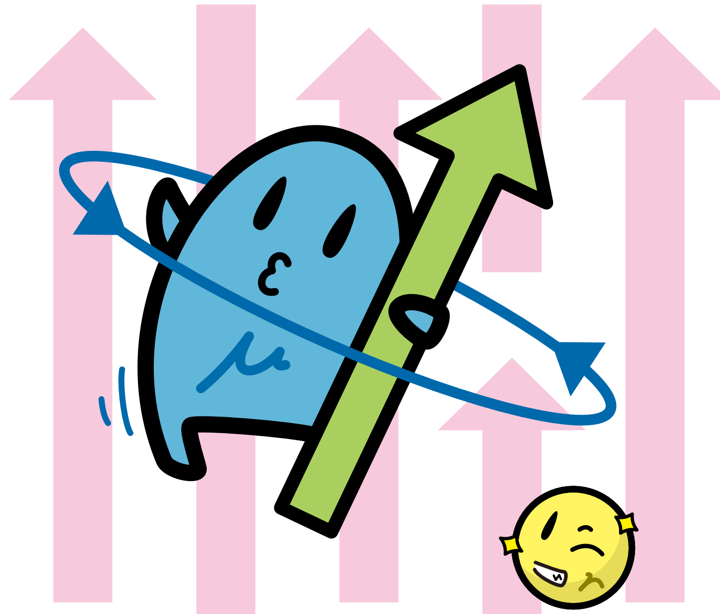

HLBL Contribution to $(g-2)_\mu$

— Dispersive Approach —

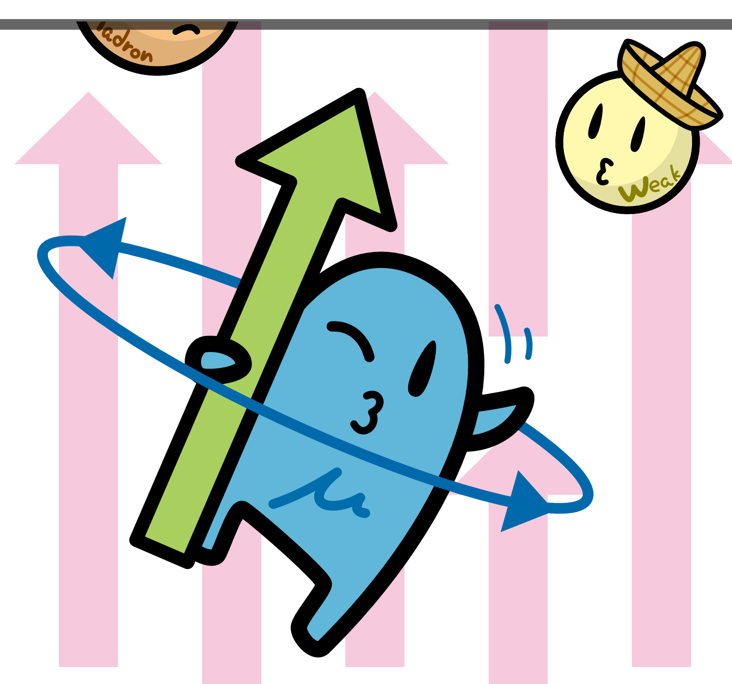

MODEL DEPENDENCE

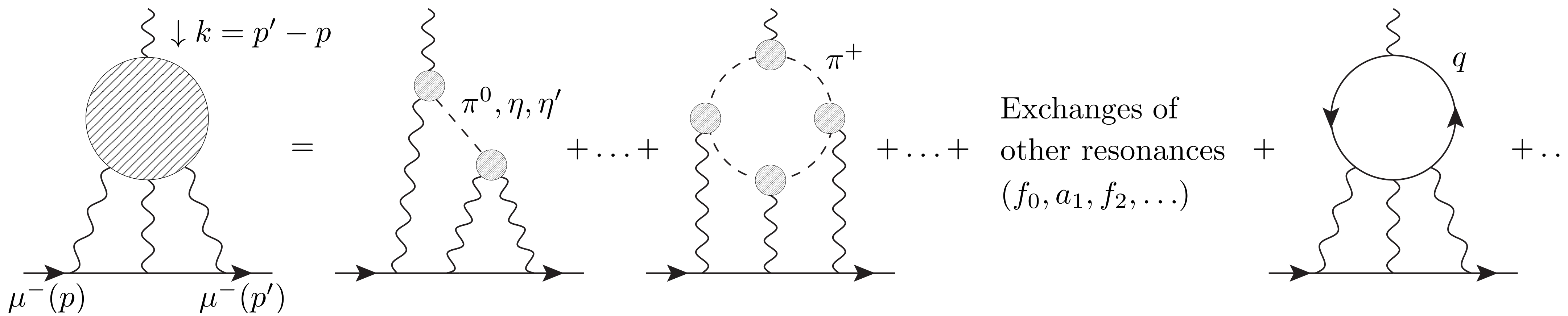

FIG. 1. HLbL in the muon $g - 2$ in model calculations. The blobs on the right-hand side of the equal sign are form factors that describe the interaction of photons with hadrons.

- Model calculations:
  - Identification of contributions is not unique (off-shell contributions, form factors)
  - Possible double counting of high-energy contributions (dressed constituent quark-loop & mesonic contributions)

MODEL DEPENDENCE

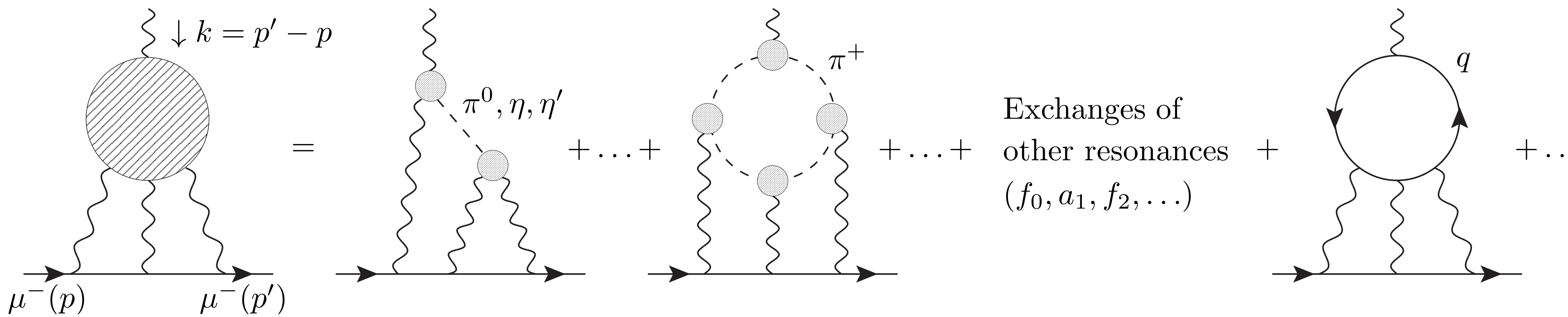

FIG. 1. HLbL in the muon $g-2$ in model calculations. The blobs on the right-hand side of the equal sign are form factors that describe the interaction of photons with hadrons.

- Model calculations:
  - Identification of contributions is not unique (off-shell contributions, form factors)
  - Possible double counting of high-energy contributions (dressed constituent quark-loop & mesonic contributions)
- Dispersive approach:
  - *If an amplitude can be reconstructed from its singularities, and these are related by unitarity to physical sub-amplitudes obtained by cutting the hadronic blobs in all possible ways and taking into account all possible (on-shell) intermediate states, then the whole amplitude can be split into a number of contributions clearly identified by the (on-shell) intermediate states.*

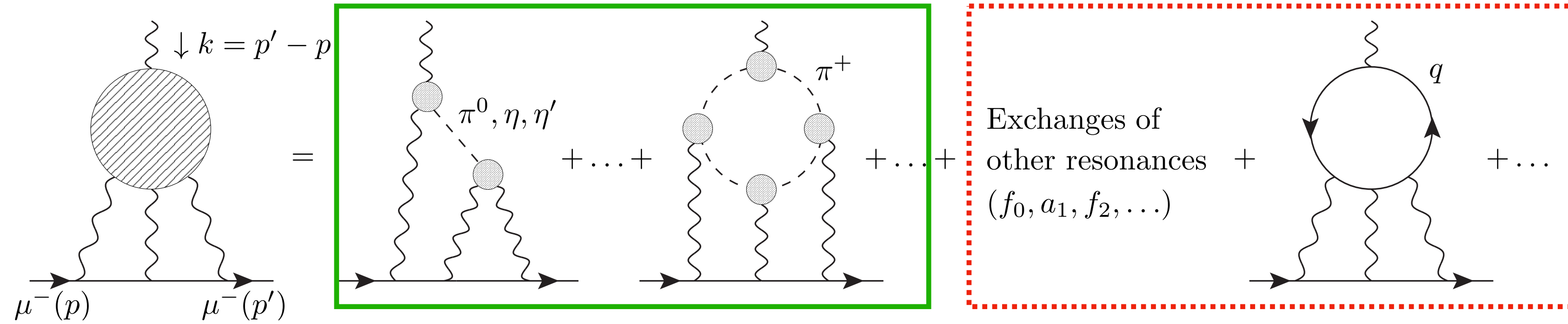

pseudoscalar poles	$93.8(4.0)$	**well determined contributions**
pion box	$-15.9(2)$	
S-wave $\pi\pi$ rescattering	$-8(1)$	
kaon box	$-0.5(1)$	

Scalars+tensors $\gtrsim 1$ GeV	$\sim -1(3)$	**major source of uncertainty**
axial vectors	$\sim 6(6)$	
short distance	$\sim 15(10)$	
heavy quarks	$\sim 3(1)$	

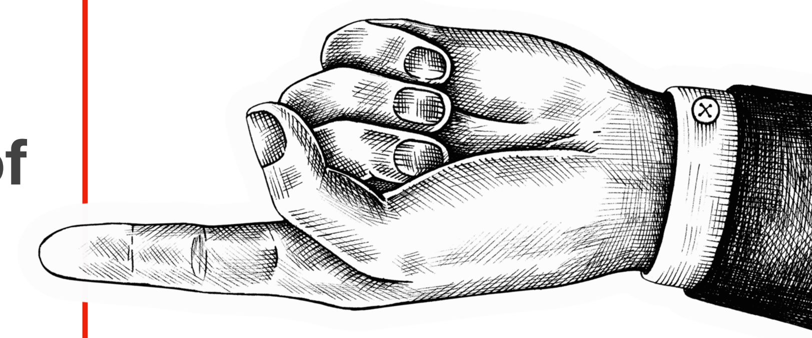

Lattice: $a_\mu^{\mathrm{HLbL}} = 109.6(15.9) \times 10^{-11}$ Chao et al. (2021, 2022)

$= 124.7(14.9) \times 10^{-11}$ Blum et al. (2023)

HLBL CONTRIBUTIONS TO $(g-2)_\mu$

$$a_\mu^{\mathrm{HLbL}} = \frac{2\alpha^3}{3\pi^2}\int_0^\infty dQ_1 \int_0^\infty dQ_2 \int_{-1}^{1} d\tau \sqrt{1-\tau^2}\, Q_1^3 Q_2^3 \sum_{i=1}^{12} T_i(Q_1, Q_2, \tau)\, \bar{\Pi}_i(Q_1, Q_2, \tau)$$

$$Q_i^2 = -\,q_i^2\,,\, Q_3^2 = Q_1^2 + Q_2^2 + 2\tau Q_1 Q_2$$

known kernel functions (main contribution from energies below 1.5 GeV)

combinations of the scalar functions Π_i

HLBL CONTRIBUTIONS TO $(g-2)_\mu$

$$a_\mu^{\mathrm{HLbL}} = \frac{2\alpha^3}{3\pi^2}\int_0^\infty dQ_1 \int_0^\infty dQ_2 \int_{-1}^{1} d\tau \sqrt{1-\tau^2}\, Q_1^3 Q_2^3 \sum_{i=1}^{12} T_i(Q_1, Q_2, \tau)\, \bar{\Pi}_i(Q_1, Q_2, \tau)$$

known kernel functions (main contribution from energies below 1.5 GeV)

combinations of the scalar functions Π_i

$$Q_i^2 = -\, q_i^2\,,\, Q_3^2 = Q_1^2 + Q_2^2 + 2\tau Q_1 Q_2$$

$$a_\mu^{\mathrm{HLbL}} = a_\mu^{\pi^0-\mathrm{pole}} + a_\mu^{\pi-\mathrm{box}} + a_\mu^{\pi\pi} + \cdots$$

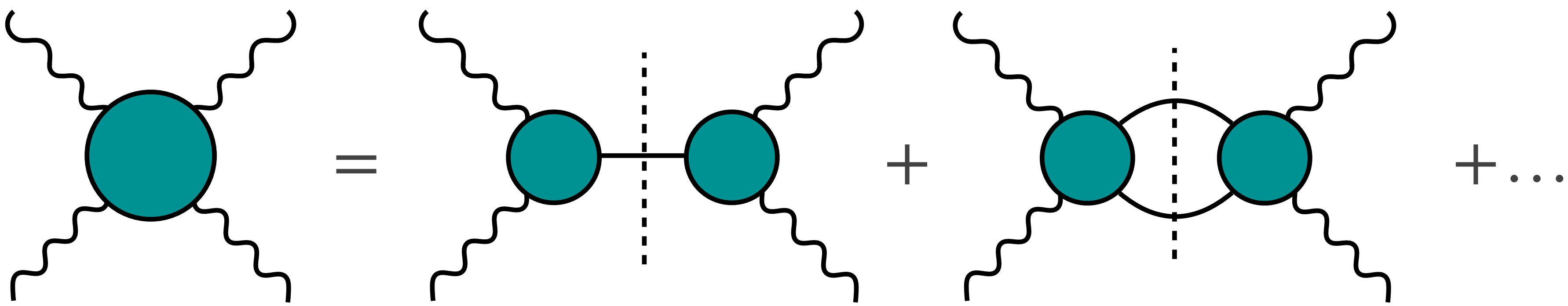

HLBL CONTRIBUTIONS TO $(g-2)_\mu$

$$a_\mu^{\mathrm{HLbL}} = \frac{2\alpha^3}{3\pi^2}\int_0^\infty dQ_1 \int_0^\infty dQ_2 \int_{-1}^{1} d\tau \sqrt{1-\tau^2}\, Q_1^3 Q_2^3 \sum_{i=1}^{12} T_i(Q_1,Q_2,\tau)\, \bar{\Pi}_i(Q_1,Q_2,\tau)$$

$$Q_i^2 = -q_i^2\,,\, Q_3^2 = Q_1^2 + Q_2^2 + 2\tau Q_1 Q_2$$

known kernel functions (main contribution from energies below 1.5 GeV)

combinations of the scalar functions Π_i

$$a_\mu^{\mathrm{HLbL}} = a_\mu^{\pi^0-\mathrm{pole}} + a_\mu^{\pi-\mathrm{box}} + a_\mu^{\pi\pi} + \cdots$$

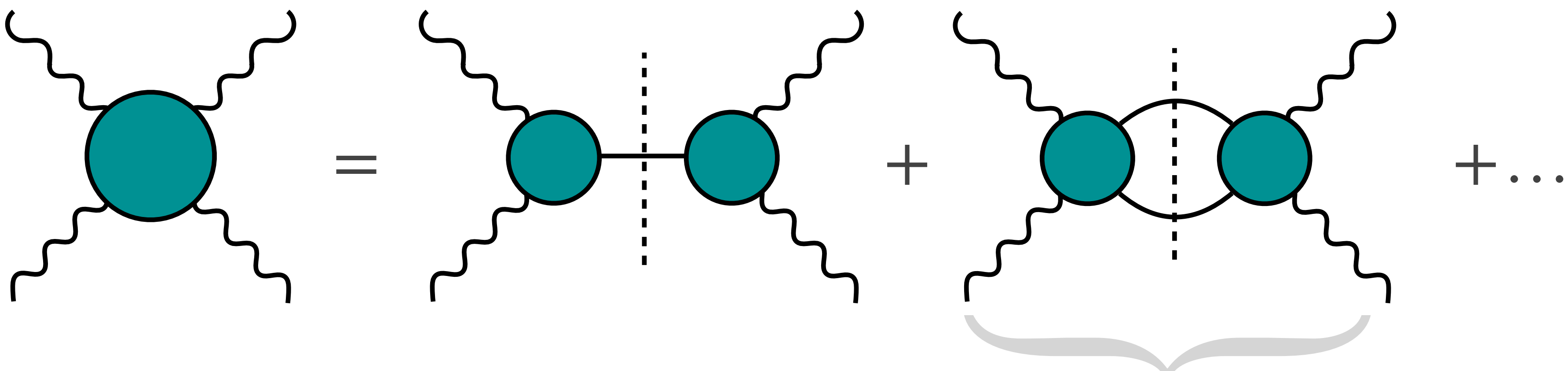

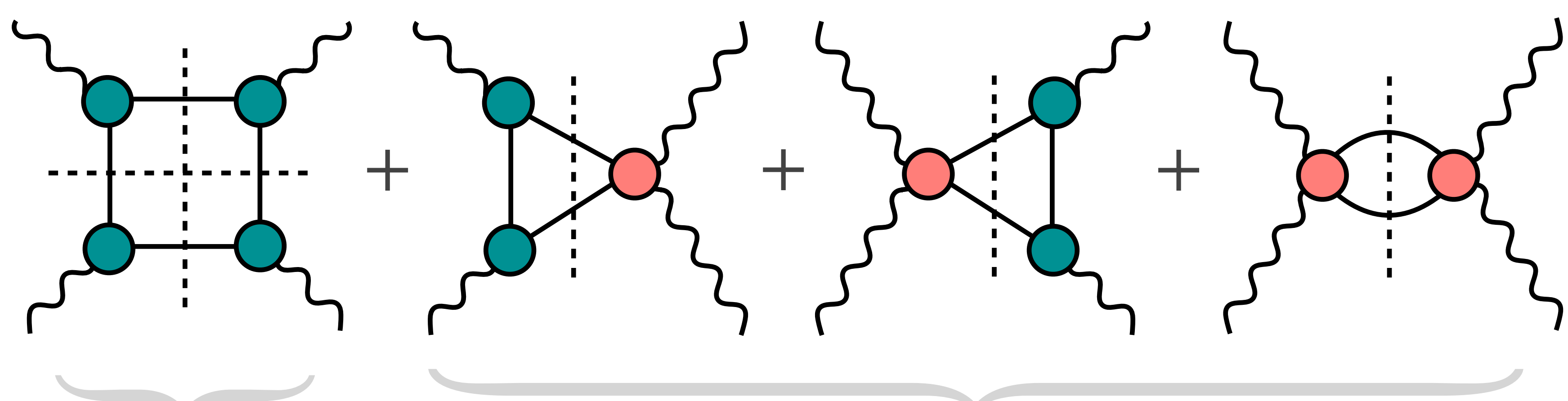

HLBL — DISPERSION RELATIONS

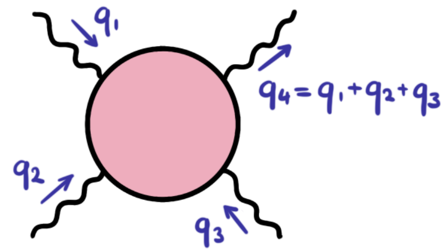

- Dispersive approaches apply different cuts on LbL amplitude

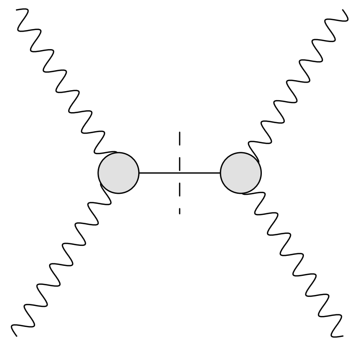

input: disp. representation of space-like doubly-virtual pion transition form factor

- Mandelstam double-spectral representation with two-pion primary cut
  - Poles in sub-processes $\gamma^* \gamma^* \to \pi\pi$ and crossed sub-process $\gamma^* \pi \to \gamma^* \pi$

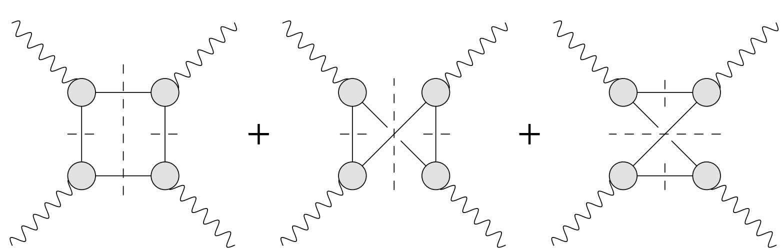

$$= F_\pi^V(q_1^2)F_\pi^V(q_2^2)F_\pi^V(q_3^2)F_\pi^V(q_4^2) \times$$

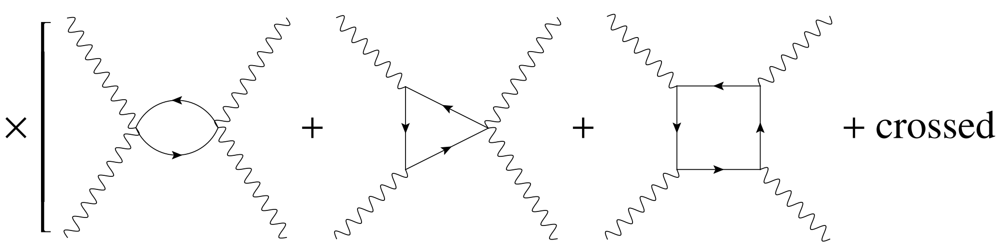

input: disp. fit of space-like and time-like data for pion vector form factor

  - Multi-particle cuts in sub-processes $\gamma^* \pi \to \gamma^* \pi$

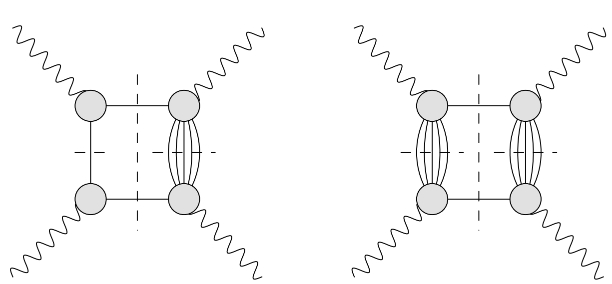

input: $\gamma^* \gamma^* \to \pi\pi$ partial waves

HLBL — EMPIRICAL INPUT

Andrzej Kupsc

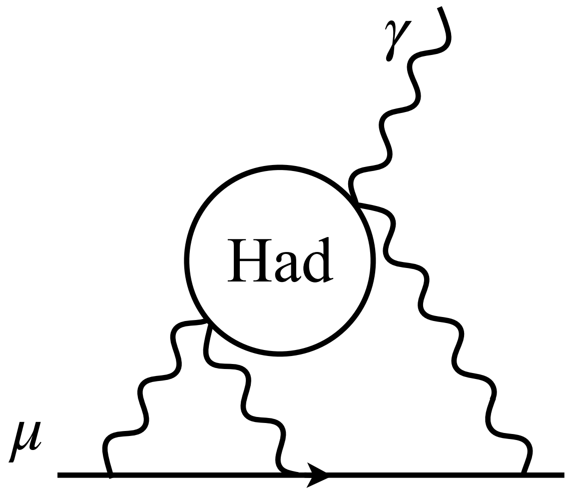

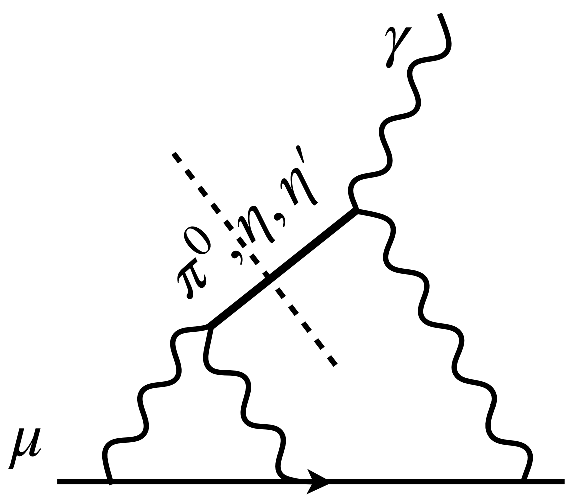

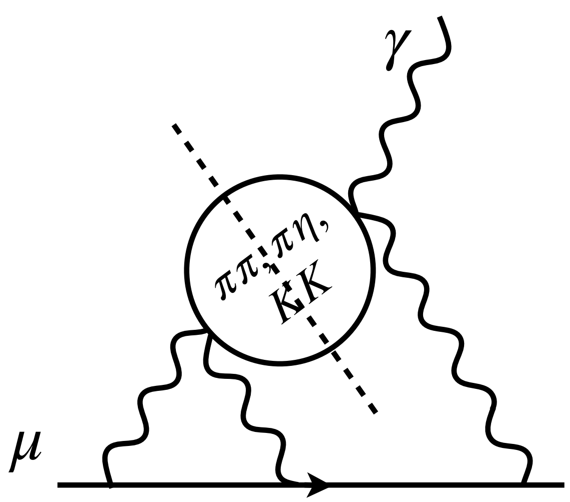

$q^2 > 0$ **timelike** γ^*:

- Dalitz decay

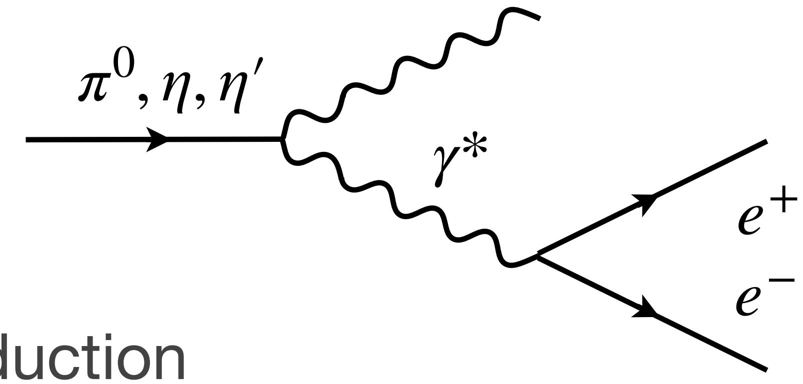

- Radiative production

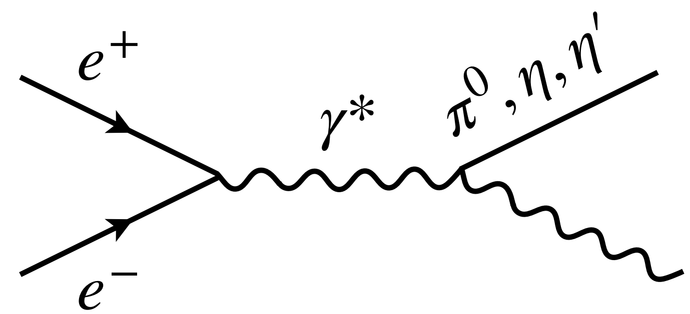

$q^2 < 0$ **spacelike** γ^*

- Two-photon collisions

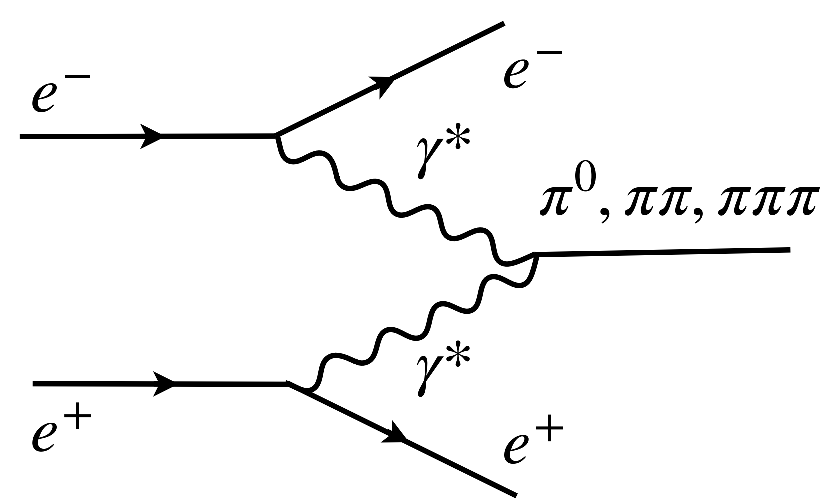

HLBL — EMPIRICAL INPUT

Andrzej Kupsc

Hadronic light-by-light scattering: data input

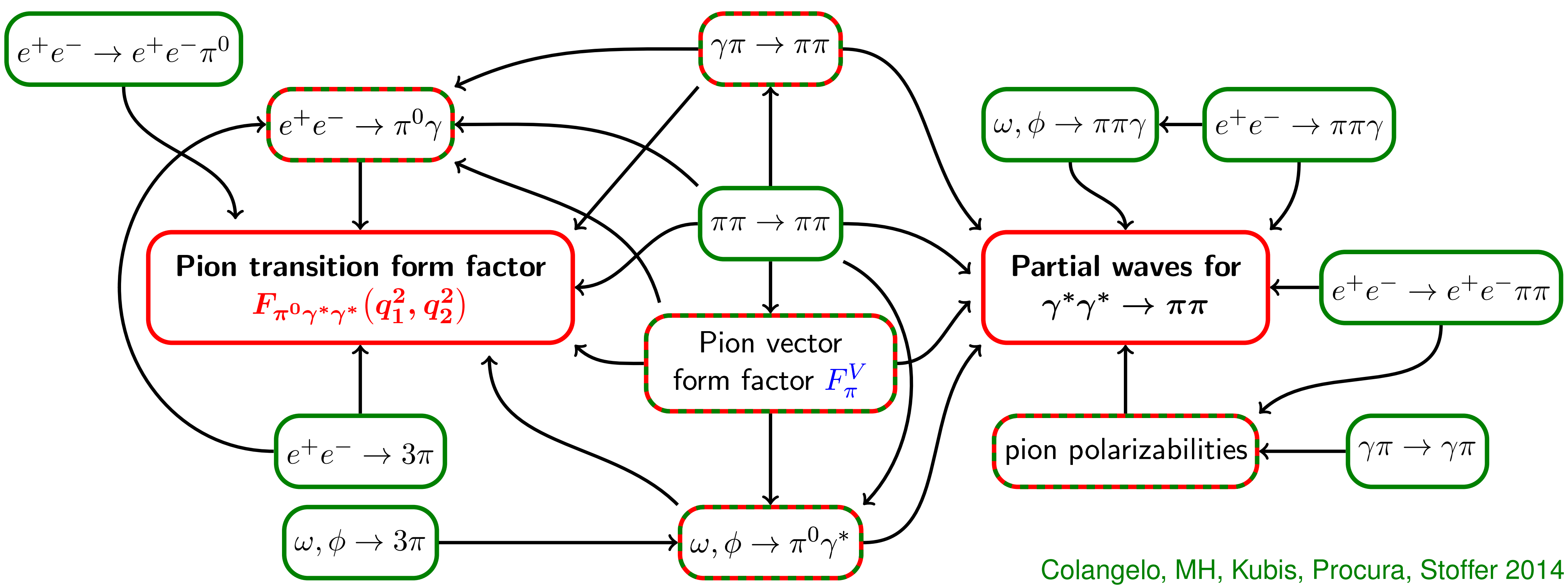

Colangelo, MH, Kubis, Procura, Stoffer 2014

- Reconstruction of $\gamma^*\gamma^* \to \pi\pi, \pi^0$: combine experiment and theory constraints
- Need input on $\gamma^*\gamma^*$ matrix elements for as many states as possible

HLBL — EMPIRICAL INPUT

Andrzej Kupsc

Aoyama, et al., Phys. Rept. 887 (2020) 1-166

issue	experimental input [I] or cross-checks [C]
axials, tensors, higher pseudoscalars	$\gamma^{(*)}\gamma^* \to 3\pi,\ 4\pi,\ K\bar{K}\pi,\ \eta\pi\pi,\ \eta'\pi\pi$ [I]
missing states	inclusive $\gamma^{(*)}\gamma^* \to$ hadrons at 1–3 GeV [I]
dispersive analysis of $\eta^{(\prime)}$ TFFs	$e^+e^- \to \eta\pi^+\pi^-$ [I]
	$\eta' \to \pi^+\pi^-\pi^+\pi^-$ [I]
	$\eta' \to \pi^+\pi^-e^+e^-$ [I]
	$\gamma\pi^- \to \pi^-\eta$ [C]
dispersive analysis of π^0 TFF	$\gamma\pi \to \pi\pi$ [I]
	high accuracy Dalitz plot $\omega \to \pi^+\pi^-\pi^0$ [C]
	$e^+e^- \to \pi^+\pi^-\pi^0$ [C]
	$\omega, \phi \to \pi^0 l^+ l^-$ [C]
pseudoscalar TFF	$\gamma^{(*)}\gamma^* \to \pi^0, \eta, \eta'$ at arbitrary virtualities [I,C]
pion, kaon, $\pi\eta$ loops (including scalars and tensors)	$\gamma^{(*)}\gamma^* \to \pi\pi,\ K\bar{K},\ \pi\eta$ at arbitrary virtualities, partial waves [I,C]

Table 14: Priorities for new experimental input and cross-checks.

Experimental inputs (BES III) — *Christoph Redmer*
Kobayashi Hall, KEK Tsukuba campus — 09:10 - 09:35

Dispersive improvement of HLbL in soft kinematics — *Jan-Niklas Toelstede*
Kobayashi Hall, KEK Tsukuba campus — 13:30 - 13:55

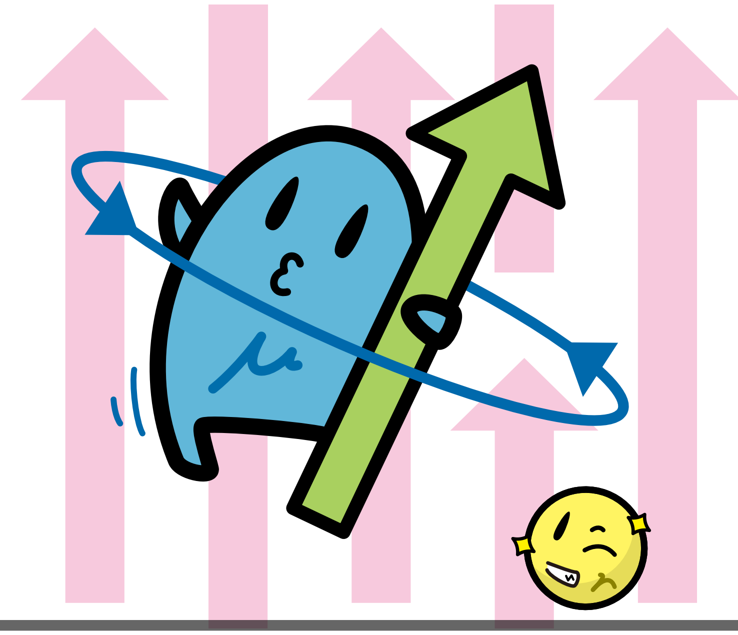

HLBL Contribution to $(g-2)_\mu$

— Pion & Kaon Loops —

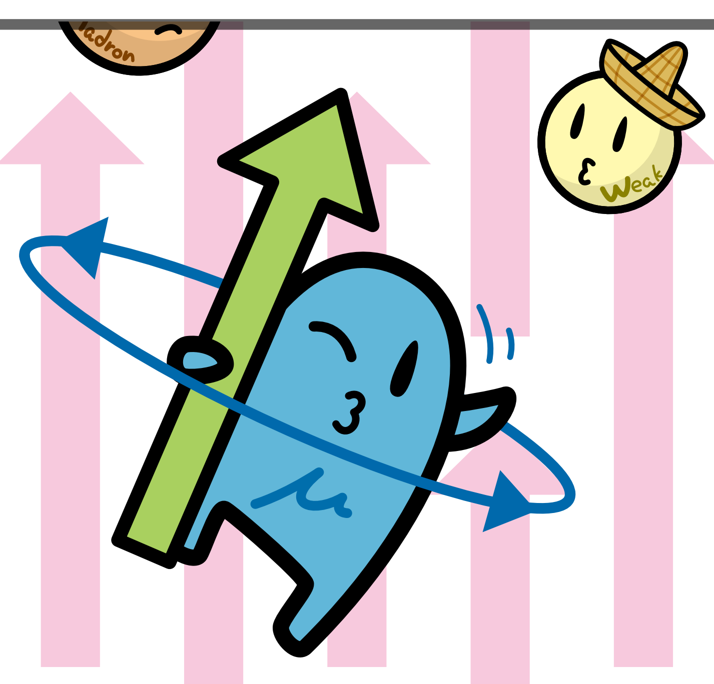

PION & KAON BOX

- Step 1: fixed-s dispersion relation for $\gamma^* \gamma^* \to \pi^+\pi^-$:
  - Requires BTT tensor decomposition for $\gamma^* \gamma^* \to \pi^+\pi^-$
  - Coincides with scalar QED supplemented with electromagnetic form factors

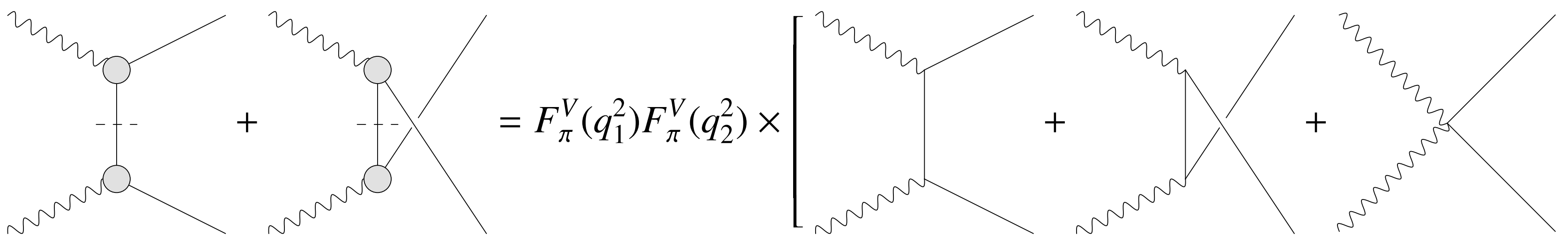

PION & KAON BOX

- Step 1: fixed-s dispersion relation for $\gamma^*\gamma^* \to \pi^+\pi^-$:
  - Requires BTT tensor decomposition for $\gamma^*\gamma^* \to \pi^+\pi^-$
  - Coincides with scalar QED supplemented with electromagnetic form factors

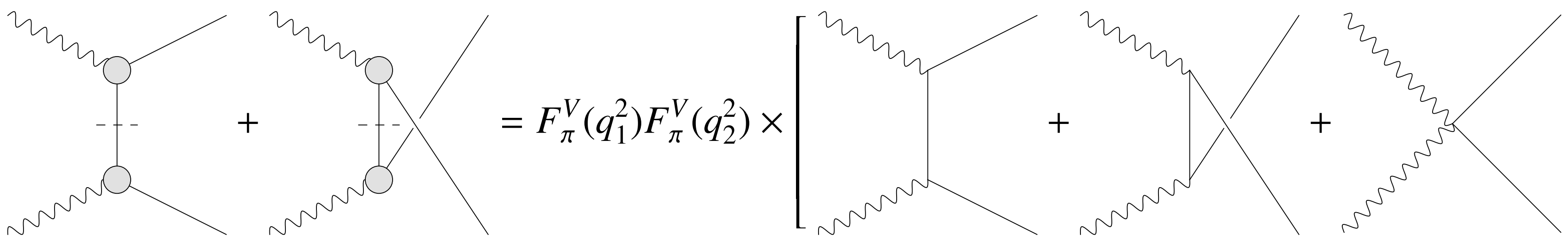

- Step 2: double-dipsersion relation for pion box:

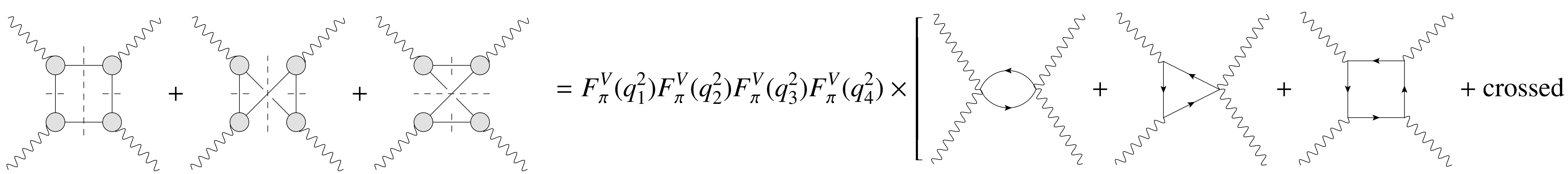

$$\Pi_i^{\pi\text{-box}}(s,t,u;q_i^2) = F_\pi^V(q_1^2)F_\pi^V(q_2^2)F_\pi^V(q_3^2)F_\pi^V(q_4^2)$$
$$\times\left(\frac{1}{\pi^2}\int ds'dt'\,\frac{\rho_{i;st}(s',t')}{(s'-s)(t'-t)} + \frac{1}{\pi^2}\int ds'du'\,\frac{\rho_{i;su}(s',u')}{(s'-s)(u'-u)} + \frac{1}{\pi^2}\int dt'du'\,\frac{\rho_{i;tu}(t',u')}{(t'-t)(u'-u)}\right)$$

PION & KAON BOX

- Step 1: fixed-s dispersion relation for $\gamma^* \gamma^* \to \pi^+\pi^-$:
  - Requires BTT tensor decomposition for $\gamma^* \gamma^* \to \pi^+\pi^-$
  - Coincides with scalar QED supplemented with electromagnetic form factors

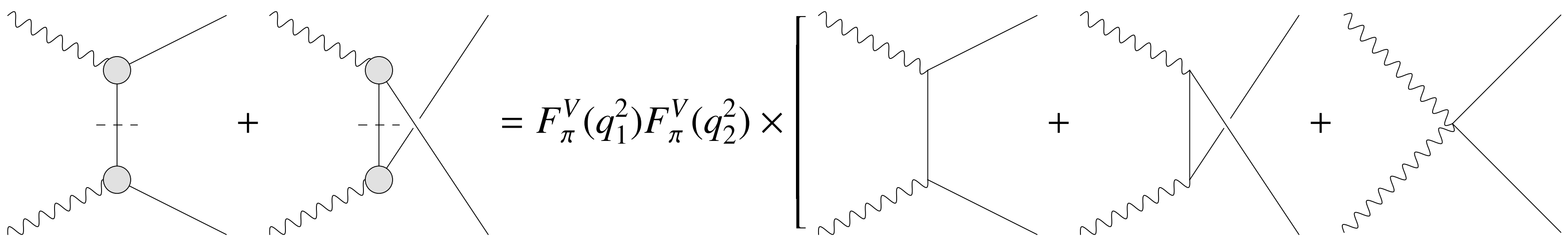

- Step 2: double-dipsersion relation for pion box:

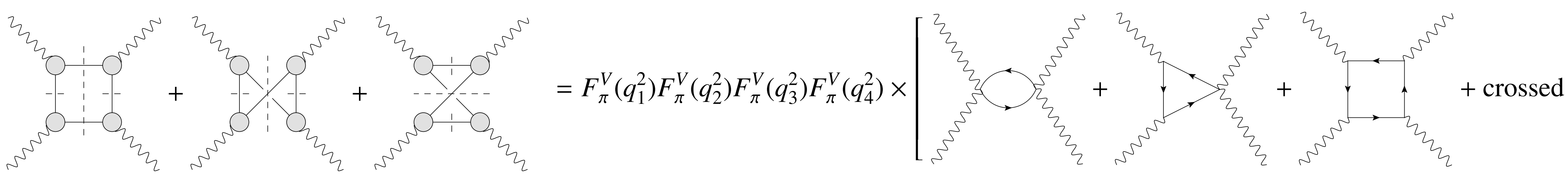

$$\Pi_i^{\pi\text{-box}}(s,t,u;q_i^2) = F_\pi^V(q_1^2) F_\pi^V(q_2^2) F_\pi^V(q_3^2) F_\pi^V(q_4^2)$$
$$\times \left(\frac{1}{\pi^2} \int ds' dt' \frac{\rho_{i;st}(s',t')}{(s'-s)(t'-t)} + \frac{1}{\pi^2} \int ds' du' \frac{\rho_{i;su}(s',u')}{(s'-s)(u'-u)} + \frac{1}{\pi^2} \int dt' du' \frac{\rho_{i;tu}(t',u')}{(t'-t)(u'-u)} \right)$$

- Equivalently for kaon box $\bar{\Pi}_i^{K\text{-box}}(q_1^2,q_2^2,q_3^2) = F_K^V(q_1^2) F_K^V(q_2^2) F_K^V(q_3^2) \frac{1}{16\pi^2} \int_0^1 dx \int_0^{1-x} dy\, I_i^K(x,y)$

PION & KAON BOX

- Step 1: fixed-s dispersion relation for $\gamma^*\gamma^* \to \pi^+\pi^-$:
  - Requires BTT tensor decomposition for $\gamma^*\gamma^* \to \pi^+\pi^-$
  - Coincides with scalar QED supplemented with electromagnetic form factors

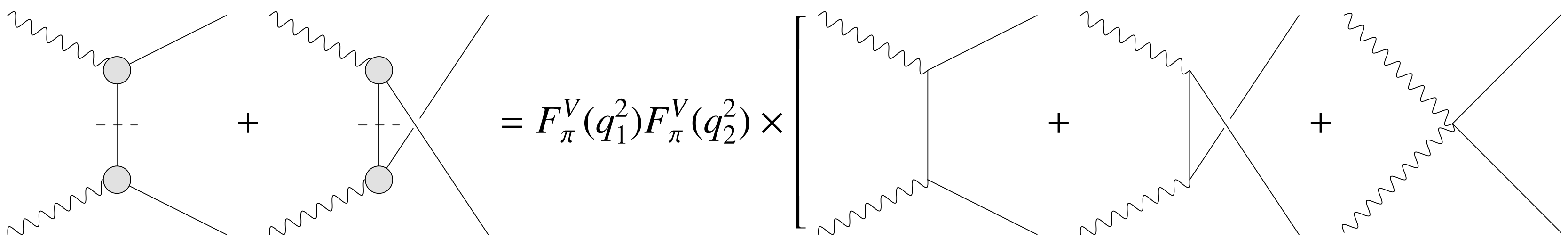

- Step 2: double-dipsersion relation for pion box:

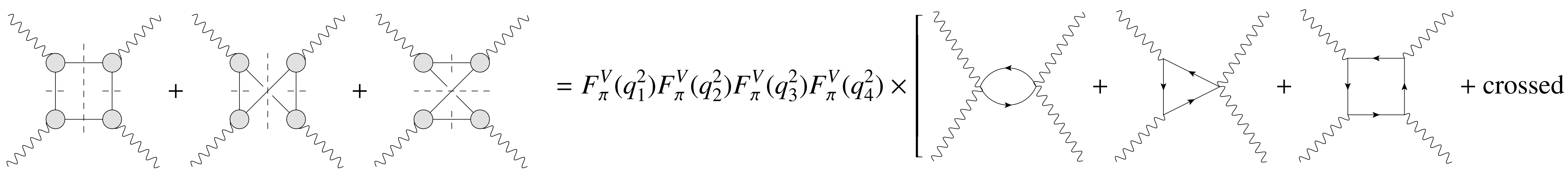

$$\Pi_i^{\pi\text{-box}}(s,t,u;q_i^2) = F_\pi^V(q_1^2)F_\pi^V(q_2^2)F_\pi^V(q_3^2)F_\pi^V(q_4^2)$$
$$\times\left(\frac{1}{\pi^2}\int ds'dt'\frac{\rho_{i;st}(s',t')}{(s'-s)(t'-t)} + \frac{1}{\pi^2}\int ds'du'\frac{\rho_{i;su}(s',u')}{(s'-s)(u'-u)} + \frac{1}{\pi^2}\int dt'du'\frac{\rho_{i;tu}(t',u')}{(t'-t)(u'-u)}\right)$$

- Equivalently for kaon box $\bar{\Pi}_i^{K\text{-box}}(q_1^2,q_2^2,q_3^2) = F_K^V(q_1^2)F_K^V(q_2^2)F_K^V(q_3^2)\frac{1}{16\pi^2}\int_0^1 dx\int_0^{1-x} dy\, I_i^K(x,y)$
- Empirical input: pion and kaon vector form factors

Martin Hoferichter

D. Stamen, D. Hariharan, M. Hoferichter, B. Kubis, P. Stoffer, EPJC 82 (2022) 5, 432

PION & KAON BOX

$$a_\mu^{\pi-\text{box}} = -\,15.9(2)\times 10^{-11}$$
$$a_\mu^{K-\text{box}} = -\,0.5(1)\times 10^{-11}$$

- Step 1: fixed-s dispersion relation for $\gamma^*\gamma^* \to \pi^+\pi^-$:
  - Requires BTT tensor decomposition for $\gamma^*\gamma^* \to \pi^+\pi^-$
  - Coincides with scalar QED supplemented with electromagnetic form factors

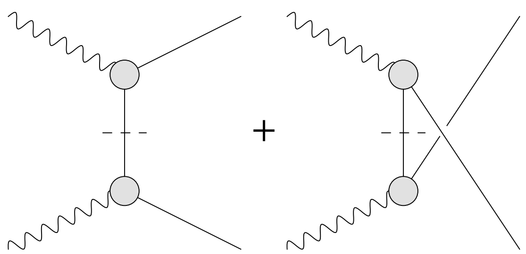

$= F_\pi^V(q_1^2)F_\pi^V(q_2^2)\times$

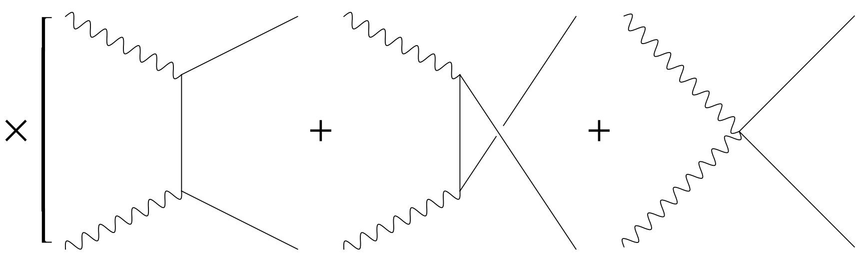

- Step 2: double-dipsersion relation for pion box:

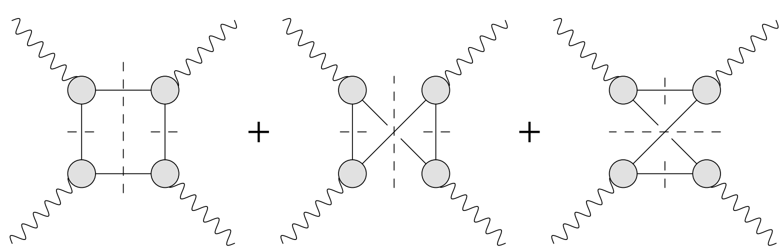

$= F_\pi^V(q_1^2)F_\pi^V(q_2^2)F_\pi^V(q_3^2)F_\pi^V(q_4^2)\times$

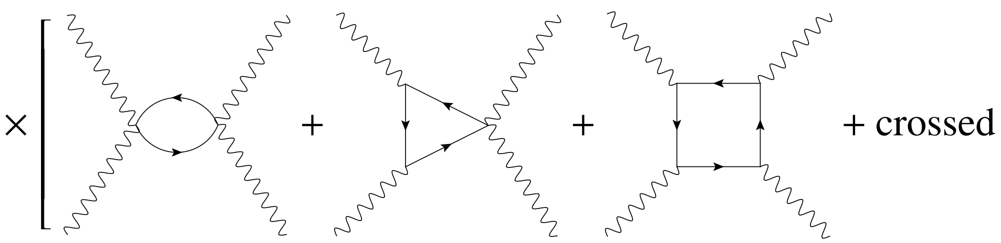

$$\Pi_i^{\pi\text{-box}}(s,t,u;q_i^2) = F_\pi^V(q_1^2)F_\pi^V(q_2^2)F_\pi^V(q_3^2)F_\pi^V(q_4^2)$$
$$\times\left(\frac{1}{\pi^2}\int ds'dt'\,\frac{\rho_{i;st}(s',t')}{(s'-s)(t'-t)} + \frac{1}{\pi^2}\int ds'du'\,\frac{\rho_{i;su}(s',u')}{(s'-s)(u'-u)} + \frac{1}{\pi^2}\int dt'du'\,\frac{\rho_{i;tu}(t',u')}{(t'-t)(u'-u)}\right)$$

- Equivalently for kaon box $\bar{\Pi}_i^{K\text{-box}}(q_1^2,q_2^2,q_3^2) = F_K^V(q_1^2)F_K^V(q_2^2)F_K^V(q_3^2)\frac{1}{16\pi^2}\int_0^1 dx\int_0^{1-x} dy\, I_i^K(x,y)$
- Empirical input: pion and kaon vector form factors

D. Stamen, D. Hariharan, M. Hoferichter, B. Kubis, P. Stoffer, EPJC 82 (2022) 5, 432

Martin Hoferichter

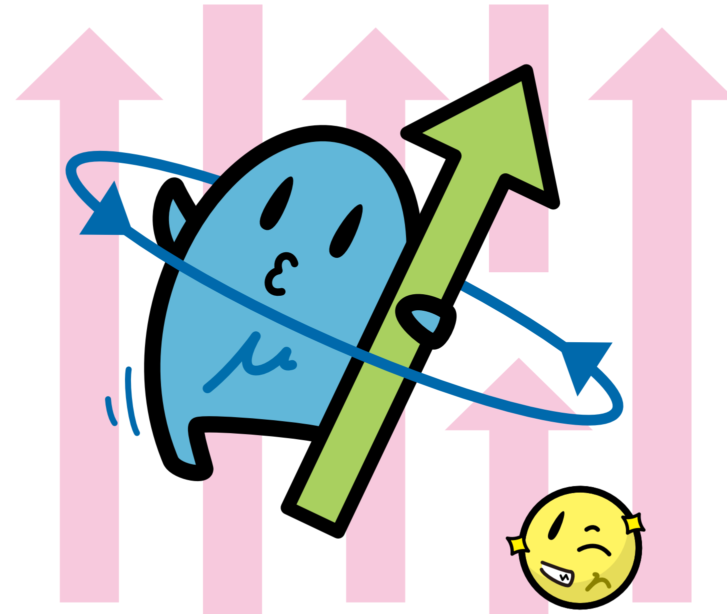

HLBL Contribution to $(g-2)_\mu$

— Rescattering —

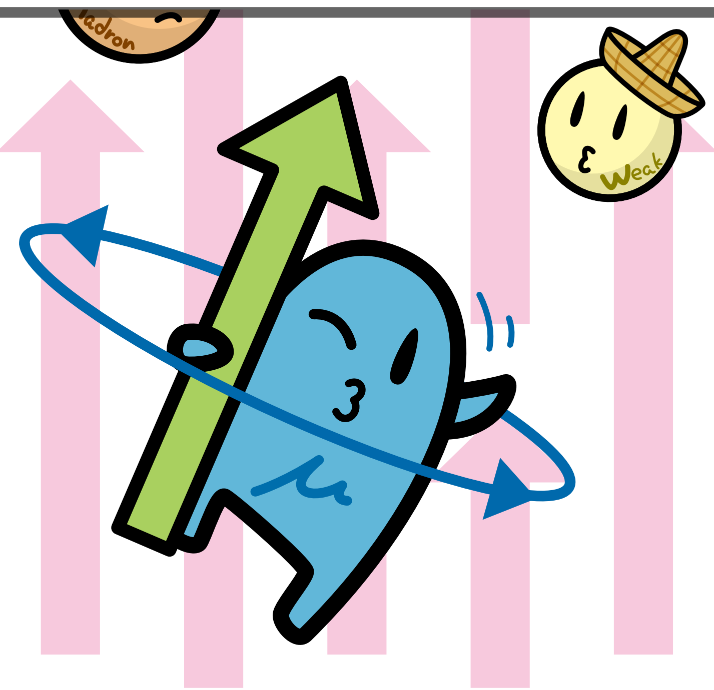

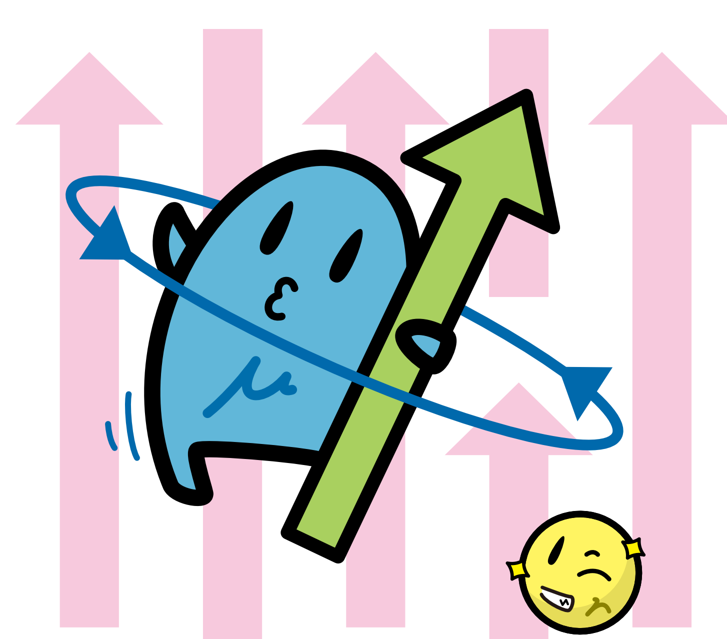

Oleksandra Deineka
(MTHS school, Bochum)

HLBL Contribution to $(g-2)_\mu$

— Rescattering —

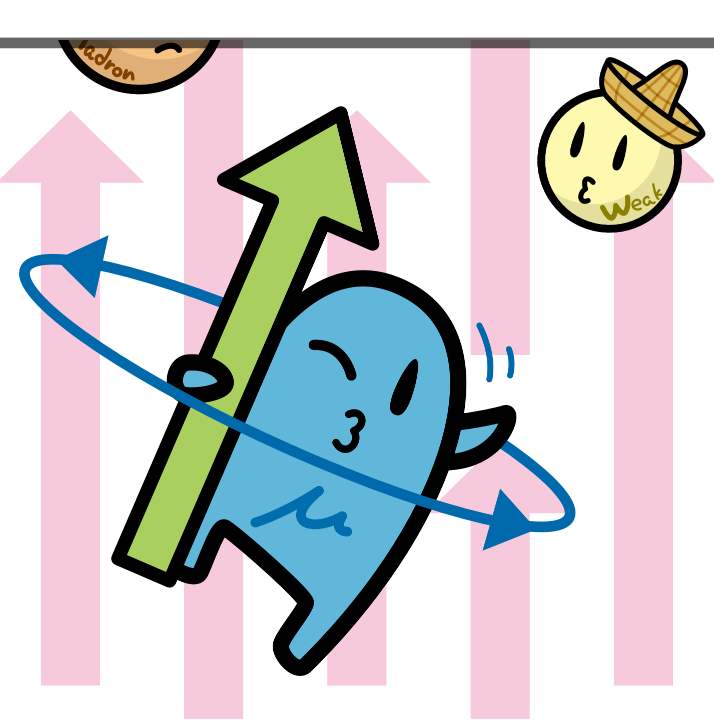

PION RESCATTERING

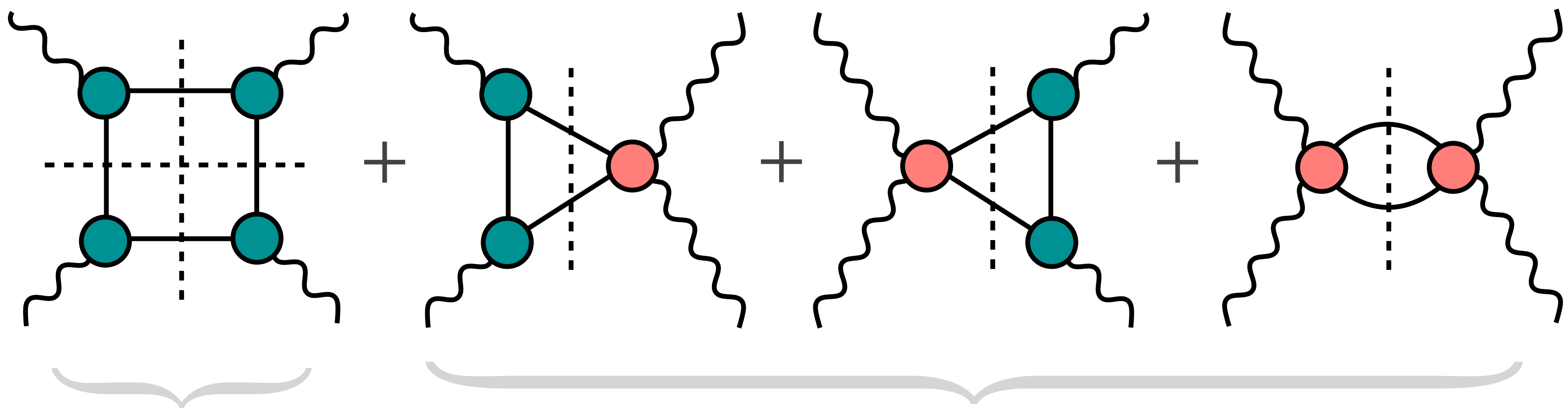

pion/kaon box rescattering contribution

PION RESCATTERING

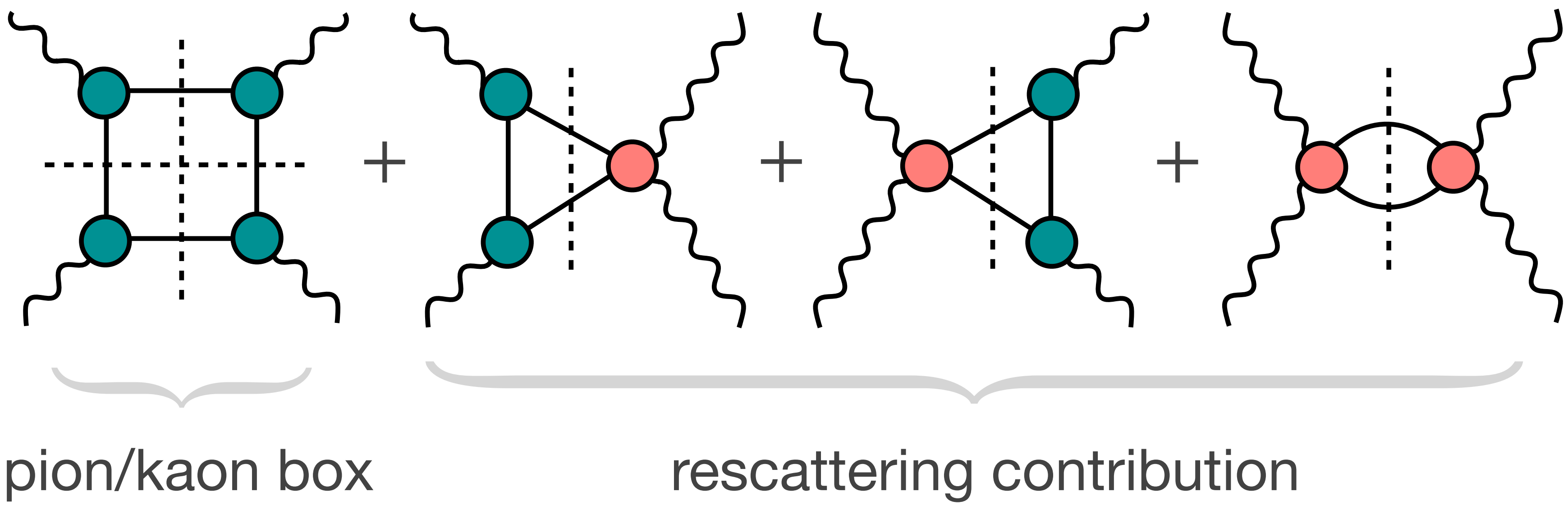

Important ingredients:
$\gamma^*\gamma^* \to \pi\pi, \pi\eta, \dots$
for spacelike γ^*

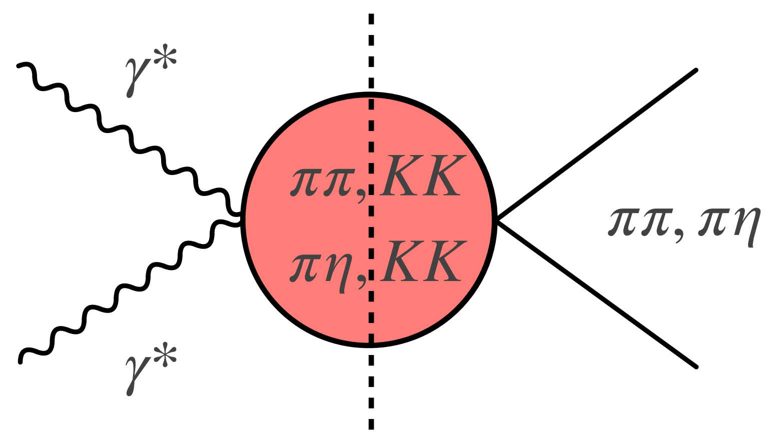

PION RESCATTERING

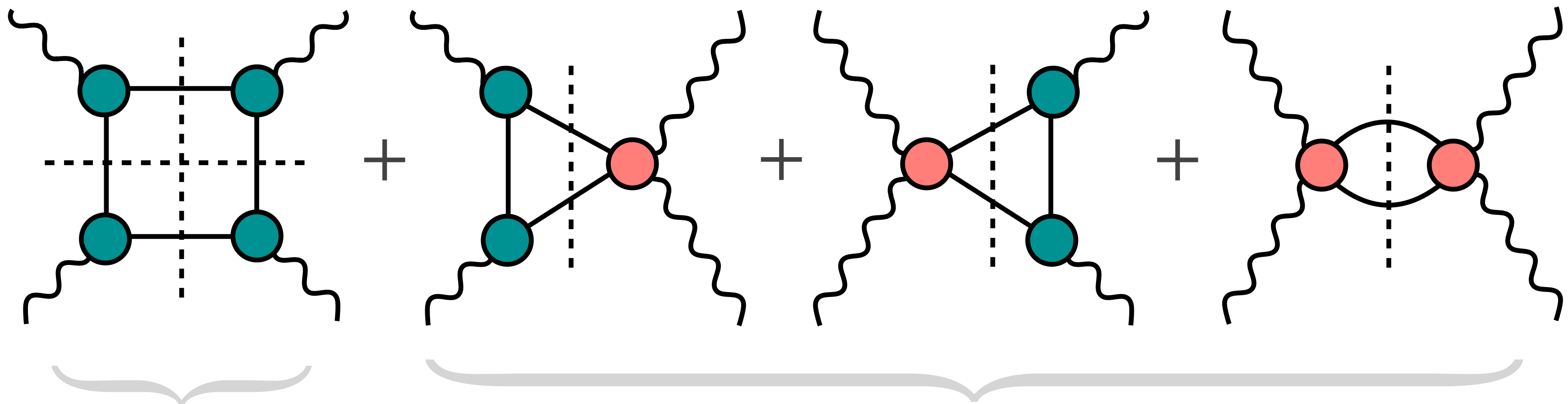

pion/kaon box | rescattering contribution

Important ingredients:
$\gamma^*\gamma^* \to \pi\pi, \pi\eta, \ldots$
for spacelike γ^*

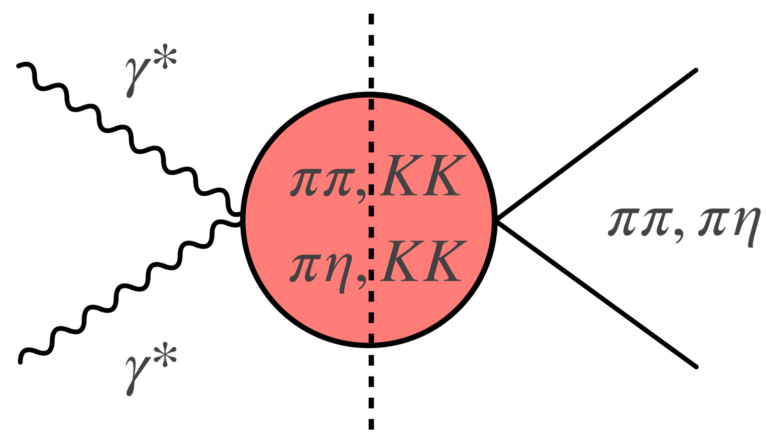

so far included:

S-wave $\pi\pi$ re-scattering

PION RESCATTERING

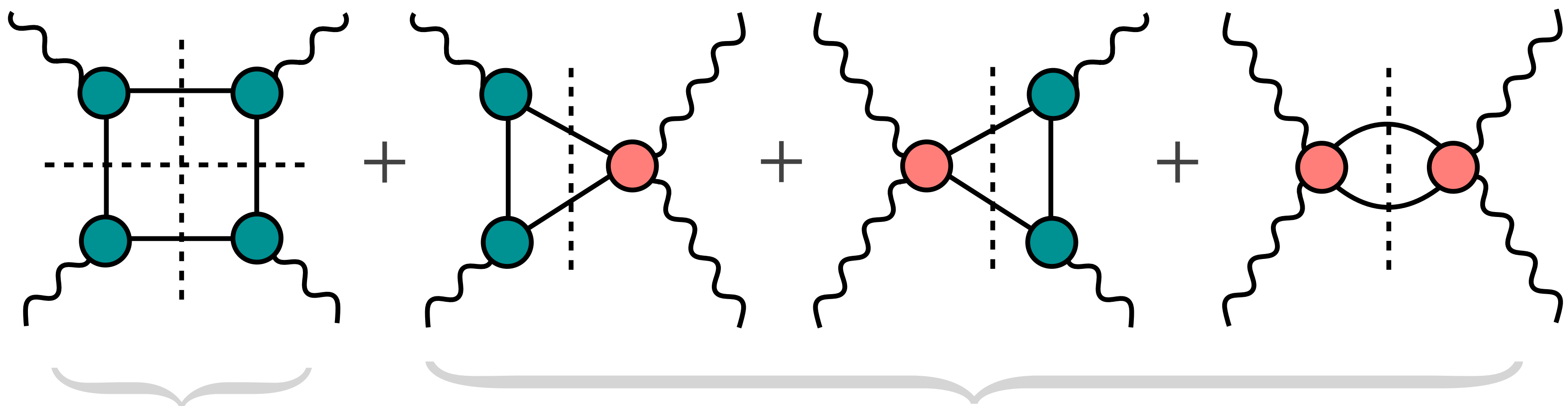

pion/kaon box

rescattering contribution

Important ingredients:
$\gamma^*\gamma^* \to \pi\pi, \pi\eta, \ldots$
for spacelike γ^*

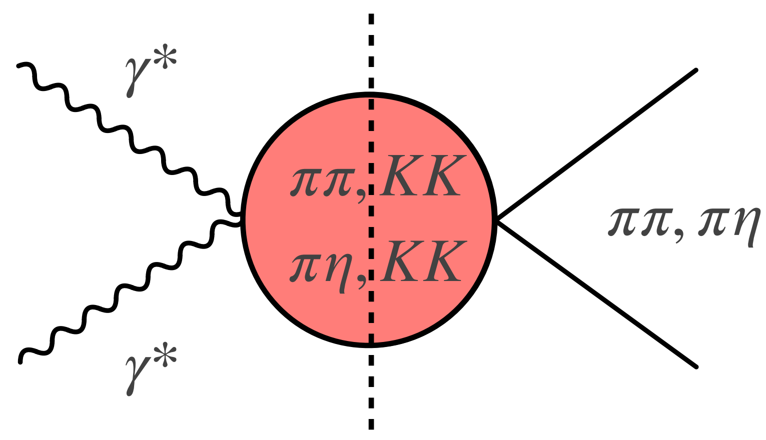

<u>so far included</u>:

S-wave $\pi\pi$ re-scattering

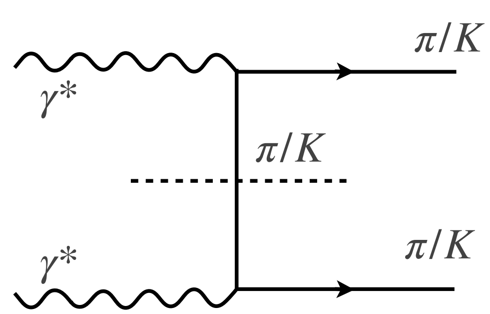

with π-pole left-hand cut

PION RESCATTERING

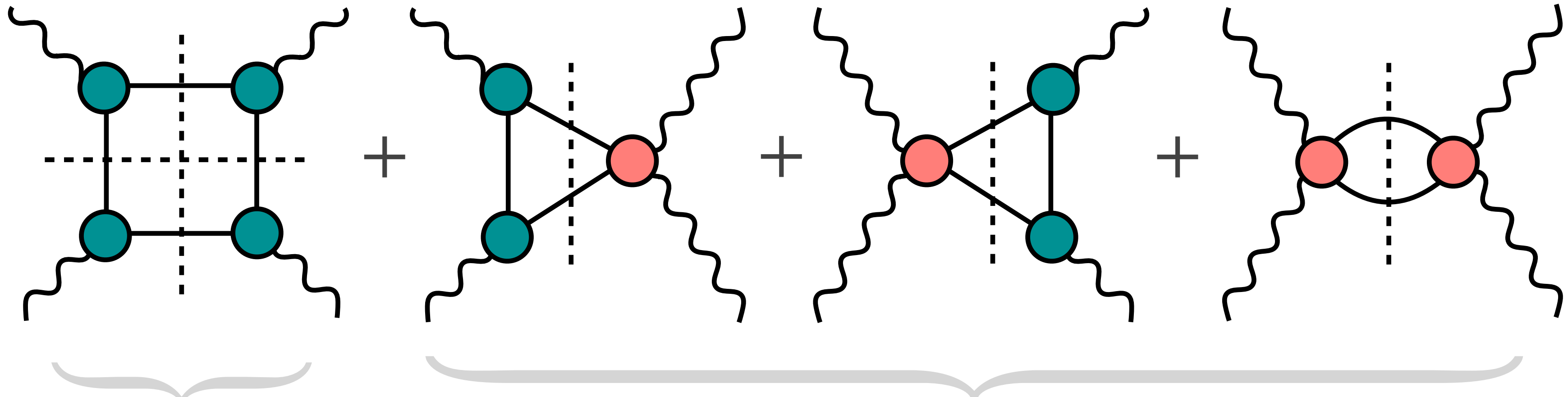

pion/kaon box

rescattering contribution

$$a_{\mu, J=0}^{\pi\pi,\pi-\text{pole, LHC}} = -8(1) \times 10^{-11}$$

Important ingredients:
$\gamma^*\gamma^* \to \pi\pi, \pi\eta, \ldots$
for spacelike γ^*

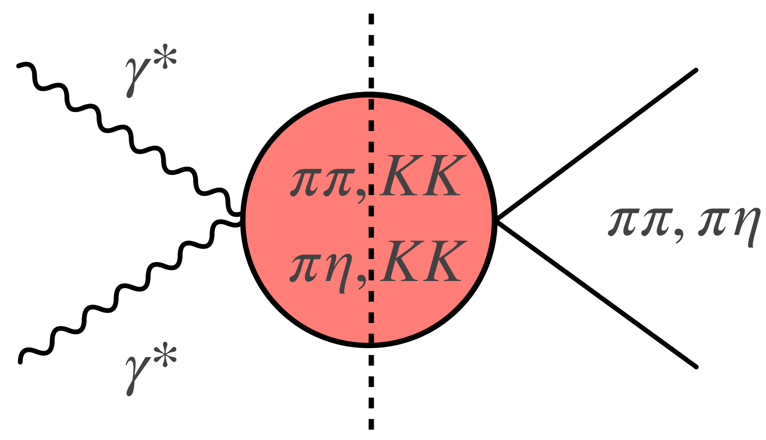

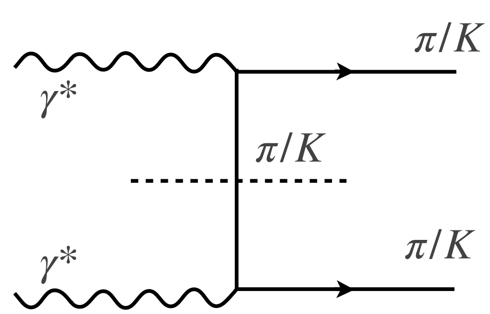

<u>so far included</u>:

S-wave $\pi\pi$ re-scattering

with π-pole left-hand cut

HELICITY PARTIAL WAVES

S-wave amplitudes free from kinematic constraints

$$\bar{h}^{(0)}_{i=1,2} = \frac{\bar{h}^{(0)}_{++} \mp Q_1 Q_2 \bar{h}^{(0)}_{00}}{s - s^{(\mp)}_{\text{kin}}}\,, \qquad s^{(\pm)}_{\text{kin}} \equiv -\,(Q_1 \pm Q_2)^2$$

Can write a **dispersion relation**

$$\bar{h}^{J}_{i}(s) = \int_{-\infty}^{s_L} \frac{ds'}{\pi} \frac{\text{Disc}\,\bar{h}^{(J)}_{i}(s')}{s' - s} + \int_{s_{th}}^{\infty} \frac{ds'}{\pi} \frac{\text{Disc}\,\bar{h}^{(J)}_{i}(s')}{s' - s}$$

Coupled-channel unitarity

$$\text{Disc}\,h^{(J)}_{i,a}(s) = \sum_{b=1,2} t^{(J)*}_{ab}(s)\,\rho_b(s)\,h^{(J)}_{i,b}(s)$$

hadronic scattering amplitude

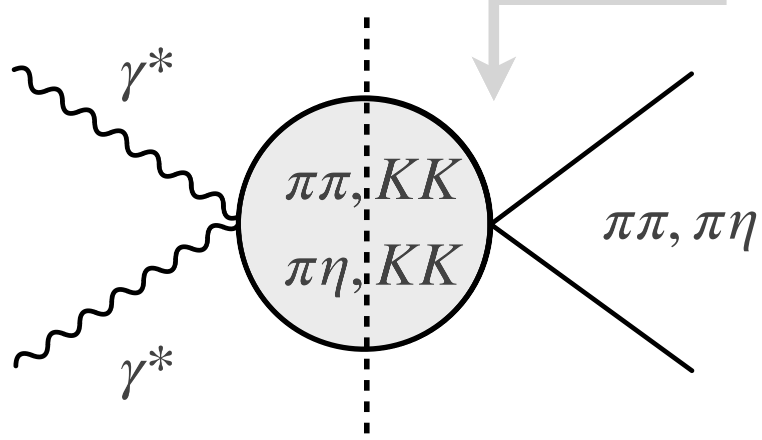

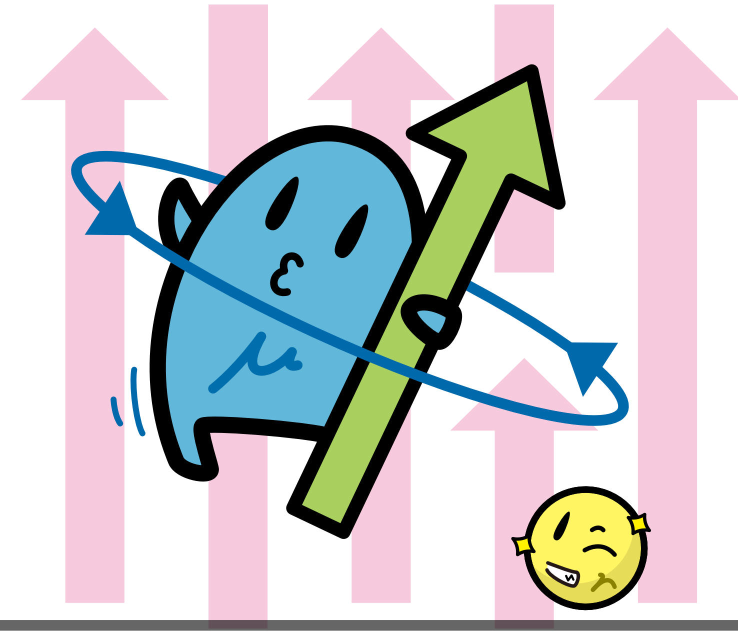

HLBL Contribution to $(g-2)_\mu$

— Scalars & Tensors —

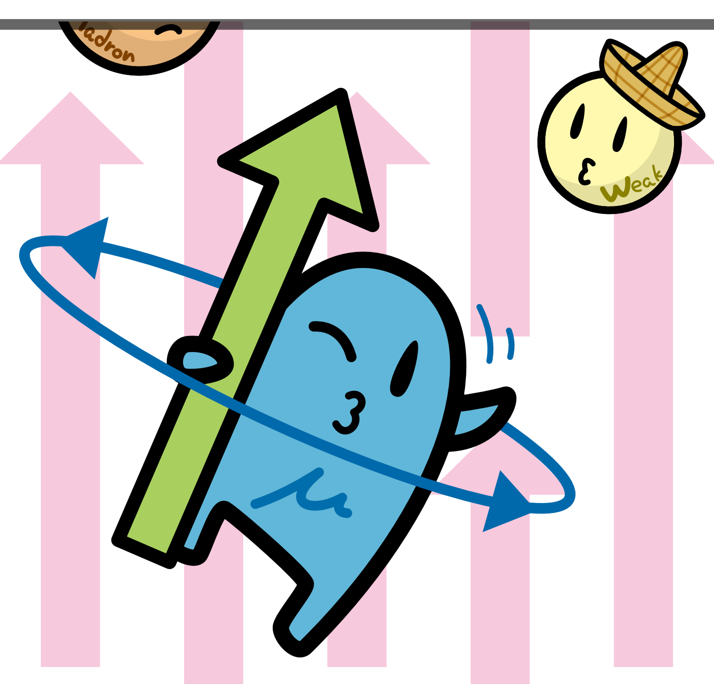

$f_0(980) + a_0(980)$

$\gamma\gamma \to \pi^0\pi^0$

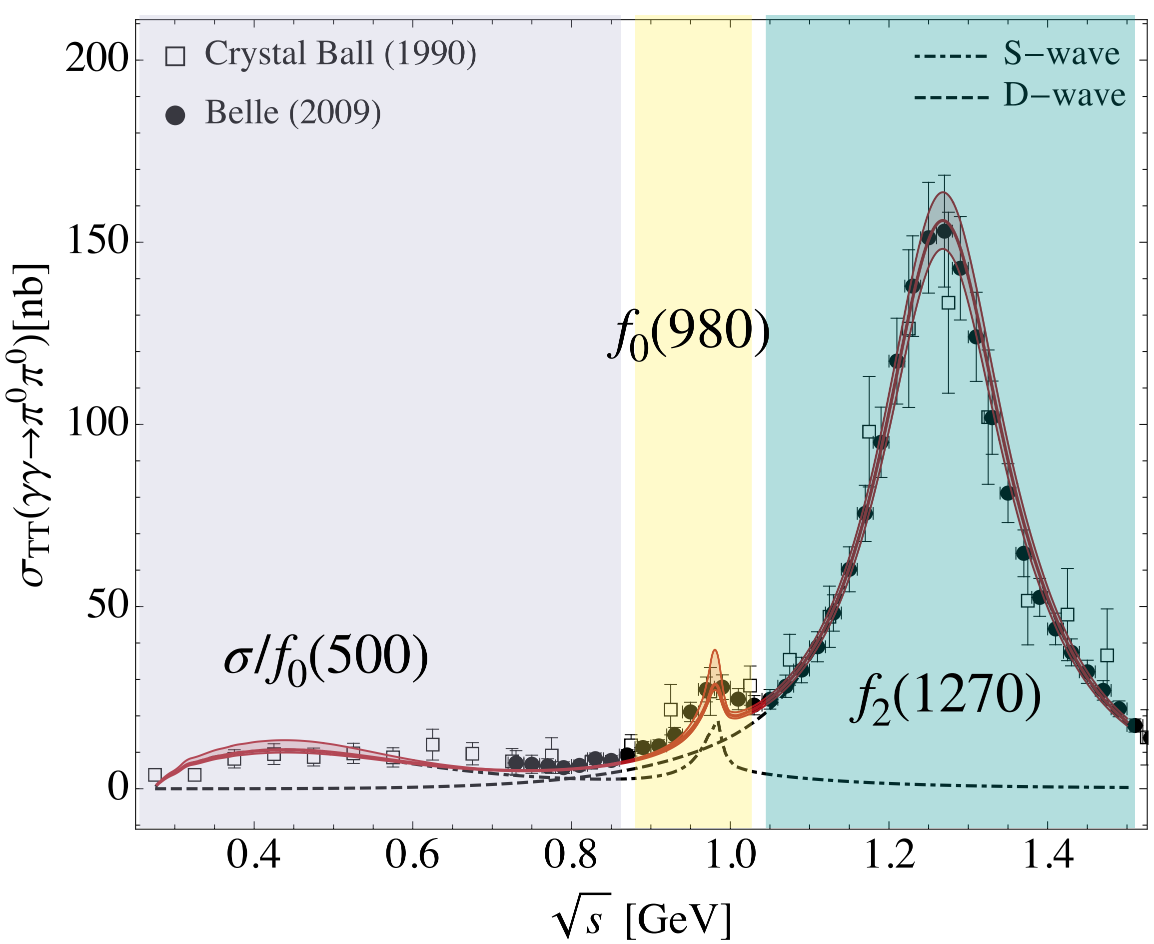

$\gamma\gamma \to \pi^0\eta$

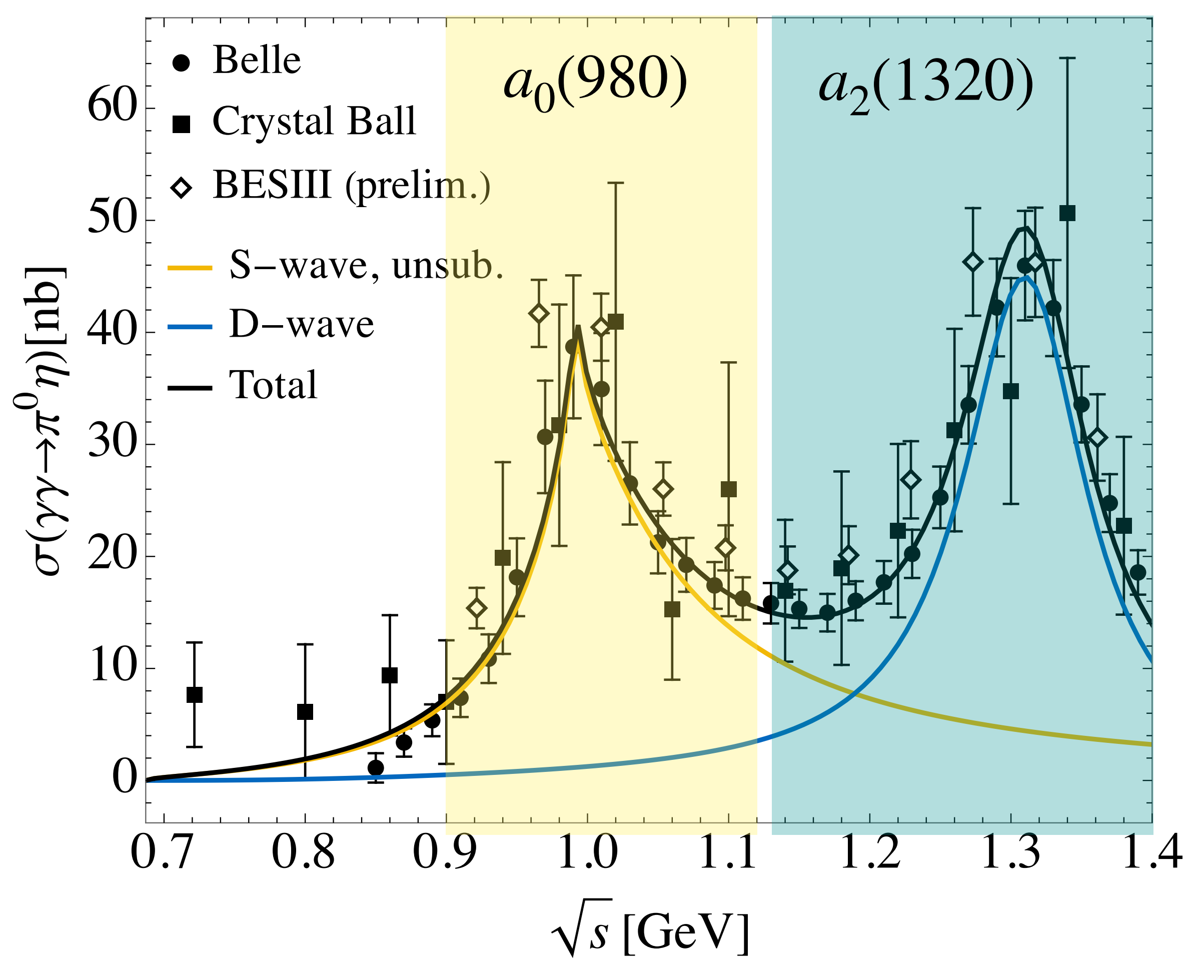

$$a_\mu^{\mathrm{HLbL}}[f_0(980)] = -0.2(2)\times 10^{-11}$$ [Danilkin, Hoferichter, Stoffer (2021)]

$$a_\mu^{\mathrm{HLbL}}[a_0(980)]_{\mathrm{resc.}} = -0.46(2)\times 10^{-11}$$ [Deineka, Danilkin, Vanderhaeghen (2024)]

$$a_\mu^{\mathrm{HLbL}}[\mathrm{tensors}] = 0.9(1)\times 10^{-11}$$

- Broad $f_0(500)$ resonance is covered by present $\pi\pi$ re-scattering implementation
- Heavier resonances require D- and higher waves, as well as coupled-channel ($\pi\pi$, $\pi^0\eta$, KK)

$f_0(980) + a_0(980)$

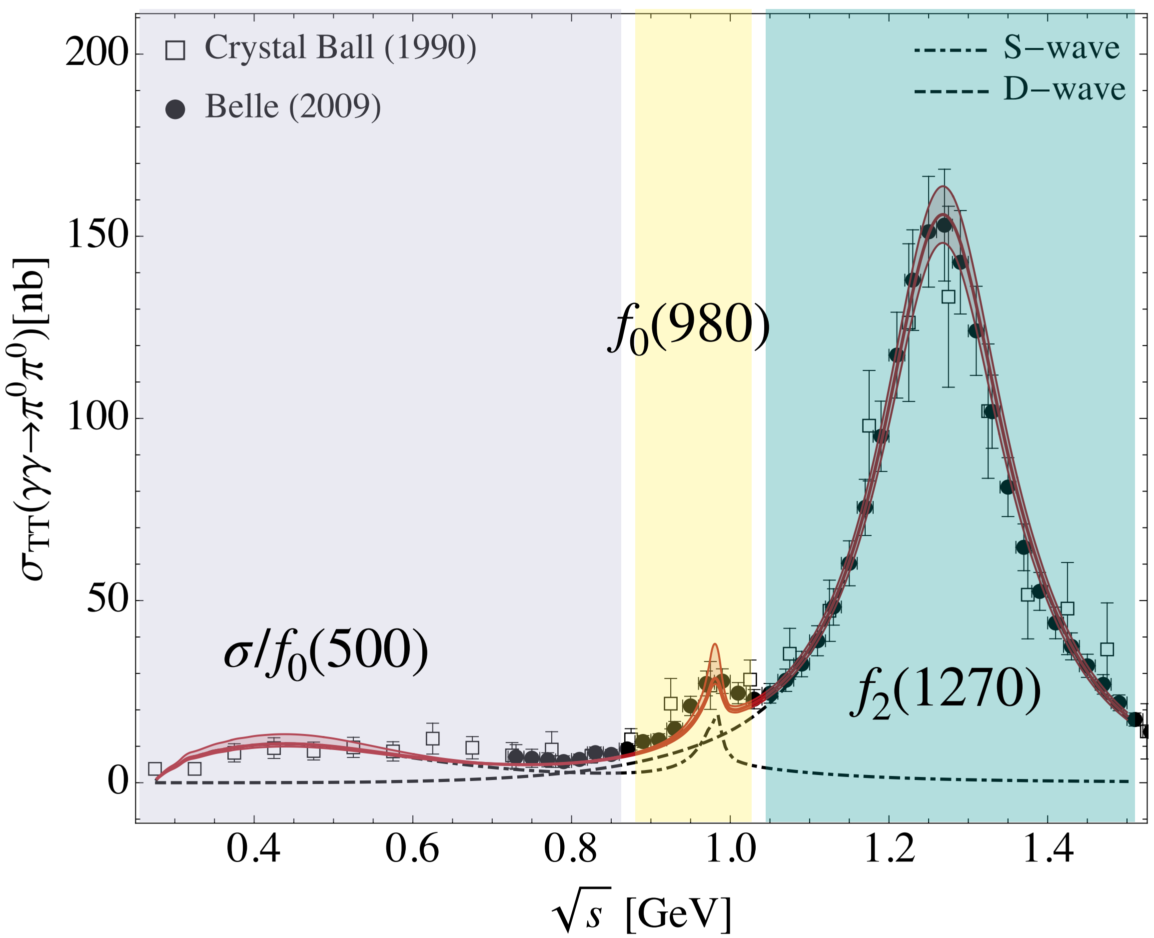

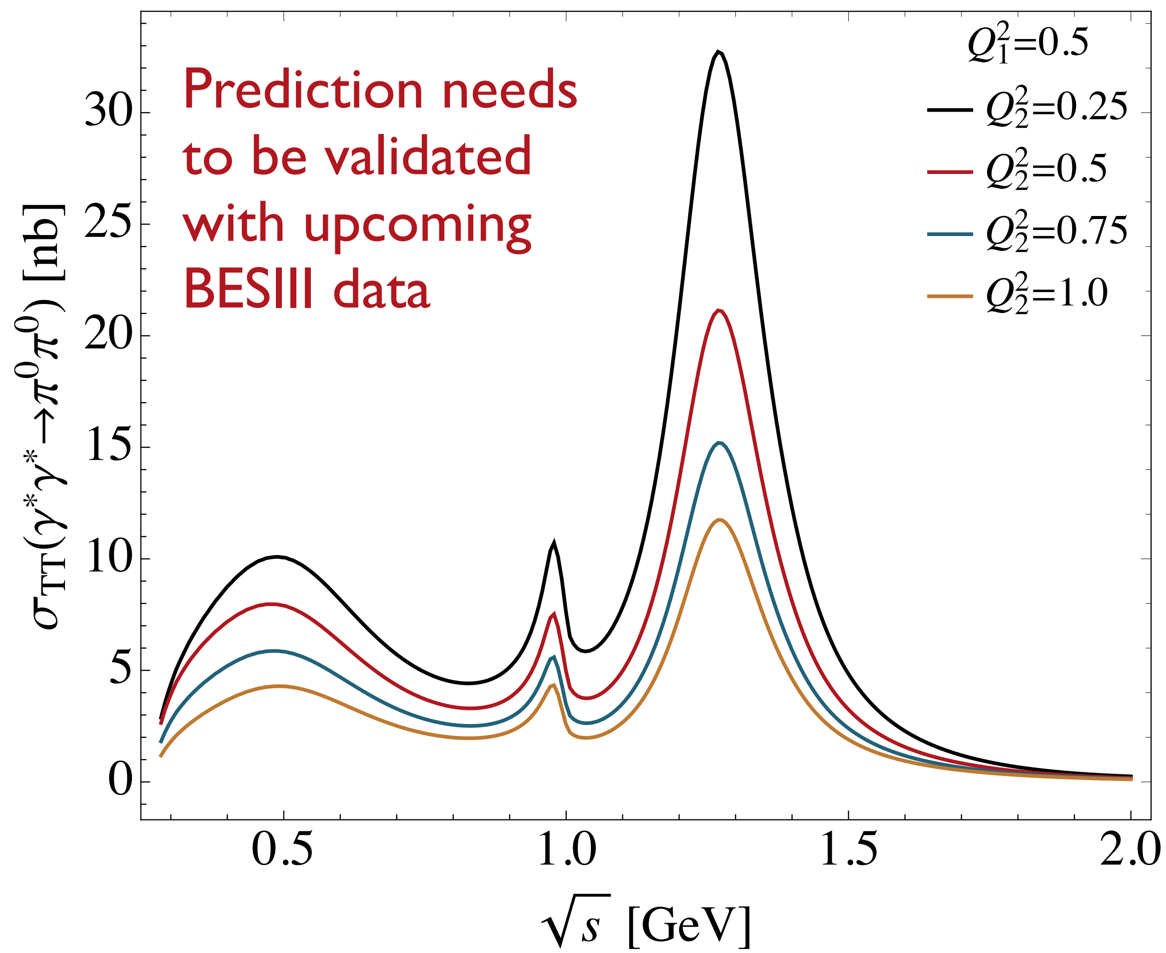

$$a_\mu^{\text{HLbL}}[f_0(980)] = -0.2(2) \times 10^{-11}$$ [Danilkin, Hoferichter, Stoffer (2021)]

$$a_\mu^{\text{HLbL}}[a_0(980)]_{\text{resc.}} = -0.46(2) \times 10^{-11}$$ [Deineka, Danilkin, Vanderhaeghen (2024)]

$$a_\mu^{\text{HLbL}}[\text{tensors}] = 0.9(1) \times 10^{-11}$$

- Broad $f_0(500)$ resonance is covered by present $\pi\pi$ re-scattering implementation
- Heavier resonances require D- and higher waves, as well as coupled-channel ($\pi\pi$, $\pi^0\eta$, KK)

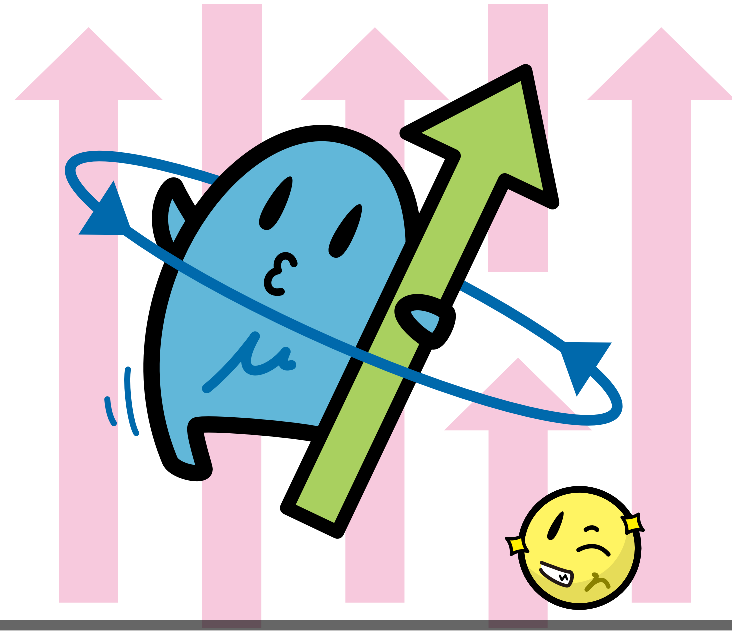

HLBL Contribution to $(g-2)_\mu$

— Pseudoscalar Meson Contributions —

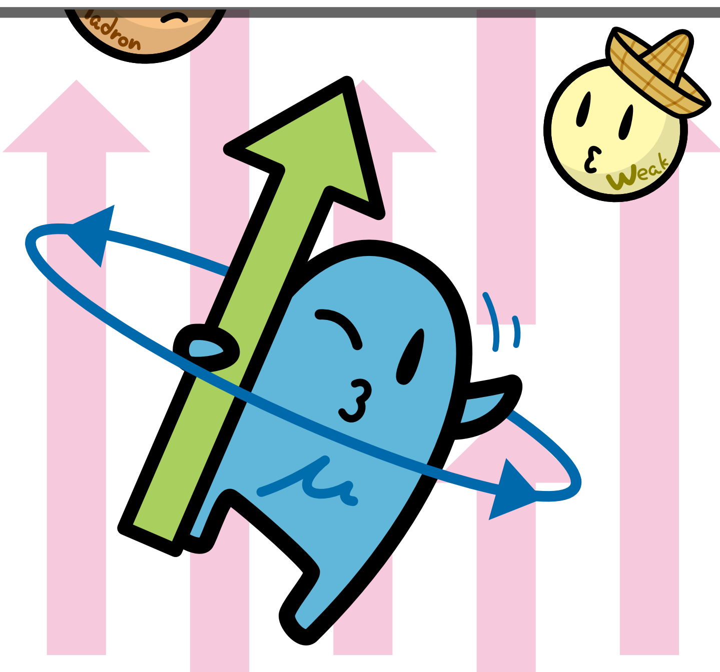

PSEUDOSCALAR-POLE CONTRIBUTION

$$\Pi_1^{\mathrm{P-pole}} = -\frac{F_{P\gamma^*\gamma^*}(-Q_1^2, -Q_2^2)\, F_{P\gamma\gamma^*}(-Q_3^2)}{Q_3^2 + M_P^2}$$

$P = \pi^0,\, \eta,\, \eta'$

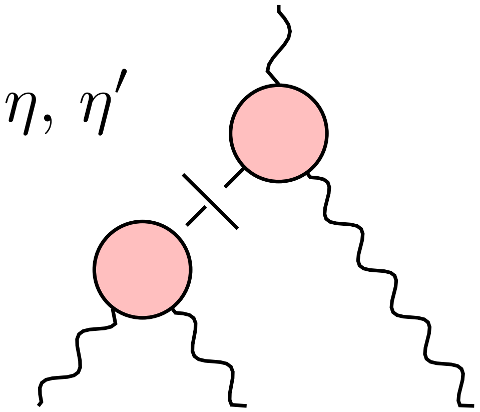

$$a_\mu^{\mathrm{HLbL}} = \frac{2\alpha^3}{3\pi^2} \int_0^\infty dQ_1 \int_0^\infty dQ_2 \int_{-1}^{1} d\tau \sqrt{1-\tau^2}\, Q_1^3 Q_2^3 \sum_{i=1}^{12} T_i(Q_1, Q_2, \tau)\, \bar{\Pi}_i(Q_1, Q_2, \tau)$$

PSEUDOSCALAR-POLE CONTRIBUTION

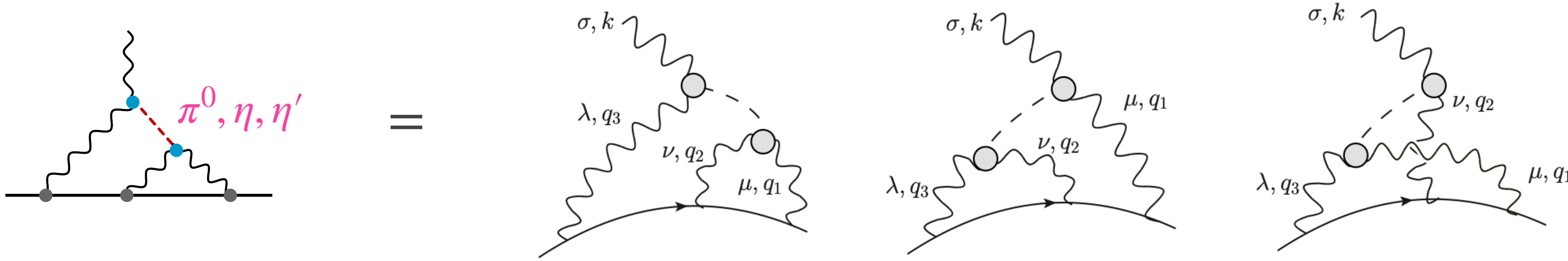

$$a_\mu^{P-\text{pole}} = \left(\frac{\alpha}{\pi}\right)^3 \int \mathrm{d}Q_1 \mathrm{d}Q_2 \mathrm{d}\tau \Big[w_1(Q_1, Q_2, \tau)\, F_{P\gamma^*\gamma^*}(-Q_1^2, -Q_3^2) F_{P\gamma^*\gamma}(-Q_2^2, 0)$$

$$+ w_2(Q_1, Q_2, \tau)\, F_{P\gamma^*\gamma^*}(-Q_1^2, -Q_2^2) F_{P\gamma^*\gamma}(-Q_3^2, 0) \Big]$$

on-shell pseudoscalar transition form factors (TFFs)

kernel functions are peaked at low energies

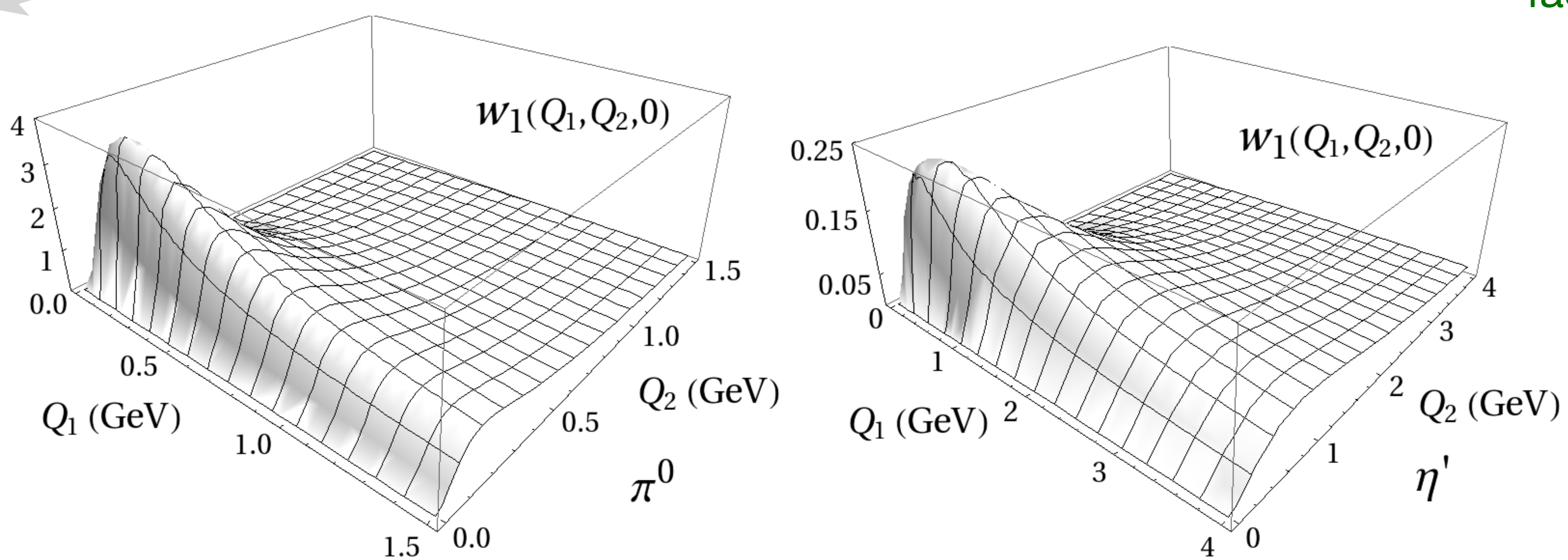

Figure 58: Weight function $w_1(Q_1, Q_2, 0)$ for π^0 (left) and η' (right); cf. Eq. (4.19). Reprinted from Ref. [19].

PSEUDOSCALAR TRANSITION FORM FACTOR

- On-shell pseudoscalar ($P = \pi^0, \eta, \eta'$) transition form factor $F_{P\gamma^*\gamma^*}(q_1^2, q_2^2)$:

$$i\int \mathrm{d}^4x\, e^{iq_1\cdot x}\,\langle 0\,|\,T\{j_\mu(x)j_\nu(0)\}\,|\,P(q_1+q_2)\rangle = \epsilon_{\mu\nu\rho\sigma}q_1^\rho q_2^\sigma F_{P\gamma^*\gamma^*}(q_1^2, q_2^2)$$

- Normalized to the two-photon decay:

$$\Gamma(P\to\gamma\gamma) = \frac{\pi\alpha^2 M_P^3}{4}F_{P\gamma\gamma}^2, \qquad F_{P\gamma\gamma} = F_{P\gamma^*\gamma^*}(0{,}0)$$

- SDCs for pseudoscalar transition form factors (e.g., for the pion):
    - Chiral Anomaly: $F_{\pi^0\gamma\gamma}(0{,}0) = -\dfrac{1}{4\pi^2 f_\pi}$
    - Brodsky-Lepage limit: $\lim\limits_{Q^2\to\infty} F_{\pi^0\gamma\gamma^*}(Q^2) = -\dfrac{2f_\pi}{Q^2}$
    - Symmetric pQCD limit: $\lim\limits_{Q^2\to\infty} F_{\pi^0\gamma^*\gamma^*}(Q^2, Q^2) = -\dfrac{2f_\pi}{3Q^2}$

PION TFF — DISPERSIVE APPROACH

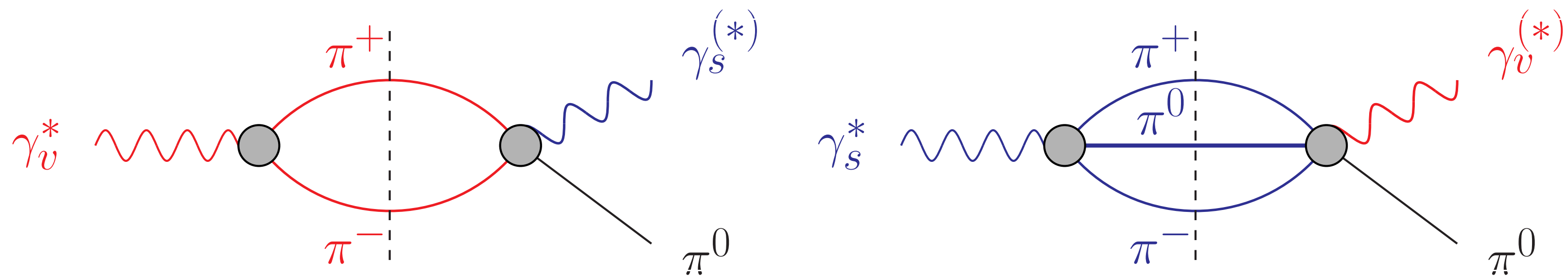

Bastian Kubis (g-2 school 2021)

$$F_{\pi^0\gamma^*\gamma^*} = F^{\text{disp}}_{\pi^0\gamma^*\gamma^*} + F^{\text{eff}}_{\pi^0\gamma^*\gamma^*} + F^{\text{asym}}_{\pi^0\gamma^*\gamma^*}$$

M. Hoferichter, B.-L. Hoid, B. Kubis, S. Leupold, and S. P. Schneider, JHEP 10, 141 (2018)

- Dispersive part:

$$F^{\text{disp}}_{\pi^0\gamma^*\gamma^*}(-Q_1^2,-Q_2^2) = F^{\text{disp}}_{vs}(-Q_1^2,-Q_2^2) + F^{\text{disp}}_{vs}(-Q_2^2,-Q_1^2) = \frac{1}{\pi^2}\int_{4M_\pi^2}^{s_{iv}} \mathrm{d}x \int_{s_{\text{thr}}}^{s_{is}} \mathrm{d}y\, \frac{\rho(x,y)}{(x+Q_1^2)(y+Q_2^2)} + \{q_1 \leftrightarrow q_2\}$$

with $\rho(x,y) = \dfrac{(x/4 - M_\pi^2)^{3/2}}{12\pi\sqrt{x}} \mathrm{Im}[(F_\pi^V(x))^* f_1(x,y)]$

- Asymptotic contribution to ensure pQCD limit:

$$F^{\text{asym}}_{\pi^0\gamma^*\gamma^*}(-Q_1^2,-Q_2^2) = 2f_\pi \int_{s_m}^{\infty} \mathrm{d}x \frac{Q_1^2 Q_2^2}{(x+Q_1^2)^2(y+Q_2^2)^2}$$

- Effective pole ($M_{\text{eff}} \sim 1.5 - 2\,\text{GeV}$) parametrising heavier intermediate states:

$$F^{\text{eff}}_{\pi^0\gamma^*\gamma^*}(-Q_1^2,-Q_2^2) = \frac{g_{\text{eff}}}{4\pi^2 f_\pi} \frac{M_{\text{eff}}^4}{(M_{\text{eff}}^2+Q_1^2)(M_{\text{eff}}^2+Q_2^2)}$$

EMPIRICAL INPUT — REMINDER

Hadronic light-by-light scattering: data input

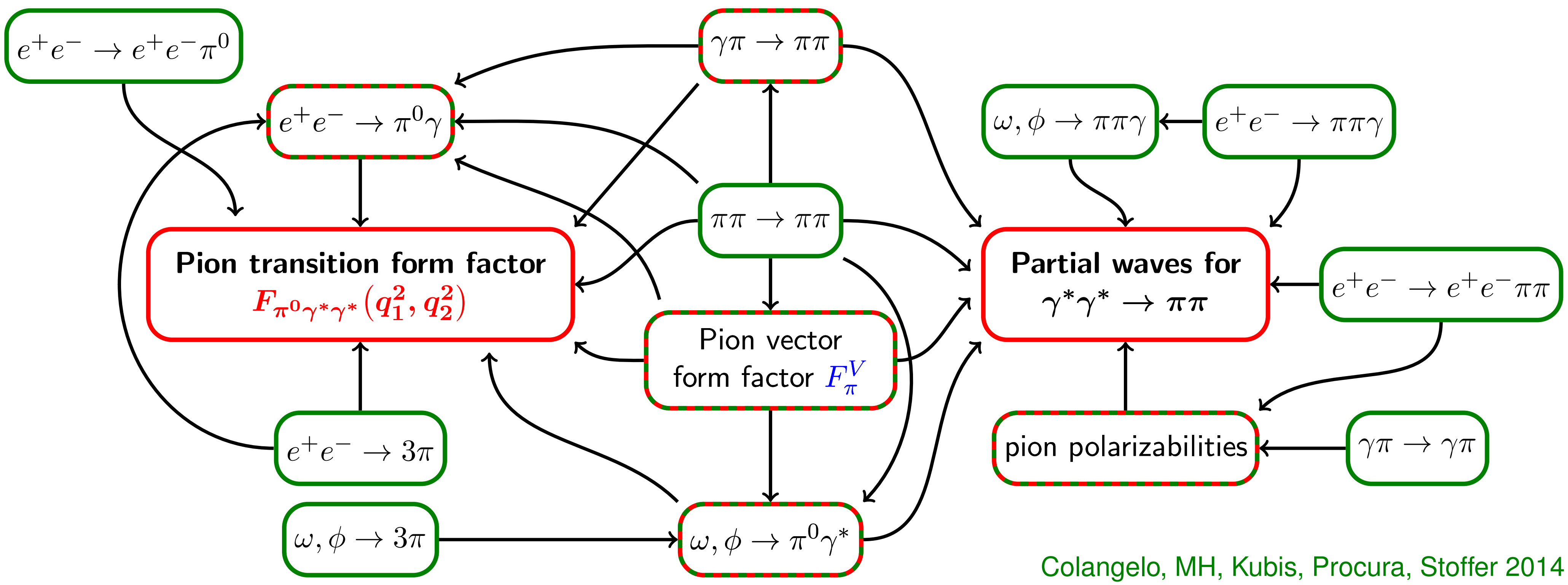

Colangelo, MH, Kubis, Procura, Stoffer 2014

- Reconstruction of $\gamma^*\gamma^* \to \pi\pi, \pi^0$: combine experiment and theory constraints
- Need input on $\gamma^*\gamma^*$ matrix elements for as many states as possible

PION

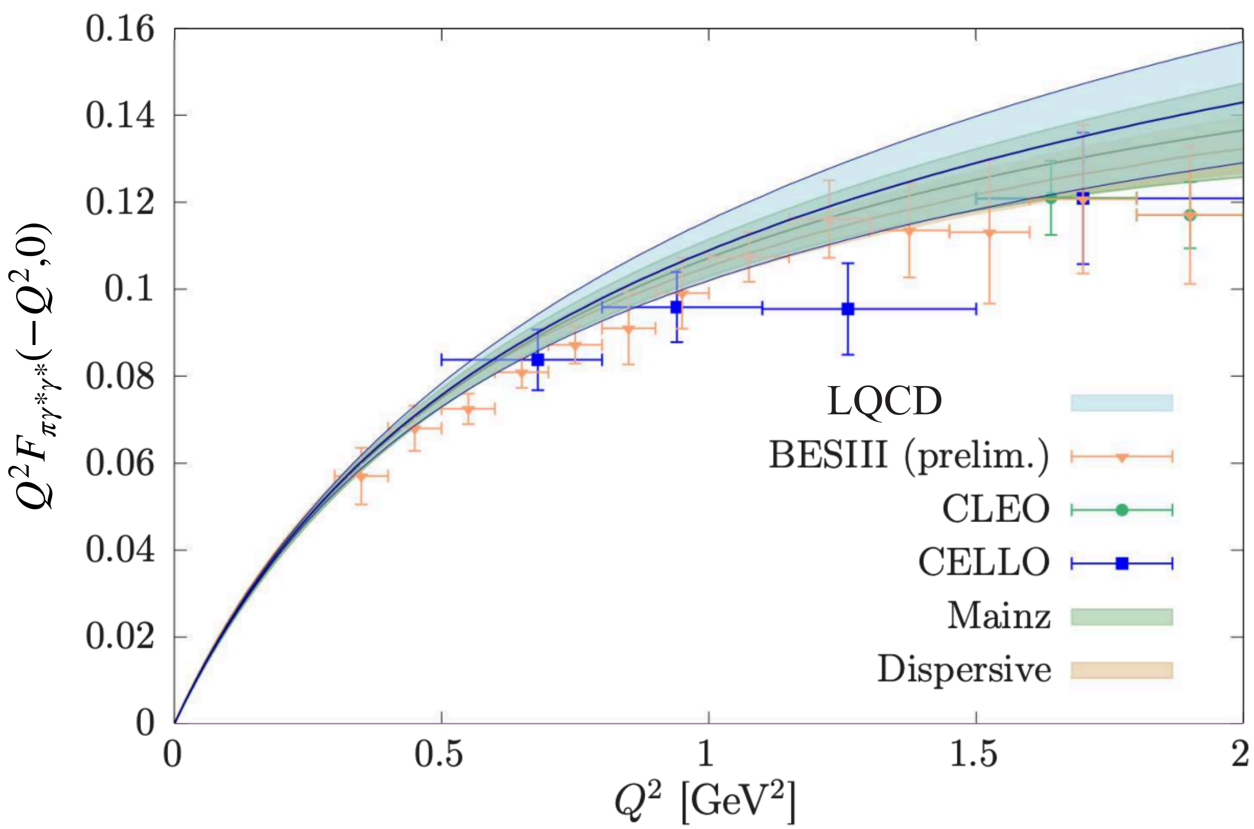

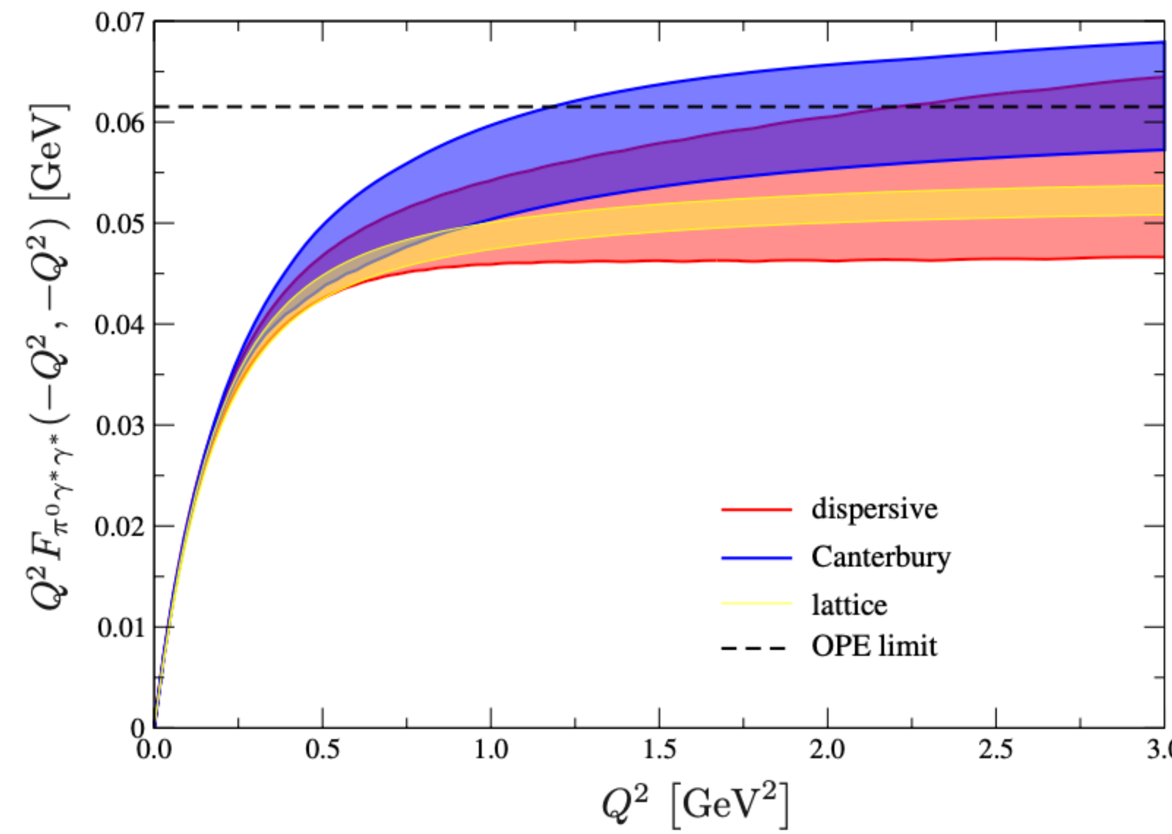

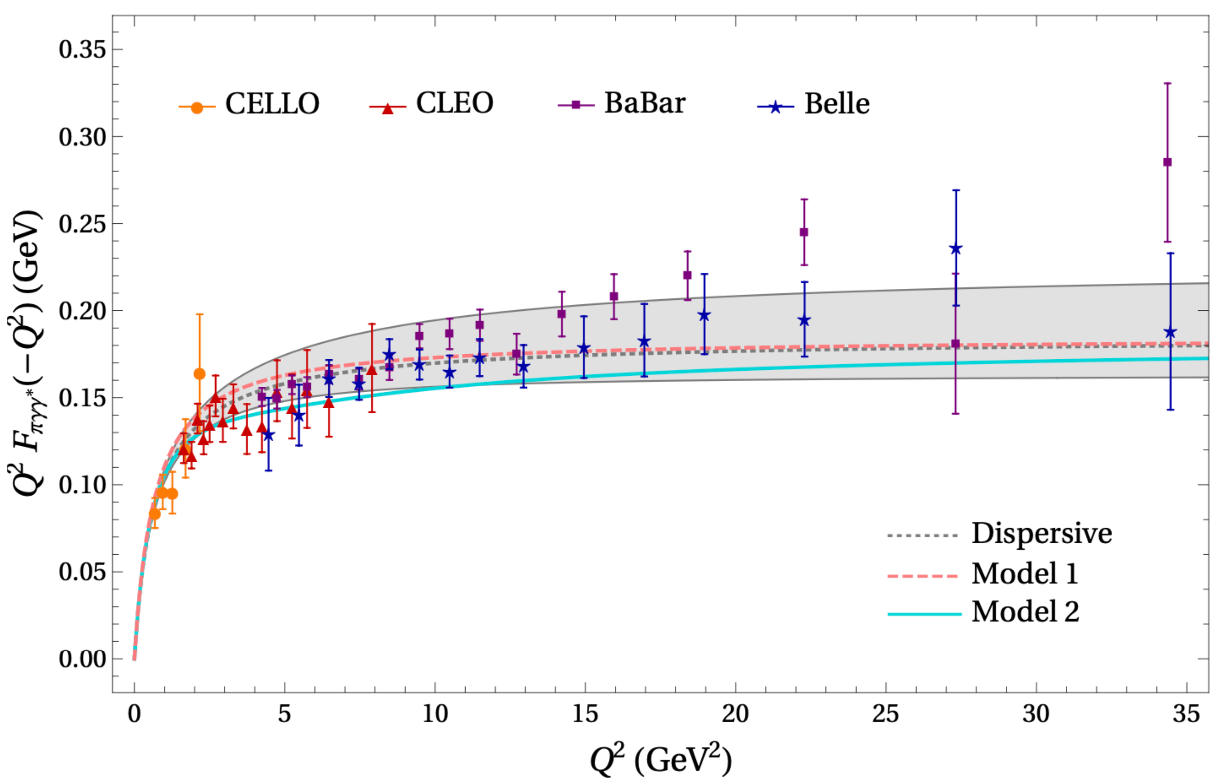

$$a_\mu^{\pi^0\text{-pole}}(\text{disp}) = 63.0^{+2.7}_{-2.1} \times 10^{-11}$$

$$a_\mu^{\pi^0\text{-pole}}(\text{CA}) = 63.6(2.7) \times 10^{-11}$$

$$a_\mu^{\pi^0\text{-pole}}(\text{lattice}) = 62.3(2.3) \times 10^{-11}$$

ETA & ETA’

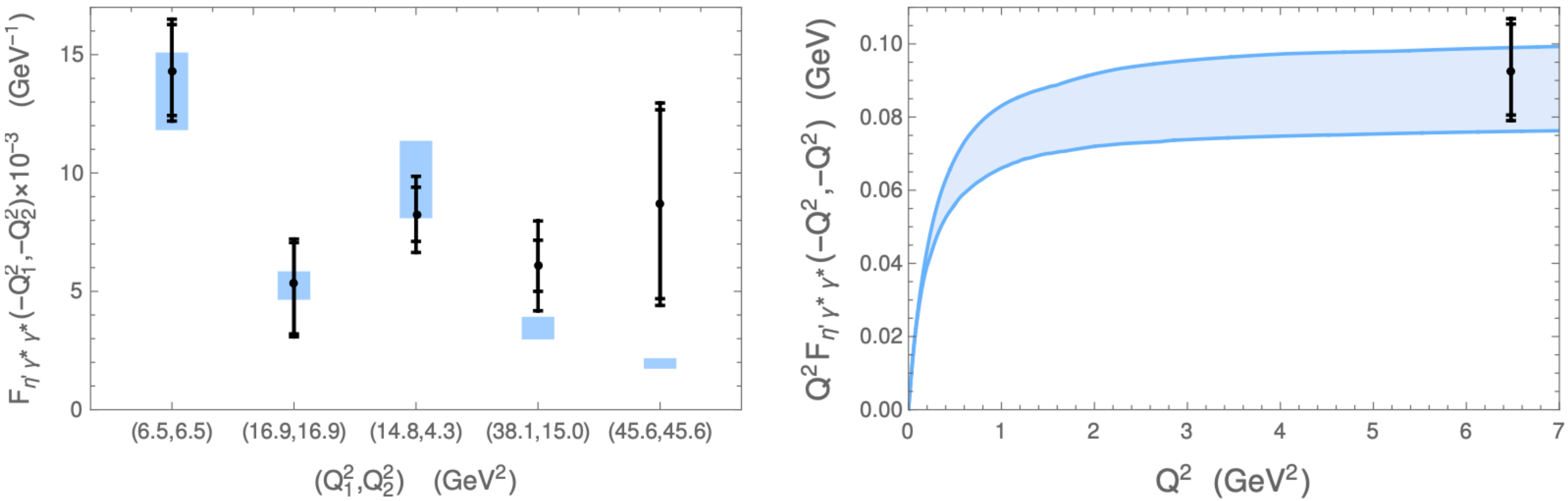

Figure 59: Left: BABAR data points [108] with statistical errors (inner bars) and statistical and systematic combined (outer bars) in black, together with the CA prediction including errors (blue bands). Right: The analogous plot for the diagonal $Q^2 F_{\eta'\gamma^*\gamma^*}(-Q^2,-Q^2)$ TFF.

$$a_\mu^{\eta\text{-pole}} = 16.3(1.0)_{\text{stat}}(0.5)_{a_{P;1,1}}(0.9)_{\text{sys}} \times 10^{-11} \to 16.3(1.4) \times 10^{-11}$$
$$a_\mu^{\eta'\text{-pole}} = 14.5(0.7)_{\text{stat}}(0.4)_{a_{P;1,1}}(1.7)_{\text{sys}} \times 10^{-11} \to 14.5(1.9) \times 10^{-11}$$

Update on eta, eta' poles *Simon Holz*

Kobayashi Hall, KEK Tsukuba campus 11:20 - 11:45

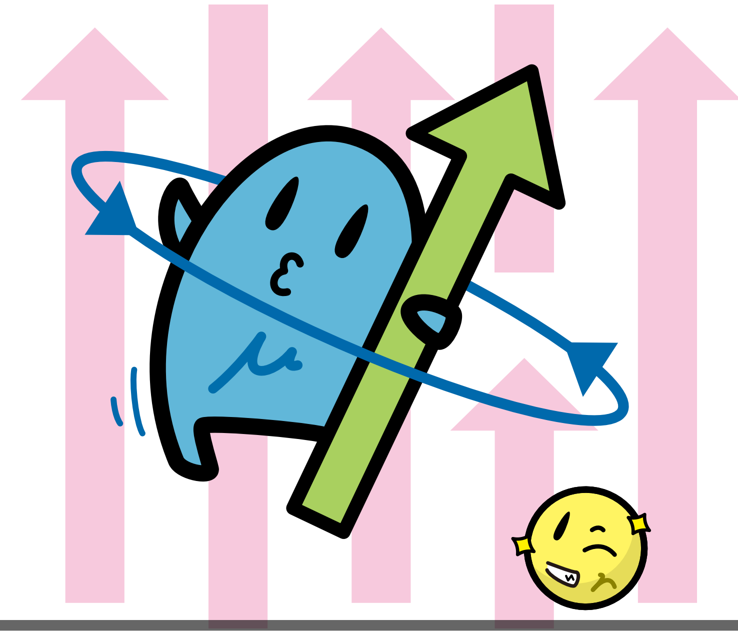

HLBL Contribution to $(g-2)_\mu$

— Short Distance Constraints —

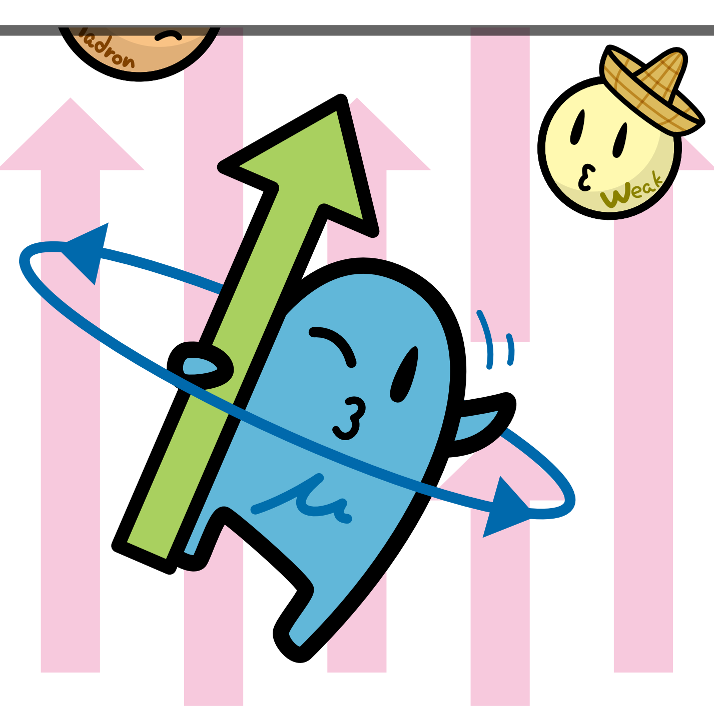

LONGITUDINAL SHORT-DISTANCE CONSTRAINTS

- Pseudoscalar-pole (in particular Pion-pole) contributions are the leading HLbL contributions

- Mixed- and high-energy regions need to be estimated for a full evaluation

- Issue: pseudoscalar-pole contribution does not have the asymptotic behaviour dictated by QCD

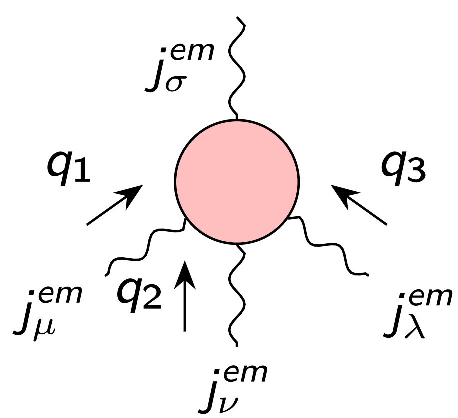

$$\xrightarrow{\text{OPE}} \quad \frac{2}{\hat{q}^2}\,\epsilon_{\mu\nu\alpha\beta}\,\hat{q}^\alpha$$

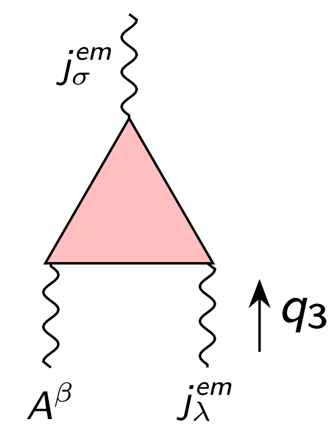

with
$\hat{q} := \frac{q_1 - q_2}{2}$

- Effective solution proposed by Melnikov & Vainshtein (MV) is incompatible with low-energy properties of the HLbL tensor
K. Melnikov and A. Vainshtein, Phys. Rev. D 70, 113006 (2004)

- SDCs can be satisfied with a summation over an infinite tower of pseudoscalar poles

SHORT-DISTANCE CONSTRAINTS

- Tower of excited pseudo scalars (Regge model)
  Colangelo, FH, Hoferichter Laub, Stoffer 20/21
- Tower of axial-vectors (holographic QCD model)
  Leutgeb, Rebhan 19/21 & Cappiello, Cata, D'Ambrosio, Greynat, Iyer 20

Update on hQCD	*Anton Rebhan*
Kobayashi Hall, KEK Tsukuba campus	10:30 - 10:55

- Calculation of (non-) perturbative corrections to the OPE
  Bijnens, Hermansson-Truedsson, Laub, Rodriguez-Sanchez 20/21

Short-distance constraints in the Melnikov-Vainshtein limit	*Nils Hermansson-Truedsson*
Kobayashi Hall, KEK Tsukuba campus	09:35 - 10:00

- Interpolants between energy regions
  Lüdtke, Procura 20
- General considerations
  Knecht 20 & Masjuan, Roig, Sanchez-Puertas 20 & Colangelo, FH, Hoferichter Laub, Stoffer 21

48. C5 Short distance constraints from HLbL contribution to the muon anomalous magnetic moment
Daniel Gerardo Melo Porras
02/09/2024, 16:52
Poster pitch talk

SDC FOR MIXED- AND HIGH ENERGIES

- Relevant part of the HLbL tensor:

$P = \pi^0,\ \eta,\ \eta'$

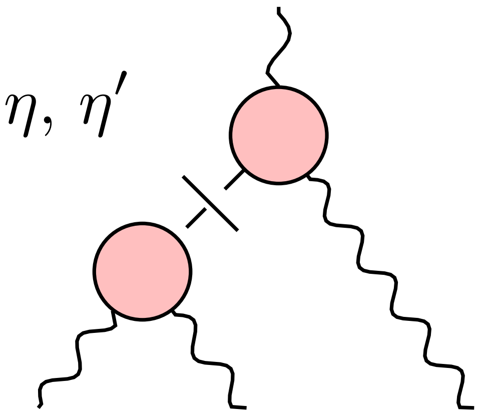

$$\Pi_1^{\mathrm{P-pole}} = -\frac{F_{P\gamma^*\gamma^*}(-Q_1^2, -Q_2^2)\, F_{P\gamma\gamma^*}(-Q_3^2)}{Q_3^2 + M_P^2}$$

G. Colangelo, et al., JHEP 1704 (2017) 161

- Longitudinal part is intimately related to the pseudoscalar poles but cannot be saturated by π^0, η, η' alone, nor by any finite number of poles

- SDCs for asymptotic $(Q^2 \equiv Q_1^2 \approx Q_2^2 \approx Q_3^2 \gg \Lambda^2_{\mathrm{QCD}})$ and mixed energy region $(Q^2 \equiv Q_1^2 \approx Q_2^2 \gg Q_3^2)$ follow from the operator product expansion (OPE):

$$\lim_{Q\to\infty} \sum_{n=0}^{\infty} \hat{\Pi}_1^{\pi(n)-\mathrm{pole}}(Q^2, Q^2, Q^2) = -\frac{1}{9\pi^2}\frac{1}{Q^4}$$

$$\lim_{Q_3\to\infty} \lim_{Q\to\infty} \sum_{n=0}^{\infty} \hat{\Pi}_1^{\pi(n)-\mathrm{pole}}(Q^2, Q^2, Q_3^2) = -\frac{1}{6\pi^2}\frac{1}{Q^2 Q_3^2}$$

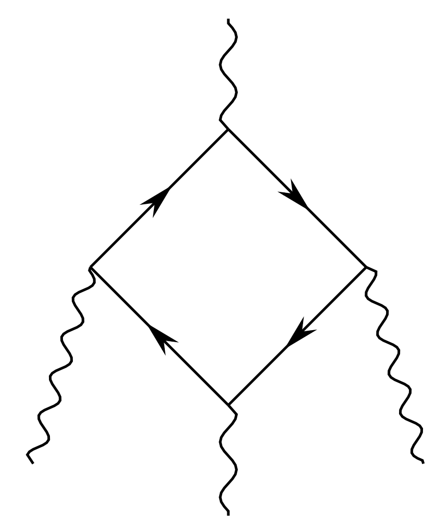

- Leading term in the OPE for HLbL corresponds to the perturbative quark loop

Bijnens et al., 1908.03331 (2019)

SDC FOR TRANSITION FORM FACTOR

- SDCs for pseudoscalar transition form factor
  - Chiral Anomaly: $F_{\pi^0\gamma\gamma}(0,0) = -\dfrac{1}{4\pi^2 f_\pi}$
  - Brodsky-Lepage limit: $\lim\limits_{Q^2\to\infty} F_{\pi^0\gamma\gamma^*}(Q^2) = -\dfrac{2f_\pi}{Q^2}$
  - Symmetric pQCD limit: $\lim\limits_{Q^2\to\infty} F_{\pi^0\gamma^*\gamma^*}(Q^2, Q^2) = -\dfrac{2f_\pi}{3Q^2}$

SDC FOR TRANSITION FORM FACTOR

- SDCs for pseudoscalar transition form factor
  - Chiral Anomaly: $F_{\pi^0\gamma\gamma}(0,0) = -\dfrac{1}{4\pi^2 f_\pi}$
  - Brodsky-Lepage limit: $\lim\limits_{Q^2\to\infty} F_{\pi^0\gamma\gamma^*}(Q^2) = -\dfrac{2f_\pi}{Q^2}$
  - Symmetric pQCD limit: $\lim\limits_{Q^2\to\infty} F_{\pi^0\gamma^*\gamma^*}(Q^2,Q^2) = -\dfrac{2f_\pi}{3Q^2}$
- Melnikov & Vainshtein replaced the external photon vertex with the transition form factor at real-photon point (dropped Q^2 dependence)
  - Prescription is incompatible with low-energy properties of the HLbL tensor

$a_\mu^{\pi^0-\text{pole}} = 62.6 \times 10^{-11}$

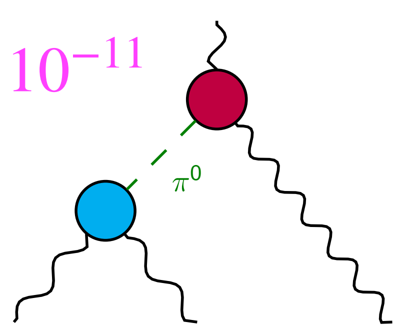

$a_\mu^{\pi^0-\text{pole}} = 76.5 \times 10^{-11}$

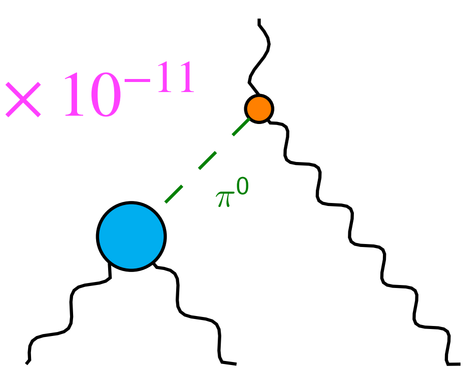

$$-\frac{\mathcal{F}_{\pi^0\gamma^*\gamma^*}(Q_1^2,Q_2^2)\mathcal{F}_{\pi^0\gamma\gamma^*}(Q_3^2)}{Q_3^2+m_{\pi^0}^2} \longrightarrow -\frac{2f_\pi}{3Q^2}\,\frac{1}{Q_3^2}\,\frac{2f_\pi}{Q_3^2}$$

$$\overline{\Pi}_1^{\text{OPE},(3)} \longrightarrow -\frac{1}{6\pi^2 Q^2 Q_3^2} = -\frac{2f_\pi}{3Q^2}\,\frac{1}{Q_3^2}\,\frac{1}{4\pi^2 f_\pi}$$

INFINITE TOWERS OF MESONS

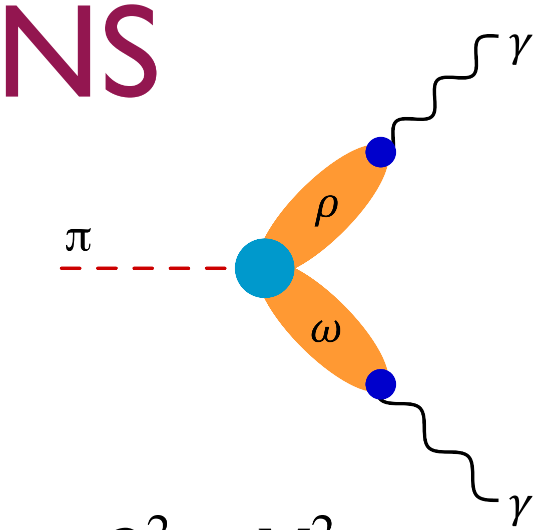

- Start from a large-N$_c$ Regge model:

Broniowski and Ruiz Arriola, Phys. Rev. D74, 034008 (2006)

$$F_{\pi^0\gamma^*\gamma^*}(-Q_1^2,-Q_2^2) \propto \sum_{V_\rho,V_\omega}\left[\frac{1}{D^1_{V_\rho}D^2_{V_\omega}}+\frac{1}{D^1_{V_\omega}D^2_{V_\rho}}\right]$$

with $D^i_X := Q_i^2 + M_X^2$

- Symmetric Momenta: $F_{\pi^0\gamma^*\gamma^*}(-Q^2,-Q^2) \propto \sum_{n=0}^{\infty}\frac{1}{[Q^2+M^2_{V(n)}]^2}$

$$= \frac{1}{\sigma_V^4}\,\psi^{(1)}\left(\frac{M_V^2+Q^2}{\sigma_V^2}\right)$$

- Each term in the sum is of $\mathcal{O}(1/Q^4)$, but the infinite sum satisfies the symmetric pQCD limit $\lim_{Q^2\to\infty} F_{\pi^0\gamma^*\gamma^*}(Q^2,Q^2) = -\frac{2f_\pi}{3Q^2}$

INFINITE TOWERS OF MESONS

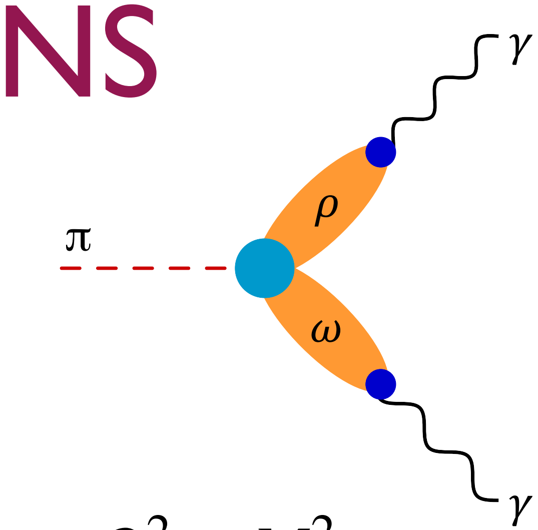

- Start from a large-N$_c$ Regge model:

Broniowski and Ruiz Arriola, Phys. Rev. D74, 034008 (2006)

$$F_{\pi^0\gamma^*\gamma^*}(-Q_1^2, -Q_2^2) \propto \sum_{V_\rho, V_\omega} \left[\frac{1}{D^1_{V_\rho} D^2_{V_\omega}} + \frac{1}{D^1_{V_\omega} D^2_{V_\rho}} \right] \qquad \text{with } D^i_X := Q_i^2 + M_X^2$$

  - Symmetric Momenta: $F_{\pi^0\gamma^*\gamma^*}(-Q^2, -Q^2) \propto \sum_{n=0}^{\infty} \frac{1}{[Q^2 + M^2_{V(n)}]^2}$

$$= \frac{1}{\sigma_V^4} \psi^{(1)} \left(\frac{M_V^2 + Q^2}{\sigma_V^2} \right)$$

  - Each term in the sum is of $\mathcal{O}(1/Q^4)$, but the infinite sum satisfies the symmetric pQCD limit $\lim_{Q^2\to\infty} F_{\pi^0\gamma^*\gamma^*}(Q^2, Q^2) = -\frac{2f_\pi}{3Q^2}$

- In the same way, the SDCs on the HLbL tensor will be satisfied

LARGE-Nc REGGE MODEL

- Vector-meson-dominance model for transition form factors of radially-excited pseudoscalar mesons
  - Large-N$_c$ limit — spectrum of the theory in any sector (set of quantum numbers) reduces to an infinite tower of narrow resonances
  - Regge ansatz for masses of radially-excited mesons $M^2_{V(n)} = M^2_{V(0)} + n\,\sigma_V^2$
  - Minimal model that satisfies all constraints on the transition form factors and HLbL tensor
  - Reproduce phenomenological constraints

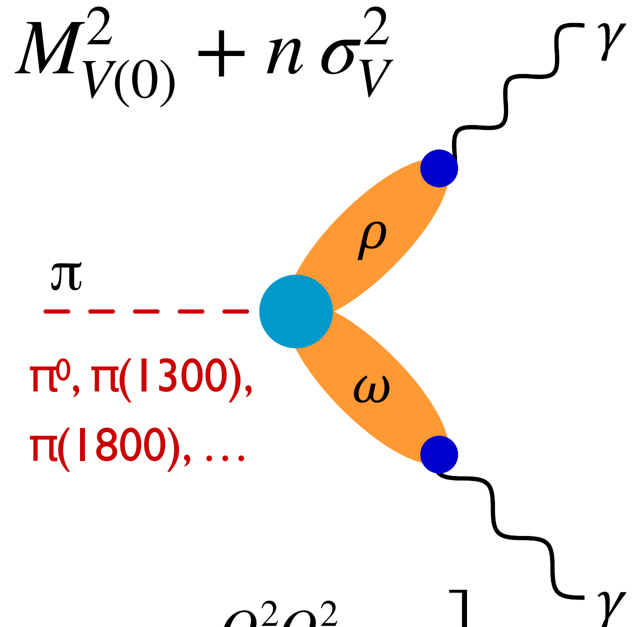

$$F_{\pi(n)\gamma^*\gamma^*}(-Q_1^2,-Q_2^2) = \frac{1}{8\pi^2 F_\pi}\Bigg\{\left(\frac{M_\rho^2 M_\omega^2}{D^1_{\rho(n)}D^2_{\omega(n)}} + \frac{M_\rho^2 M_\omega^2}{D^2_{\rho(n)}D^1_{\omega(n)}}\right)\left[c_{\text{anom}} + \frac{1}{\Lambda^2}\left(c_A M^2_{+,n} + c_B M^2_{-,n}\right) + c_{\text{diag}}\frac{Q_1^2 Q_2^2}{\Lambda^2(Q_+^2 + M^2_{\text{diag}})}\right]$$
$$+\frac{Q_-^2}{Q_+^2}\left[c_{\text{BL}} + \frac{1}{\Lambda^2}\left(c_A M^2_{-,n} + c_B M^2_{+,n}\right)\right]\left(\frac{M_\rho^2 M_\omega^2}{D^1_{\rho(n)}D^2_{\omega(n)}} - \frac{M_\rho^2 M_\omega^2}{D^2_{\rho(n)}D^1_{\omega(n)}}\right)\Bigg\}$$

with $M^2_{\pm,n} = \frac{1}{2}\left(M^2_{\omega(n)} \pm M^2_{\rho(n)}\right), \quad Q_\pm^2 = Q_1^2 \pm Q_2^2, \quad D_V^j = Q_j^2 + M_V^2$

PION TRANSITION FORM FACTOR

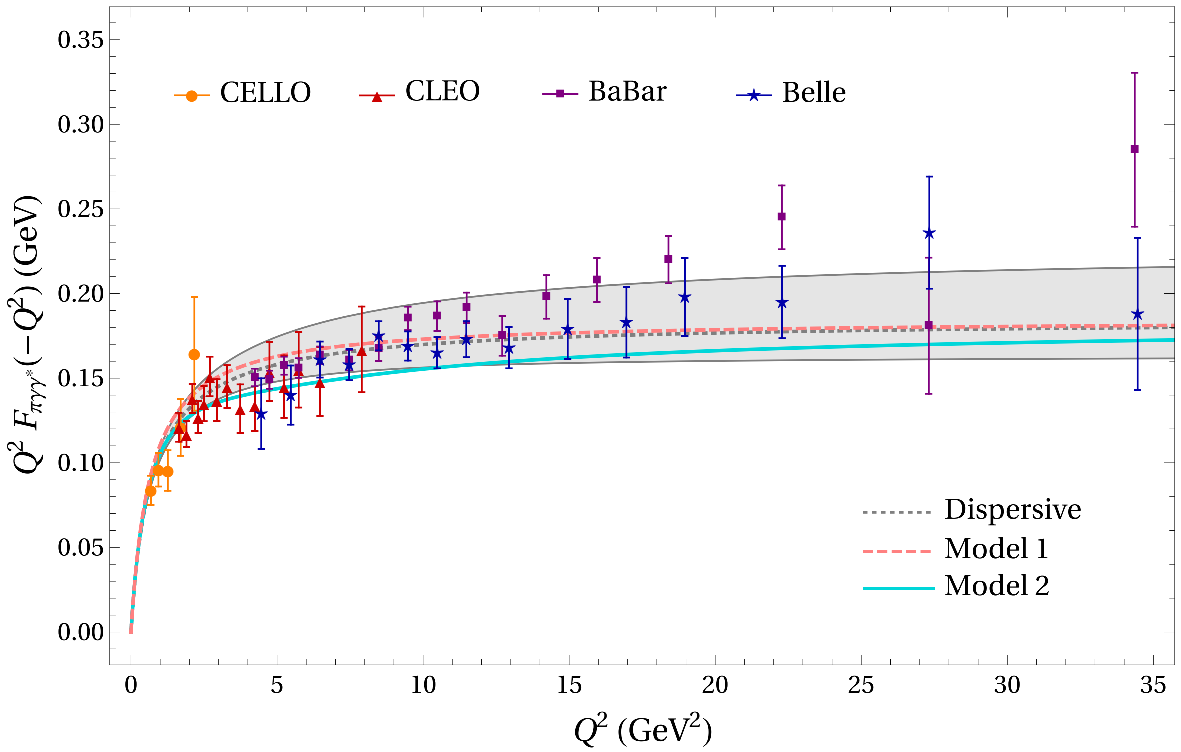

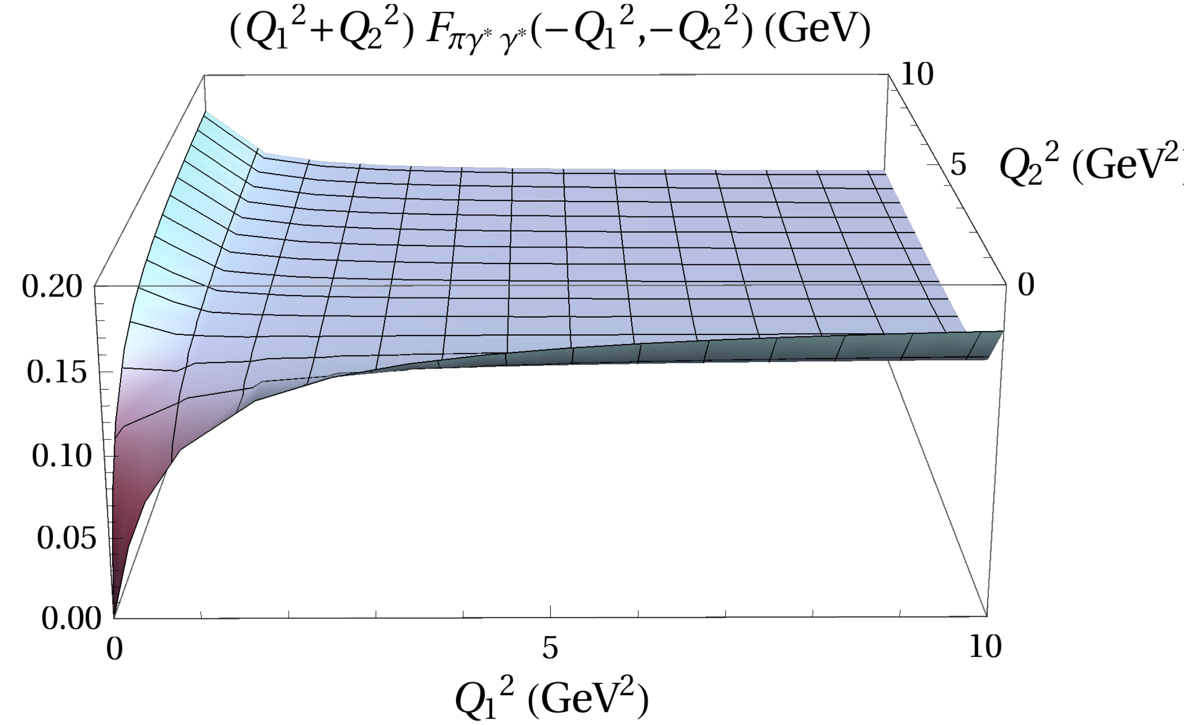

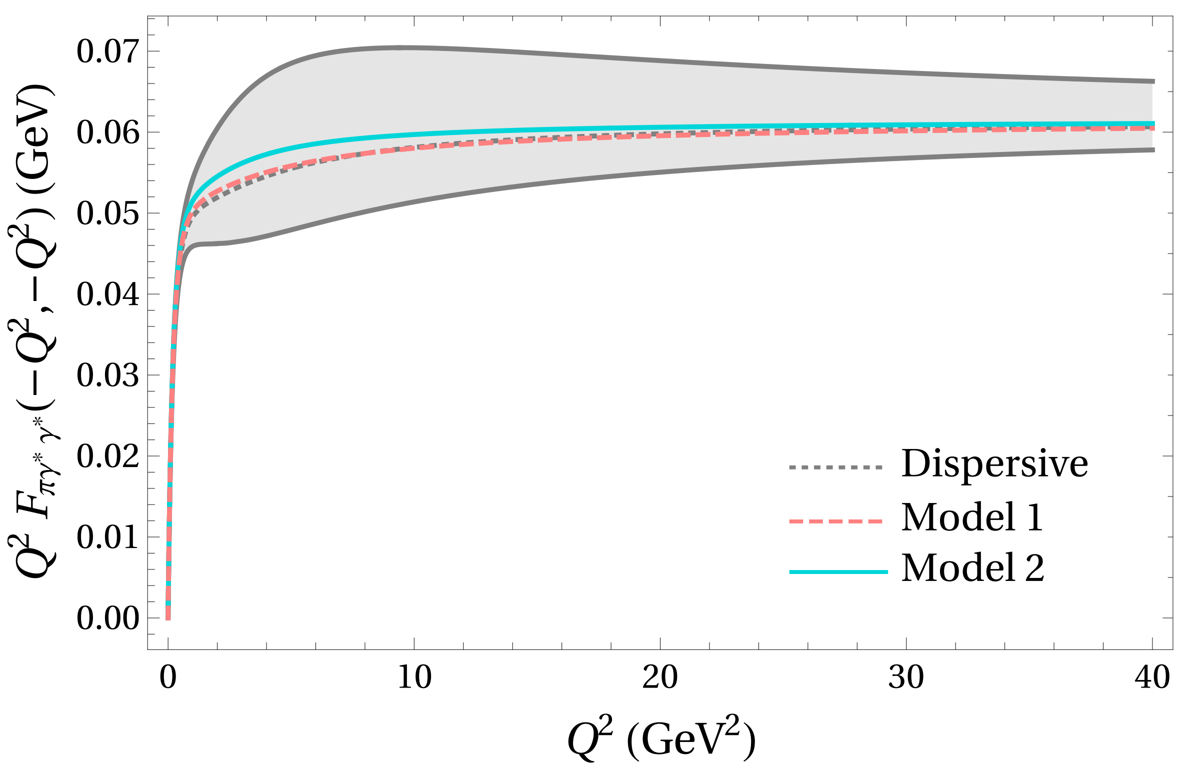

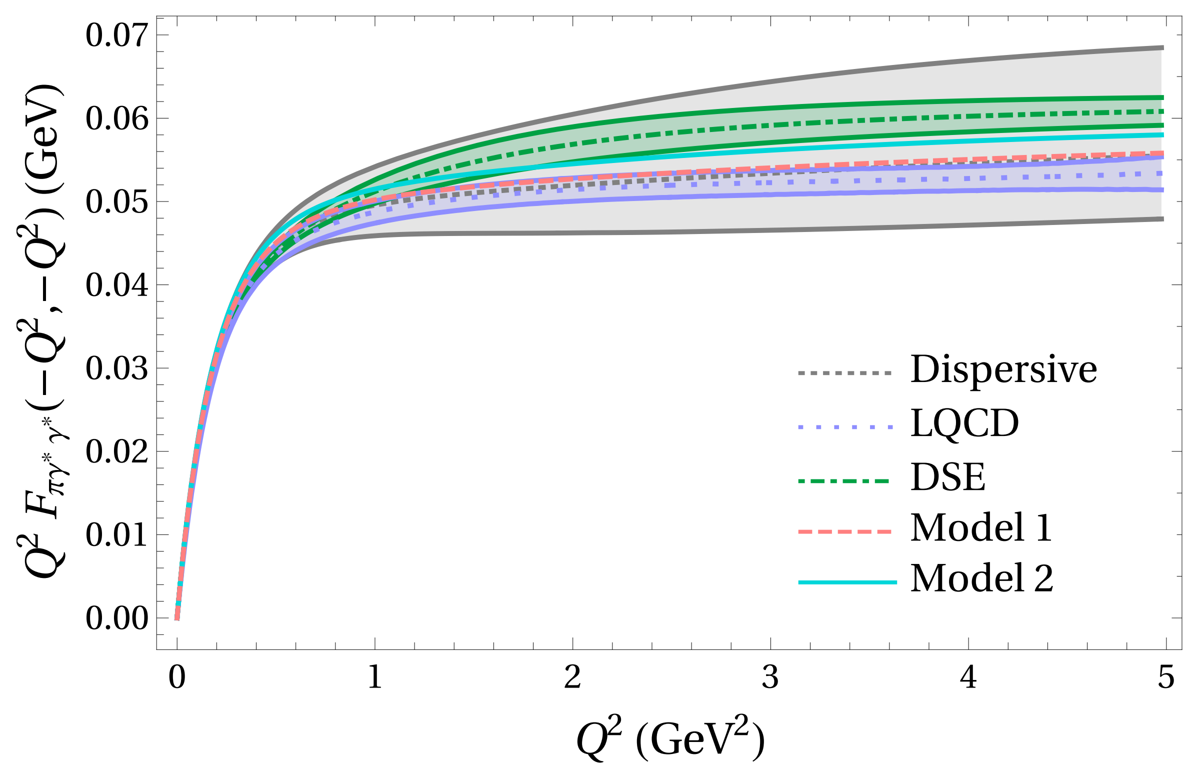

ETA TRANSITION FORM FACTORS

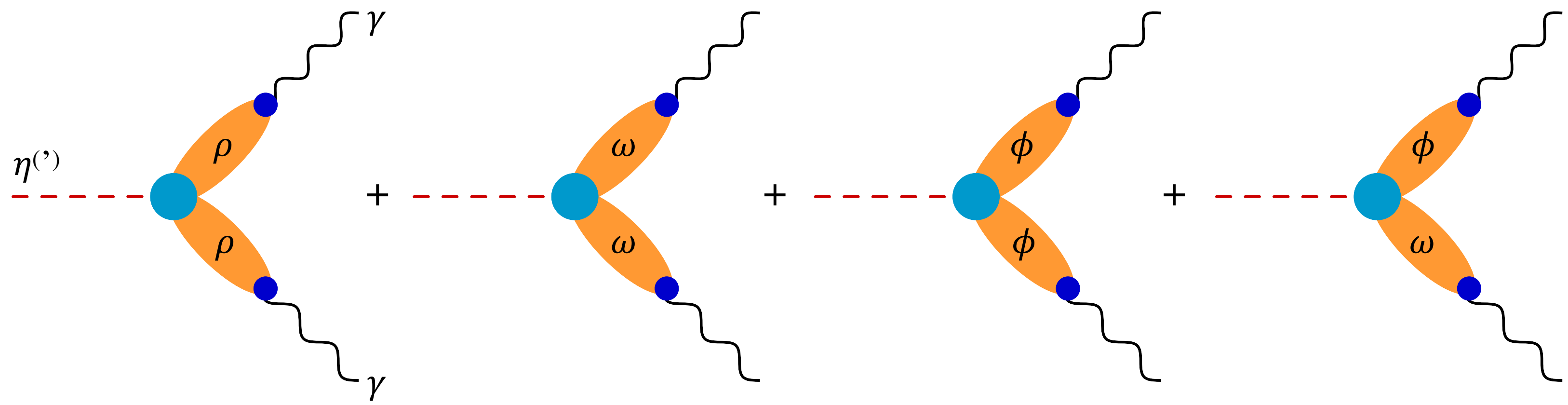

- Vector-meson-dominance model with of isoscalar-isoscalar and isovector-isovector pairs
- Relative coupling strengths follow from effective Lagrangian
- $\eta - \eta'$ and $\phi - \omega$ mixings must be considered

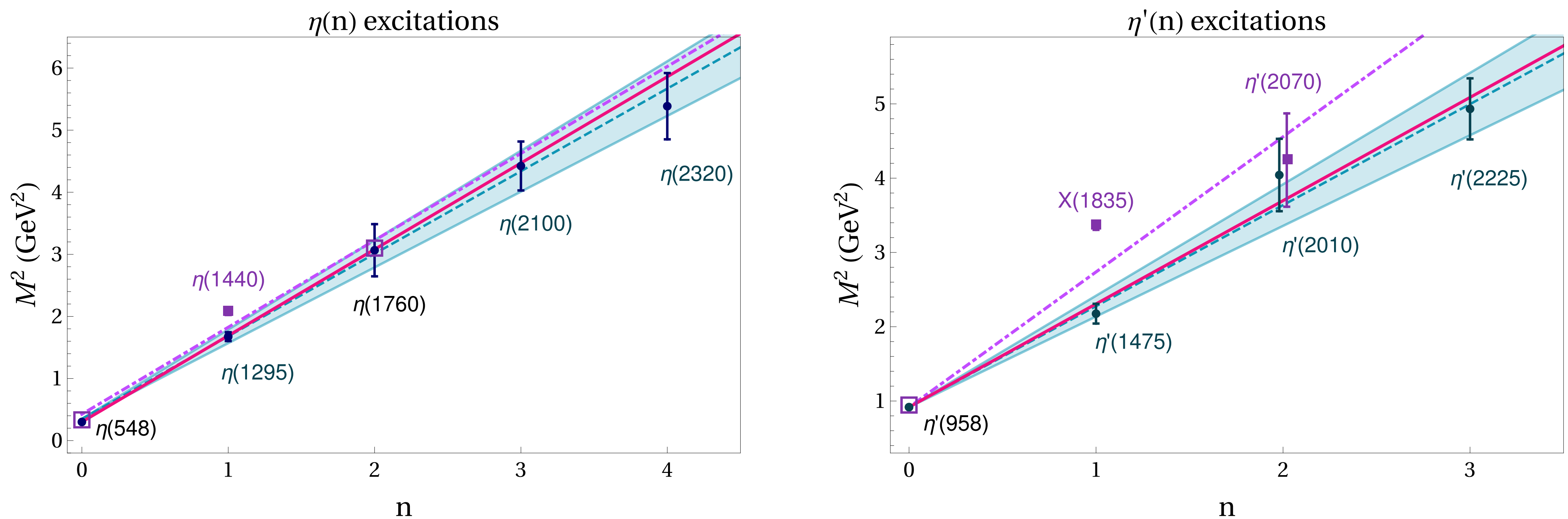

ETA TRANSITION FORM FACTORS

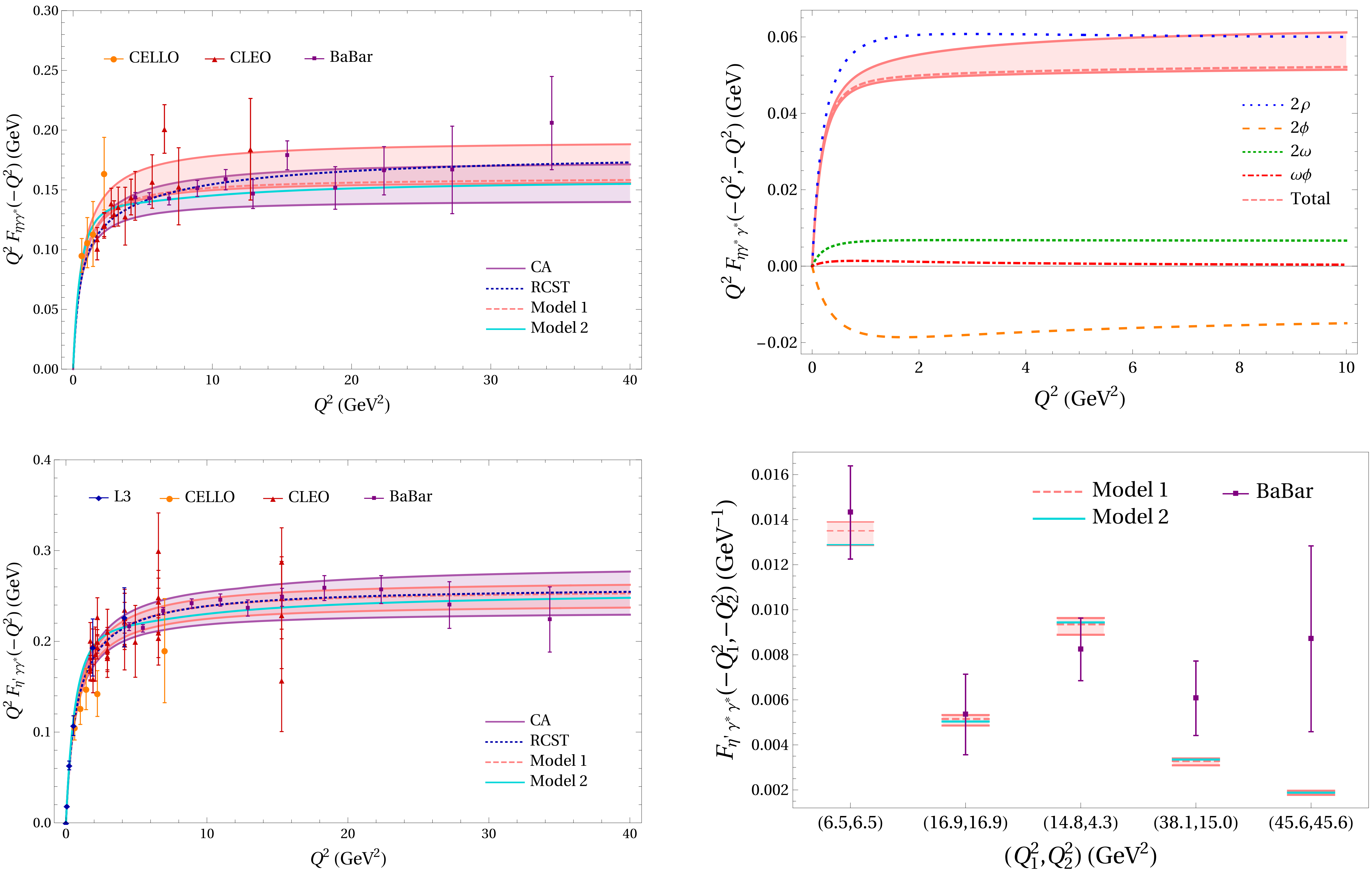

SUM OF PSEUDOSCALAR-POLE CONTRIBUTIONS

$$\Delta a_\mu^{P-\text{poles}}(n_{\max}) = \sum_{n=1}^{n_{\max}} a_\mu^{P(n)-\text{pole}}$$

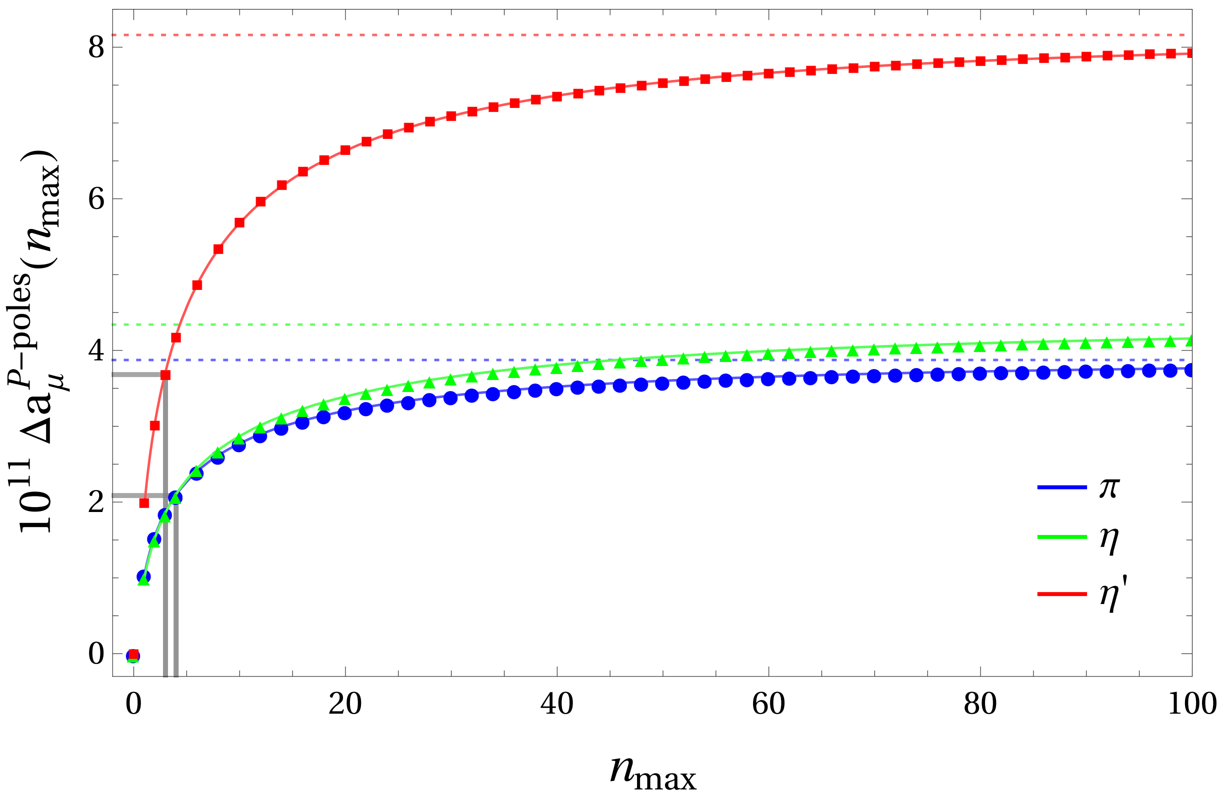

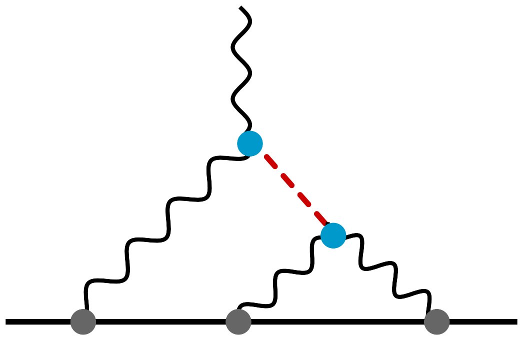

$$\Delta a_\mu^{\pi-\text{poles}} = 2.7\,(0.4)_{\text{Model}}\,(1.2)_{\text{syst}} \times 10^{-11} = 2.7\,(1.3) \times 10^{-11}$$

$$\Delta a_\mu^{\eta-\text{poles}} = 3.4\,{}^{+0.9}_{-0.7}\Big|_{\text{Model}}\,(0.9)_{\text{syst}} \times 10^{-11} = 3.4\,{}^{+1.3}_{-1.1} \times 10^{-11}$$

$$\Delta a_\mu^{\eta'-\text{poles}} = 6.5\,(1.1)_{\text{Model}}\,(1.7)_{\text{syst}} \times 10^{-11} = 6.5\,(2.0) \times 10^{-11}$$

- Total effect of excited pseudoscalar mesons: $\Delta a_\mu^{\text{PS}-\text{poles}} = \Delta a_\mu^{\pi-\text{poles}} + \Delta a_\mu^{\eta-\text{poles}} + \Delta a_\mu^{\eta'-\text{poles}}$

$$= 12.6\,{}^{+1.6}_{-1.5}\Big|_{\text{Model}}\,(3.8)_{\text{syst}} \times 10^{-11}$$

$$= 12.6(4.1) \times 10^{-11}$$

SUM OF PSEUDOSCALAR-POLE CONTRIBUTIONS

$$\Delta a_\mu^{P-\text{poles}}(n_\text{max}) = \sum_{n=1}^{n_\text{max}} a_\mu^{P(n)-\text{pole}}$$

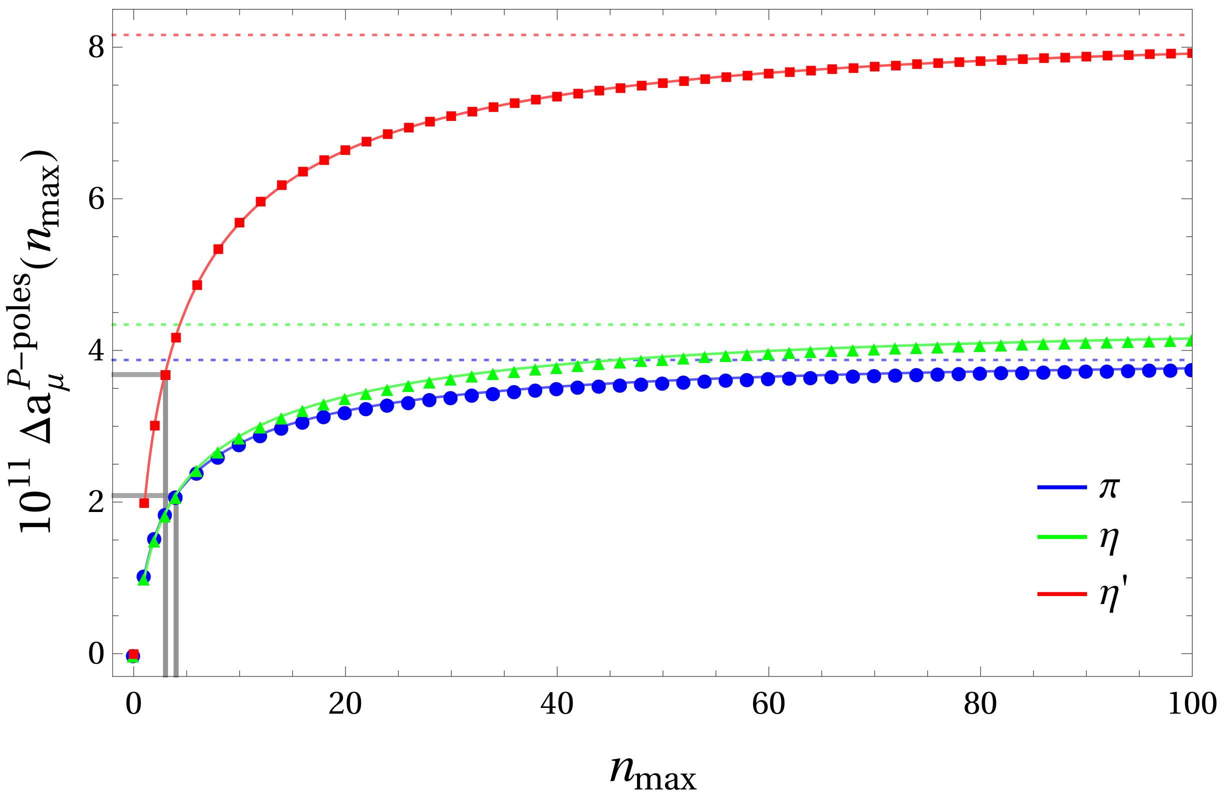

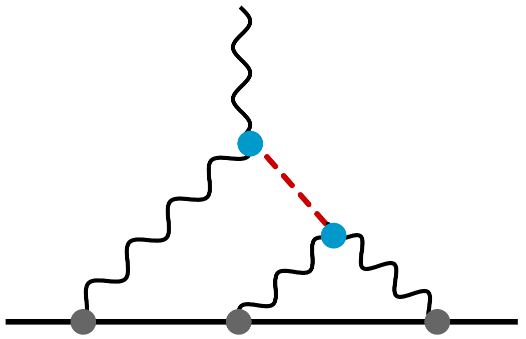

$$\Delta a_\mu^{\pi-\text{poles}} = 2.7\,(0.4)_\text{Model}\,(1.2)_\text{syst} \times 10^{-11} = 2.7\,(1.3) \times 10^{-11}$$

$$\Delta a_\mu^{\eta-\text{poles}} = 3.4\,{}^{+0.9}_{-0.7}\Big|_\text{Model}\,(0.9)_\text{syst} \times 10^{-11} = 3.4\,{}^{+1.3}_{-1.1} \times 10^{-11}$$

$$\Delta a_\mu^{\eta'-\text{poles}} = 6.5\,(1.1)_\text{Model}\,(1.7)_\text{syst} \times 10^{-11} = 6.5\,(2.0) \times 10^{-11}$$

- Total effect of excited pseudoscalar mesons: $\Delta a_\mu^{\text{PS}-\text{poles}} = \Delta a_\mu^{\pi-\text{poles}} + \Delta a_\mu^{\eta-\text{poles}} + \Delta a_\mu^{\eta'-\text{poles}}$

$$= 12.6\,{}^{+1.6}_{-1.5}\Big|_\text{Model}\,(3.8)_\text{syst} \times 10^{-11}$$

$$= 12.6(4.1) \times 10^{-11}$$

- Original and updated MV result:

$$\Delta a_\mu^{\pi-\text{poles}}\Big|_\text{MV} = 13.5 \times 10^{-11} \quad [16.2 \times 10^{-11}]$$

$$\Delta a_\mu^{\eta-\text{poles}}\Big|_\text{MV} = 5.0 \times 10^{-11} \quad [10.0 \times 10^{-11}]$$

$$\Delta a_\mu^{\eta'-\text{poles}}\Big|_\text{MV} = 5.0 \times 10^{-11} \quad [12.1 \times 10^{-11}]$$

MATCHING TO PERTURBATIVE QUARK LOOP

$$a_\mu^{\mathrm{HLbL}} = \frac{2\alpha^3}{3\pi^2}\int_0^\infty dQ_1 \int_0^\infty dQ_2 \int_{-1}^1 d\tau\, \sqrt{1-\tau^2}\, Q_1^3 Q_2^3 \sum_{i=1}^{12} T_i(Q_1,Q_2,\tau)\bar{\Pi}_i(Q_1,Q_2,\tau)$$

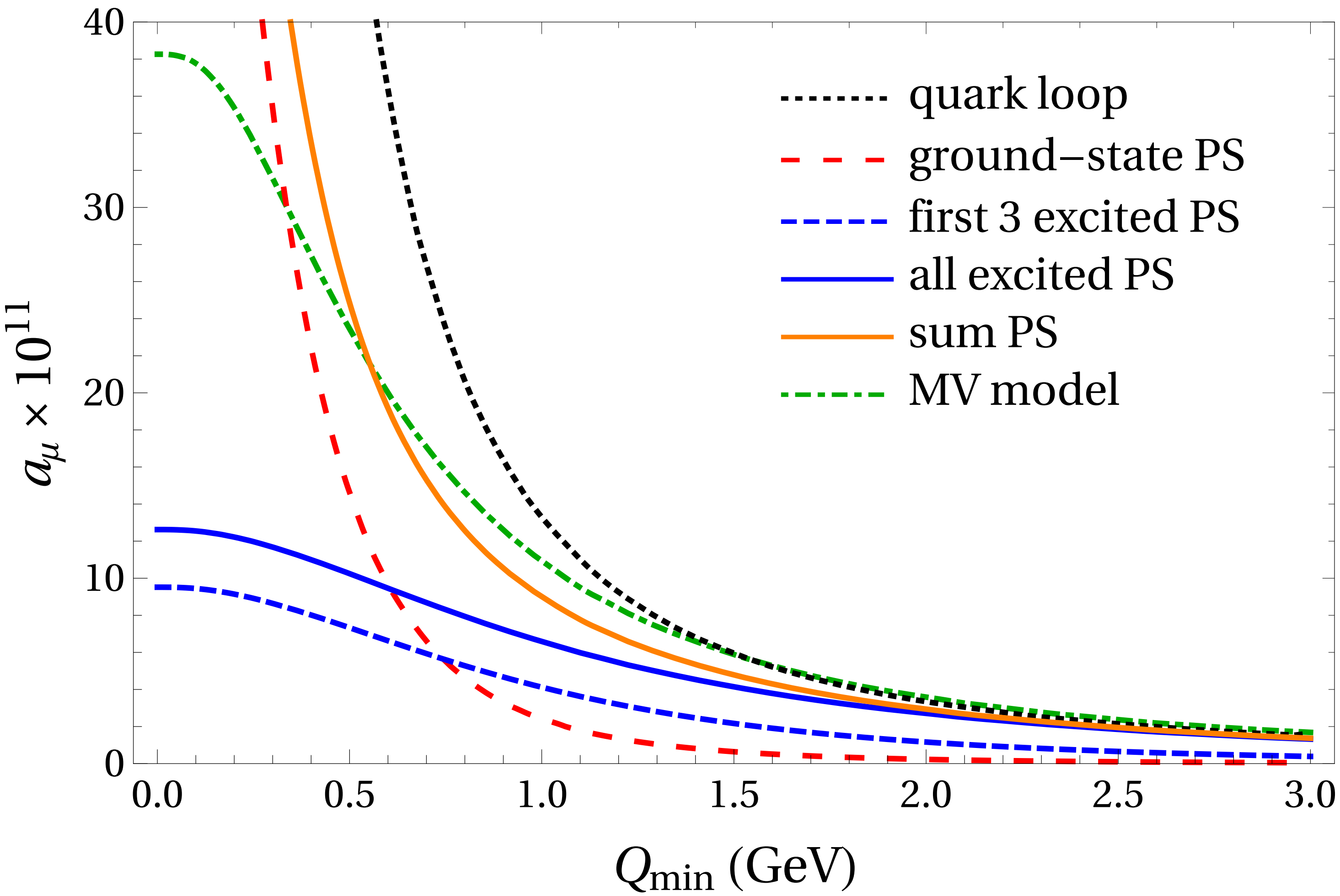

high-energy region:
$Q_i \geq Q_{\min}$

$$\Delta a_\mu^{\mathrm{PS-poles}}\Big|_{\mathrm{MV}} = 23.5 \times 10^{-11} \quad [38 \times 10^{-11}]$$

$$\Delta a_\mu^{\mathrm{LSDC}} = \left[8.7(5.5)_{\mathrm{PS-poles}} + 4.6(9)_{q-\mathrm{loop}}\right] \times 10^{-11} \sim 13(6) \times 10^{-11}$$

MATCHING TO PERTURBATIVE QUARK LOOP

$$a_\mu^{\mathrm{HLbL}} = \frac{2\alpha^3}{3\pi^2}\int_0^\infty dQ_1 \int_0^\infty dQ_2 \int_{-1}^1 d\tau\,\sqrt{1-\tau^2}\,Q_1^3 Q_2^3 \sum_{i=1}^{12} T_i(Q_1,Q_2,\tau)\bar{\Pi}_i(Q_1,Q_2,\tau)$$

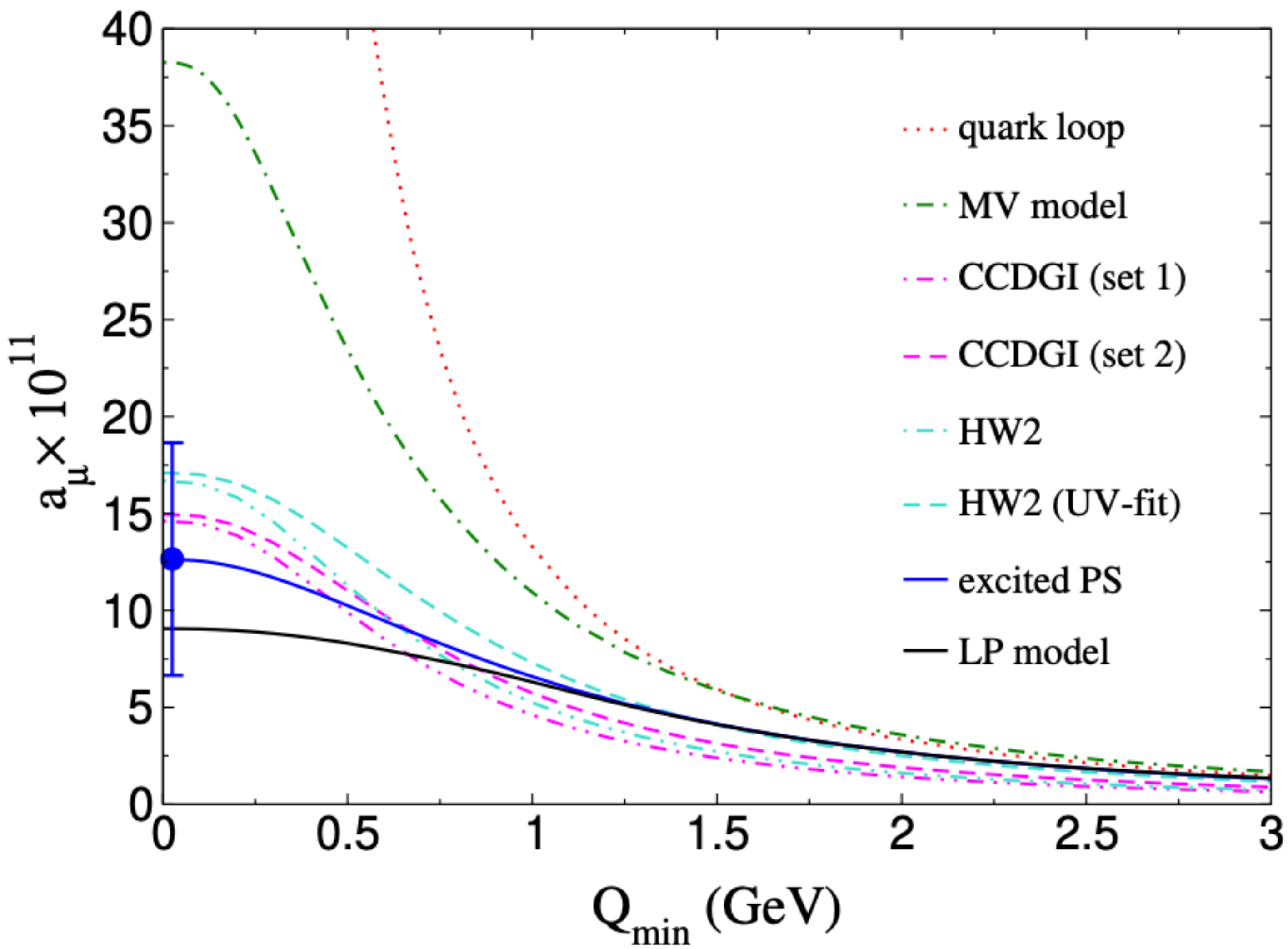

high-energy region:
$Q_i \geq Q_{\min}$

$$\Delta a_\mu^{\mathrm{PS-poles}}\Big|_{\mathrm{MV}} = 23.5 \times 10^{-11} \quad [38 \times 10^{-11}]$$

$$\Delta a_\mu^{\mathrm{LSDC}} = \left[8.7(5.5)_{\mathrm{PS-poles}} + 4.6(9)_{q-\mathrm{loop}}\right] \times 10^{-11} \sim 13(6) \times 10^{-11}$$

LOW- AND MIXED ENERGY REGION

$$a_\mu^{\mathrm{HLbL}} = \frac{2\alpha^3}{3\pi^2}\int_0^\infty dQ_1 \int_0^\infty dQ_2 \int_{-1}^1 d\tau\,\sqrt{1-\tau^2}\,Q_1^3 Q_2^3 \sum_{i=1}^{12} T_i(Q_1,Q_2,\tau)\bar{\Pi}_i(Q_1,Q_2,\tau)$$

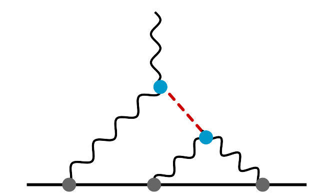

with $Q_3^2 = Q_1^2 + 2Q_1Q_2\tau + Q_2^2$

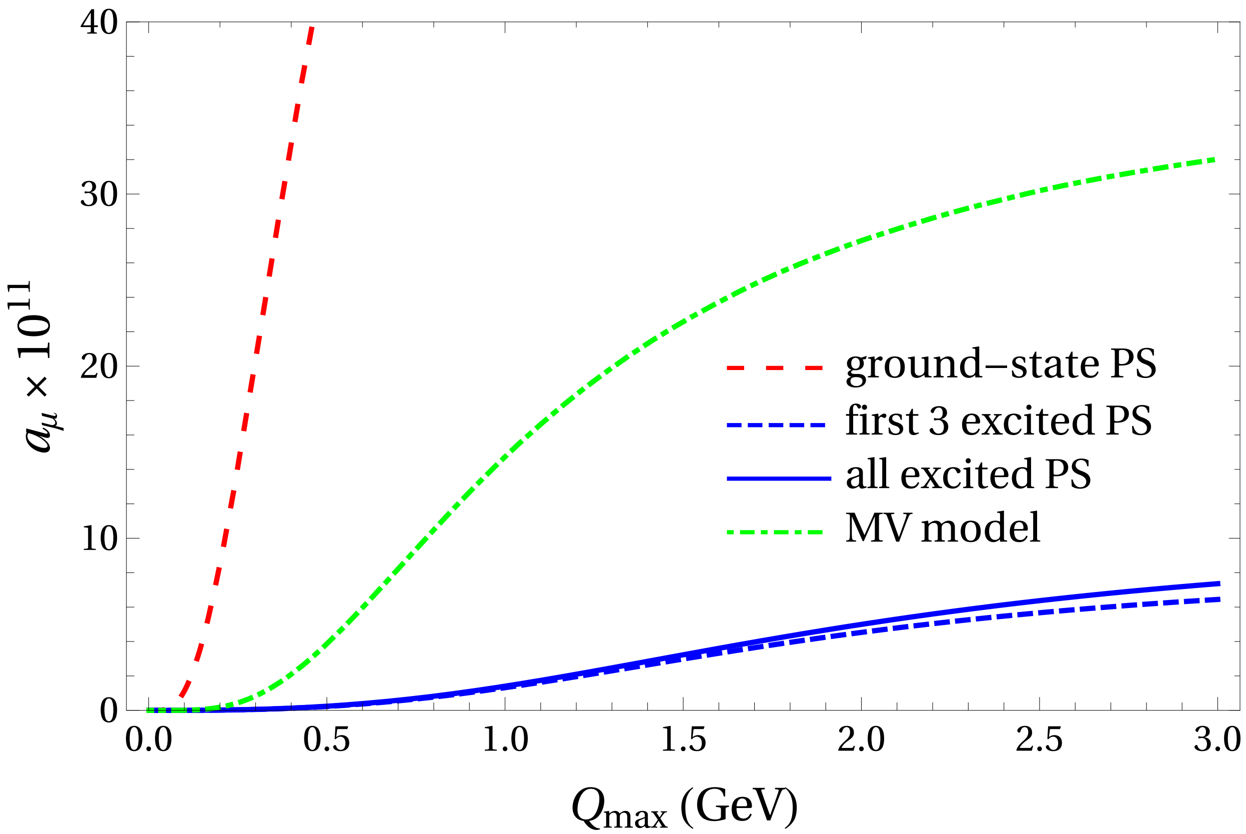

low-energy region

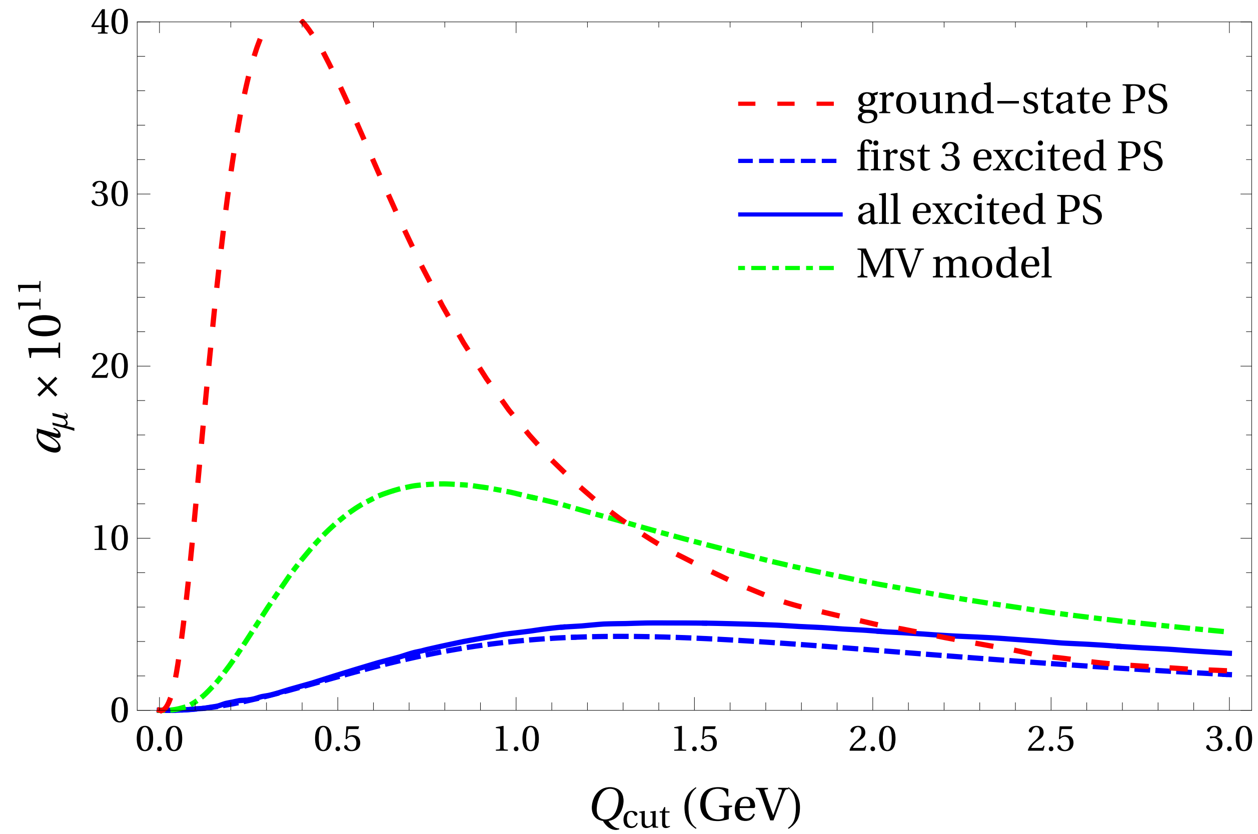

mixed-energy region

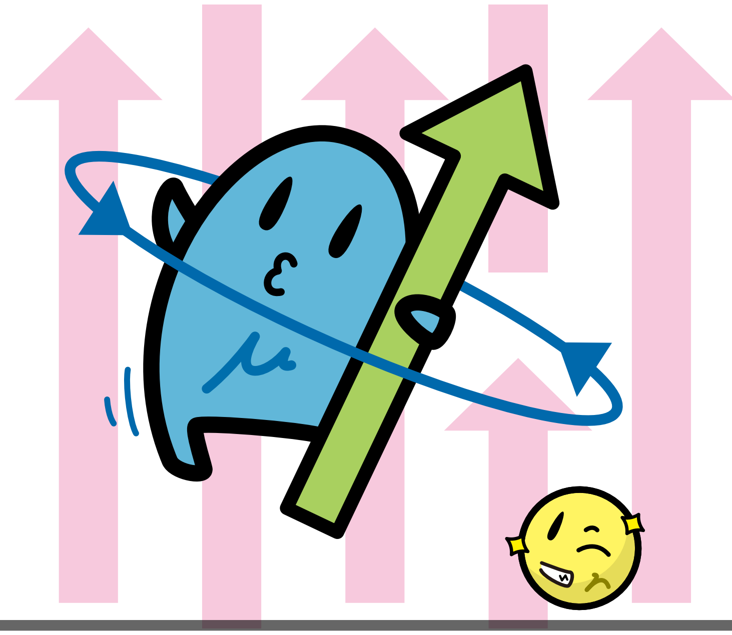

HLBL Contribution to $(g-2)_\mu$

— Quark Loop —

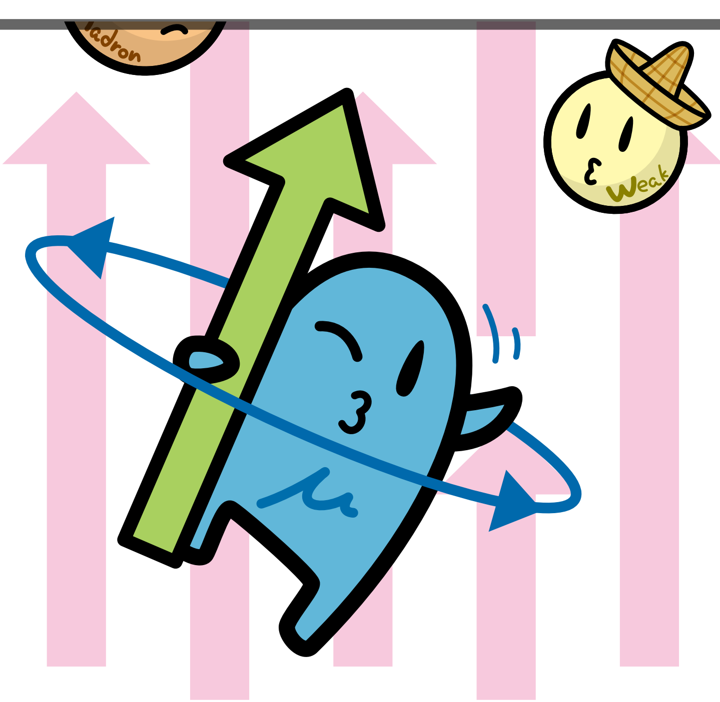

QUARK LOOP

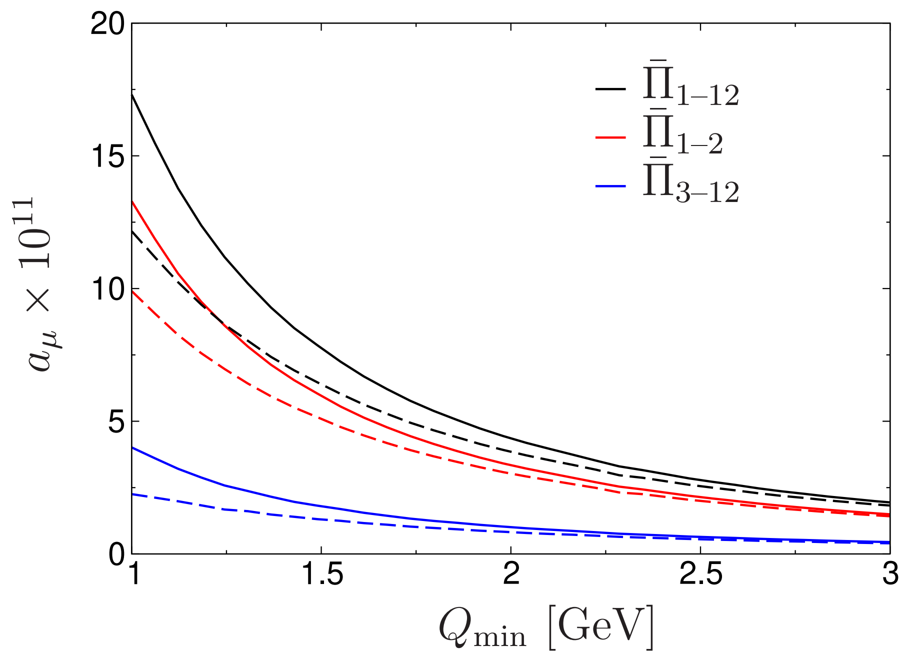

Figure 70: Contribution of the pQCD quark loop to a_μ for $Q_i \geq Q_{\min}$. Solid lines for vanishing quark masses, dashed lines for $m_q = 0.3$ GeV. The total contribution from $\bar{\Pi}_{1-12}$ is shown in black, together with the partial ones from $\bar{\Pi}_{1-2}$ (red) and $\bar{\Pi}_{3-12}$ (blue).

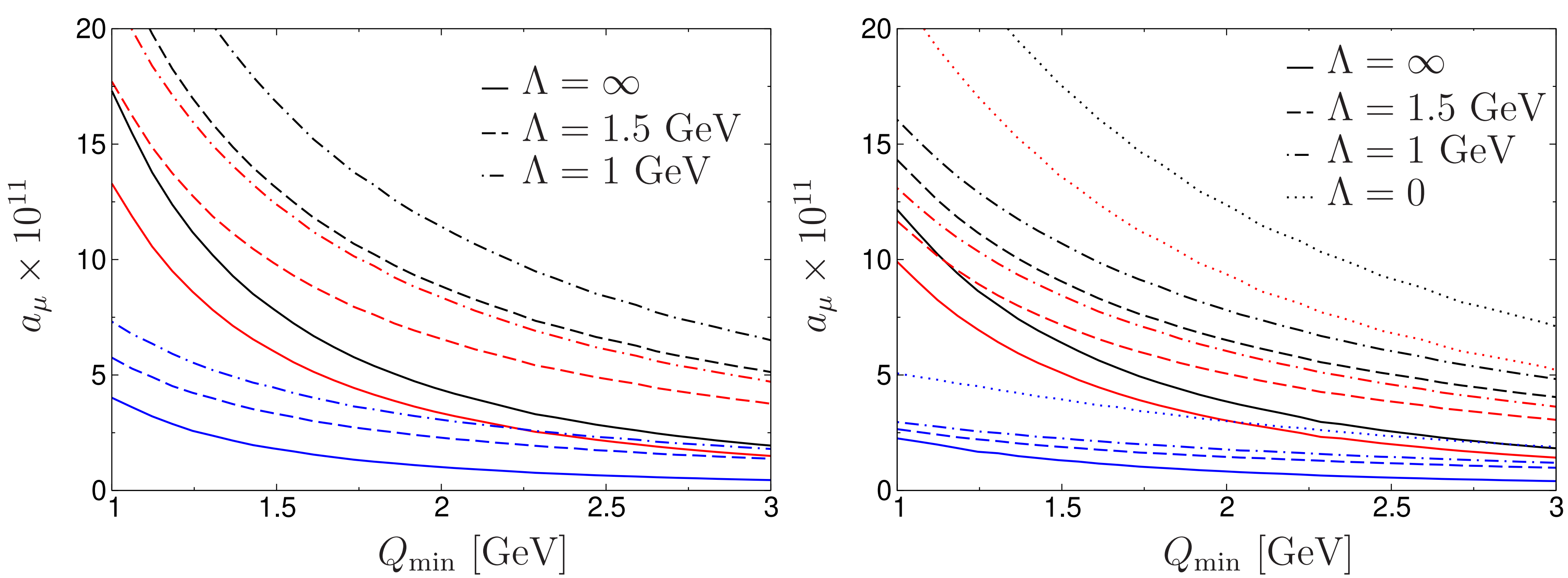

Figure 71: Contribution of the pQCD quark loop to a_μ for $Q_{1,2} \geq Q_{\min}$ and Q_3^2 damped by $Q_3^2/(Q_3^2 + \Lambda^2)$ below $Q_{\min}$ (plus crossed), see main text, for vanishing quark mass (left) and $m_q = 0.3$ GeV (right). Color coding as in Fig. 70, which is reproduced in the limit $\Lambda \to \infty$. The limit $\Lambda \to 0$ does not exist for $m_q = 0$. Left diagram reprinted from Ref. [553].

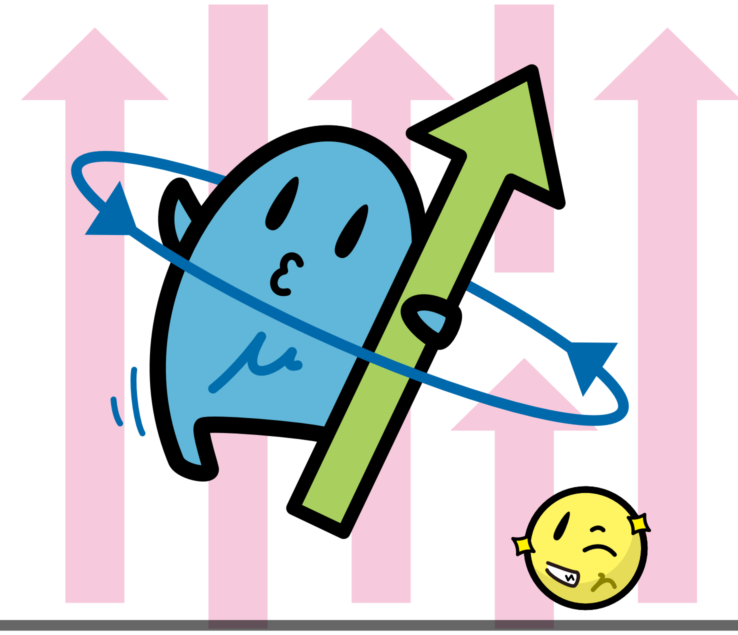

HLBL Contribution to $(g-2)_\mu$

— Axial Vectors —

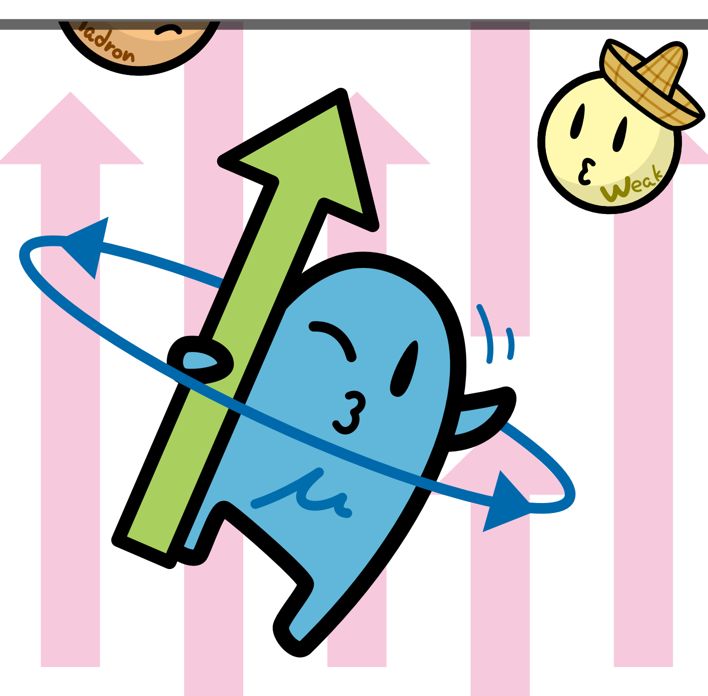

$a_1(1260) + f_1(1285) + f_1(1420)$

	$a_\mu^{\mathrm{HLbL}}[\mathrm{axials}] \times 10^{11}$
Melnikov, Vainshtein ‘04	22(5)
Pauk, Vanderhaeghen ’14 (w/o a1)	6.4(2.0)
Jegerlehner ‘17	7.6(2.7)
Roig, Sanchez-Puertas ‘20	0.8(+3.5,-0.8)
Leutgeb, Rebhan ’19 ‘21	17
Capiello et al. ‘20	~14

- Axial vectors are affected by basis ambiguities

  41. B8 Hadronic contributions to light-by-light scattering in new basis
  Maximilian Zillinger
  02/09/2024, 16:38
  Poster pitch talk

- Model-independent treatment of axial vectors particularly urgent

Determination of axial-vector TFFs

- Three independent TFFs, accessible in
  - $e^+e^- \to e^+e^- f_1$ (space-like)
  - $f_1 \to \rho\gamma$, $f_1 \to \phi\gamma$
  - $f_1 \to e^+e^-$
  - $\boldsymbol{e^+e^- \to f_1\pi^+\pi^-}$

$\hookrightarrow$ global analysis in VMD parameterizations

- Constraint from $e^+e^- \to f_1\pi^+\pi^-$ for the first time allows for unambiguous solutions
- Most information available for f_1

$\hookrightarrow$ f_1' and a_1 from $U(3)$ symmetry

- Analysis of consequences for HLbL in progress

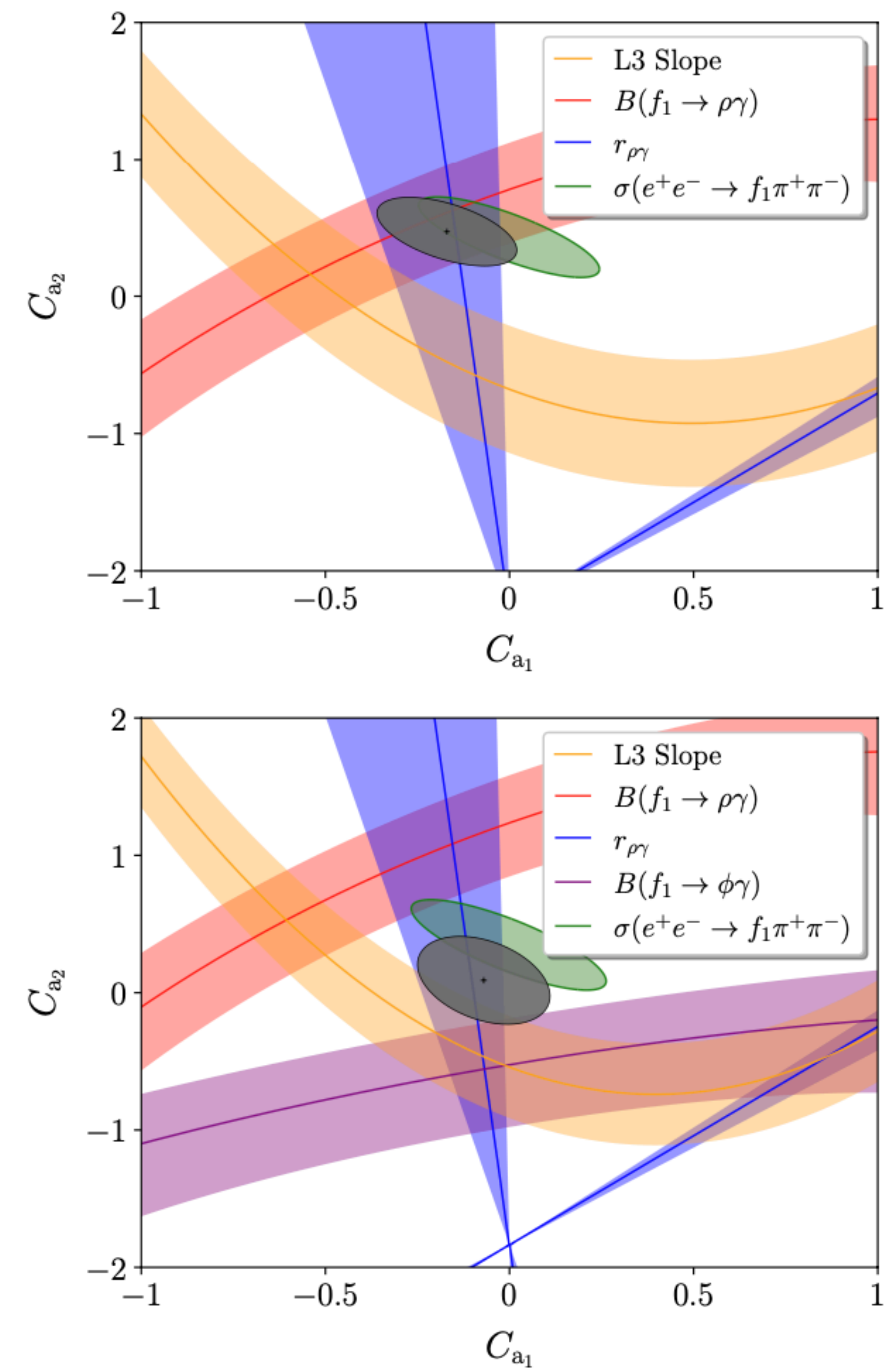

MH, Kubis, Zanke 2023

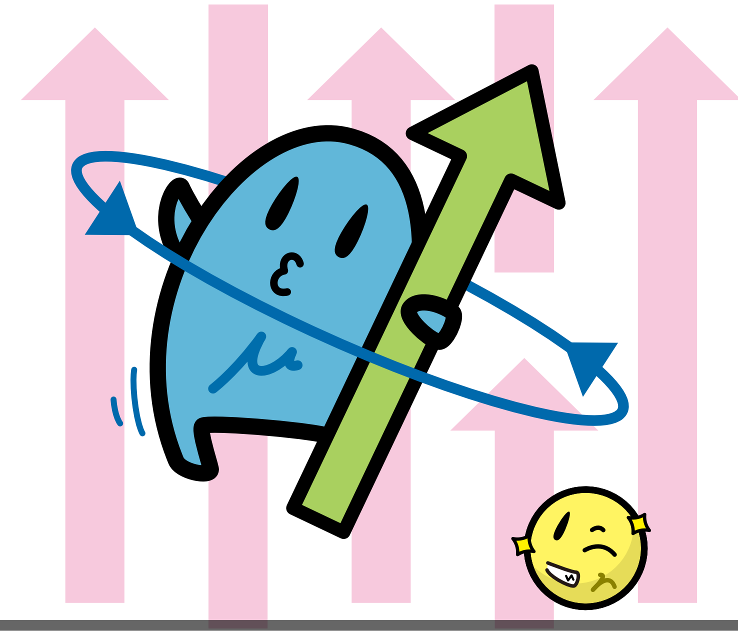

HLBL CONTRIBUTION TO $(g-2)_\mu$

— NLO —

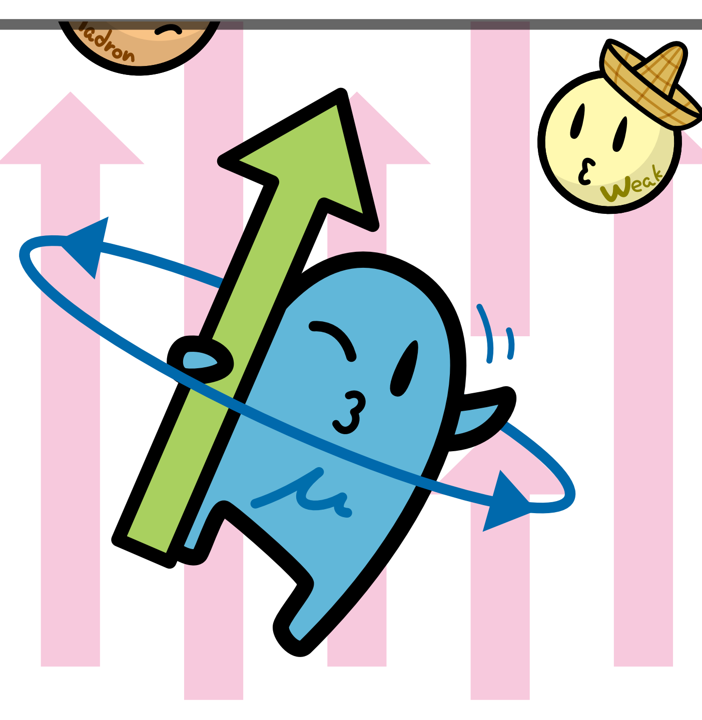

HLBL AT NLO

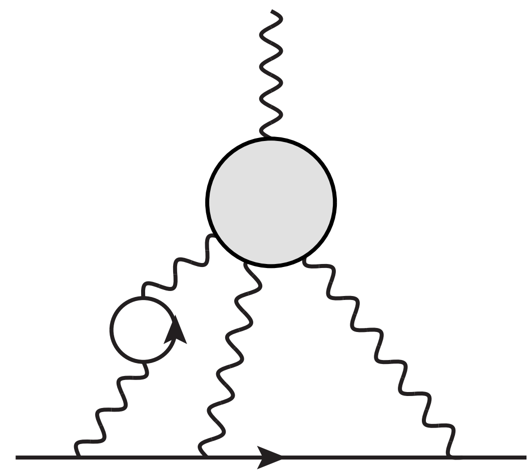

- Higher-order corrections in α can be logarithmically enhanced, e.g., HVP at $\mathcal{O}(\alpha^4)$:

$$a_\mu^{\text{HVP, NNLO}} = 12.4(1) \times 10^{-11} \sim 12.5\,\% \times a_\mu^{\text{HVP, NLO}}$$

- Naïve expectation:

electron VP for $m_e \to 0$

$$\text{\# dressed photon propagators} \longrightarrow 3 \times \frac{\alpha}{\pi} \times \frac{2}{3} \log \frac{m_\mu}{m_e} \sim 2.5\,\%$$

- Electron vacuum polarization correction to pion-pole contribution:

$$a_\mu^{\pi^0\text{-pole, NLO}} = 1.5 \times 10^{-11} \sim 2.6\,\% \times a_\mu^{\pi^0\text{-pole}}$$

- Total estimate: $a_\mu^{\text{HLbL, NLO}} = 2(1) \times 10^{-11}$

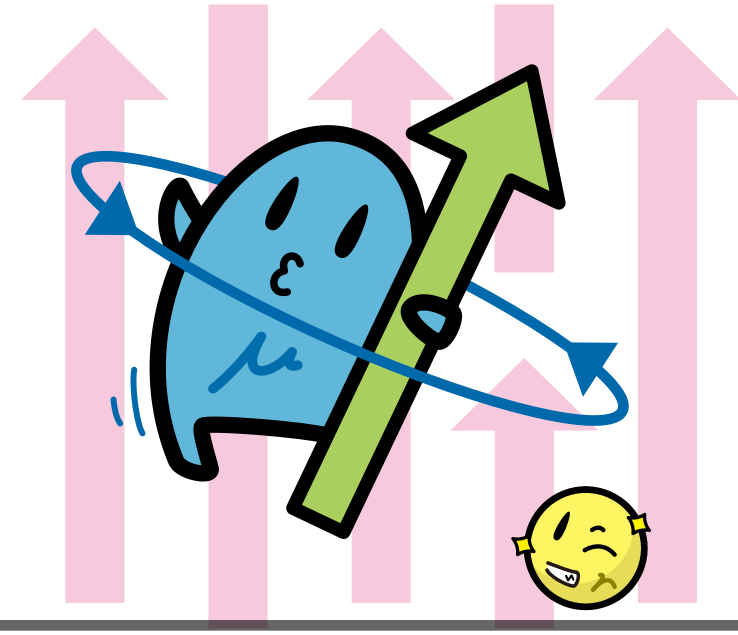

Recent Progress

— Precision Goal 10% —

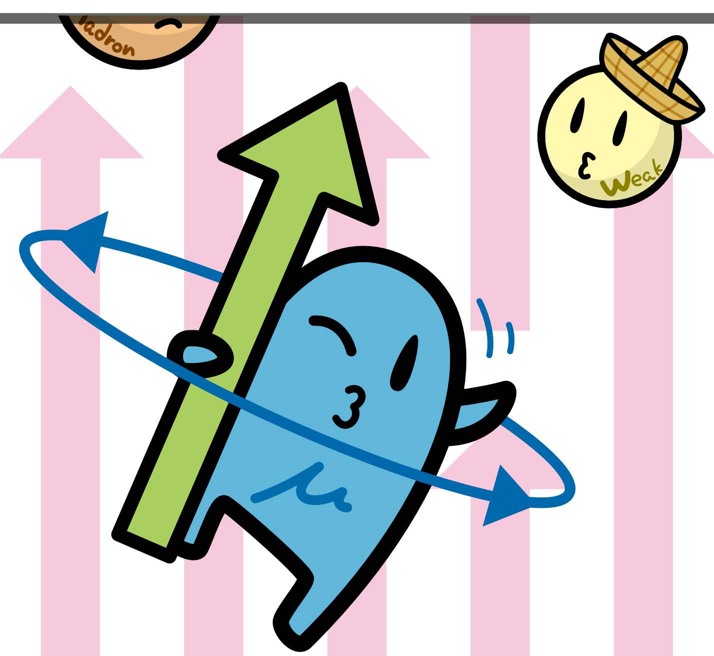

Gilberto Colangelo
(CD24, Bochum)

Recent progress on HLbL

- **Pseudoscalars**:
  dispersive analysis for $\eta^{(\prime)}$ almost completed $\rightarrow$ talk by S. Holz
- **Axials**:
  - TFF analyzed in terms of VMD, including phenom. constraints Hoferichter, Kubis, Zanke '23
  - Optimized basis (no singularities, ok for pion box) Hoferichter, Stoffer, Zillinger '24
- **Tensors**: no proper basis for general kinematics
  $\Rightarrow$ dispersion relation for $g-2$ kinematics ($q_4 = 0$) Lüdtke, Procura, Stoffer '23
- **SDC**:
  - complete analysis in QCD at NLO in all regimes (Melnikov-Vainshtein and beyond) Bijnens, Hermansson-Truedsson, Rodríguez-Sánchez, '23 and in progress, $\rightarrow$ talk by J. Bijnens
  - hQCD models have been further refined (axial-vector contrib. $\gtrsim$ than in WP) Leutgeb, Mager, Rebhan '23

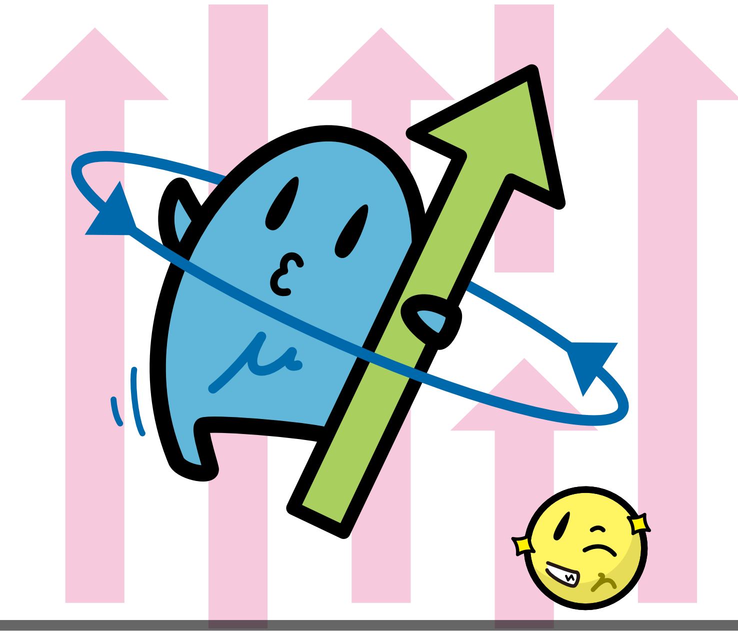

Thank You For Your Attention!

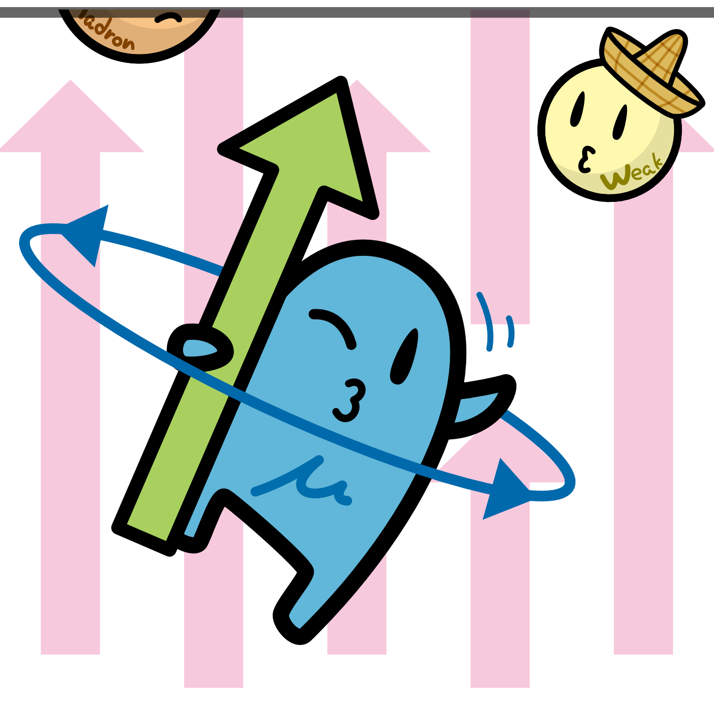

Back-up Slides

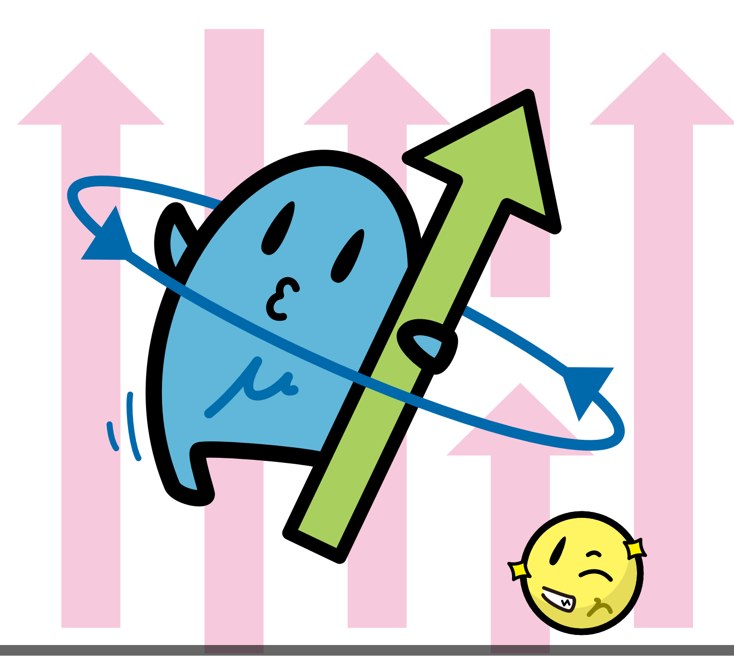

slides courtesy of
Oleksandra Deineka
(MTHS school, Bochum)

HLBL Contribution to $(g-2)_\mu$

— Rescattering —

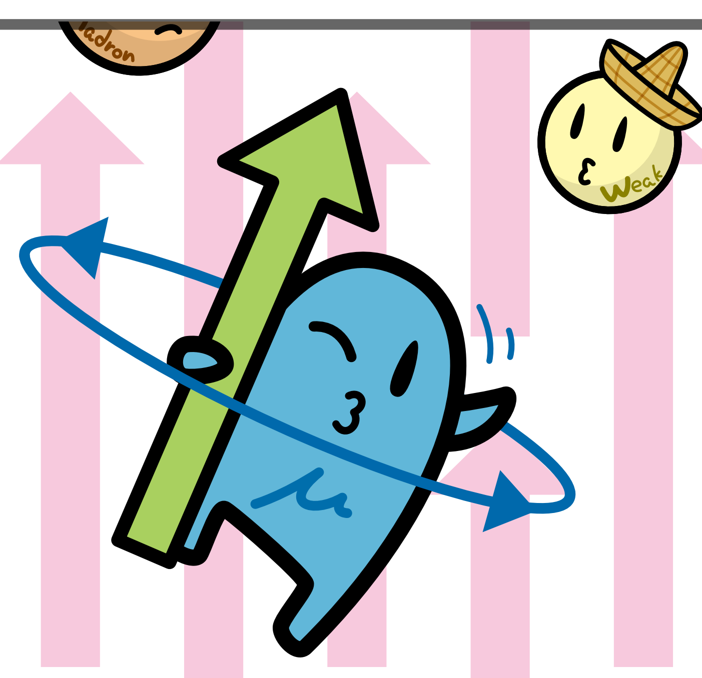

Two pseudoscalar contribution

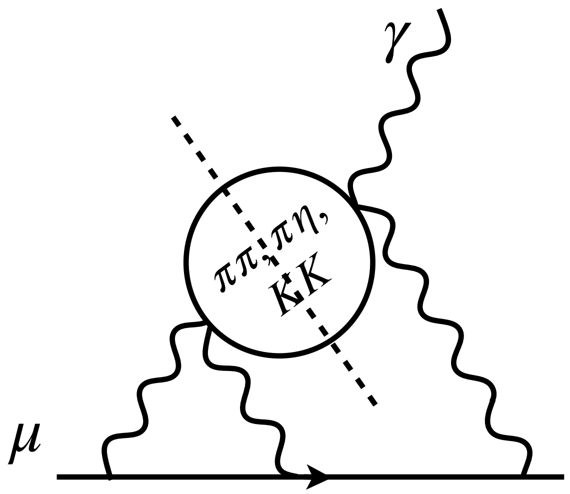

Important ingredients:
$\gamma^*\gamma^* \to \pi\pi, \pi\eta, \ldots$
for spacelike γ^*

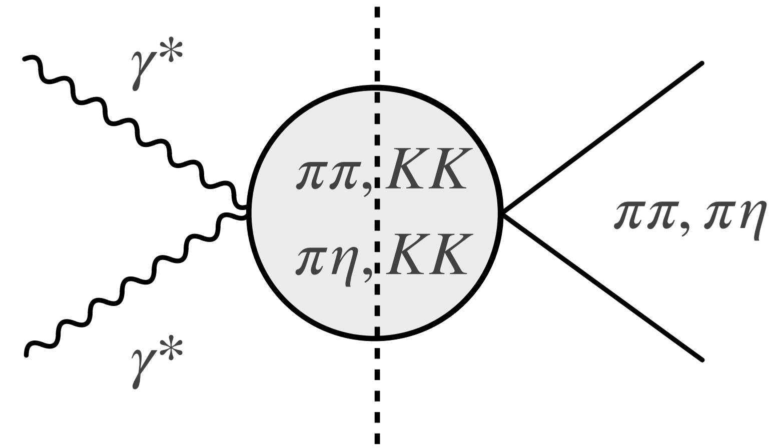

$\gamma\gamma \to \pi^0\pi^0$

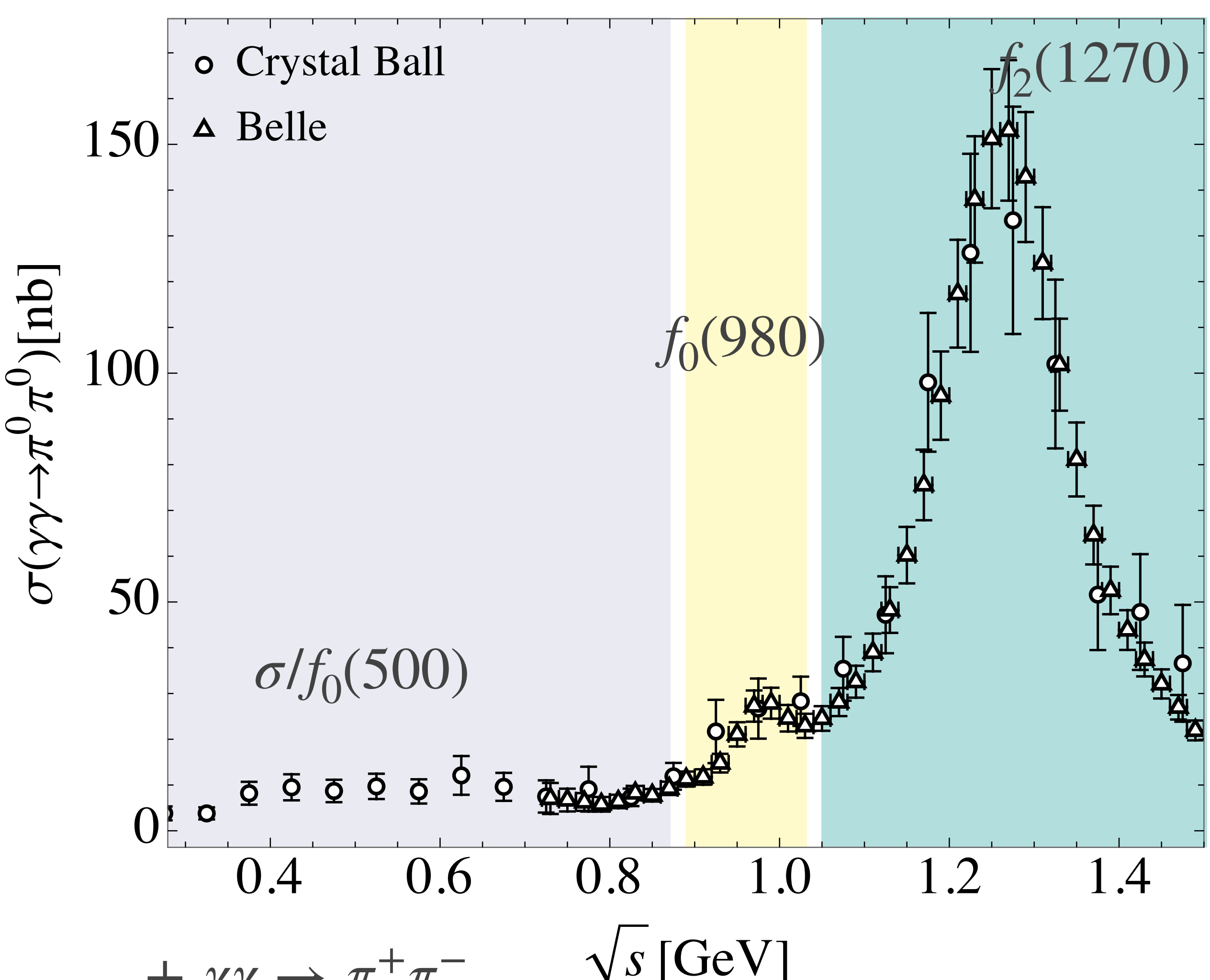

$+ \gamma\gamma \to \pi^+\pi^-$

$\gamma\gamma \to \pi^0\eta$

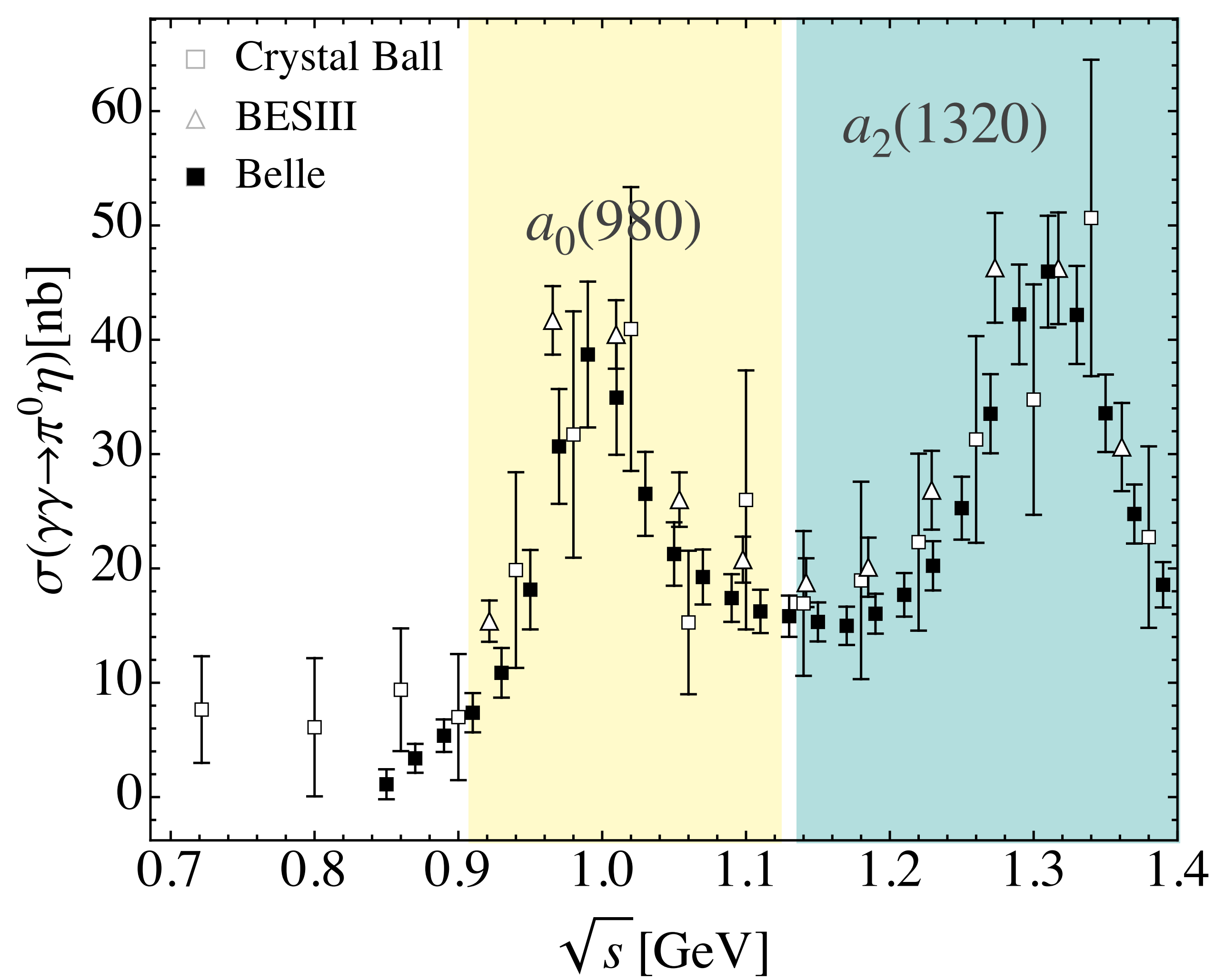

Two pseudoscalar contribution

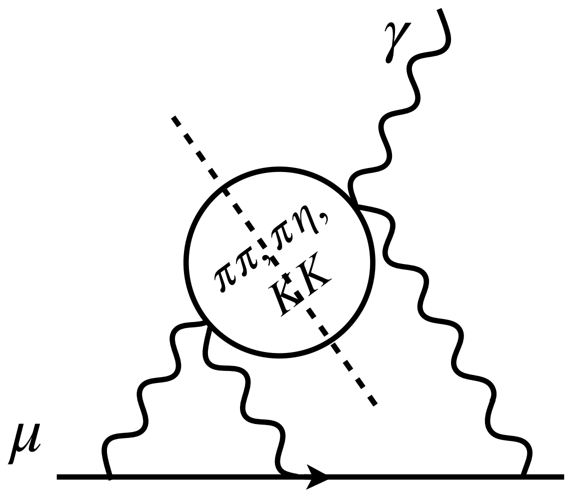

Important ingredients:
$\gamma^*\gamma^* \to \pi\pi, \pi\eta, \ldots$
for spacelike γ^*

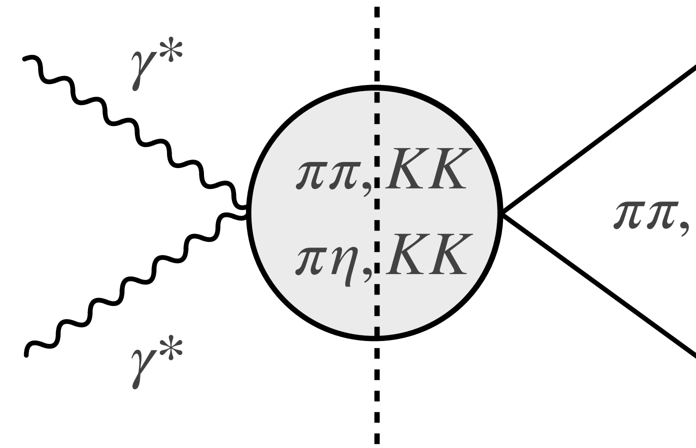

$$a_\mu^{HLbL} = \frac{2\alpha^3}{3\pi^2} \int_0^\infty dQ_1 \int_0^\infty dQ_2 \int_{-1}^1 d\tau \sqrt{1-\tau^2} Q_1^3 Q_2^3 \sum_{i=1}^{12} T_i(Q_1, Q_2, \tau) \bar{\Pi}_i(Q_1, Q_2, \tau)$$

$\bar{\Pi}_i$ for the re-scattering contribution in the S-wave

Colangelo et. al (2017)

$$\bar{\Pi}_i^{J=0} \sim \frac{1}{\pi} \int_{s_{th}}^\infty ds' \frac{1}{\lambda_{12}(s')(s'-q_3^2)^2} \left(f(s') \mathrm{Im} \bar{h}^{(0)}_{++,++}(s') - g(s') \mathrm{Im} \bar{h}^{(0)}_{00,++}(s') \right)$$

+crossed

helicity amplitudes

$\gamma^*\gamma^* \to \gamma^*\gamma^*$

$\gamma^*\gamma^* \to \pi\pi$

$\gamma^*\gamma^* \to \pi\eta$

$\gamma^*\gamma^* \to KK$

Unitarity $\mathrm{Im} \bar{h}^{(0)}_{\lambda_1\lambda_2,\lambda_3\lambda_4}(s) = \bar{h}^{(0)}_{\lambda_1\lambda_2}(s) \rho_{\pi\pi/\pi\eta}(s) \bar{h}^{(0)*}_{\lambda_3\lambda_4}(s) + \bar{k}^{(0)}_{\lambda_1\lambda_2}(s) \rho_{KK}(s) \bar{k}^{(0)*}_{\lambda_3\lambda_4}(s)$

phase-space factor

Dispersion relation

S-wave amplitudes free from kinematic constraints

$$\bar{h}^{(0)}_{i=1,2} = \frac{\bar{h}^{(0)}_{++} \mp Q_1 Q_2 \bar{h}^{(0)}_{00}}{s - s^{(\mp)}_{\text{kin}}}, \quad s^{(\pm)}_{\text{kin}} \equiv -(Q_1 \pm Q_2)^2$$

Can write a **dispersion relation**

$$\bar{h}^J_i(s) = \int_{-\infty}^{s_L} \frac{ds'}{\pi} \frac{\text{Disc}\,\bar{h}^{(J)}_i(s')}{s'-s} + \int_{s_{th}}^{\infty} \frac{ds'}{\pi} \frac{\text{Disc}\,\bar{h}^{(J)}_i(s')}{s'-s}$$

Coupled-channel unitarity

$$\text{Disc}\,h^{(J)}_{i,a}(s) = \sum_{b=1,2} t^{(J)*}_{ab}(s)\,\rho_b(s)\,h^{(J)}_{i,b}(s)$$

hadronic scattering amplitude

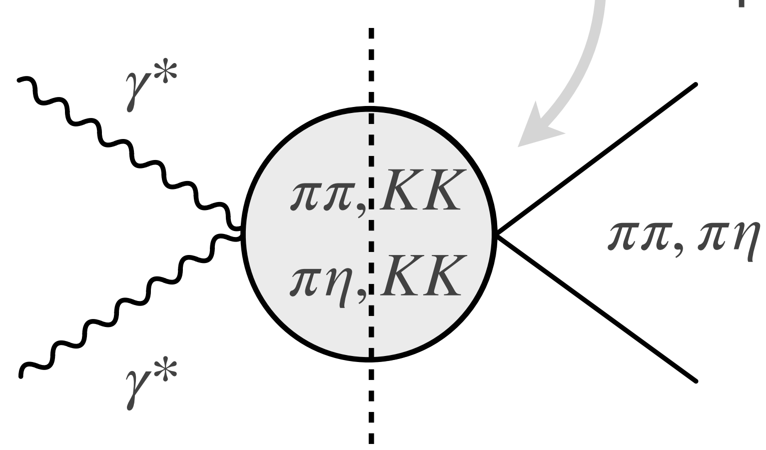

Hadronic input

Unitarity relation for the hadronic amplitude

$$\text{Disc}\, t_{ab}(s) = \sum_c t_{ac}(s)\rho_c(s)t^*_{cb}(s)$$

Once-subtracted dispersion relation

$$t_{ab}(s) = U_{ab}(s) + \frac{s}{\pi}\sum_c \int_{s_{thr}}^{\infty} \frac{ds'}{s'} \frac{\text{Disc}\, t_{ab}(s')}{s'-s}$$

Can be solved by means of **N/D ansatz**

$$t_{ab}(s) = \sum_c D^{-1}_{ac}(s)\, N_{cb}(s)$$

contributions from the right-hand cuts

contributions from the left-hand cuts

Chew, Mandelstam (1960)
Luming (1964)
Johnson, Warnock (1981)

Conformal mapping expansion for hadronic left-hand cuts

Gasparyan, Lutz (2010)

$$U(s) = \sum_{n=0}^{\infty} C_n(\xi(s))^n$$

Hadronic input

$$U(s) = \sum_{n=0}^{\infty} C_n(\xi(s))^n$$

coefficients fitted to the data

$\{\pi\pi, KK\}$: fit to the hadronic data/Roy analysis

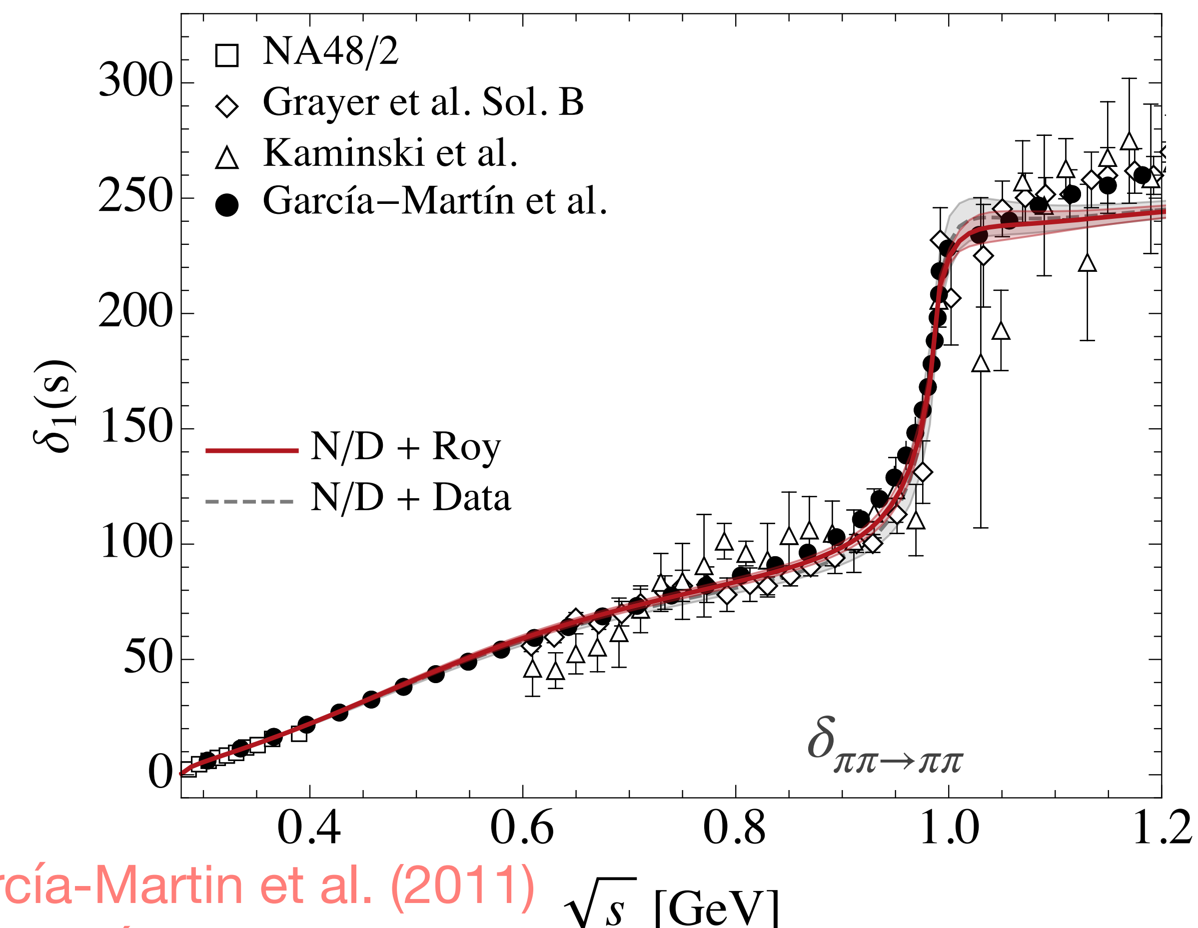

García-Martin et al. (2011)
Peláez, Rodas (2020)

Danilkin, D., Vanderhaeghen (2020)

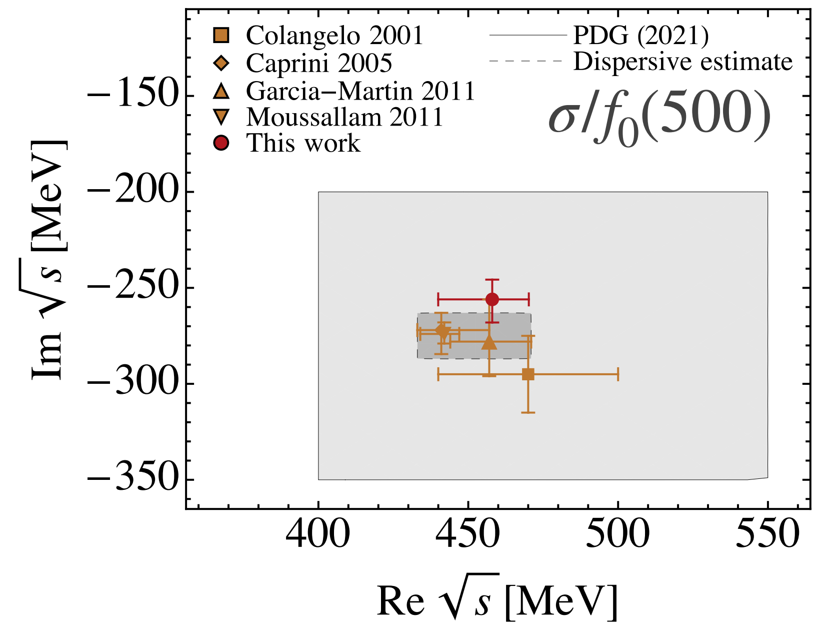

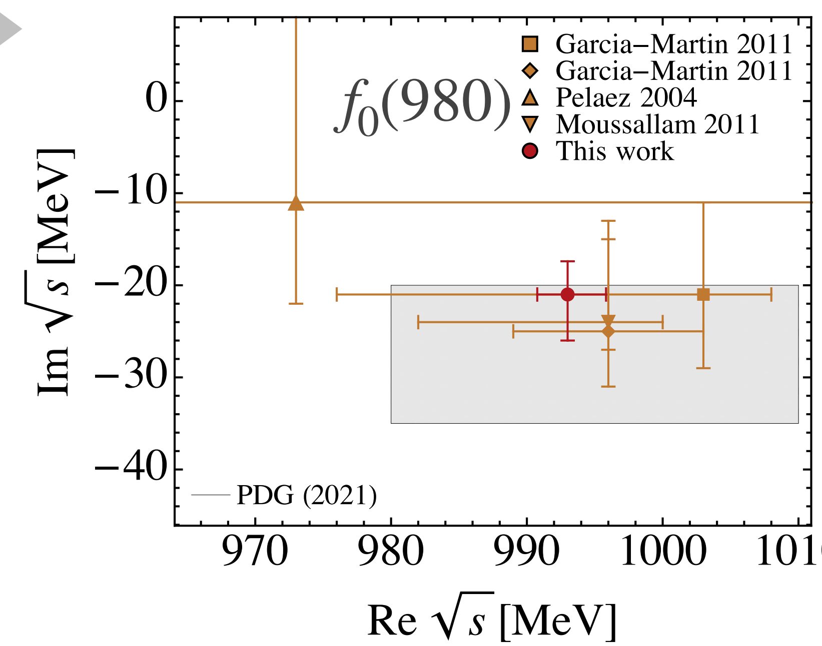

$\{\pi\eta, KK\}$: **no hadronic data available**, coefficients C_n fitted to the cross-section data on $\gamma\gamma \to \pi^0\eta\,, \gamma\gamma \to K_sK_s$

$\gamma\gamma$ left-hand cuts

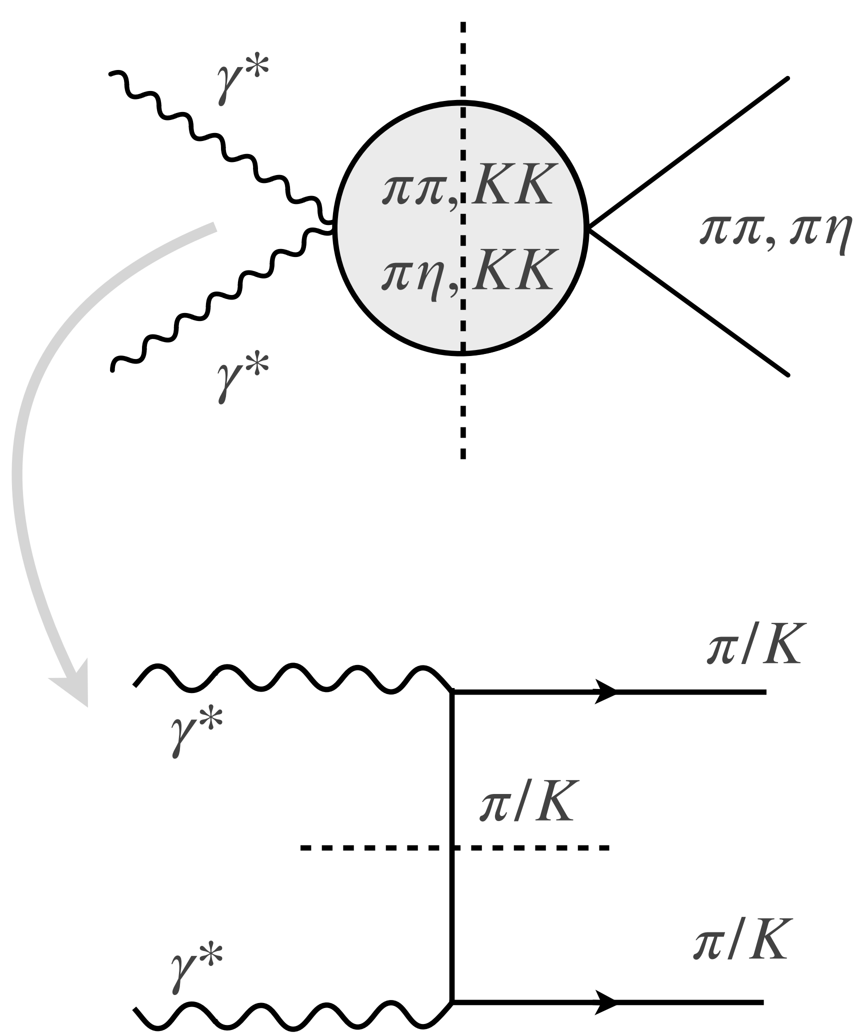

For the S-wave use **Born left-hand cut** only

The generalization to the case of off-shell photons require knowledge of electromagnetic pion/kaon form factors

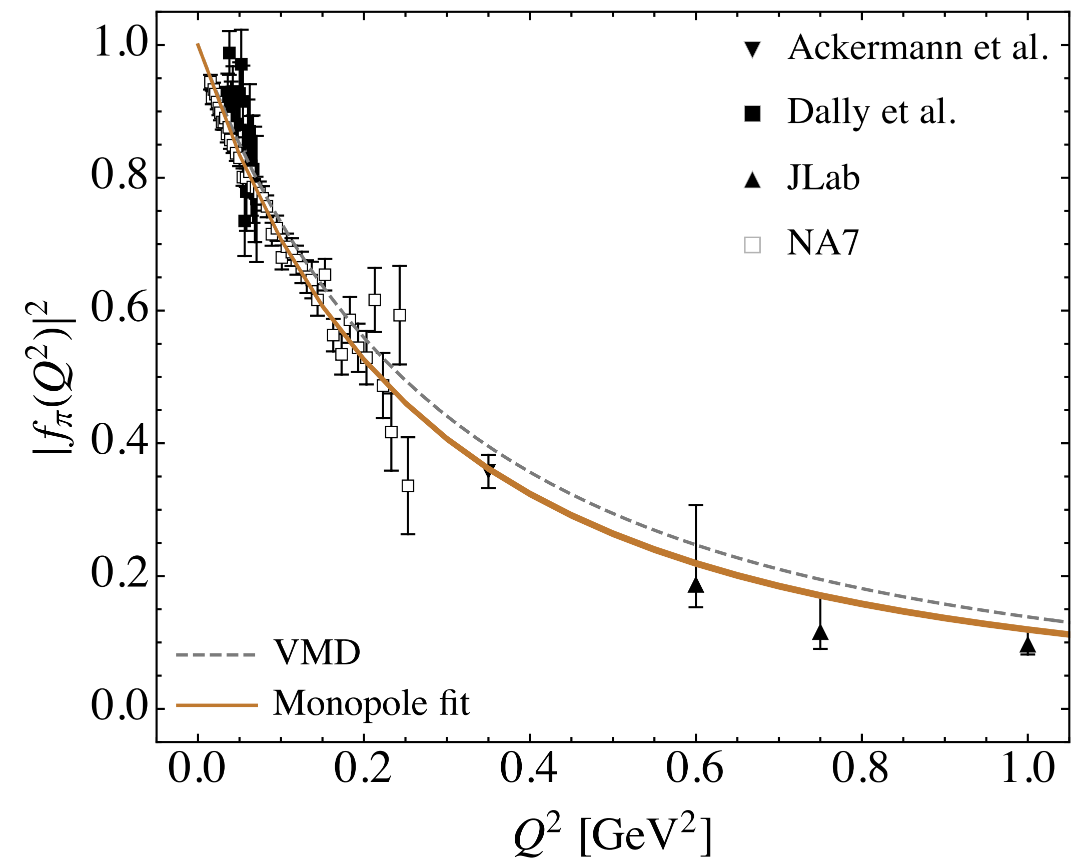

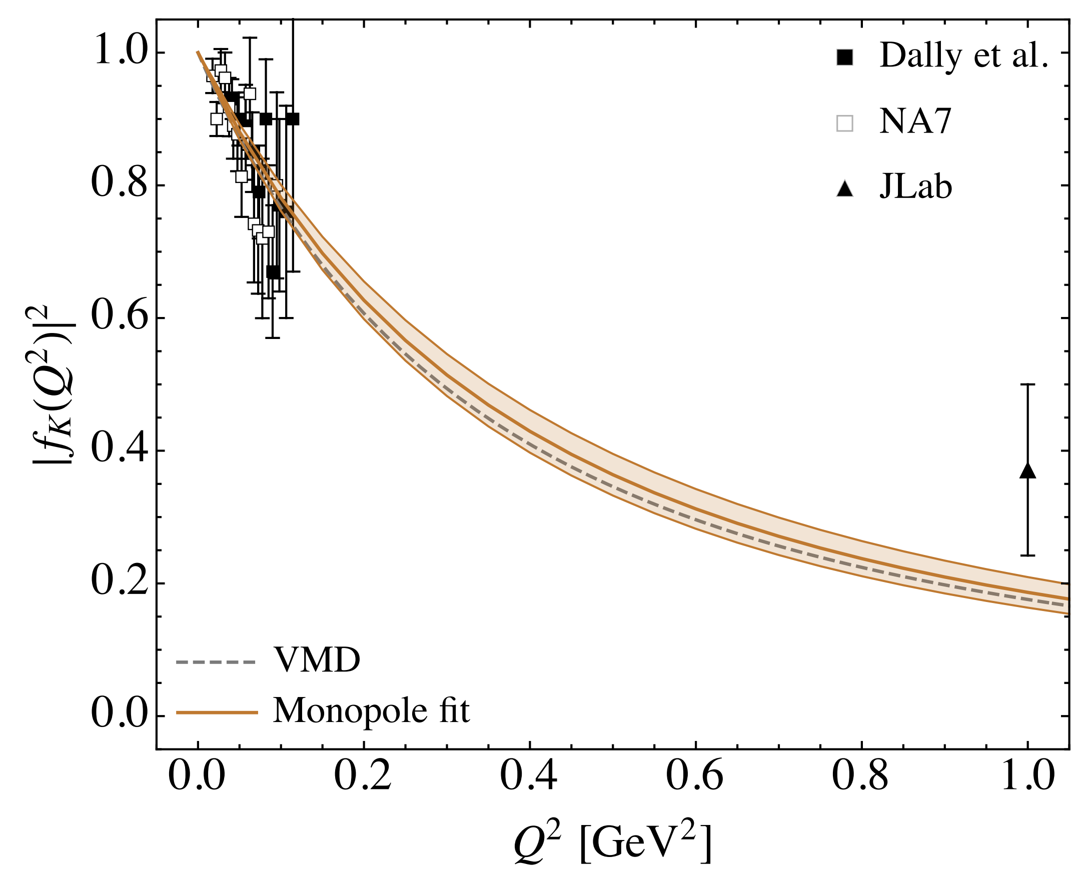

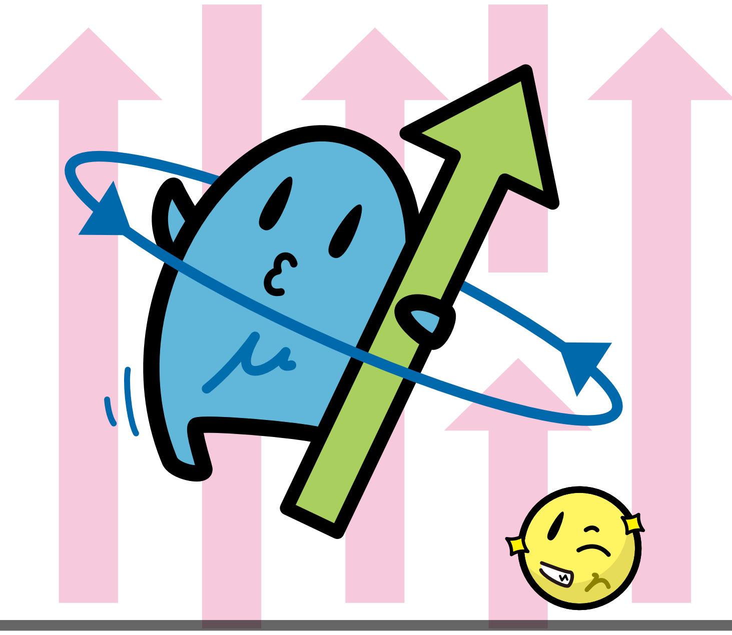

HLBL Contribution to $(g-2)_\mu$

— Short Distance Constraints —

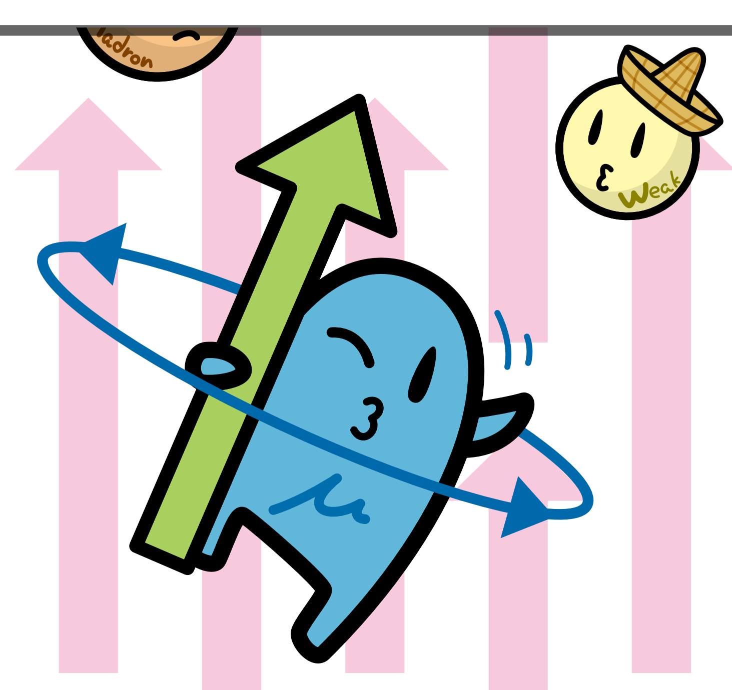

OPE AND NON-RENORMALIZATION THEOREMS

- Isospin-triplet component: $\hat{\Pi}_1(q_1^2, q_2^2, q_3^2, 0; s, t, u) = \dfrac{F_{\pi\gamma^*\gamma^*}(q_1^2, q_2^2) F_{\pi\gamma\gamma^*}(q_3^2)}{s - M_\pi^2} + \ldots$
- $g-2$ limit ($q_4 \to 0$) changes the kinematics into $s = q_3^2, t = q_2^2$ and $u = q_1^2$:

$$\bar{\Pi}_1(q_1^2, q_2^2, q_3^2) := \hat{\Pi}_1(q_1^2, q_2^2, q_3^2, 0; q_3^2, q_2^2, q_1^2) = \frac{F_{\pi\gamma^*\gamma^*}(q_1^2, q_2^2) F_{\pi\gamma\gamma^*}(q_3^2)}{q_3^2 - M_\pi^2} + G(q_1^2, q_2^2, q_3^2)$$

- OPE limit $\hat{q}^2 := q_1^2 = q_2^2 \gg \Lambda_{\text{QCD}}^2$ and no constraint on q_3:

$$\bar{\Pi}_1(\hat{q}^2, \hat{q}^2, q_3^2) = -\frac{2F_\pi}{3\hat{q}^2}\left[\frac{F_{\pi\gamma\gamma}}{q_3^2} + \frac{F_{\pi\gamma\gamma^*}(q_3^2) - F_{\pi\gamma\gamma}}{q_3^2} + \mathcal{O}(M_\pi^2)\right] + G(\hat{q}^2, \hat{q}^2, q_3^2) + \mathcal{O}(\hat{q}^{-3})$$

- Known behaviour in the chiral limit: $\bar{\Pi}_1(\hat{q}^2, \hat{q}^2, q_3^2)\Big|_{m_q=0} = -\dfrac{1}{6\pi^2}\dfrac{1}{\hat{q}^2 q_3^2} + \mathcal{O}(\hat{q}^{-3})$
- Therefore: $G(\hat{q}^2, \hat{q}^2, q_3^2)\Big|_{m_q=0} = \dfrac{2F_\pi}{3\hat{q}^2}\dfrac{F_{\pi\gamma\gamma^*}(q_3^2) - F_{\pi\gamma\gamma}}{q_3^2}\Bigg|_{m_q=0} + \mathcal{O}(\hat{q}^{-3})$

OPE AND NON-RENORMALIZATION THEOREMS

- Non-renormalization theorem tells us that the q_3^2 dependence of the leading term is exact ($\hat{q}^2 := q_1^2 = q_2^2 \gg \Lambda_{\text{QCD}}^2$):

$$G(\hat{q}^2, \hat{q}^2, q_3^2)\Big|_{m_q=0} = \frac{2F_\pi}{3\hat{q}^2} \frac{F_{\pi\gamma\gamma^*}(q_3^2) - F_{\pi\gamma\gamma}}{q_3^2}\Bigg|_{m_q=0} + \mathcal{O}(\hat{q}^{-3})$$

- $\bar{\Pi}_1^{\text{MV}}(q_1^2, q_2^2, q_3^2) = \dfrac{F_{\pi\gamma^*\gamma^*}(q_1^2, q_2^2) F_{\pi\gamma\gamma}}{q_3^2 - M_\pi^2}$ implicitly assumes

$$G(q_1^2, q_2^2, q_3^2)_{\text{MV}} = -F_{\pi\gamma^*\gamma^*}(q_1^2, q_2^2) \frac{F_{\pi\gamma\gamma^*}(q_3^2) - F_{\pi\gamma\gamma}}{q_3^2 - M_\pi^2}$$

- Melnikov & Vainshtein model extrapolates a constraint only valid at asymptotically high energies to all possible q_1^2, q_2^2, thus distorts the low-energy properties of the HLbL tensor K. Melnikov and A. Vainshtein, 1911.05874

- Our model $G_{\text{eP}}(q_1^2, q_2^2, q_3^2) = \sum\limits_{i=1} \dfrac{F_{\pi\gamma^*\gamma^*}(q_1^2, q_2^2) F_{\pi\gamma\gamma^*}(q_3^2)}{q_3^2 - M_{\pi(i)}^2}$ satisfies SDC only away from the chiral limit and for $q_3^2 \gg \Lambda_{\text{QCD}}$: $\lim\limits_{\hat{q}^2 \to \infty} \hat{q}^2 G_{\text{eP}}(\hat{q}^2, \hat{q}^2, q_3^2) = -\dfrac{1}{6\pi^2 q_3^2} + \mathcal{O}(q_3^{-3})$

HOLOGRAPHIC QCD — HW2 MODEL

- $$\bar{\Pi}_1^{\mathrm{HW2}} = F_{\pi\gamma^*\gamma^*}(q_1^2, q_2^2)\left[\frac{F_{\pi\gamma\gamma}}{q_3^2 - M_\pi^2} + \frac{M_\pi^2(F_{\pi\gamma\gamma^*}(q_3^2) - F_{\pi\gamma\gamma})}{q_3^2(q_3^2 - M_\pi^2)}\right] - \frac{F_{\pi\gamma\gamma}^2}{q_3^2}\int_0^{z_0} dz\alpha'(z)v_1(z)v_2(z)\bar{v}_3(z)$$
  where $v_i(z) = zQ_i\left[K_1(zQ_i) + \frac{K_0(z_0Q_i)}{I_0(z_0Q_i)}I_1(zQ_i)\right]$, $\alpha(z) = 1 - z^2/z_0^2$ and $z_0 = (\sqrt{2}\pi F_\pi)^{-1}$ J. Leutgeb and A. Rebhan, 1912.01596 & L. Cappiello, et al., 1912.02779
  - Corrections to the $1/q_3^2$ behaviour vanish in the chiral limit
- $$G_{\mathrm{HW2}}(q_1^2, q_2^2, q_3^2) = F_{\pi\gamma^*\gamma^*}(q_1^2, q_2^2)\frac{F_{\pi\gamma\gamma^*}(q_3^2) - F_{\pi\gamma\gamma}}{q_3^2} - \frac{F_{\pi\gamma\gamma}^2}{q_3^2}\int_0^{z_0} dz\alpha'(z)v_1(z)v_2(z)\bar{v}_3(z)$$
  where $\bar{v}_i(z) = v_i(z) - 1$
- Pseudoscalar TFF with correct normalization, BL and symmetric pQCD limits:
  $$F_{\pi\gamma^*\gamma^*}(q_1^2, q_2^2) = -F_{\pi\gamma\gamma}\int_0^{z_0} dz\,\alpha'(z)v_1(z)v_2(z)$$

COMPARISON OF SDC MODELS

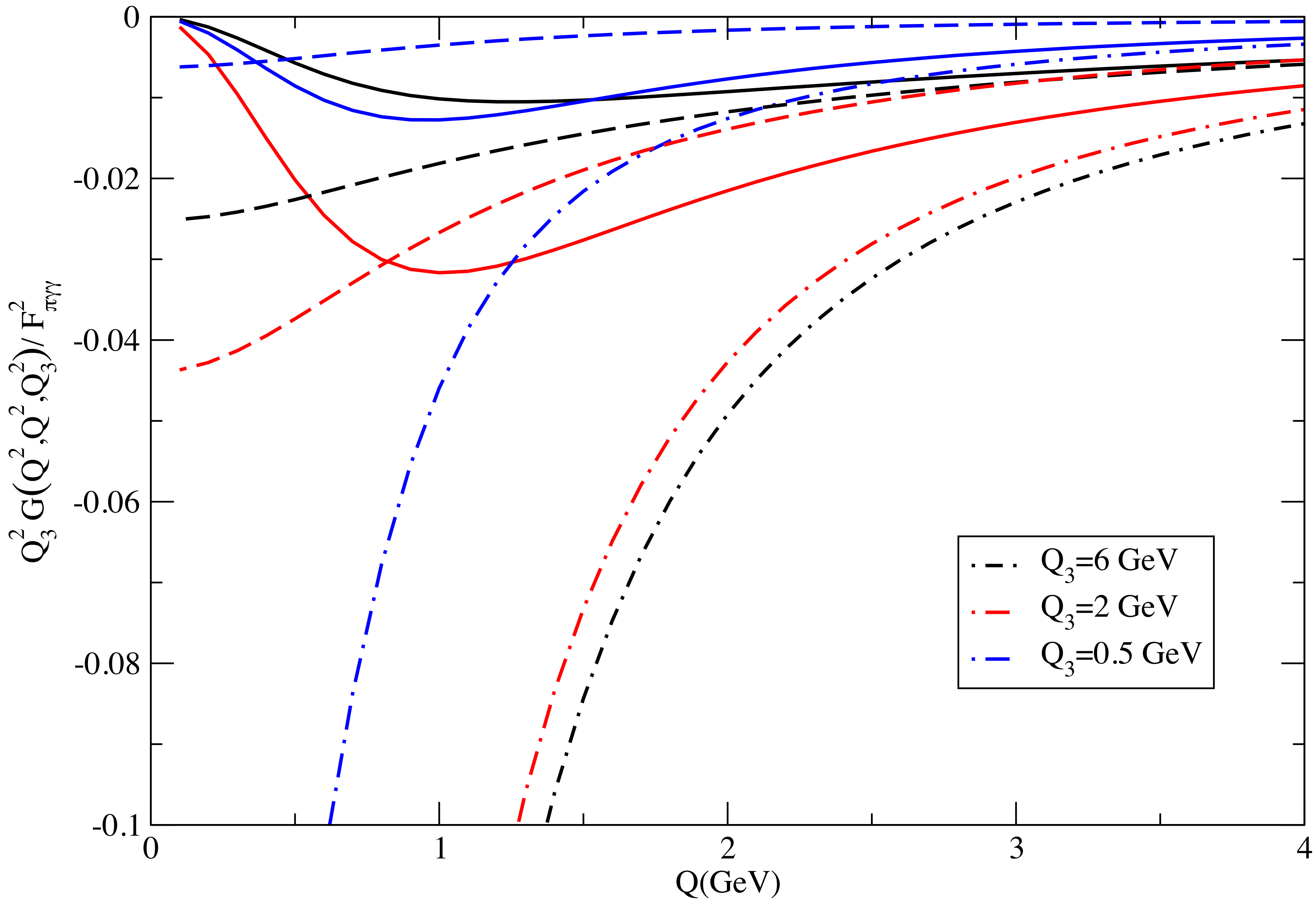

HW2 axial-vector tower (solid)

pseudoscalar tower (dashed)

Melnikov & Vainshtein (dot-dashed)

CONTRIBUTION TO g-2

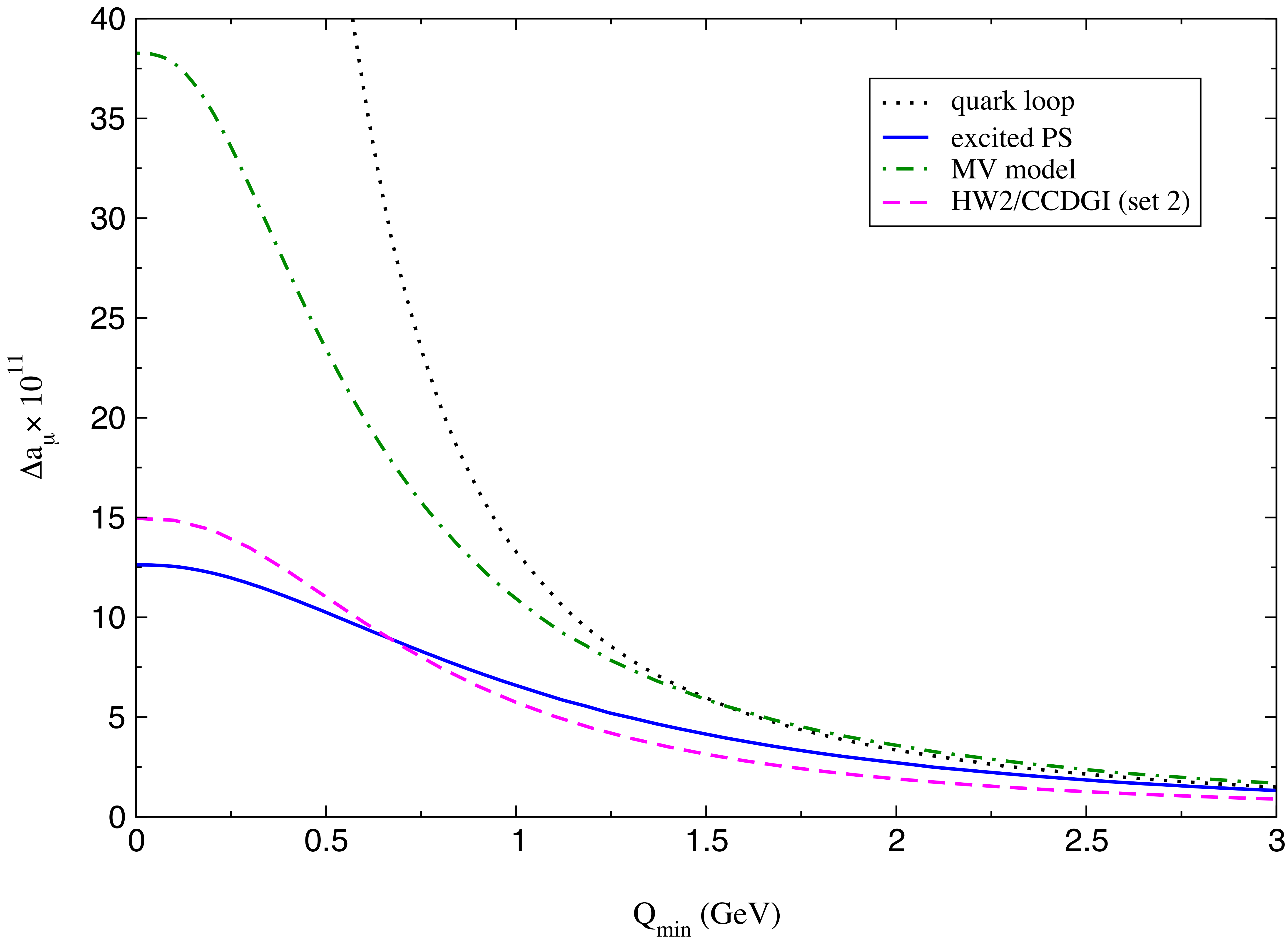

GROUND-STATE AXIAL-VECTOR

- Is it possible to satisfy the MV SDC by means of a single axial-vector meson (per isospin channel)? — incompatible with L3 data

- Symmetry properties of axial-vector TFFs:
$$F_1(q_1^2, q_2^2) = -F_1(q_2^2, q_1^2), \quad F_2(q_2^2, q_1^2) = -F_3(q_1^2, q_2^2)$$
$$G_2(q_1^2, q_2^2) = (q_1^2 - q_2^2)F_1(q_1^2, q_2^2) + q_1^2 F_2(q_1^2, q_2^2) + q_2^2 F_2(q_2^2, q_1^2)$$
$$G_1(q^2) = F_1(q^2, 0) + F_2(q^2, 0) = \frac{G_2(q^2, 0)}{q^2}$$

- Assuming the basis: $G(q_1^2, q_2^2, q_3^2) = \dfrac{G_2(q_1^2, q_2^2) G_1(q_3^2)}{M_A^6}$, the constraint factorizes:
$$\lim_{\hat{q}^2 \to \infty} x \frac{G_2(\hat{q}^2, \hat{q}^2)}{M_A^4} = -\frac{2}{3\hat{q}^2} + \mathcal{O}(\hat{q}^{-3}),$$
$$\frac{G_1(q_3^2)}{x M_A^2} = -F_\pi \frac{F_{\pi\gamma\gamma^*}(q_3^2) - F_{\pi\gamma\gamma}}{q_3^2}$$

AXIAL-VECTOR TRANSITION FORM FACTOR